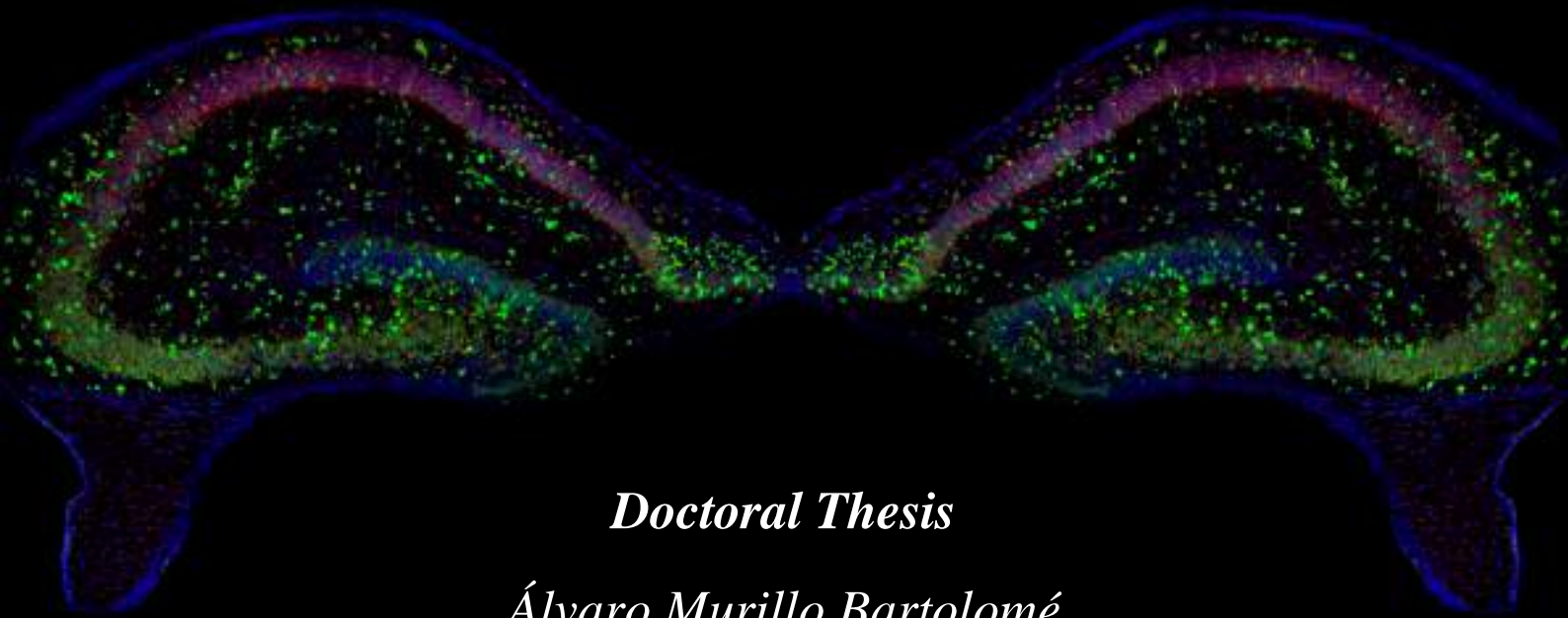




**Effects of GluN3A silencing in  
Huntington's disease and  
systematic mapping of its  
expression in the mouse forebrain**



*Doctoral Thesis*

*Álvaro Murillo Bartolomé*

**Thesis Director:** Isabel Pérez Otaño

**Thesis co-Director:** Sonia Marco Martínez

Universidad Miguel Hernández

PhD Program in Neuroscience

Instituto de Neurociencias de Alicante, 2021





# Effects of GluN3A silencing in Huntington's disease and systematic mapping of its expression in the mouse forebrain

*Doctoral Thesis presented by*

*Álvaro Murillo Bartolomé*

**Thesis Director:**

Isabel Pérez Otaño

**Thesis co-Director:**

Sonia Marco Martínez

San Juan de Alicante, 2021

*PhD Program in Neuroscience*

*Instituto de Neurociencias – UMH-CSIC*







San Juan de Alicante, February 16<sup>th</sup> 2021

To whom it may concern,

The doctoral thesis entitled “*Effects of GluN3A silencing in Huntington's disease and systematic mapping of its expression in the mouse forebrain*” has been developed by myself, Álvaro Murillo Bartolomé. This thesis is presented in a publication format. It is based on experimental studies undertaken at the Neuroscience Institute of Alicante during the PhD program in neuroscience of the Miguel Hernández University.

Yours sincerely,

D. Álvaro Murillo Bartolomé





San Juan de Alicante, February 16<sup>th</sup> 2021

To whom it may concern,

The doctoral thesis entitled “*Effects of GluN3A silencing in Huntington's disease and systematic mapping of its expression in the mouse forebrain*” has been developed by myself, Álvaro Murillo Bartolomé. This thesis includes the following publications, I am the first author of one of them. I declare that the publications have not been used and will not be used in any other thesis in agreement with my thesis director Isabel Pérez Otaño and my thesis co-director Sonia Marco Martínez.

1. Marco, Sonia, Alvaro Murillo and Isabel Pérez-Otaño. 2018. “RNAi-Based GluN3A Silencing Prevents and Reverses Disease Phenotypes Induced by Mutant Huntingtin.” *Molecular Therapy* 26(8):1965–72. doi: 10.1016/j.ymthe.2018.05.013
2. “Alvaro Murillo, Ana Isabel Navarro, Eduardo Puelles, Yajun Zhang, Timothy J. Petros, and Isabel Perez-Otano. 2020. “Temporal Dynamics and Neuronal Specificity of *Grin3a* Expression in the Mouse Forebrain.” *Cerebral Cortex*. Dec 9:bhaa330. doi: 10.1093/cercor/bhaa330”.

Yours sincerely,

D. Álvaro Murillo Bartolomé







San Juan de Alicante, 16 de Febrero 2021

D<sup>a</sup>. Isabel Pérez Otaño, Profesora de Investigación CSIC

AUTORIZA la presentación de la Tesis Doctoral titulada “*Effects of GluN3A silencing in Huntington's disease and systematic mapping of its expression in the mouse forebrain*” y realizada por D Álvaro Murillo Bartolomé, bajo mi inmediata dirección y supervisión como directora de su Tesis Doctoral en el Instituto de Neurociencias (UMH-CSIC) y que presenta para la obtención del grado de Doctor por la Universidad Miguel Hernández.

Y para que conste, a los efectos oportunos, firmo el presente certificado.

Dra. Isabel Pérez Otaño





San Juan de Alicante, 16 de Febrero 2021

D<sup>a</sup>. Sonia Marco Martínez, científico contratado.

AUTORIZA la presentación de la Tesis Doctoral titulada "*Effects of GluN3A silencing in Huntington's disease and systematic mapping of its expression in the mouse forebrain*" y realizada por D Álvaro Murillo Bartolomé, bajo mi inmediata dirección y supervisión como co-directora de su Tesis Doctoral en el Instituto de Neurociencias (UMH-CSIC) y que presenta para la obtención del grado de Doctor por la Universidad Miguel Hernández.

Y para que conste, a los efectos oportunos, firmo el presente certificado.

Dra. Sonia Marco Martínez





San Juan de Alicante, 16 de Febrero 2021

Dña. Elvira de la Peña García, Coordinadora del programa de doctorado en Neurociencias del Instituto de Neurociencias de Alicante, centro mixto de la Universidad Miguel Hernández (UMH) y de la Agencia Estatal Consejo Superior de Investigaciones Científicas (CSIC),

CERTIFICO:

Que la Tesis Doctoral titulada "*Effects of GluN3A silencing in Huntington's disease and systematic mapping of its expression in the mouse forebrain*" ha sido realizada por D Álvaro Murillo Bartolomé, bajo la dirección de D<sup>a</sup> Isabel Pérez Otaño como directora y D<sup>a</sup> Sonia Marco Mantinez como co-directora, y doy mi conformidad para que sea presentada a la Comisión de Doctorado de la Universidad Miguel Hernández.

Y para que conste, a los efectos oportunos, firmo el presente certificado.

Dra. Elvira de la Peña García





«A veces vale la pena derretirse por algunas personas»

- Olaf -

**AGRADECIMIENTOS**





Este viaje duro y emocionante ya se está acabando. Duro, sí, pero de lo fácil uno no se enorgullece. Emocionante, vibrante y apasionante son los calificativos que me trae a la cabeza los años vividos durante la tesis. Esos adjetivos me llevaban, en ciertos experimentos, a estar en plena madrugada, festivos y fines de semana en el laboratorio dando lo mejor de mí. Historias de fracasos, de alegrías, de fraternidad, etc durante los últimos años de la mano de GluN3A solo llenarían una pequeña parte de un enorme libro que se podría escribir de mi tesis.

Toda historia empieza con un prólogo y la mía empezó en Salamanca, en un pequeño laboratorio dirigido por Felipe X. Pimentel y coprotagonizado por Emilio Boada. Este último, realizó la obra más importante que está dirigiendo mi vida, fue el inductor de la pasión que tengo hacia la ciencia.

En 2015, dado que el mundo no se acabó en 2012, la Dra. Isabel Pérez Otaño posibilitó mi incorporación a su grupo de laboratorio en el CIMA de Pamplona, donde encontré un ambiente acogedor por parte de todos. De ella, como gran mentora, me llevo el buen hacer de la ciencia, las miradas críticas a los artículos científicos y que en ningún caso procrastinar es una opción. No echaré de menos su despacho sofocante en invierno, pero si las largas horas de análisis donde ella veía cosas que yo ni con mil ojos me hubiera fijado, enseñándome así a hacerme las preguntas adecuadas. Gracias también al ministerio de economía y competitividad por darme la oportunidad de realizar mi tesis con la ayuda financiera de la contratación de doctores en formación.

Mis primeros pasos en el laboratorio los hice de la mano de la Dra. Sonia Marco, codirectora de mi tesis y casera durante unos meses, para la cual no existen palabras en el mundo que se acerquen a lo agradecido que estoy. Siempre enérgica y siempre trabajadora, me enseñaba con pasión, arrojo y paciencia el trabajo diario. Tanto las alegrías y como los fracasos los afrontábamos juntos. Me acuerdo con nostalgia de las “charlas” largas donde ella hablaba y yo escuchaba. Con mucho cariño ella me echaba broncas horas después de los fallos que yo cometía inicialmente, ya que veía en mi la cara de pesadumbre ante los errores cometidos y como ella decía “no te quiero hundir más”.

Otra gran mención es para el Dr. Luis García Rabaneda con el que no compartí muchos experimentos, pero sí enseñanzas y discusiones en bares, paseos, marchas...sobre ciencia. Siempre ha sido una ayuda y una persona con la que poder hablar de cualquier cosa. Junto a él y a la Dra. Eva Liñeiro, su mujer, construimos un círculo vicioso de cenas y cervezas que empezó en su fantástica boda.

Para mi sevillana favorita, la futura doctora María José Conde Dusman, solo tengo palabras de cariño. La verdad es que no sabía dónde nombrar a esta “moza”, ya que hemos estado juntos por varios años desde el master hasta el final de la tesis. Luchadora y capaz hasta la medula, trabajamos codo con codo durante un par de meses en los que el cambio de medio durante horas en las campanas se hacía más ameno.

Por supuesto gracias al Dr. John Wesseling por sus tantas ideas constructivas a mis proyectos; al Dr. Partha Narayan Dey que me quitó el miedo al inglés; a la Dra. Rebeca Martínez Turrillas y a la Dra. Daniela Urribarri por sus ayudas en el día a día del laboratorio y por supuesto a Víctor Darío Ramos por sus enseñanzas en microscopía y por los buenos momentos que pasamos juntos.

Mi cuadrilla formada por Ángela, Antonio, Luis, Pablo, Eva y Juan, con los que tan buenos ratos pase y a los que echo mucho de menos, mil gracias!!!!por mantenerme cuerdo con los potes y las salidas al campo en los largos inviernos norteños.

Por el devenir de la vida, una mudanza acaeció sobre el laboratorio, permitiéndome conocer a gente maravillosa también el instituto de neurociencias de Alicante. Allí, compañeros de laboratorio me ayudaron muchísimo. Como Ana Navarro Navarro, que tuvo que aguantar mis desastres organizativos. La Dra. Noelia Campillo o Noelia Zurdo, que me hacían la vida del laboratorio más fácil. Gracias también a Alice Staffa, por enseñarme a decir la palabra “perfecto” con acento italiano y a Sergio del Olmo por iniciarme en el mundo de la electrofisiología. También agradezco su apoyo a la Dra. Eva Liñeiro, a Neus Vidal, al Dr. Oliver Crawley, al Dr. David Litvin y a Sara Mico con los que no compartí mucho tiempo, pero estarán en mi memoria.

Tengo que hacer especial mención a mi compañero de trabajo, de gimnasio, de cenas, de fiestas, de piso... en resumen, a mi “compañero de vida” Oscar Elia Zudaire. Cuando nos veíamos mal el uno al otro siempre había una cena o play station que pudiera mejorar la situación del afectado. Preguntas como “voy a poner la lavadora, ¿quieres meter algo en ella?” eran la envidia de verdaderas parejas. Sin una discusión y con opiniones muy similares en mil cosas pasamos meses geniales. Solo me queda la espinita del buceo, pero algún día...

La colaboración en los experimentos de hibridación *in situ* me dieron la oportunidad de conocer a gente genial. Gracias a el Dr. Eduardo Puelles, cuyos conocimientos anatómicos me dejaban fascinado. Al Dr. Diego Echevarría, el cual siempre tenía un buen consejo y un dulce en la mano. Y a Paqui Almagro, la mami de todos.

Por supuesto, un especial agradecimiento a mis 4 chicas favoritas Aida, Vero, Raquel y Rita. Con las que tan buenos momentos he compartido dentro y fuera del trabajo. Experiencias, cariño, conocimiento y una gran amistad es lo que me llevo de todas ellas. De Aida tengo que hacer mención sus vaivenes mentales, pero también su fidelidad a la amistad, la cual nunca falto. De mi vecina, Vero, nunca olvidare sus críticas hacia mi inteligencia emocional, aunque era claramente superior a la media según sus cálculos, así como su valentía al enfrentarse a la adversidad. De Raquel, que es la más madura, aunque es la más joven de las 3, recordaré sus amables consejos y su felicidad intrínseca que era contagiosa. La gallardía es claramente la seña de identidad de Rita, mi vilera favorita.

Gracias a toda la gente de mi pueblo (Casaseca de Campeán), Héctor, Pablo, Abel, Ángel, Lara, Jose, Friaza, Alex, Vero, Laura... cuyas preguntas como “¿trabajas en festivo? ¿no te pagan las horas extras? ¿cuándo te conviertes en doctor?” hacían sacar en mí una sonrisa áspera. No mucha gente me lo podía decir ya que la población es pequeña, pero, aunque pocos allí vivimos, orgullosos decimos “de Casaseca somos hijos nacidos”.

A una persona muy especial, Laura, a la que tanto quiero solo decirle que gracias por ser mi apoyo y por estar siempre a mi lado en mis buenos y mis malos momentos de estrés. Por todos los ánimos que me das y los consejos. Gracias por escuchar y por

aguantarme. Los pequeños viajes que nos hacemos me permiten seguir cuerdo en este mundo de locura. Elegiste estar, aun estas y seguirás estando día a día en mi vida.

A mi “pápa” por todos sus consejos, apoyo y locuras. La frase “las cosas solo se pueden hacer de dos formas, bien o como siempre” me acompaña día a día en mi vida personal y el trabajo.

A mi “gorda” por aguantar tantos meses seguidos sin poderme ver, por la ayuda financiera, sin la cual no hubiera podido ni siquiera iniciar la carrera. Gracias por todo su cariño y afecto. Una madre siempre siempre siempre siempre está ahí. Por mas palabras que use no se podría expresar todo mi amor. Gracias también a Berna, que gracias a su mera existencia mantenía lejos de mi a mi madre dejándome mas libre.

A mi hermano, que tiempo atrás, cuando yo estaba castigado y hacia experimentos en casa, me decía que algún día encontraría alguna cura como investigador ¡gracias por la premonición! Mucho nos pegábamos de pequeños, pero mucho nos queremos.

Hay gente que se ha ido de este mundo antes de verme como doctor. Ellos son mis abuelos maternos, Primitivo e Inés. Mis segundos padres, a los que proceso cariño, gratitud y amor infinito.

Por supuesto al resto de mi familia, abuelos, tios, primos...

A todos y cada uno de vosotros, mil gracias por haberme acompañado en este camino tan arduo y largo. **Mi gratitud es eterna con todos vosotros.**

*En memoria de mis abuelos: Primitivo e Inés.*



«La ciencia es la progresiva aproximación  
del hombre al mundo real»

- Max Planck -

**TABLE OF CONTENTS**



<b>LIST OF FIGURES AND TABLES</b>	p. 1
<b>ABSTRACT/RESUMEN</b>	p. 7
<b>INTRODUCTION</b>	p. 13
1. Huntington's disease (HD)	p. 13
1.1 HD symptoms.	p. 13
1.2 Neuropathology of HD.	p. 14
1.3 Basal ganglia.	p. 17
1.3.1 Affectation of basal ganglia pathways in HD.	p. 19
1.4 <i>HTT</i> expression.	p. 19
1.5 <i>HTT</i> : structure and function.	p. 21
1.6 HD etiology.	p. 22
1.7 Gain or loss of functions of mHTT.	p. 24
1.8 Mouse models of HD.	p. 25
1.8.1 Transgenic mice expressing N-terminal portion of mHTT.	p. 25
1.8.2 Full-length mHTT transgenic mice.	p. 27
1.8.3 Knock-in transgenic mice.	p. 29
1.8.4 Synaptic alterations in mouse models of HD	p. 31
2. Ionotropic glutamate receptors.	p. 32
2.1 NMDARs.	p. 33
2.1.1 NMDARs subunit basic structure.	p. 33
2.1.2 Classical NMDAR properties and function.	p. 34
2.2 GluN3A-Containing NMDARs.	p. 36
2.2.1 Unique features of GluN3A subunits.	p. 36
2.2.2 Receptor assembly.	p. 39
2.2.3 Biophysical properties.	p. 39
2.2.4 GluN3A-interacting proteins.	p. 41
2.2.5 GluN3A expression in the CNS.	p. 42
2.2.5.1 Developmental time-course.	p. 42
2.2.5.2 GluN3A subcellular localization.	p. 43

2.2.5.3 Areas and cell types with GluN3A expression.	p. 45
2.2.6 GluN3A-NMDARs gate synapse and circuit maturation.	p. 45
2.2.7 GluN3A in diseases.	p. 48
2.2.7.1 GluN3A in HD.	p. 48
3. Gene silencing.	p. 49
3.1 RNA interference (RNAi).	p. 49
3.1.1 Short hairpin RNA (shRNA).	p. 51
3.2 AAVs.	p. 52
3.2.1 Recombinant AAVs (rAAVs).	p. 53
3.3 shRNA-AAVs as a therapeutic tool.	p. 53
<b>HYPOTHESIS AND SPECIFIC AIMS.</b>	p. 57
<b>MATERIAL AND METHODS</b>	p. 61
1. AAV-shGluN3A vector.	p. 61
2. rAAV production.	p. 62
3. Stereotaxic injections.	p. 64
4. Spine measurement by Golgi impregnation.	p. 64
5. Western blot.	p. 65
5.1 Protein sample preparation.	p. 65
5.2 SDS-PAGE electrophoresis.	p. 65
5.3 Protein transfer to PVDF membranes.	p. 66
5.4 Immunodetection.	p. 66
6. <i>In situ</i> hybridization.	p. 67
6.1 <i>Grin3a</i> mRNA cloning	p. 67
6.1.1 Riboprobe design and synthesis.	p. 67
6.1.2 Insert and vector digestion, and ligation.	p. 68
6.1.3 Bacterial transformation.	p. 68
6.1.4 Plasmid amplification.	p. 69
6.2 Riboprobe synthesis.	p. 69



6.3 Colorimetric ISH: Hybridization, immunodetection and amplification	p. 69
6.4 FISH: Hybridization, immunodetection and amplification	p. 71
6.4.1 Double FISH	p. 71
7. RNAscope.	p. 72
8. Immunohistochemistry.	p. 73
8.1 Immunohistochemistry in slices from injected mice.	p. 73
8.2 Immunohistochemistry after FISH.	p. 74
9. Image acquisition and analysis.	p. 74
10. Animals.	p. 75
10.1 Mouse models.	p. 75
10.2 Real-time PCR for HD mouse model genotyping.	p. 76
11. Behavioral tests.	p. 77
12. Statistical analysis.	p. 77
<b>RESULTS.</b>	p. 81
<b>First chapter.</b> “RNAi-Based GluN3A Silencing Prevents and Reverses Disease Phenotypes Induced by Mutant huntingtin”	p. 81
<b>Second chapter.</b> “Temporal Dynamics and Neuronal Specificity of <i>Grin3a</i> Expression in the Mouse Forebrain”	p. 96
<b>DISCUSSION.</b>	p. 117
<b>CONCLUSIONS.</b>	p. 131
<b>APPENDIX.</b>	p. 137
Abbreviations.	p. 137
<b>BIBLIOGRAPHY</b>	p. 151





«Los científicos no persiguen la verdad; es ésta la que los  
persigue a ellos»

- Karl Schlecta -

**FIGURES AND TABLES**



List of figures

**INTRODUCTION**

<b>Figure 1.</b> Variation of the brain anatomy in an HD patient.	p.15
<b>Figure 2.</b> Alterations in morphology of MSNs in HD.	p.17
<b>Figure 3.</b> Basal ganglia circuitry models of HD.	p.20
<b>Figure 4.</b> Onset of HD symptoms depends on the number of CAGs.	p.23
<b>Figure 5.</b> Timeline of behavioral and neuropathological symptoms in the YAC128 HD mouse model.	p.29
<b>Figure 6.</b> Transmembrane topology of GluN3A NMDAR subunit, sites for modulation and protein-protein interactions.	p.38
<b>Figure 7.</b> NMDARs composition alternatives.	p.40
<b>Figure 8.</b> GluN3A protein expression during rodent brain development.	p.42
<b>Figure 9.</b> Location of GluN3A-containing NMDARs at the synapse.	p.44
<b>Figure 10.</b> GluN3A-containing NMDARs in synapse plasticity and maturation.	p.47
<b>Figure 11.</b> GluN3A-containing NMDARs location in HD dendritic spines.	p.49
<b>Figure 12.</b> Genetic deletion of GluN3A in YAC128 prevents dendritic spine density loss and ameliorates motor dysfunction.	p.50

**MATERIAL AND METHODS**

<b>Figure 13.</b> ShGluN3A characterization.	p.61
<b>Figure 14.</b> Schematic drawing of the generated rAAV plasmid carrying shGluN3A.	p.62
<b>Figure 15.</b> Schematic showing transfection of HEK293T cells with the 3 necessary plasmids to generate encapsidated rAAV.	p.62
<b>Figure 16.</b> Schematic of mice placed into a stereotaxic frame with the skull surface exposed and two burr holes in the bone.	p.64
<b>Figure 17.</b> <i>Grin3a</i> riboprobe characterization.	p.68

## RESULTS.

### First chapter.

- Figure 1.** Silencing GluN3A in MSNs by intrastriatal injection of rAAV9-driven shRNAs p.82
- Figure 2.** *In vivo* transduction efficiency in immunohistochemically identified cell-types. p.83
- Figure 3.** GluN3A silencing prevents and reverses spine loss. p.84
- Figure 4.** rAAV9-shGluN3A improves motor coordination in YAC128 mice. p.85
- Figure 5.** Rescue of balance deficits by rAAV9-shGluN3A in YAC128 mice. p.86
- Supplementary Figure 1.** Comparison of transduced striatal area between rAAV serotypes upon a single injection into the striatum. p.90
- Supplementary Figure 2.** Long-lasting transduction of striatal neurons by rAAV9-shGluN3A. p.91
- Supplementary Figure 3.** Body weight and muscular strength are not affected by rAAV9-shGluN3A intrastriatal injection. p.92

### Second chapter.

- Figure 1.** *Grin3a* expression is down-regulated into adulthood. p.98
- Figure 2.** Regional distribution of *Grin3a* expression in early postnatal development. p.99
- Figure 3.** Embryonic *Grin3a* expression. p.100
- Figure 4.** Emergence and down-regulation of *Grin3a* expression throughout postnatal developmental stages. p.101
- Figure 5.** Dynamic temporal patterns of *Grin3a* expression across cortical layers and sensory modalities. p.102
- Figure 6.** *Grin3a* expression in excitatory and inhibitory neurons. p.103
- Figure 7.** *Grin3a* expression in molecularly defined interneuron populations. p.104

**Supplementary Figure 1.** Adult *Grin3a* expression in the thalamus and cortical amygdala. p.109

**Supplementary Figure 2.** Dorso-ventral gradient of *Grin3a* expression in adult CA1 hippocampus. p.110

**Supplementary Figure 3.** High *Grin3a* mRNA expression in a subpopulation of GABAergic neurons. p.111

## DISCUSSION

**Figure 18.** Correlation between T1w:T2w ratios and *Grin3a* relative expression p.122

**Figure 19.** High *Grin3a* mRNA levels in Sst interneurons. p.126

## List of tables

### INTRODUCTION.

**Table 1.** Commonly used transgenic mice models of HD. p.30

### MATERIAL AND METHODS.

**Table 2.** rAAV constructs used for cell infection. p.63

**Table 3.** Primary antibodies used for immunodetection in WB. p.67

**Table 4.** List of antibodies used for ISH. p.72

**Table 5.** Primary antibodies used for immunostaining. p.73

**Table 6.** Secondary antibodies used for immunostaining. p.74

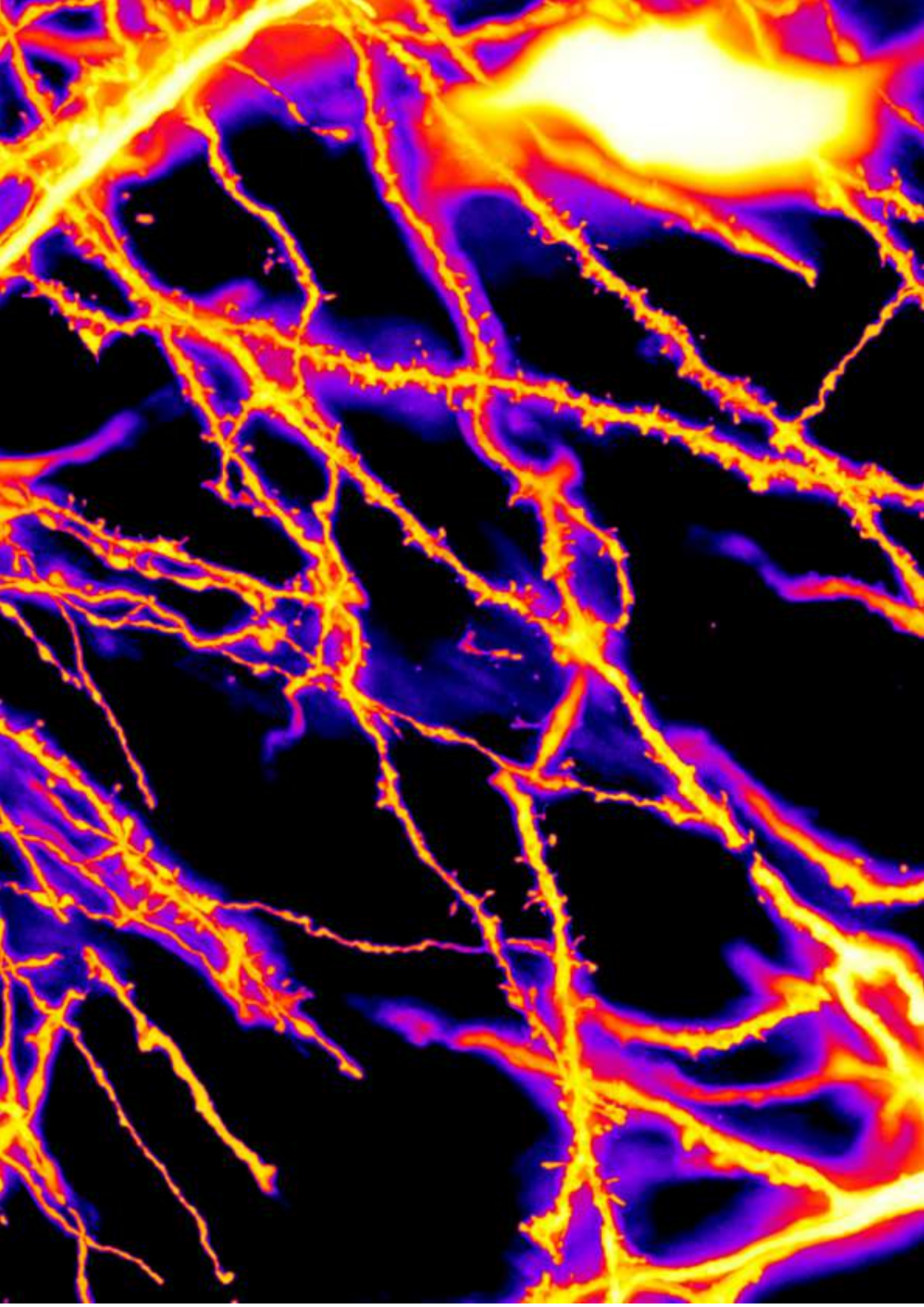
**Table 7.** Nucleotide sequence of the different primers used for qPCR genotyping. p.76

### RESULTS.


#### Second chapter.

**Supplementary Table 1.** Semi-quantitative analysis of *Grin3a* mRNA levels at postnatal times of maximal expression (P6-P9). p.112

**Supplementary Table 2.** Statistical analyses of the time-courses of *Grin3a* emergence and down-regulation in primary somatosensory (SS1) and visual cortex (V1). p.114







«El aspecto más triste de la vida es que la ciencia reúne el conocimiento más rápidamente que la sociedad la sabiduría»

- Isaac Asimov -

**ABSTRACT**





Developing new therapeutic strategies to treat neurodegenerative diseases is a public health priority due to the current lack of therapies and enormous cost of medical care, the increase in cases with population aging, and the human suffering for patients and their families. A pre-eminent example is Huntington disease (HD), a progressive, rare and inherited neurological disease that usually manifests in adulthood and is characterized by a triad of symptoms: involuntary movements known as chorea which result from dysfunction and later degeneration of medium-sized spiny neurons (MSNs) in the striatum; cognitive impairment; and psychiatric disturbances. While the disease-causing mutation, an abnormal expansion of a polyglutamine stretch in the N-terminal region of a protein called huntingtin (HTT), has been known for almost 3 decades, to date there is no cure and symptomatic treatments offer only minor palliative effects. Our group recently discovered a key early HD pathogenic mechanism: dysregulated synaptic expression of juvenile NMDA-type glutamate receptors containing GluN3A subunits (GluN3A-NMDARs), which drives the aberrant pruning of synapses formed by cortical afferents onto MSNs.

In this Thesis, we set out to design and evaluate a new gene therapy approach to correct the aberrant GluN3A expression. We began by testing the ability of recombinant adeno-associated vectors (rAAVs) encoding RNAi triggers to drive sustained GluN3A silencing in MSNs, the vulnerable population. Upon a single stereotaxic injection into the mouse striatum, rAAV9-shGluN3A reduced GluN3A expression with high efficiency (>85% silencing), and selectivity. Silencing was maintained over long periods of time, up to 11 months after a single administration, and ameliorated synaptic and motor deficits in YAC128 mice, a well-established HD model. Notably, rAAV9-shGluN3A injections were effective when timed with disease initiation, but also when delivered at later disease stages. Our findings provide proof-of-principle validation of the effectiveness of GluN3A-directed gene therapies in HD mouse models, a necessary step for advancing into clinically relevant settings.

Targeting GluN3A subunits would be predicted to have minimal side-effects due to their low expression in adult brain in non-pathological settings,

which appears as a significant advantage compared to other NMDAR-based strategies. Yet the information currently available is sparse and recent work suggests that GluN3A also operates in adult brains to control a variety of behaviors. Thus for the second part of my Thesis, I conducted a systematic analysis of *Grin3a* expression in the mouse brain that combined high-sensitivity colorimetric and fluorescence *in situ* hybridization (FISH) with labeling for specific neuronal subtypes. We found that, while GluN3A expression peaks postnatally, significant levels remain into adulthood in specific brain regions including the amygdala, medial habenula, association cortices and high-order thalamic nuclei. The time-course of emergence and down-regulation of *Grin3a* expression varies across brain region, cortical layer of residence and sensory modality, in a pattern that correlates with previously reported hierarchical gradients of brain maturation and functional specialization. *Grin3a* is expressed in both excitatory and inhibitory neurons, with strong mRNA levels being a distinguishing feature of somatostatin interneurons. Our study provides a comprehensive map of *Grin3a* distribution across the murine lifespan and paves the way for dissecting the diverse functions of GluN3A in health and disease.

## RESUMEN

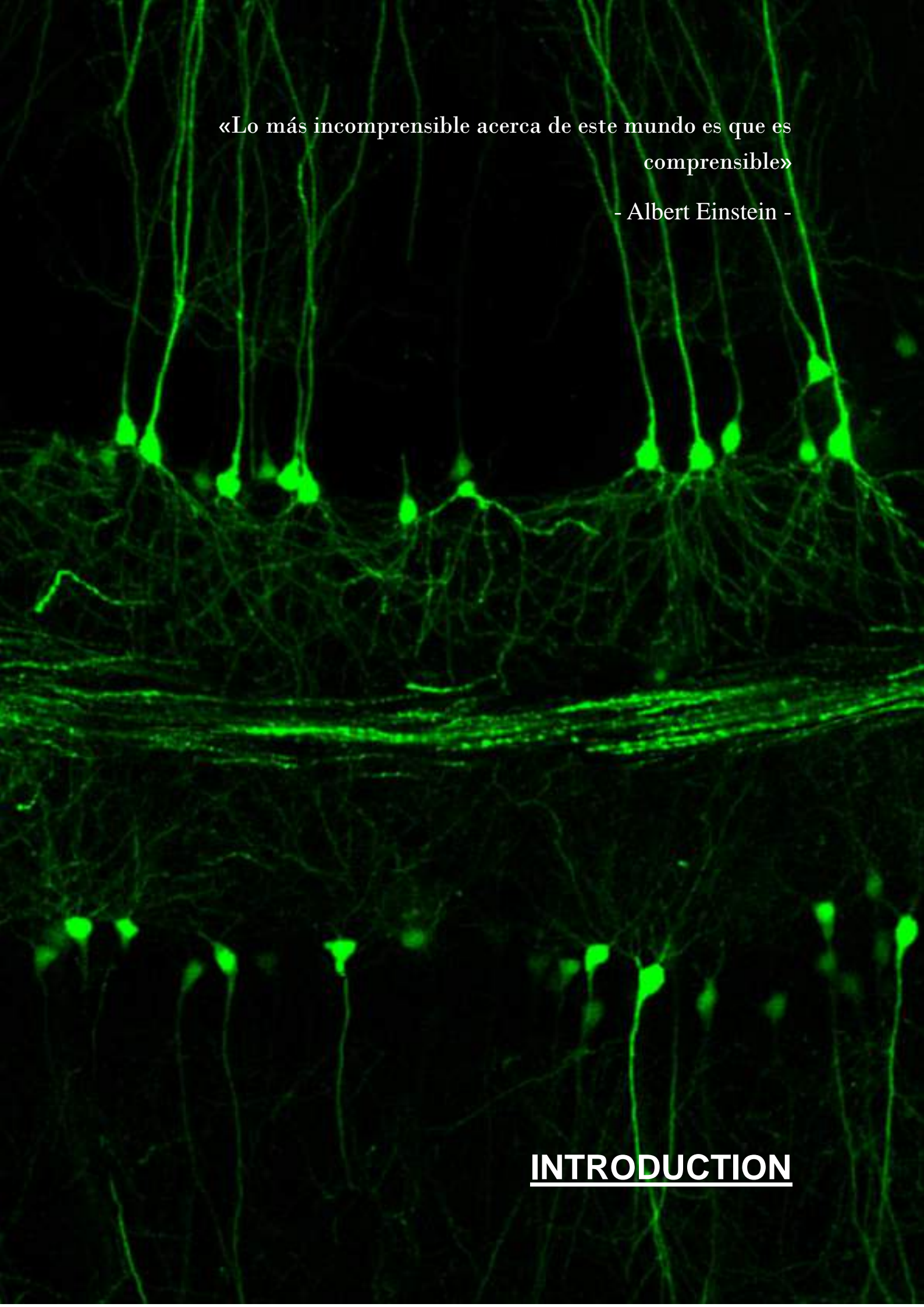
El desarrollo de nuevas estrategias terapéuticas para tratar enfermedades neurodegenerativas es una prioridad debido a la falta actual de terapias y al enorme coste de la atención médica, el incremento de casos con el envejecimiento de la población y el sufrimiento de los pacientes y sus familiares. Un ejemplo preeminente es la enfermedad de Huntington (EH), una enfermedad neurológica progresiva, rara y hereditaria que normalmente se manifiesta en la edad adulta y se caracteriza por una tríada de síntomas: movimientos involuntarios conocidos como corea causados por la disfunción y posterior degeneración de las neuronas espinosas de tamaño medio (MSNs) del cuerpo estriado, deterioro cognitivo y alteraciones psiquiátricas. Si bien la mutación causante de la enfermedad, una expansión anormal de una región poliglutaminica en la porción N-terminal de una proteína llamada huntingtina (HTT), se conoce desde hace casi 3 décadas, hasta la fecha no existe cura y los tratamientos sintomáticos ofrecen solo efectos paliativos menores. Nuestro grupo descubrió recientemente un mecanismo patogénico temprano clave en la EH: la expresión sináptica desregulada de los receptores de glutamato de tipo NMDA juveniles que contienen subunidades GluN3A (GluN3A-NMDAR), que produce la poda/eliminación aberrante de las sinapsis formadas las aferencias corticales en las MSNs.

En esta tesis, nos propusimos evaluar un nuevo enfoque de terapia génica para corregir la expresión aberrante de GluN3A. Comenzamos probando la capacidad de los vectores adenoasociados recombinantes (rAAV) que codifican los ARN de interferencia para desencadenar el silenciamiento sostenido de GluN3A en las MSNs, la población vulnerable. Tras una única inyección estereotáxica en el cuerpo estriado del ratón, rAAV9-shGluN3A redujo la expresión de GluN3A con alta eficiencia (silenciamiento > 85%) y selectividad. El silenciamiento se mantuvo durante largos períodos de tiempo, hasta 11 meses después de una sola administración, y mejoró los déficits sinápticos y motores en ratones YAC128, un modelo de EH bien establecido. Es destacable que las inyecciones de rAAV9-shGluN3A fueron efectivas

cuando se sincronizaron con el inicio de la enfermedad, pero también cuando se administraron en etapas posteriores de la enfermedad. Nuestros hallazgos proporcionan una validación de prueba de concepto de la efectividad de las terapias génicas dirigidas hacia GluN3A en modelos murinos de EH, un paso necesario para avanzar hacia ámbitos clínicamente relevantes.

Cabe esperar que la utilización de subunidades de GluN3A como diana provoque efectos secundarios mínimos debido a su baja expresión en el cerebro adulto en entornos no patológicos, lo cual supondría una clara ventaja frente a otras estrategias dirigidas a otros NMDARs. Sin embargo, la información actualmente disponible es escasa y un trabajo reciente sugiere que GluN3A también opera en cerebros adultos para controlar una variedad de comportamientos. Por lo tanto, para la segunda parte de mi tesis, realicé un análisis sistemático de la expresión de *Grin3a* en el cerebro de ratón que combina hibridación *in situ* colorimétrica de alta sensibilidad y fluorescencia con marcaje para subtipos neuronales específicos. Descubrimos que, aunque la expresión de GluN3A alcanza su punto máximo en edades postnatales, niveles significativos permanecen hasta la edad adulta en regiones cerebrales específicas, como la amígdala, la habénula medial, las cortezas asociativas y los núcleos talámicos de alto orden.

La aparición y regulación negativa temporal de la expresión de *Grin3a* varía a lo largo de las regiones del cerebro, la capa cortical de residencia y la modalidad sensorial, en un patrón que correlaciona con gradientes jerárquicos de maduración cerebral y especialización funcional reportados anteriormente. *Grin3a* se expresa tanto en neuronas excitadoras como inhibitoras, siendo los altos niveles de ARN mensajero un rasgo distintivo de interneuronas de somatostatina. Nuestro estudio proporciona un mapa completo de la distribución de *Grin3a* murino a lo largo de la vida y allana el camino para analizar las diversas funciones de GluN3A en condiciones fisiológicas y patológicas.



«Lo más incomprensible acerca de este mundo es que es comprensible»

- Albert Einstein -

**INTRODUCTION**







## 1. Huntington's disease (HD)

HD is a dominantly inherited neurodegenerative disorder caused by the presence of an abnormally long polyglutamine stretch in the HTT protein (Wexler *et al.*, 1991). Although a pre-symptomatic diagnostic (even prenatally or at a pre-implantation stage) is possible, no specific treatment is available, with only palliative drugs that offer very partial relief. The incidence of HD in white people is about 5-7 affected individuals per 100,000 (Walker, 2007). In African (Harry *et al.*, 1981; Joubert *et al.*, 1987) and Asian populations the rate is lower, in the latter only 0.5 per 100,000 individuals (Takano *et al.*, 1998). Otherwise, areas colonized by a few founders, such as the region around Lake Maracaibo (Young *et al.*, 1986) and Tasmania (Pridmore, 1990), present epidemic rates (1625-3530 affected persons per 100,000 individuals). The certainty in mutant HTT (mHTT) carriers that the disease will manifest or the onset of symptoms make the incidence of suicide in people with HD 5-11 times higher than the average in other populations, being suicide the cause of death in 5.7% of HD patients (Reed *et al.*, 1958; Kessler *et al.*, 1989).

### 1.1 HD symptoms

Diagnosis takes place typically around 35-40 years of age (Paulsen *et al.*, 2005) when the initial motor symptoms, consisting on abrupt involuntary movements (chorea) that interfere with voluntary movement, emerge. They affect legs and arms, but also the body trunk and ocular muscles (Van Vugt *et al.*, 2001). This initial period is known as the hyperkinetic stage and is followed by a hypokinetic phase where dystonia and rigidity affect the muscles (Mahant *et al.*, 2003). Motor symptoms are the most striking, but 79% of HD patients show also cognitive decline, attention deficits, and difficulty in acquiring new knowledge (Naarding *et al.*, 2001). In fact, cognitive impairment is estimated to emerge 10 years prior to motor dysfunction onset (Duff *et al.*, 2010; Tabrizi *et al.*, 2013). Furthermore, 33% of the patients show prominent psychiatric disturbances before the onset of motor alterations, that manifest as mood and personality disorders in HD

(Maio *et al.*, 1993; Shiwach, 1994). In addition, 40% of patients suffer from depression due to the changes in their lives and the burden on people around them (Folstein *et al.*, 1983). Loss of weight occurs as a consequence of some HD symptoms, such as depression, increased motor activity during the first stages or deglutition difficulty (called dysphagia) in the hypokinetic phase (Kagel *et al.*, 1992; Djoussé *et al.*, 2002). HD patients could suffer epileptic attacks (Srivastava *et al.*, 1999) and hallucinations (Rosenblatt *et al.*, 2000). HD patients die commonly by respiratory disease (44.2% of the cases), cardiovascular problems (Solberg *et al.*, 2018) or due to infection of ulcers derived from immobility (Dubinsky, 2005), typically 20 years after being diagnosed (Folstein *et al.*, 1983).

## 1.2 Neuropathology of HD

The neuropathological changes observed in HD brains target predominantly the caudate and putamen, with atrophy of these regions and expansion of the ventricles (Vonsattel *et al.*, 1985). Both nuclei (called striatum in rodents) conform the largest subcortical structure in the mammalian brain with an estimated volume of 10 cm<sup>3</sup> in humans (Schröder *et al.*, 1975), and are involved in the processing of motor information arriving from the cortex. Possibly secondary to anatomical atrophy of the caudate and putamen and degeneration of the corticostriatal pathway, the number of pyramidal neurons in the cortex is reduced and cortical atrophy is observed at later stages of the disease (Figure 1) (Macdonald *et al.*, 2002). Over time, significant loss of pyramidal neurons in other regions such as the hippocampus CA1 and angular gyrus is also noticeable (Spargo *et al.*, 1993; Macdonald *et al.*, 1997).

The atrophy of the caudate and putamen is due to degeneration and death of MSNs, that are the most vulnerable cell population in HD (Reiner *et al.*, 1988). Other striatal populations involved in regulating motor function include cholinergic interneurons (Bolam *et al.*, 1984), GABAergic neurons that express parvalbumin protein (Gerfen *et al.*, 1985) and somatostatin (Sst) neurons (Vincent *et al.*, 1983) and are relatively spared.

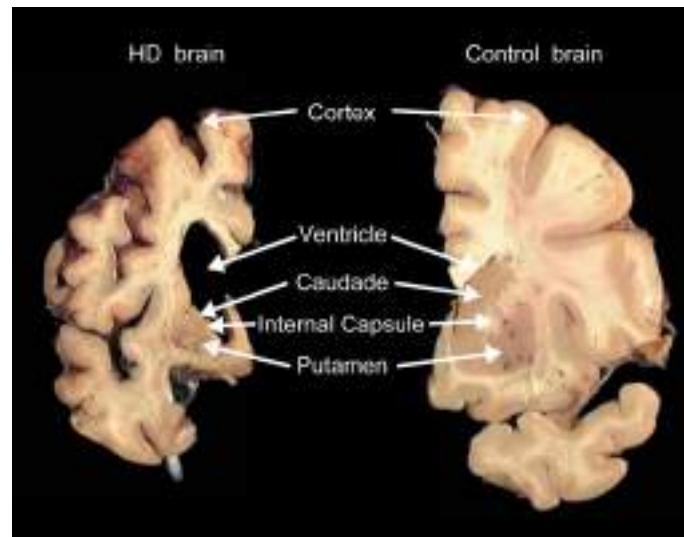


Figure 1. Variation of the brain anatomy in an HD patient. Macroanatomical changes in ventricles, cortices and caudate/putamen are seen in HD brain (left) compared with a control brain (right). Modified from Reiner *et al.*, 2011.

MSNs are GABAergic projection neurons and constitute 90-95% of all neurons of the striatum. They can be identified by the expression of Glutamic Acid Decarboxylase (GAD) (Gerfen, 1988), Calbindin-D<sub>28k</sub> and DARPP-32 (dopamine and cAMP regulated phosphoprotein of 32 KD) (Pickel and Heras, 1996, Ouimet *et al.*, 1998; Fienberg *et al.*, 2000). MSNs are characterized by a medium-sized soma (10-20  $\mu\text{m}$  in diameter) from which several dendrites radiate (3 to 7), covering an area of 0,2-0,28  $\text{mm}^2$  (Ferrante *et al.*, 1991; Wilson *et al.*, 2004). The dendrites are mostly smooth for the first 30  $\mu\text{m}$ , which generally corresponds to primary dendrites. From there, they branch repeatedly and show very high spine densities, hence their name, in secondary and subsequent dendrites (Gerfen *et al.*, 1988). Two different subpopulations of MSNs can be identified based on the expression of dopamine receptor 1 or 2 (D1 or D2 receptors respectively). Both D1- and D2-expressing MSNs display similarly high spine densities and are intermixed with each other within the striatum (Gagnon *et al.*, 2017). Although the proportion of D1/D2-MSNs is maintained throughout most of the striatum, intermediate ventromedial caudate-putamen, a small portion of the whole striatum, show more D1-MSNs (Ren *et al.*, 2017). Dendritic spines are small membrane protrusions of neuronal dendrites with different sizes (from 0.01  $\mu\text{m}^3$  to 0.8  $\mu\text{m}^3$ ) and shapes

(mushroom, thin, stubby and cupshaped) (Hering 2001) and are the site where most excitatory synapses form. Dendritic spines of MSNs receive glutamatergic synaptic inputs from the cortex (Gerfen, 1984; Selemon *et al.*, 1985; Donoghue *et al.*, 1986) and thalamus (Vogt *et al.*, 1941; Powell *et al.*, 1956), as well as modulatory dopaminergic afferents from SNr (Lynd-Balta *et al.*, 1994; Haber *et al.*, 2000) and SNc (Gerfen *et al.*, 1984), and GABAergic terminals from striatal interneurons and axonal collaterals from other MSNs (Gerfen, 1988), making up to 10,000 synapses onto a single MSN.

Gross anatomical atrophy only becomes evident when the disease has progressed inexorably. However, longitudinal imaging studies in humans have shown functional and microstructural morphological alterations in MSNs at much earlier pre-manifest and presymptomatic stages (Tabrizi *et al.*, 2011; Tabrizi *et al.*, 2013; Ross *et al.*, 2014). For instance, reductions in caudate-putamen volumes measured by magnetic resonance are observed before manifest motor symptoms and also a decrease in grey- and white-matter volumes (Tabrizi *et al.*, 2011; Tabrizi *et al.*, 2013), that affect the corpus callosum (Rosas *et al.*, 2010). Some of these alterations have been related to a decrease in cognitive abilities in HD patients who have not yet developed overt motor symptoms (Tabrizi *et al.*, 2011; Tabrizi *et al.*, 2013).

Work in humans and mice has placed synaptic alterations at the center-stage of the neurodegeneration process, with changes in the number and morphology of dendritic arbors and spines. Several post-mortem studies examined the morphology of MSNs of HD patients at different stages of the disease using the classical Golgi impregnation. A remarkable decrease in spine density accompanied with abnormalities in the size and shape of spines, and altered appearance of dendritic endings were observed (Figure 2) (Graveland *et al.*, 1985b; Ferrante *et al.*, 1991).

In MSNs of HD mice models, the synaptic properties are altered prior to the onset of behavioral symptoms, such as the increase of spontaneous excitatory postsynaptic currents (Raymond *et al.*, 2011). Furthermore, reduction in the density of dendritic spines has been observed in presymptomatic stages in several mouse models (Richards *et al.*, 2011; Marco *et al.*, 2013; Simmons *et*

*al.*, 2013; Wu *et al.*, 2016), which has been directly related to the aberrant expression of GluN3A (Marco *et al.*, 2013). Alterations in dendritic spine density in HD mouse models are not due to a decrease in the number of new spines but to instability during spine maturation (Murmu *et al.*, 2013).

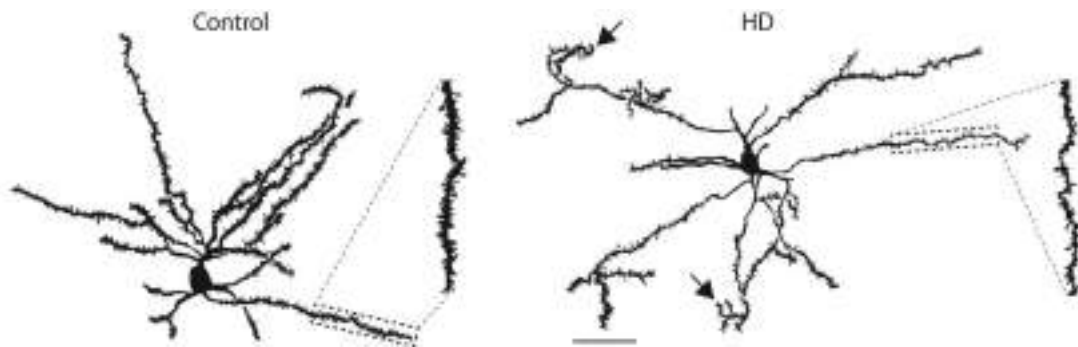


Figure 2. Alterations in morphology of MSNs in HD. Drawings of MSNs from a HD patient (right) showing recurving distal dendritic segments (arrows), abnormal dendritic growth and decrease in spine density (high magnification) in comparison with MSNs from a control individual (left). Scale bar: 50  $\mu\text{m}$ . Modified from Ferrante *et al.*, 1991.

### 1.3 Basal ganglia

The basal ganglia consist of several subcortical nuclei involved mainly in motor control, but also in motor learning, executive functions and emotions. Strictly, the basal ganglia include two nuclei that are deeply embedded in brain hemispheres: striatum and globus pallidus (formed by external and internal segment, divided by myelinated fibres known as the medial medullary lamina). Other areas involved in those processes are the subthalamic nucleus (STN; located in the diencephalon) and substantia nigra (SN; in mesencephalon).

Basal ganglia nuclei can be categorized based on afferent or efferent projection axons (Lanciego *et al.*, 2012):

1) Input nuclei: caudate and putamen that receive incoming information from cortex and thalamus.

2) Intrinsic nuclei: STN, substantia nigra *pars compacta* (SNc) and external segment of the globus pallidus (GPe). All receive and send information to other basal ganglia nuclei.

3) Output nuclei send the information to the thalamus and are the substantia nigra *pars reticulata* (SNr) and the internal segment of the globus pallidus (GPi).

All these nuclei are part of a motor refinement circuit. The caudate and putamen receive information from the cortex (Gerfen, 1984; Selemon *et al.*, 1985; Donoghue *et al.*, 1986), thalamus (Vogt *et al.*, 1941; Powell *et al.*, 1956), SNc (Gerfen *et al.*, 1985) and SNr (Lynd-Balta *et al.*, 1994; Haber *et al.*, 2000), and drift information through two routes, called the direct and the indirect pathway. Each of these routes is defined by the MSNs that send the projections and the nuclei innervated by these projections (Albin *et al.*, 1989; DeLong, 1990; Kawaguchi *et al.*, 1990; Parent *et al.*, 2000; Wu *et al.*, 2000):

1. Direct pathway: MSNs in this route predominantly express the D1 receptor (Beckstead *et al.*, 1988; Gerfen *et al.*, 1990). Their striatofugal inhibitory projections innervate the SNr and GPi (Beckstead *et al.*, 1986).
2. Indirect pathway: MSNs in this route express D2 receptors and their axons innervate the GPe (Beckstead *et al.*, 1988; Gerfen *et al.*, 1990). GABAergic neurons from GPe innervate the STN (Shink *et al.*, 1996) which in turn sends projections to the SNr and GPi (Ilinsky *et al.*, 1987; Percheron *et al.*, 1996).

Thus, both direct and indirect pathways innervate SNr and GPi. Although both inhibitory efferent nuclei innervate the thalamus, significant differences can be observed. While pallido-thalamic projections innervate the densicellular and parvicellular territories of the ventral-anterior thalamic nucleus (VA), nigro-thalamic projections target the magnocellular division (ventro-medial and ventro-lateral thalamic nucleus, VM and VL respectively) (Ilinsky *et al.*, 1987; Percheron *et al.*, 1996) (Figure 3, left panel). The circuit is completed with thalamo-striatal and thalamo-cortical efferents. Thalamic axon terminals target projection neurons (MSNs) and interneurons of the striatum (Vogt *et al.*, 1941; Meredith *et al.*, 1990; Lapper *et al.*, 1992; Dubé *et al.*, 1998). The thalamus also

innervates layer IV of neocortex, several layers of motor and prefrontal cortices (Caviness *et al.*, 1980).

### 1.3.1 Alteration of basal ganglia pathways in HD.

The motor regulatory pathways described above are affected in HD due to cell loss in the striatum. D2-expressing MSNs are lost first followed by death of D1-MSNs, which modifies the flow of motor information between basal ganglia nuclei (Reiner *et al.*, 1988; Gerfen *et al.*, 1990; Glass *et al.*, 2000; Deng *et al.*, 2004). The reduction in the number of D2-MSNs produces a decrease of the STN activity due to the incapacity of striatum to inhibit GPe. At the same time, the imbalance between D1- and D2- MSNs increases SNc activity and produces an hyperactivation of the direct pathway (Jahanshahi *et al.*, 2010). This leads to the inability of this circuit to inhibit thalamic nuclei, which results in a hyperactivation of the cortex causing hyperkinesia (Figure 3, middle panel) (Albin *et al.*, 1989) which is one of the hallmarks of the disease.

Other HD characteristic symptoms are hypokinesia/bradykinesia, which occur later in disease progression as a result of loss of D1-MSNs. Reduced inhibition of the GPi and SNr produces hyperinhibition of thalamus which stops activating the neocortex (Figure 3, right panel) (Albin *et al.*, 1990).

## 1.4 *HTT* expression

HD is caused by an expansion of the trinucleotides CAG in the human huntingtin gene (*HTT*), located in the short arm of the chromosome 4 at position 16.3 (4p16.3) (HDCRG, 1993). The *HTT* gene is large, with 67 exons spanning 180 kb, and encodes two transcripts. In adult and fetal brain, the larger transcript (13.7 kb) is predominantly expressed in the central nervous system (CNS) whereas the smaller transcript (10.3 kb) is more widely expressed in peripheral tissues (Li *et al.*, 1993; Hughes *et al.*, 2014; Ruzo *et al.*, 2015). Northern blot and *in situ* hybridization analysis demonstrate that: 1) *HTT* is expressed ubiquitously since early development and persists into adulthood,

showing higher levels in brain and testes (Li *et al.*, 1993; Strong *et al.*, 1993) and: 2) levels are not altered in the basal ganglia of HD patients (Landwehrmeyer *et al.*, 1995).

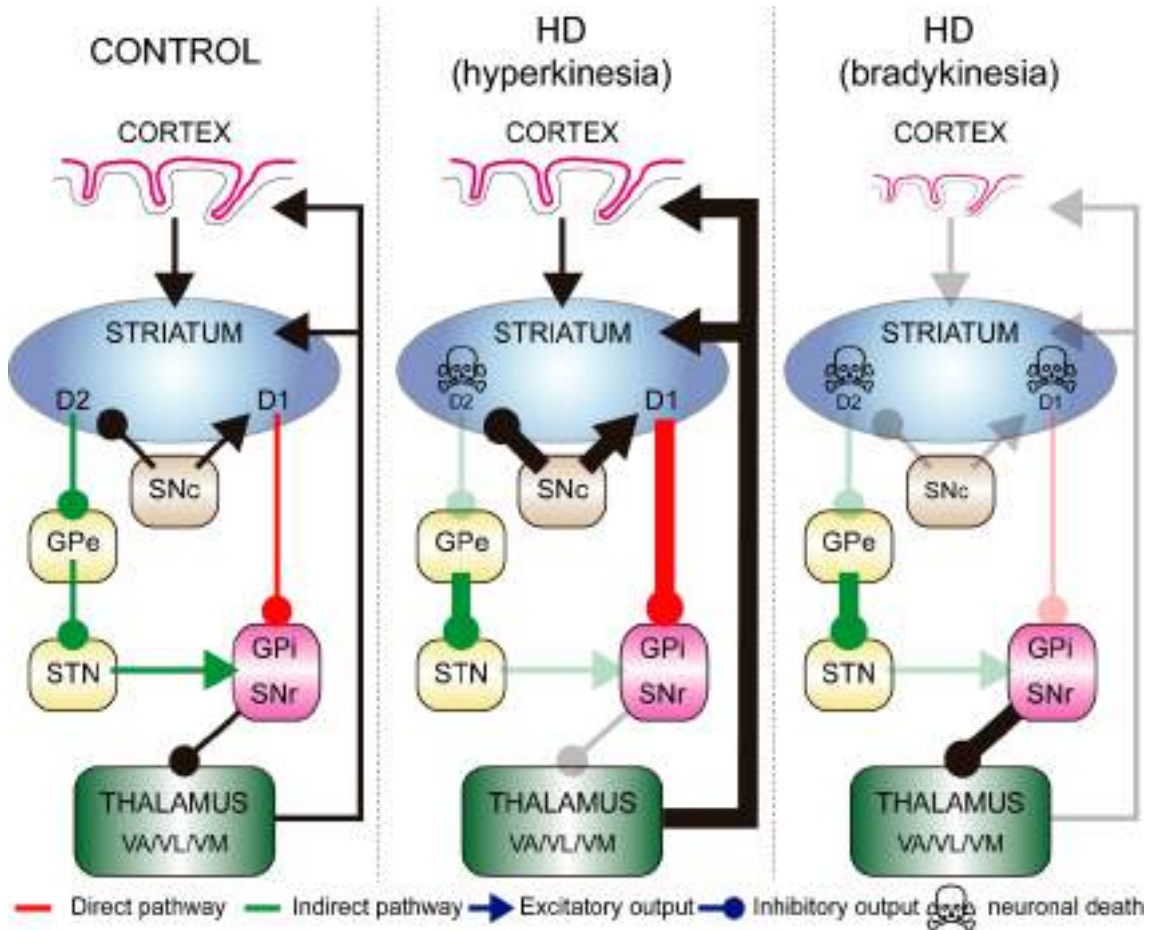


Figure 3. Basal ganglia circuitry models of HD. Left panel: schematic drawing of the direct and indirect pathways in non-pathological conditions. Cortical and thalamic afferents target the striatum, exciting both D1 and D2 MSNs. SNc activate D1 cells and inhibit D2 neurons. D2 cells inhibit GPe in the indirect pathway (in green) which in turn inhibit STN reducing the activation of GPi and SNr. D1 neurons inhibit in the direct pathway (in red) regions GPi and SNr. Both inhibit thalamic nuclei, which activate striatum and neocortex through glutamatergic axons. Middle panel: early symptomatic stages of HD are caused by an alteration in the basal ganglia circuitry due to the death of D2-positive neurons and activation of SNc. This produces a decrease of the activity of the indirect pathway and increase of direct pathway activity. All this culminates in hyperactivation of thalamic-striatal and thalamic-cortical axons. Right panel: late HD is characterised by D1 cell death and SNc activity loss. Direct and indirect pathways are deregulated producing hyperinhibition of thalamic nuclei that together with neocortex dystrophy prevent striatal activation. Transparent arrows: loss of function; Wider arrows: gain of function. Abbreviations: D1,



dopamine receptor 1 positive neurons; D2, dopamine receptor 2 positive neurons; GPe, external segment of the globus pallidus; GPi, internal segment of the globus pallidus; SNc, substantia nigra *pars compacta*; SNr, substantia nigra *pars reticulata*; STN, subthalamic nucleus; VA, ventral-anterior thalamic nucleus; VL, ventral-lateral thalamic nucleus; VM, ventral-medial thalamic nucleus.

### 1.5 HTT: structure and function

HTT is a well-conserved 348-kDa protein of 3.144 amino acids; in fact, it shows one of the highest protein homologies among mammalian species (Tartari *et al.*, 2008). The N-terminal HTT domain, encoded by exon 1, contains an alpha-helix (Atwal *et al.*, 2007) followed by a polymorphic polyglutamine (polyQ) stretch. An increase in the number of glutamine residues has been observed throughout evolution (Tartari *et al.*, 2008). In humans not affected by HD, the polyQ tract contains 9 to 35 consecutive glutamine amino acids, with an average between 17 and 20 repeats (Kremer *et al.*, 1994). The polyQ stretch is followed by a proline-rich domain (PRD) which is polymorphic in the human population (Tartari *et al.*, 2008).

The rest of the protein (99.8%) is not well characterised as research has mainly focused on the exon 1, where HD mutations are found. The region encoded by exons 2-67 contains several HEAT (Huntingtin, Elongator factor3, PR65/A regulatory subunit of PP2A, and Tor1) repeats that mediate intra- and interprotein interactions (Palidwor *et al.*, 2009). HTT undergoes post-translational modifications such as phosphorylation, ubiquitination, sumoylation, acetylation and palmitoylation (Saudou *et al.*, 2016). Polymorphic domains and post-translational modifications allow HTT to adopt up to a hundred structurally distinguishable conformations (Seong *et al.*, 2010). The subcellular location of HTT is mostly cytoplasmic although it can be found in the nucleus (Hoogeveen *et al.*, 1993).

The function of HTT is not clearly known. HTT interacts with more than 200 proteins, although this analysis was made in affinity-purified complexes and should be validated by co-localization and functional experiments (Ratovitski *et al.*, 2012; Schaefer *et al.*, 2012). The number of glutamines in the polyQ stretch

changes the pattern of HTT protein interactions, yielding interactions with proteins that normally do not interact with HTT, or altering the affinity of HTT for its normal partners (Goehler *et al.*, 2004; Culver *et al.*, 2012; Ratovitski *et al.*, 2012; Shirasaki *et al.*, 2012). HTT interacts with proteins involved in a wide range of cellular processes (Harjes *et al.*, 2003) such as endocytosis, vesicle trafficking and recycling, cell division coordination, cell cycle regulation, autophagy and transcription among others (Gutekunst *et al.*, 1995; Engelender *et al.*, 1997; Li *et al.*, 1998; Steffan *et al.*, 2000; Engqvist-Goldstein *et al.*, 2001; Pal *et al.*, 2006; Kaltenbach *et al.*, 2007; Colin *et al.*, 2008; del Toro *et al.*, 2009; Keryer *et al.*, 2011; Elias *et al.*, 2014).

## 1.6 HD etiology

Increased number of glutamines in the polyQ domain beyond a threshold alters protein-protein interactions and leads to aggregation of HTT. Up to 35 consecutive glutamines are considered normal, but above 27 poses a risk for the next generation. Thirty-six to 40 CAG repeats in *HTT* may cause HD. Above 40 glutamines, all individuals develop HD and there is an inverse correlation between number of glutamine repeats and age of onset (Figure 4) (Squitieri *et al.*, 2002). Although that is a general rule to categorize possible HD patients, cases with only 34 CAG repeats and even with just 29 have been reported (Kenney *et al.*, 2007; Andrich *et al.*, 2008). Juvenile onset cases occur in patients with more than 100 CAG repeats, with symptoms beginning under 20 years of age (Cannella *et al.*, 2004).

A characteristic of HD is the presence of aggregates containing mHTT and some of its interacting partners. Sequestration of key intracellular proteins into aggregates is thought to interfere with their function and lead to cell dysfunction and eventually death (Davies *et al.*, 1997). Yet in HD brains, aggregates have been found to be more frequent in cortex than in striatum, which is puzzling, given that the striatum is the vulnerable region (Gutekunst *et al.*, 1999). This led to propose that aggregates might have a protective function. For instance, increased proteolysis in HD promotes the accumulation of small

N-terminal mHTT segments that contain long polyQ stretches and generate cytotoxicity.

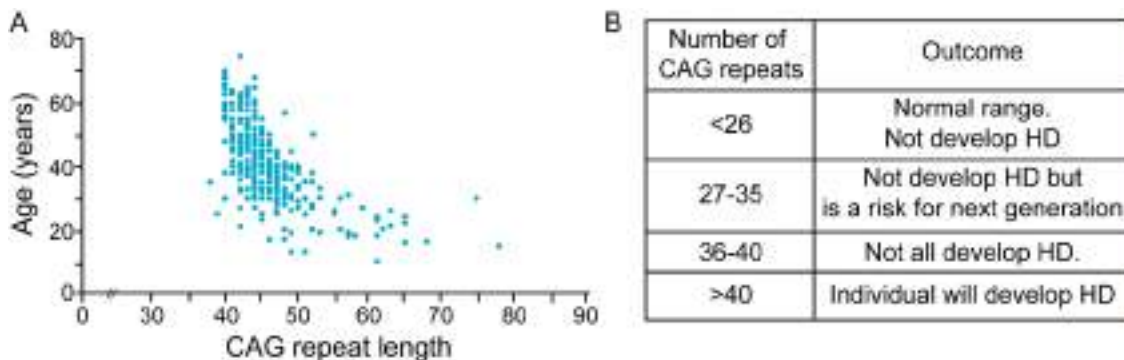


Figure 4. Onset of HD symptoms depends on the number of CAGs. (A) Composite graph plotting number of CAG repeats versus age (in years) of HD symptoms onset. The graph shows an inverse correlation between both axes. Modified from Walker, 2007. (B) Table of CAG repeat ranges for HD onset. Less than 35 CAG repeats do not lead to the disease. However, the descendants of carriers of 27 to 35 repeats are at a risk of developing HD. From 36 to 40 CAG repeats, not all individuals will suffer from the disease, but over 40 they will.

Aggregates could then prevent cell damage by limiting the action of proteases on mHTT (Saudou *et al.*, 1998; Benn *et al.*, 2005; Graham *et al.*, 2006). Also, mHTT aggregate formation reduces levels of oligomeric mHTT decreasing the risk of neuronal death (Arrasate *et al.*, 2004). No consensus has been reached on the toxicity or protective function of these aggregates (Arrasate and Finkbeiner 2012).

A prominent example of protein interactions affected by the polyQ length is the protein kinase C and casein kinase substrate in neurons 1 (PACSIN1). Increases in the number of glutamines in the polyQ stretch enhances the affinity of PACSIN1 for mHTT and drives the sequestration of PACSIN1 into somatic and neuropil mHTT aggregates (Modregger *et al.*, 2002; Marco *et al.*, 2013). In line with this, a dramatic loss of PACSIN1 immunoreactivity was observed in processes of cortical neurons of presymptomatic patients (Diprospero *et al.*, 2004). Moreover, biochemical analysis showed that in HD brains PACSIN1 appears more concentrated in microsomal than synaptosomal fractions, indicating that the subcellular location of this protein is altered (Modregger *et al.*, 2002; Diprospero *et al.*, 2004).

## 1.7 Gain or loss of functions of mHTT

Mutant proteins could cause disease via loss or gain of function. There are reports supporting either notion. For example, conditional *HTT* knockout in adult mice results in progressive neurodegeneration, particularly in the striatum, with HD symptoms (Dragatsis *et al.*, 2000), suggesting that loss of HTT function originate HD. Moreover, overexpression of WT HTT in YAC128 mice protects from MSN death (Leavitt *et al.*, 2006). Negative dominance is another type of loss of function where the mutant protein interferes with WT conformation and activity. For instance, overexpression of mHTT inhibits the roles of HTT in transcription (Zuccato *et al.*, 2003). In addition, reduction of HTT levels in HD and WT mice produces pathological effects (Van Raamsdonk *et al.*, 2005b). Furthermore, heterozygous HTT KO mice show HD-like symptoms (Nasir *et al.*, 1995; O'Kusky *et al.*, 1999). Thus, all these studies support the idea that at least part of the pathological events in HD may be attributable to the loss of the normal HTT function.

However, the inverse correlation between the number of glutamine repeats and age of HD onset has lent support to the gain of function hypothesis, specifically a gain of toxicity. For instance, cytotoxicity could be caused by abnormal interactions of mHTT with other proteins, interfering with several cellular pathways such as endocytosis, axonal transport, autophagy, metabolic, gene transcription, etc (Walker *et al.*, 2007). Mice expressing only the *HTT* exon 1 develop similar cognitive and motor symptoms to those observed in the disease, reinforcing the idea of gain of function as the cause of HD (Mangiarini *et al.*, 1996). Besides, other human genetic disorders produced by polyQ expansion as spinocerebellar ataxia, spinobulbar muscular atrophy and dentatorubropallidoluysian atrophy, have been attributed to a gain of function conferred by the polyQ stretch (Komure *et al.*, 1995; Mariotti *et al.*, 2000; O'Hearn *et al.*, 2001; Piccioni *et al.*, 2001).

## 1.8 Mouse models of HD

Different animal models have been generated to study HD. *Drosophila Melanogaster* and *Caenorhabditis elegans* animal models show neuronal polyQ inclusions and progressive degeneration (Faber *et al.*, 1999; Marsh *et al.*, 2003). However, mice HD models were the first to appear. Initially, excitotoxic damage by kainic acid in striatum tissue was used as a model of HD because it kills MSNs and mimics some HD symptoms (Coyle *et al.*, 1976). Other excitotoxins such as quinolinic acid and 3-nitropropionic acid have been used (Beal *et al.*, 1986; Beal *et al.*, 1993).

The discovery that HD is caused by a genetic mutation prompted the emergence of animal models based on the expression of the mutated gene, making HD one of the neurodegenerative diseases with better animal models. Genetic models recapitulate some electrophysiological, neurochemical, histopathological and behavioural alterations of HD (Mangiarini *et al.*, 1996). They can be classified into three groups based on the type of transgene, all of them with altered polyQ stretch (Table 1).

- 1) Transgenic mice expressing an N-terminal region of mHTT. A portion of the *HTT* gene of human or chimeric human/mouse origin is randomly inserted.
- 2) Transgenic mice expressing full-length *HTT* gene randomly inserted.
- 3) Knock-in mice strains with a pathological CAG repeat length introduced in the polyQ stretch locus of the endogenous *Htt* gene.

Nevertheless, each model has strengths and limitations for modelling specific symptoms of this hereditary disease (Pouladi *et al.*, 2013).

### 1.8.1 Transgenic mice expressing N-terminal portion of mHTT

Exon 1 fragments have been detected in HD patients (Neueder *et al.*, 2017). and expression of a truncated N-terminal mHTT protein, omitting the rest of the protein, is sufficient to mimic some HD symptoms in mouse models

- R6/1 and R6/2

R6 mice were the first transgenic mouse model created to study HD. R6/1 and R6/2 carry exon 1 of the human *HTT* gene carrying 116 and 144 CAG repeats, respectively (Mangiarini *et al.*, 1996). R6/1 mice express around 31% of *HTT* mRNA and R6/2 75% compared to the endogenous level, respectively (Mangiarini *et al.*, 1996).

These mice recapitulated the importance of CAG repeats on age of onset seen in humans. R6/2 motor symptoms commence at around 3 weeks of age with locomotor hyperactivity, which is not observed until 13-20 weeks of age in R6/1 mice (Hansson *et al.*, 2001; Luesse *et al.*, 2001). Locomotor hyperactivity in R6/2 mice is followed by gradual reduction of motor activity from 8 weeks of age (Carter *et al.*, 1999). Concerning lifespan, R6/1 live longer than 1 year while R6/2 die at 13-16 weeks of age (Sathasivam *et al.*, 1999). R6/2 brains weigh 20% less than WT at 12 weeks of age (Kosinski *et al.*, 1999) and R6/1 striatum area is reduced 17% at 18 weeks of age, which is not due to neuronal death but to loss of the neuropil (Hansson *et al.*, 1999; Turmaine *et al.*, 2000; Klapstein *et al.*, 2001). mHTT aggregates appear in striatum and cortex in R6/2 at 3-4 weeks of age, whereas inclusions do not appear until 8 weeks of age in R6/1 striatum (Hansson *et al.*, 2001; Meade *et al.*, 2002).

- N171-82Q

This transgenic mouse expresses exon 1 and exon 2 of *HTT* (171 amino acids in total) with 82 glutamines in the polyQ stretch (Schilling *et al.*, 1999). N-terminal fragment expression is driven by the mouse prion promoter (*Prnp*) appearing only in neurons, not in other cell types in the CNS (Schilling *et al.*, 1999). The main characteristics include the significant body weight loss and the lack of hyper and hypokinesia, although these mice show motor and memory deficits (Ramaswamy *et al.*, 2009). The neuropathological features include striatal neuronal loss, striatal atrophy and ventricular enlargement at 16 weeks of age (Yu *et al.*, 2003; McBride *et al.*, 2006). The N171-82Q line has a lifespan that ranges from 4 to 6 months (Martin *et al.*, 2009).

- Tg100

It expresses around 3 Kb of the *HTT* gene with 100 CAG repeats under the rat neuron specific enolase promoter (Laforet *et al.*, 2001). At 3 months of age mHTT inclusions appear in MSNs and cortex, altering the morphology of dendrites and leading to motor symptoms at 3-6 months of age (Laforet *et al.*, 2001).

- HD94

HD94 is a transgenic conditional knockout mouse that expresses exon 1 of mHTT with 94 glutamines under the control of the CaMKII $\alpha$  promoter, which restricts its expression to forebrain neurons (Yamamoto *et al.*, 2000; Wang *et al.*, 2013). The expression of the transgene can be stopped with doxycycline. These mice are hypokinetic by 9 months. Cytoplasmic aggregates appear in the soma and neuropil of striatal and cortical neurons at 2 months of age. Although death of MSNs is not detected, striatal atrophy is observed from 18 weeks to 2 years of age, when these mice die. All these phenotypes can be rescued with doxycycline administration beginning at 18 weeks of age, and maintaining the treatment for 16 weeks (Yamamoto *et al.*, 2000).

Although these mouse models recapitulate some HD symptoms, the use of only the HTT N-terminal domain does not mimic molecular defects caused by interaction of other HTT regions with cellular proteins.

### 1.8.2 Full-length mHTT transgenic mice

The lack of robust motor deficits or cell death in the models mentioned above prompted the generation of full-length HTT models. Because the R6, N171-82Q, Tg100 and HD94 mice only express the N-terminal portion of mHTT, crucial HD aspects might be missing. While conventional transgenic technology did not allow to introduce a gene as large as *HTT*, transgenic mice carrying full-length *HTT* were eventually created using a yeast artificial chromosome (YAC) vector system which expressed the entire human *HTT* gene under the human *HTT* gene promoter (Hodgson *et al.*, 1999; Slow *et al.*, 2003). The first YAC HD

mouse was the YAC72 carrying 72 CAG repeats. YAC72 presented significant neurodegeneration in the striatum at 12 months, motor deficits at 16 months but rare apparition of macro-aggregates (Hodgson *et al.*, 1999; Seo *et al.*, 2008).

Due to delayed symptom onset in YAC72 mice, YAC128 mice, carrying full-length human mHTT with a 128 polyQ tail, were generated (Slow *et al.*, 2003). These mice present a motor learning deficit in rotarod testing at 2 months of age and cognitive deficits in a simple swimming test at 8 months of age (Van Raamsdonk *et al.*, 2005b). The symptoms probably reflect loss of synaptic connectivity produced by spine loss in MSNs, that is detectable by 3 months of age (Marco *et al.*, 2013). Motor skills undergo a progressive decline, which begins to manifest at 6 months of age in rotarod and in swimming T-maze tests (Slow *et al.*, 2003; Van Raamsdonk *et al.*, 2005b). After a hyperkinetic period, that starts at 3 months of age, hypokinetic symptoms appear at 12 months of age (Slow *et al.*, 2003). Modest striatal atrophy (9% with respect to WT mice) is found in 36 weeks-old mice but loss of neurons in striatum (15%) and cortex are significant at 1 year of age (Slow *et al.*, 2003). Neuronal death in striatum and cortex affect directly to brain weight, whereas other regions as cerebellum are not affected (Slow *et al.*, 2003). Nuclear diffuse mHTT immunoreactivity appears in 3-month-old striatum while it is not until 12 months that are present in CA1 and cortical neurons (Van Raamsdonk *et al.*, 2005a). Although electron microscopy (EM) analysis demonstrate micro-aggregates of mHTT in 1-year-old YAC128 mice, is not until 18 months of life that macro-aggregates appear in MSNs (Slow *et al.*, 2003). Both presymptomatic and symptomatic YAC128 mice show consistent resistance to excitotoxic stress (Graham *et al.*, 2009). YAC128 mice show a normal lifespan. Nevertheless, survival analysis of males and females reveals a reduction in life expectancy in males (Van Raamsdonk *et al.*, 2005b).



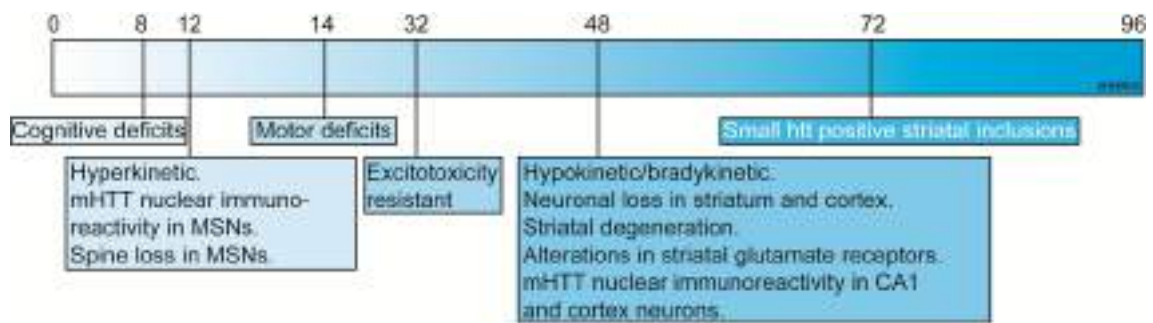


Figure 5. Timeline (in weeks) of behavioral and neuropathological symptoms in the YAC128 HD mouse model chosen for this study

- BACHD

The BACHD mouse was generated by injection of a bacterial artificial chromosome (BAC) into fertilized mice eggs. The BAC contains the entire 170 Kb human *HTT* locus with a 97 mixed CAA-CAG repeats flanked by LoxP ends, that generate a 97polyQ tail (Gray *et al.*, 2008). This conditional mutant HD mouse model presents body gain starting at 6 months of age that is maintained to death. Also at that age, these mice display atrophy of 30% in striatum and in cortex. mHTT aggregates appear in cortex and striatum in 1-year-old mice. At 2 months of age, these mice exhibit a subtle but significant decrease in rotarod performance. The BACHD mouse model has the advantage that does not show instability in the germline in polyQ repeats due to the alternating CAA-CAG in the transgene (Gray *et al.*, 2008).

### 1.8.3 Knock-in transgenic mice

These mice were generated by homologous recombination, where the endogenous polyQ stretch in *Htt* was replaced with a pathological polyQ. This non-random technique avoids possible insertions that alter other genes.

Mice with different glutamine repetitions were developed to recapitulate all pathological stages of the disease:

- HdhQ72/Q80 (Shelbourne *et al.*, 1999).
- HdhQ111 (Wheeler *et al.*, 1999).
- HdhQ94 (Levine *et al.*, 1999).
- CAG150 (Lin *et al.*, 2001).
- CAG140 (Menalled *et al.*, 2003).

In contrast to what happens in humans, mice with more CAGs repeats show a delay in the appearance of pathology. One example is in HdhQ150, that show first motor symptoms at 16-24 months of age, while HdhQ94 mice, with a shorter polyQ stretch, present hyperactivity and hypoactivity at 2 and 4 months respectively (Levine *et al.*, 1999; Menalled *et al.*, 2002; Heng *et al.*, 2007). All mice present normal lifespan although mHTT aggregates appear in all the cases at different ages or locations (Menalled *et al.*, 2002; Wheeler *et al.*, 2002; Kennedy *et al.*, 2003; Heng *et al.*, 2007; Hickey *et al.*, 2008).

Table 1. Commonly used transgenic mice models of HD.

Strain name	Transgenic /Knock-in	Gene Characteristics	Promoter	Number of glutamines	Motor symptom Onset (months)	References
<b>R6/1</b>	Transgenic fragment	Exon 1 of human <i>HTT</i> gene	1 kb of Human <i>HTT</i>	116	1.5	Mangiarini <i>et al.</i> , 1996; Carter <i>et al.</i> , 1999
<b>R6/2</b>	Transgenic fragment	Exon 1 of human <i>HTT</i> gene	1 kb of Human <i>HTT</i>	144	4,5	Mangiarini <i>et al.</i> , 1996; Hodges <i>et al.</i> , 2008
<b>N171-82Q</b>	Transgenic fragment	First 171 amino acids of human <i>HTT</i>	Prnp	82	3	Schilling <i>et al.</i> , 1999; Schilling <i>et al.</i> , 2004
<b>Tg100</b>	Transgenic fragment	First 3 kb of human <i>HTT</i> cDNA	Rat NSE	100	3	Laforet <i>et al.</i> , 2001
<b>HD94</b>	Transgenic fragment	Chimeric human/mouse <i>HTT</i> exon 1	TetO + tT	94	1,5	Yamamoto <i>et al.</i> , 2000
<b>YAC72</b>	Transgenic full-length	Full length human <i>HTT</i> gene	Human <i>HTT</i>	72	16	Hodgson <i>et al.</i> , 1999; Seo <i>et al.</i> , 2008
<b>YAC128</b>	Transgenic full-length	Full length human <i>HTT</i> gene	Human <i>HTT</i>	128	6	Slow <i>et al.</i> , 2003

<b>BACHD</b>	Transgenic full-length	Full length human <i>HTT</i> gene (floxed exon 1)	Human <i>HTT</i>	97	2	Gray <i>et al.</i> , 2008
<b>HdhQ72, Q80</b>	Knock-in	Endogenous murine <i>Htt</i> gene, expanded CAG inserted	Mouse <i>Htt</i>	72,80	12	Shelbourne <i>et al.</i> , 1999; Kennedy <i>et al.</i> , 2003
<b>HdhQ111</b>	Knock-in	Endogenous murine <i>Htt</i> gene, chimeric human/mouse exon 1	Mouse <i>Htt</i>	109	24	Wheeler <i>et al.</i> , 1999; Wheeler <i>et al.</i> , 2002
<b>HdhQ94</b>	Knock-in	Endogenous murine <i>Htt</i> gene, chimeric human/mouse exon 1	Mouse <i>Htt</i>	94	2	Levine <i>et al.</i> , 1999; Menalled <i>et al.</i> , 2002
<b>HdhQ140</b>	Knock-in	Endogenous murine <i>Htt</i> gene, chimeric human/mouse exon 1	Mouse <i>Htt</i>	140	4	Menalled <i>et al.</i> , 2003; Hickey <i>et al.</i> , 2008

#### 1.8.4 Synaptic alterations in mouse models of HD

Defects in cortico-striatal synaptic communication at presymptomatic stages are one of the most consistent alterations across HD mouse models, as assessed by MRI and a variety of other methods (Raymond *et al.*, 2011). The nature of the synaptic alterations has been identified with electrophysiological methods. In R6/2 and YAC128 mice models, MSNs show first an increase in spontaneous excitatory postsynaptic currents, followed by later reduction in current densities likely reflecting spine loss (Cepeda *et al.*, 2003; André *et al.*, 2011). While initial morphological studies focused on cell death, early MSN spine loss has now been demonstrated in knock-in mouse models, BACHD, YAC128 and R6 mice (Richards *et al.*, 2011; Marco *et al.*, 2013; Simmons *et al.*, 2013; Wu *et al.*, 2016). MSN spine loss and death have been linked to alterations in NMDAR numbers, subunit composition and subcellular distributions.

- Alterations in NMDAR location: HD mice exhibit an imbalance between synaptic and extrasynaptic NMDAR, with an increase in the number of

extrasynaptic NMDARs and decreases in synaptic counterparts. The shift from synaptic to extrasynaptic NMDARs alters trophic NMDAR signalling, and has been suggested to drive MSN death in YAC128 mice (Okamoto *et al.*, 2009; Milnerwood *et al.*, 2010a)

- Alterations on NMDAR composition: the subunits that compose the NMDAR determine its down-stream signaling. In knock-in and R6/2 mice, levels of GluN2A NMDAR subunits are significantly reduced (Ma *et al.*, 2017). Abundance of GluN2B-NMDARs seems to be higher in the YAC128 striatum (Milnerwood *et al.*, 2010a). Increased NMDARs-containing GluN3A subunits are enhanced in YAC128 MSNs, which drives the loss of dendritic spines (Marco *et al.*, 2013).

Thus, the possibility of correcting early NMDAR alterations in HD to stop the pathological process from its very beginning has sparked considerable interest. Targeting aberrant GluN3A subunits raised particular attention as their expression is low in adult brains and antagonizing their functions might not be associated to the side-effects that have prevented the use of other NMDAR-based therapies (see next section).

## 2. Ionotropic glutamate receptors

Ionotropic glutamate receptors are glutamate-gated ion channels that mediate fast excitatory synaptic transmission in the CNS. They are macromolecular assemblies of four large subunits that form a central ion channel pore through which cations (principally Na<sup>+</sup> and Ca<sup>2+</sup>) flux. Four different ionotropic glutamate receptor families can be distinguished based on the molecule that activates them and their integrating subunits (Traynelis *et al.*, 2010).

- AMPA ( $\alpha$ -amino-3-hydroxy-5-methyl-4-isoxazolepropionic acid) receptors: formed by homo- or heterotetrameric assemblies of GluA1 to GluA4 proteins.
- Kainate receptors: formed by homo- or heterotetrameric assemblies of GluK1 to GluK5 subunits.

- NMDA (N-methyl-D-aspartate) receptors: formed by heterotetrameric combinations of GluN1, GluN2 (A-D) and GluN3 (A-B) subunits.
- $\delta$ -Receptors: formed by GluD1 and GluD2 subunits. Despite high homology with the other ionotropic glutamate receptors, they are not gated by glutamate and no ligand has been identified.

As mentioned, dysfunction of NMDARs has been implicated in HD, with a prominent role of subtypes containing non-conventional GluN3A-NMDARs. In this section, I will summarize our current knowledge of NMDARs with a focus on GluN3A-NMDARs.

## 2.1 NMDARs

Functional NMDAR are heterotetrameric assemblies of two mandatory GluN1 subunit and combinations of GluN2 (A-D) and GluN3 (A-B) (Monyer *et al.*, 1992; Schorge *et al.*, 2003). The specific subunit composition of NMDAR subtypes confers specific biophysical properties and protein interactions which will determine the unique trafficking, localization, signalling and functions of the receptor (Lau *et al.*, 2007; Paoletti *et al* 2013).

### 2.1.1 NMDARs subunit basic structure

All NMDAR subunits share a membrane topology characterized by an extracellular N-terminal domain, 4 membrane domains, and a cytoplasmic C-terminus domain (Paoletti *et al.*, 2007; Paoletti *et al* 2013). The extracellular domain can be divided into an N-terminal domain and a bi-lobed ligand-binding domain. The N-terminal domain on, is involved in subunit assembly and allosteric inhibition by molecules such as zinc and ifenprodil (Williams, 1993; Paoletti *et al.*, 1997; Meddows *et al.*, 2001). The ligand-binding domain has a clam-shell structure formed by two discontinuous segments, one part of the N-terminal domain and a loop formed by the amino acid sequence between transmembrane domains M3 and M4, and binds glutamate in GluN2 subunits and glycine or D-serine in GluN1 and GluN3 (Furukawa *et al.*, 2003; Furukawa

*et al.*, 2005; Yao *et al.*, 2008). NMDAR activation requires simultaneous binding of glycine and glutamate (Johnson *et al.*, 1987; Lerma *et al.*, 1990). The transmembrane domain includes three transmembrane helices (M1, M3 and M4) and a membrane re-entrant loop (M2) (Sobolevsky *et al.*, 2009). Upon assembly with other subunits, the membrane domains form a cation-permeable pore. The sequence of a key glutamine/arginine/asparagine (Q/R/N) site in M2 determines the cation permeability and confers NMDARs properties such as the ability to flux calcium and be blocked by  $Mg^{2+}$ , which are fundamental for their functions (see below) (Dingledine *et al.*, 1999). The intracellular C-terminal domain is the most diverse in amino acid sequence and has varying lengths in the different NMDAR subunits. It contains target sequences for posttranscriptional modification, such as phosphorylation sites, and protein interaction motifs that bind different partners in different subunits and are key for receptor signaling and regulation of membrane trafficking (Traynelis *et al.*, 2010).

### 2.1.2 Classical NMDAR properties and function

Classical NMDARs are heterotetrameric complexes formed by two GluN1 subunit and a combination of GluN2 subunits which yields a variety of subtypes. They are widely expressed throughout the brain, but subunit composition varies between nuclei, cell types and developmental stage (Paoletti *et al.*, 2011). Whereas the obligatory GluN1 subunit is ubiquitously expressed from embryonic stage to adulthood (Watanabe *et al.*, 1992), GluN2 subunits show different spatiotemporal expression. In embryonic brain, GluN2B and GluN2D are highly expressed, but after birth GluN2A expression appears and becomes abundantly and widely expressed in the adult CNS. GluN2C appears in the second postnatal week and its expression is mostly restricted to olfactory bulb and cerebellum (Paoletti *et al.*, 2013). Subunit exchanges modify the properties of synaptic plasticity and underlies processes such as synapse maturation, circuit refinement, acquisition of learning abilities and memory (Dumas *et al.*, 2005; Paoletti *et al.*, 2013).

NMDARs are typically concentrated at postsynaptic densities via binding to PSD95 (Prybylowski *et al.*, 2005), and other members of the PDZ-domain family (Sans *et al.*, 2000). Subcellular localization is also thought to be determined by subunit composition. GluN2A-NMDA receptors are highly concentrated at synaptic sites while GluN2B-containing NMDA receptors appear also in peri- and extrasynaptic sites (Harris *et al.*, 2007; Logan *et al.*, 2007; Raymond *et al.*, 2011).

Classical NMDAR activation requires binding of glutamate and a co-agonist (glycine or D-serine). Although the subunit stoichiometry affects cation permeability, it could be said that classical NMDARs show high-conductance channel openings, high  $\text{Ca}^{2+}$  permeability and sensitivity to  $\text{Mg}^{2+}$  blockade (Paoletti *et al.*, 2013). The activation of these receptors is also affected by substances that are endogenously found in the CNS.  $\text{Zn}^{2+}$  ions act as highly specific antagonists of GluN1-GluN2A-containing NMDARs, but protons ( $\text{H}^+$ ) preferentially inhibit GluN2D- or GluN2B-containing NMDARs (Paoletti *et al.*, 1997; Banke *et al.*, 2015).

Classical NMDARs are essential mediators of brain plasticity and convert specific neuronal activity patterns into long-term changes in synapse structure. In higher brain structures of adults, such as the cortex and hippocampus, GluN2A and GluN2B-containing NMDARs have central roles in synaptic plasticity and function (Monyer *et al.*, 1994) and mediate long-term potentiation (LTP) and long-term depression (LTD), the two main forms of synaptic long-term plasticity. According to several findings, GluN2A-containing NMDARs seem specifically important for LTP induction, whereas GluN2B-containing NMDARs would be specifically involved in LTD induction in synapses (Paoletti *et al.*, 2013). Alteration in NMDARs functions, either hyperactivity or hypofunction, at the synaptic level can cause synaptopathies such as Alzheimer's disease, Parkinson's disease, depression, autism spectrum disorders, amount others (Paoletti *et al.*, 2013).

## 2.2 GluN3A-containing NMDARs

GluN3A was the last NMDAR subunit to be discovered and has great interest due to its particular properties that differ from the classical NMDARs described above. Two independent groups identified it in 1995, and termed it with a different name, “Chi-1” or “ $\chi$ -1” and “NMDAR-like” (Ciabarra *et al.*, 1995; Sucher *et al.*, 1995). The GluN3A designation (before NR3A) was adopted later, when coimmunoprecipitation analysis showed that it can assemble with NMDAR subunits (Das *et al.*, Nature 1998). The mouse gene is *Grin3a* and the human gene *GRIN3A*. *GRIN3A* is located on human chromosome 9 (9q31.1) and spans 9 exons that encode a protein of 1115 amino acids (Ciabarra *et al.*, 1995; Sucher *et al.*, 1995; Eriksson *et al.*, 2002) and a molecular weight of 125 kD (Ciabarra *et al.*, 1997). The rodent homologous gene is located in chromosome 5 in rats and chromosome 4 in mice. *Grin3a* in rodents encodes two isoforms of the protein generated by alternative splicing, one with a short C-terminus (GluN3A-S) and a long isoform that includes 20 amino acids encoded by exon 9 (GluN3A-L) (Sun *et al.*, 1998). GluN3A-L is present only in rodents, not in humans (Andersson *et al.*, 2001).

### 2.2.1 Unique features of GluN3A subunits

GluN3A subunit functions and features are well conserved across mammalian species (Andersson *et al.*, 2001; Eriksson *et al.*, 2002) with 93% protein homology between human and rodents, and share 88% of the DNA sequence. The other non-conventional subunit, GluN3B, share 57% of the sequence with GluN3A. Lesser homology is found with GluN1 (27%) or GluN2 (24-29%) subtypes (Ciabarra *et al.*, 1995). GluN3A protein amino acid sequence and structure is similar to other NMDAR and ionotropic glutamate receptors subunits, but with crucial differences (Figure 6). In its N-terminal domain and extracellular loops, 10 asparagine residues (N145, 264, 275, 285, 296, 425, 439, 549, 565 and 886) are glycosylated to regulate trafficking of GluN3A-containing NMDARs to membrane surface (Andersson *et al.*, 2001; Skrenkova *et al.*, 2018). Also, the N-terminal domain contains a motif required for redox modulation with two cysteine residues (CC) (Andersson *et al.*, 2001). As GluN1,



GluN3 can bind glycine and D-serine, but it is not activated by glutamate (Paas *et al.*, 1998; Yao *et al.*, 2006; Yao *et al.*, 2008). A unique feature that makes GluN3A different from classical NMDAR subunits is the presence of a glycine followed by an arginine (G/R) instead of the Q/R/N site controlling ion permeability and rectification in M2 (Seeburg *et al.*, 1993, Hollmann *et al.*, 1994, Dingledine *et al.*, 1999). This finding might explain the low permeability to Ca<sup>2+</sup> (Sucher *et al.*, 1995; Nishi *et al.*, 2001; Matsuda *et al.*, 2002).

Like other NMDARs subunits, the GluN3A intracellular C-terminus domain contains putative phosphorylation sites for protein kinases A and C (PKA and PKC), calcium/calmodulin-dependent kinase II (CaMKII) and tyrosine kinases (PTK) (Ciabarra *et al.*, 1995; Sucher *et al.*, 1995; Andersson *et al.*, 2001; Nishi *et al.*, 2001; Eriksson *et al.*, 2002). Phosphorylation of residues in the C-terminal domain regulates signalling, trafficking and channel properties of other NMDAR subunits but it is yet not known how they influence GluN3A function (Chen *et al.*, 2007). The GluN3A C-terminal domain also contains trafficking motifs: an arginine/any/arginine (RXR) motif that could work as an ER retention signal (Henson *et al.*, 2010) to restrict forward secretory trafficking to only properly assembled GluN3A complexes (Perez-Otano *et al.*, 2001), and a tyrosine-based internalization motif (YWL) that mediates activity-dependent endocytosis. Phosphorylation of the YWL motif by the tyrosine kinase Src recruits the clathrin adaptor protein 2 (AP2) (Perez-Otano *et al.*, 2006; Chowdhury *et al.*, 2013). A distinguishing feature of the GluN3A C-terminal domain is the lack of a PDZ domain (Matsuda *et al.*, 2002; Eriksson *et al.*, 2007), that in other NMDAR subunits allows binding to PSD-95 and stabilizes NMDARs at postsynaptic densities within dendritic spines.

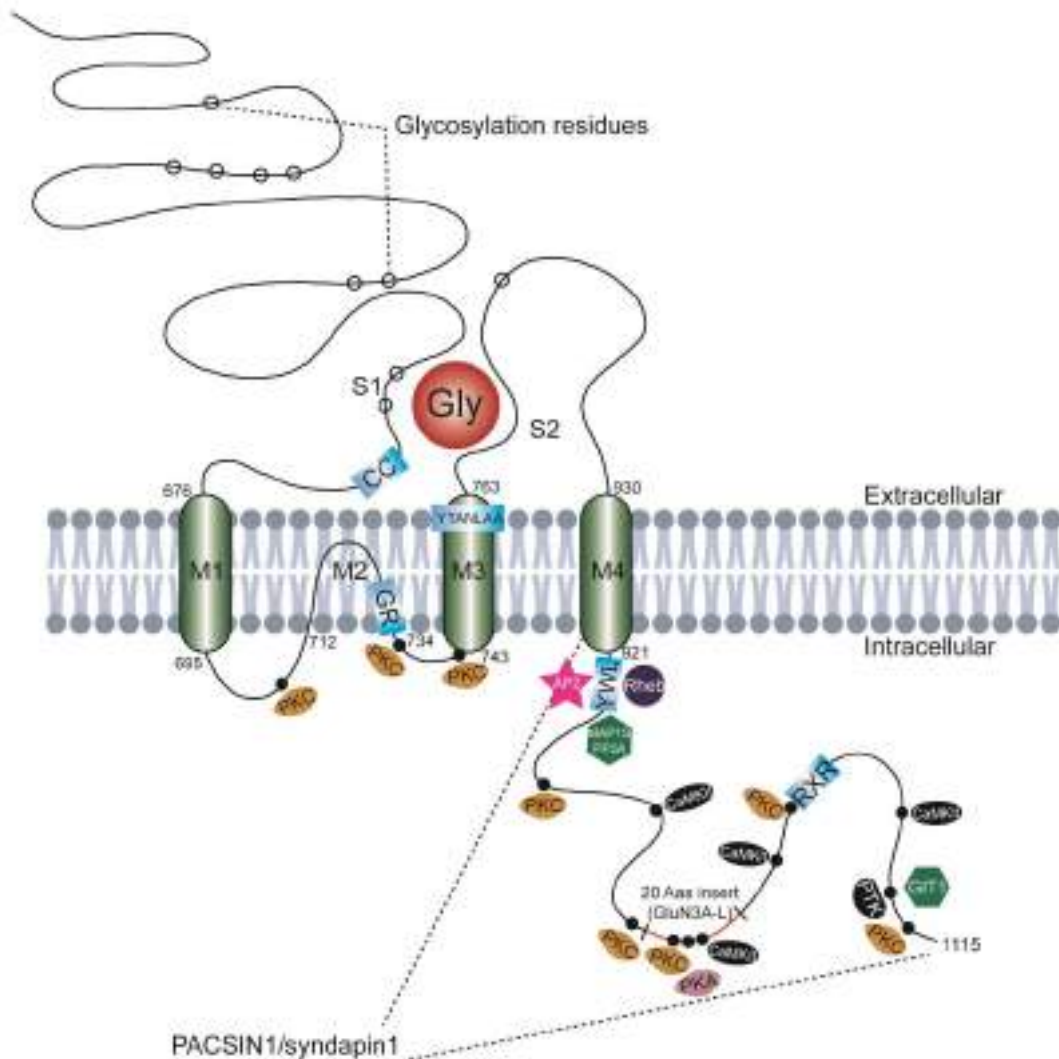


Figure 6. Transmembrane topology of GluN3A NMDAR subunit, sites for modulation and protein-protein interactions. The schematic shows the extended extracellular domain with two segments (S1 and S2) that form the binding site for Glycine (Gly) or D-serine; the transmembrane domain composed by three transmembrane helices (M1, M3 and M4) and a membrane re-entrant loop (M2); sequence motifs (-CC-, -GR-, -YTANLAAV-, -YWL-, -RXR-); and intracellular domain. Predictive glycosylation asparagine residues in extracellular domain (N145, 264, 275, 285, 296, 425, 439, 549, 565 and 886) to regulate the trafficking are indicated by open circles (○). Phosphorylation sites by protein kinases A and C (PKA and PKC), calcium/calmodulin-dependent kinase II (CaMKII) and tyrosine kinases (PTK) are present in C-terminal domain indicated by closed circles (●). Long GluN3A isoform (GluN3A-L) includes extra 20 amino acids in initial part of exon 9 (-SRWRRWTKTEGDSELSLFP-) (in red). Binding sites for intracellular proteins such as clathrin adaptor protein 2 (AP2), Ras homologue enriched in brain (RHEB), microtubule-associated proteins (MAP1S/MAP1B), GIT1 and protein kinase C and casein kinase

substrate in neurons 1 (PACSIN1/syndapin1) are indicated. Figure based on sequence data from (Andersson *et al.*, 2001).

### 2.2.2 Receptor assembly

GluN3A can assemble with both GluN1 and GluN2 subunits in heterologous cell lines. However, assembly with GluN1 is required for ER exit in such a way that homomeric GluN3A complexes or di-heteromeric GluN2A-GluN3A are retained in the ER and do not reach the plasma membrane (Perez-Otano *et al.*, 2001; Chatterton *et al.*, 2002). With these rules, two types of surface-expressed GluN3A complexes exist: di-heteromeric GluN1-GluN3A and tri-heteromeric GluN1-GluN2-GluN3A (Nishi *et al.*, 2001; Perez-Otano *et al.*, 2001; Chatterton *et al.*, 2002). Tri-heteromers containing GluN1, GluN2 and GluN3A subunits bind glutamate and NMDA and are thus bona-fide NMDARs (Pachernegg *et al.*, 2012). GluN3A has been shown to assemble with GluN2C in oligodendrocytes and with GluN2A and GluN2B in neurons (Das *et al.*, 1998; Al-Hallaq *et al.*, 2002; Nilsson *et al.*, 2007; Burzomato *et al.*, 2010; Martinez-Turrillas *et al.*, 2012).

### 2.2.3 Biophysical properties

The single-channel electrophysiological properties of isolated tri-heteromeric GluN1-GluN2A-GluN3A NMDARs have been studied (Figure 7) in patches excised from HEK293 cells and *Xenopus laevis* oocytes, (Das *et al.*, 1998; Perez-Otano *et al.*, 2001; Sasaki *et al.*, 2002). Non-conventional tri-heteromeric GluN3A-NMDARs have a smaller single-channel conductance, 28 picosiemens (pS) main conductance, than classical GluN1-GluN2A receptors (48 pS) (Perez-Otano *et al.*, 2001). GluN1-GluN2-GluN3A NMDARs also display a lower relative Ca<sup>2+</sup> permeability (permeability ratio: Ca<sup>2+</sup>/Na<sup>+</sup> or K<sup>+</sup>): 0.8 compared to 6.8 in di-heteromeric classical NMDARs (Sasaki *et al.*, 2002). Open probability is also lower: 0.03 versus 0.5, respectively (Sasaki *et al.*, 2002). The opposite applies to mean open time probability of the channel: 6.7 ms for GluN3A-NMDARs versus 3.1 ms for GluN1-GluN2A di-heteromeric NMDARs (Perez-

Otano *et al.*, 2001). Moreover, GluN3A-NMDARs are relatively insensitive to  $Mg^{2+}$  block at hyperpolarized potentials (Sasaki *et al.*, 2002; McClymont *et al.*, 2012). Because of these non-conventional NMDAR properties, GluN3A were proposed to fulfill a dominant-negative role on classical NMDAR functions (Cavara *et al.*, 2008; Low *et al.*, 2010; Pachernegg *et al.*, 2012; Kehoe *et al.*, 2013).

Although rare, di-heteromeric GluN3A-containing NMDARs exist *in vivo*. They are not activated by glutamate or NMDA, are insensitive to AP-5 (competitive NMDAR antagonist at the glutamate binding site) or open-channel blockers such as memantine or  $Mg^{2+}$ , and instead behave as excitatory glycine receptors (Chatterton *et al.*, 2002). The existence of GluN1-GluN3A excitatory receptors has been controversial because glycine triggers rapid desensitizing responses and glycine responses could not be detected in GluN3A-overexpressing transgenic mice (Chatterton *et al.*, 2002; Matsuda *et al.*, 2003; Awobuluyi *et al.*, 2007; Smothers *et al.*, 2007; Tong *et al.*, 2008). Nevertheless, experiments performed in mouse optic nerve demonstrated glycine responses of native GluN1-GluN3A NMDARs (Piña-Crespo *et al.*, 2010). Also, native GluN1/GluN3A receptors have been recently identified in juvenile mouse hippocampus and adult medial habenula (Grand *et al.*, 2018; Otsu *et al.*, 2019).

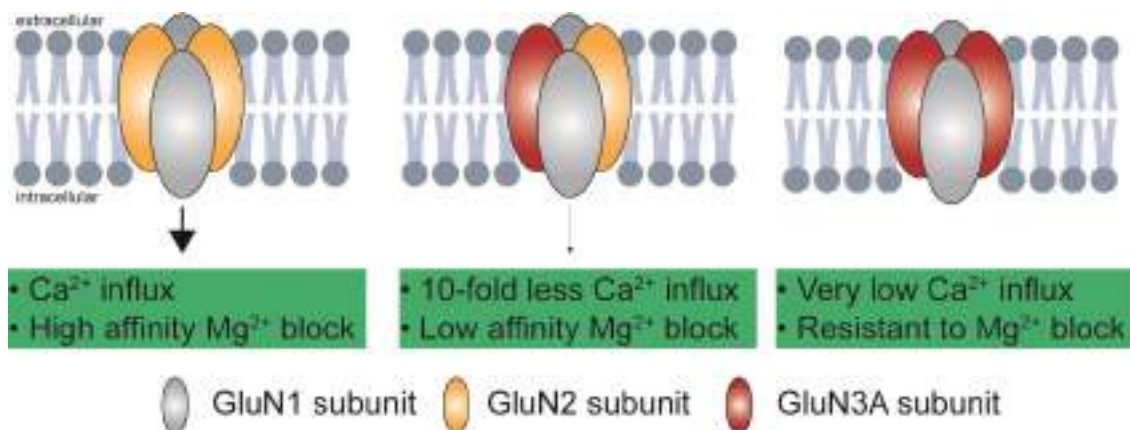


Figure 7. NMDARs composition alternatives. Tri-heteromeric (GluN1-GluN2-GluN3A) NMDARs (middle panel) exhibit reduced  $Ca^{2+}$  influx and are less sensitive to voltage-dependent block by  $Mg^{2+}$  compared with di-heteromeric (GluN1-GluN2) NMDARs (left panel). Di-heteromeric GluN3A-containing NMDARs, that are activated by glycine, exhibit resistance to  $Mg^{2+}$  blockade and are relatively  $Ca^{2+}$  impermeable (right panel).

## 2.2.4 GluN3A-interacting proteins

The C-terminal tail of GluN3A interacts with a distinct set of intracellular proteins:

- GIT1: Amino acids 1082 to 1115 of the distal C-terminal domain interact with the G-protein-coupled receptor kinase interactor 1 (GIT1) (Fiuza *et al.*, 2013). Neuronal activity dissociates GIT1 from GluN3A and favours the generation of a multiprotein complex formed by GIT1-Rac1- $\beta$ PIX (members of the Rho family of GTPases) which activates p21-activated kinase 1 (PAK1) and regulates actin dynamics in dendritic spines (Zhang *et al.*, 2003).
- Rheb: The small GTPase Ras homologue enriched in brain (Rheb) is a central activator of the mammalian target of rapamycin complex 1 (mTORC1) (Sucher *et al.*, 2011). mTORC1 signalling is involved in autophagy, spine remodelling and protein synthesis (Arsham *et al.*, 2006).
- MAP1S/MAP1B: Both are microtubule-associated proteins that bind the proximal portion of the GluN3A C-terminal domain (Eriksson *et al.*, 2007; Eriksson *et al.*, 2010).
- PP2A: Protein phosphatase 2A (PP2A) exists as a multi subunit serine-threonine phosphatase expressed in high levels in CNS (Strack *et al.*, 1998). The GluN3A binding-domain to the catalytic subunit of the complex, similar to Rheb-binding domain, is located 37 amino acids from the transmembrane domain M4 at the C-terminal tail (Chan *et al.*, 2001; Ma *et al.*, 2004). This association promotes dephosphorylation of GluN1-Ser897, attenuating NMDAR channel currents (Chan *et al.*, 2001).
- PACSIN1/syndapin1: also called “synaptic dynamin-associated protein 1” (syndapin1), is enriched in synaptic sites and interacts with dynamin and the actin cytoskeleton (Qualmann *et al.*, 1999; Kessels *et al.*, 2002; Kessels *et al.*, 2004). Neuronal activity drives the interaction of the C-terminal GluN3A domain with PACSIN1, and promotes the endocytosis of GluN3A-NMDARs (Perez-Otano *et al.*, 2006). This process permits the replacement of immature GluN3A-NMDARs with mature NMDARs and

has been linked to the maturation of neural networks. Interfering with PACSIN1 function using dominant-negative variants or because of sequestration by mHTT causes a pathological increase of GluN3A-NMDARs at the synapses (Perez-Otano *et al.*, 2006; Marco *et al.*, 2013) emphasizing the physiological importance of this interaction.

## 2.2.5 GluN3A expression in the CNS

### 2.2.5.1 Developmental time-course

The time-course of GluN3A expression in humans is characterized by a low expression during gestation, which increases soon after birth, reaches its maximum during the first year of life followed by progressive down-regulation through adolescence and into adulthood (Henson *et al.*, 2008; Henson *et al.*, 2010). In rodents, GluN3A expression increases progressively after birth with a peak around postnatal day 5-10 (P5-P10) and later declines into adulthood (Wong *et al.*, 2002) (Figure 8). The expression peak overlaps with postnatal critical periods of synaptic refinement, which has suggested a role of GluN3A in modulating experience-driven neural circuit refinements (Feldman *et al.*, 1998; Colonnese *et al.*, 2006; Perez-Otano *et al.*, 2016). The match with critical periods seems remarkable, as indicated by a delay in the decline of GluN3A expression in visual cortex where synaptic refinement takes place later (Figure 8) (Majewska *et al.*, 2003).

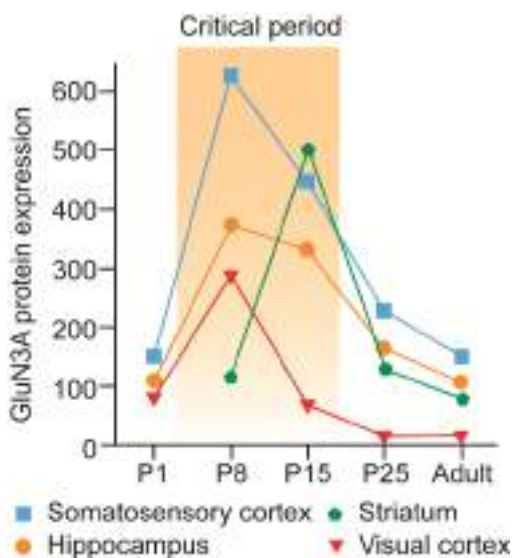


Figure 8. GluN3A protein expression during rodent brain development. Graph show GluN3A peak of expression during the critical circuit refinement period (orange shaded area) in different brain areas in the first postnatal days (P5-P10) of development. After that, sharp decrease expression occurs into adulthood. Modified from Perez-Otano *et al.*, 2016.

### 2.2.5.2 GluN3A subcellular localization

A distinguishing feature of conventional NMDARs is their high concentration in postsynaptic densities within dendritic spines, the place where most excitatory synapses are formed. However, immunogold EM and immunofluorescence analysis have revealed a special subcellular location of GluN3A (Figure 9A). In postsynaptic plasma membranes, GluN3A-NMDARs are particularly abundant in perisynaptic (within 120 nm of the postsynaptic density (PSD) edge) and extrasynaptic domains (>120 nm away from PSD) (Perez-Otano *et al.*, 2006), with only a small percentage of GluN3A-positive gold particles located at the PSD. Within PSDs, GluN3A concentrates in the edge, just the opposite to what is found in classical NMDARs (Figure 9B-C) (Racca *et al.*, 2000; Perez-Otano *et al.*, 2006). This conclusion is supported by the analysis of NMDAR components using fractionation of synaptic plasma membranes, where GluN3A distribution differs from conventional subunits, which are abundant in the highly detergent-insoluble fractions, whereas GluN3A appears mostly in TX100-soluble fraction (detergent soluble fraction) (Perez-Otano *et al.*, 2006; Martinez-Turrillas *et al.*, 2012). This “delocalization” relative to conventional NMDARs is probably due to the lack in GluN3A of a PDZ domain that links other NMDAR subunits to the PSD. GluN3A also appears in intracellular vesicles, particularly in adult neurons, likely reflecting high rates of endocytosis in spines (Figure 9B) (Perez-Otano *et al.*, 2006). Interestingly, beyond the general down-regulation of GluN3A expression, its concentration in dendritic spines also declines: it is higher at P8 and decreases from P16 into adulthood (Perez-Otano *et al.*, 2004; Henson *et al.*, 2012).

GluN3A-NMDARs are not only found in the postsynaptic spines but presynaptically, being located in specific axon terminals (Figure 9B) (Larsen *et al.*, 2011; Savtchouk *et al.*, 2019). Non-conventional presynaptic NMDARs (pre-GluN3A-NMDARs) have been found near astrocyte membranes (Savtchouk *et al.*, 2019). Down-regulation of pre-GluN3A-NMDARs is evident after the peak of expression at P8, showing the same pattern as the rest of GluN3A-NMDARs (Larsen *et al.*, 2011; Savtchouk *et al.*, 2019).

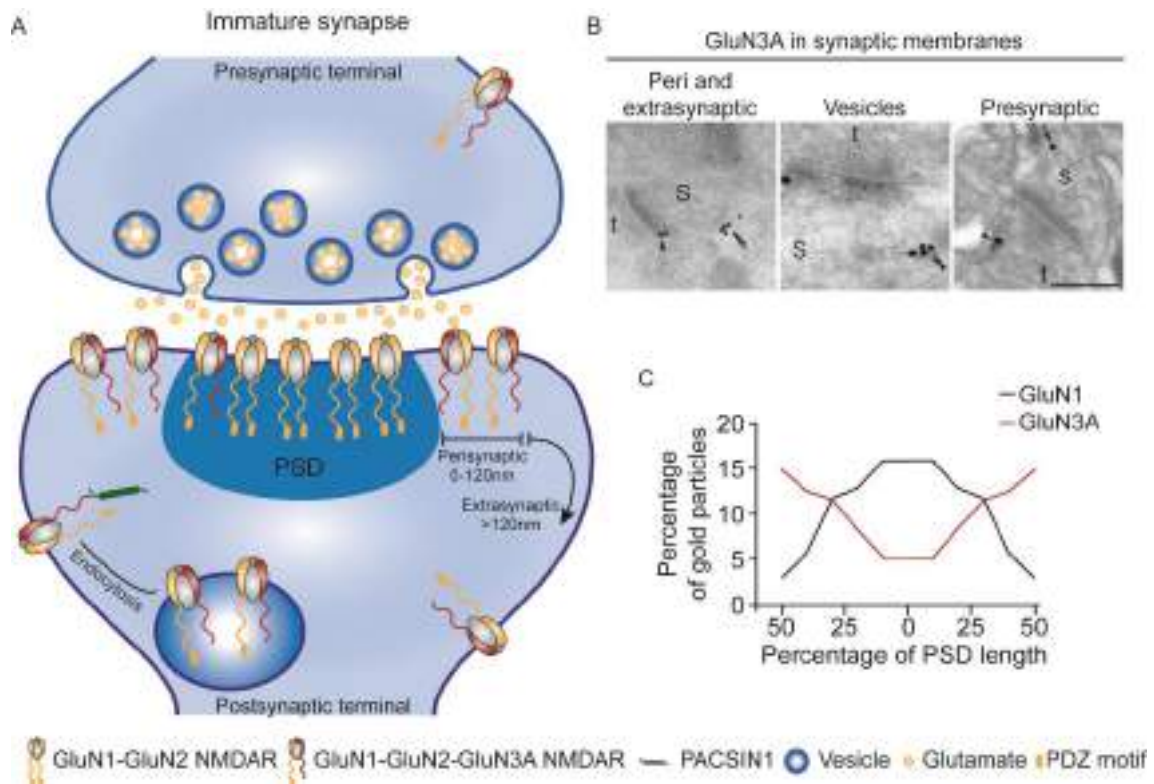


Figure 9. Location of GluN3A-containing NMDARs at the synapse. (A) Diagram showing differential membrane distribution of GluN3A-containing, mostly in perisynaptic, extrasynaptic and vesicle regions, and GluN3A-lacking NMDARs (mostly anchored to the PSD via interaction with C-terminal PDZ-domain). Diagram also illustrates presence of GluN3A NMDARs in presynaptic membranes and endocytosis pathway of non-conventional NMDARs by PACSIN1 protein. (B) EM micrographs showing immunoparticles indicating the presence of GluN3A-containing NMDARs in perisynaptic, extrasynaptic areas and in vesicles in adult rat CA1 hippocampal dendritic spines. In adult mice GluN3A also appears in axonal presynaptic membranes in medial prefrontal path input to dentate granule cells. Scale bar: 200 nm. (C) Tangential distribution of immunoparticles for GluN3A and GluN1 subunits along the PSD of CA1 hippocampal synapses where GluN3A-containing NMDARs are abundant in the periphery of the PSD. In contrast, immunoparticles for GluN1 appear mostly at the centre of the PSD. Part B is adapted from Perez-Otano *et al.*, 2006 and Savtchouk *et al.*, 2019; Part C is adapted from Perez-Otano *et al.*, 2006.



### 2.2.5.3 Areas and cell types with GluN3A expression.

In humans, GluN3A expression appears from embryonic stages in the marginal and ventricular zones, spinal cord and also in some cortical regions, where transient GluN3A levels can be detected during the second trimester of gestation (Eriksson *et al.*, 2002; Mueller *et al.*, 2003; Eriksson *et al.*, 2007; Nilsson *et al.*, 2007). Adult GluN3A levels are retained in regions or specific neuronal populations of cerebral cortex, subcortical forebrain, caudate-putamen, midbrain and hindbrain (Nilsson *et al.*, 2007; Marco *et al.*, 2013).

Analysis of GluN3A murine expression across the CNS has focused on postnatal ages, but initial studies found mRNA levels at embryonic stages in specific areas such as hippocampus, spinal cord, pons, thalamus, cortical neuroepithelium and medulla (Ciabarra *et al.*, 1995). In the first and second postnatal weeks, GluN3A appears in cortex, thalamus, hippocampus, olfactory bulb, piriform cortex, cerebellum, entorhinal cortex, striatum, amygdala, retina and medial habenula (Ciabarra *et al.*, 1995; Sucher *et al.*, 1995; Sun *et al.*, 1998; Al-Hallaq *et al.*, 2002; Wong *et al.*, 2002; Zhang *et al.*, 2002; Sucher *et al.*, 2003; Marco *et al.*, 2013; Otsu *et al.*, 2019). Although GluN3A expression is well characterized in glutamatergic neurons in cortex or CA1, it has also been detected in retinal ganglion cells, in trigeminal neurons and Sst GABAergic interneurons in visual cortex (Zhang *et al.*, 2002; Sucher *et al.*, 2003; Ishihama *et al.*, 2006; Pfeffer *et al.*, 2013). Expression has also been reported in human astrocytes and oligodendrocytes (Lee *et al.*, 2010; Jantzie *et al.*, 2015). GluN3A appears in high levels in oligodendrocyte precursors relative to other stages of their maturation (Salter *et al.*, 2005; Burzomato *et al.*, 2010; Zhan *et al.*, 2014). However, the available information continues to be sparse and a detailed analysis has been lacking.

### 2.2.6 GluN3A-NMDARs gate synapse and circuit maturation

Synapse networks build information bridges between neurons. Synapse formation occurs early in development (mostly *in utero*) and generates neuronal networks highly interconnected by weak, labile synapses. Circuits are later

refined by neuronal activity and sensory experience to yield circuits that respond to the individual environment. The refinement occurs through selective stabilization and elimination of synapses and associated dendritic spines. This process takes place throughout life but is particularly intense during critical periods of postnatal development (Rakic *et al.*, 1986; Holtmaat *et al.*, 2005; Zuo *et al.*, 2005). Conventional NMDARs have been implicated in controlling the balance between spine loss or maintenance, which has been proposed to depend on GluN2B-GluN2A ratios (Barria *et al.*, 2002; Perez-Otano *et al.*, 2004; Gambrill *et al.*, 2011).

Newer studies point towards a more prominent role of GluN3A-NMDARs in synaptic refinements through negatively modulating synaptic maturation and stabilization (Figure 10). Spine density analysis in young GluN3A-knockout (GluN3A KO) mice revealed a two-threefold increase in the number of synapses (Das *et al.*, 1998). Enhanced spine densities were associated with an earlier onset of long term potentiation (LTP) and accelerated emergence of GluN2A-NMDARs and AMPA receptors, both considered markers of synaptic maturation (Henson *et al.*, 2012). In contrast, prolonging expression of GluN3A beyond its physiological expression window reduces synaptic NMDAR currents, LTP (Tong *et al.*, 2008; Kehoe *et al.*, 2014) and spine densities in hippocampal CA1 pyramidal neurons (Roberts *et al.*, 2009). EM studies found GluN3A to be restricted to small and immature synapses, but absent from large ones (PSD length larger than 250 nm) (Roberts *et al.*, 2009). Consistent with these findings, an analysis of spine turnover demonstrated that the bidirectional changes in spine density reflect the ability of GluN3A to decrease spine stability and promote pruning (Kehoe *et al.*, 2014). Much milder increases in spine density were found in cortical neurons of adult GluN3A KO mice compared to the big changes seen in juvenile stages, which demonstrates a direct involvement of GluN3A during development (Das *et al.*, 1998; Marco *et al.*, 2013).

The behavioural consequences of GluN3A level modification are less understood. GluN3A KO mice show increased prepulse inhibition, but phenotype normalizes later on (Brody *et al.*, 2005). Enhanced spatial memory and object recognition have also been reported, but is not clear whether is due

to lack of GluN3A in juvenile or adult stages (Mohamad *et al.*, 2013). In mice in which GluN3A expression is prolonged, long-term memory storage is disrupted, but not memory acquisition, likely reflecting impaired structural plasticity (Roberts *et al.*, 2009).

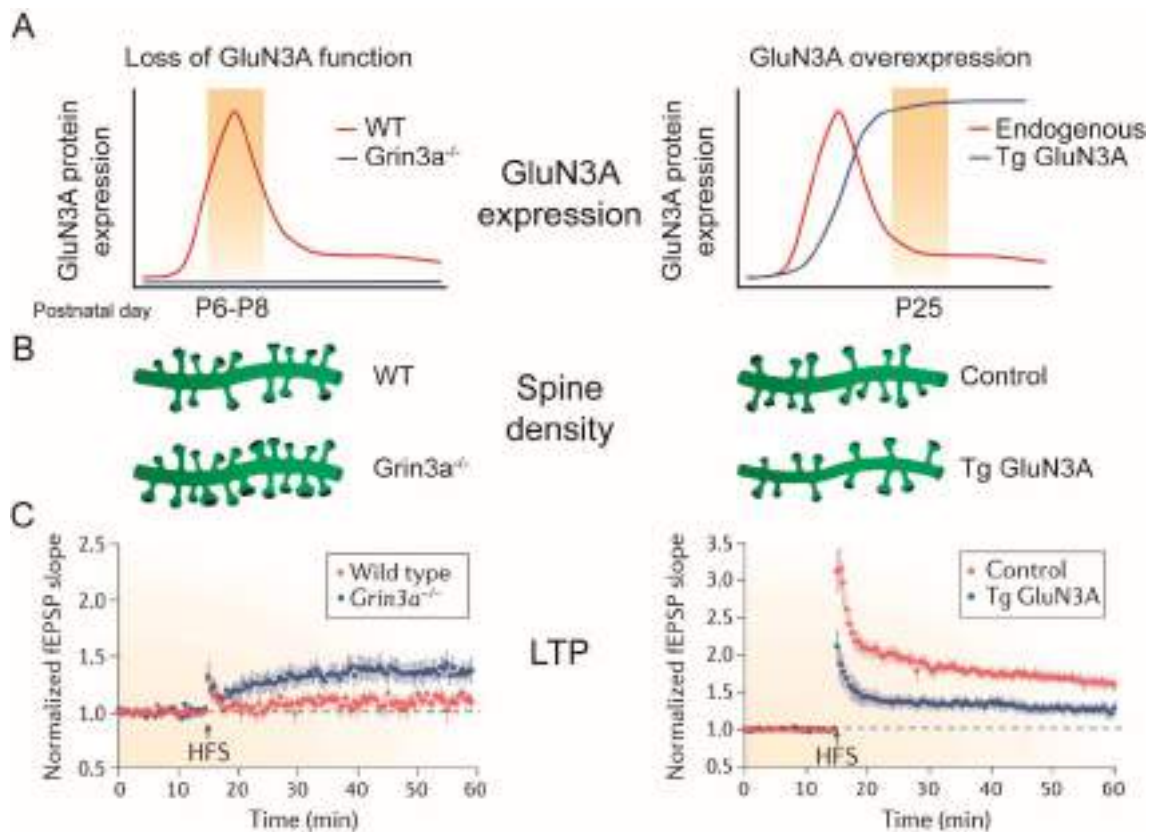


Figure 10. GluN3A-containing NMDARs in synapse plasticity and maturation. (A) Graphs show GluN3A expression time course in WT (red line), KO (*Grin3a*<sup>-/-</sup>) and transgenic mice in which GluN3A expression is prolonged (Tg GluN3A) (blue lines). The effects of loss (left panels) and gain (right panels) of GluN3A function were analysed at postnatal days (P6-P8) and P25 (when endogenous GluN3A protein level is highest or largely down-regulated, respectively). GluN3A expression was prolonged using the calcium/calmodulin-dependent protein kinase type 2 $\alpha$  (Camk2 $\alpha$ ) promoter. (B) Schematic drawing show dendritic segments from cortical neurons of GluN3A KO mice (left panel) which had increased density of spines with large spine heads, indicative of a mature morphology. Conversely, dendritic spine size and density were reduced in transgenic mice with GluN3A prolonged expression (TgGluN3A) (right panel). (C) *Grin3a*<sup>-/-</sup> CA1 neurons present an increased LTP evoked by high-frequency stimulation (HFS) of Schaffer collaterals (100Hz for 1 second) (left panel). Prolonging GluN3A expression reduced the magnitude of CA1 LTP measured at P25 (right panel). fEPSP, field excitatory postsynaptic potential. Modified from Perez-Otano *et al.*, 2016.

### 2.2.7 GluN3A in diseases

Several disorders are characterised by a loss of dendritic spines, and GluN3A implication has been suggested. To date, increased GluN3A levels have been causally linked to loss of synaptic connections in HD (Marco *et al.*, 2013). GluN3A-NMDAR levels are also increased in areas of the brain related to alcoholism or substance addiction, where they might be involved in formation of robust memories underlying relapse (Yuan *et al.*, 2013; Jin *et al.*, 2014; Yang *et al.*, 2015; Huang *et al.* 2017; Chen *et al.*, 2018; Chen *et al.*, 2020). Increased GluN3A levels have also been found in prefrontal areas in schizophrenic patients where elevated spine pruning can be observed (Glantz *et al.*, 2000; Mueller *et al.*, 2004). Interestingly, increased levels of GluN3A expression turned out to be neuroprotective in ischemic stroke, mitochondrial damage or striatal lesion with the neurotoxin 3-nitropionic acid (Nakanishi *et al.*, 2009; Henson *et al.*, 2010; Martinez-Turrillas *et al.*, 2012).

#### 2.2.7.1 GluN3A in HD

As previously mentioned, HD is characterised by spine loss in MSNs and this alteration occurs from very early stages. Work from our lab demonstrated that GluN3A levels are abnormally elevated in striatum samples of HD patients and of HD animal models including R6/1, YAC128 and knock-in mice models (Marco *et al.*, 2013). The accumulation of GluN3A-NMDARs was observed in synaptic plasma membranes without alterations at the mRNA levels, pointing towards a defect in trafficking. At a mechanistic level, the trafficking defect was identified as defective endocytosis due to sequestration of the dedicated GluN3A endocytic adaptor PACSIN1 by mHTT (Perez-Otano *et al.*, 2006; Marco *et al.*, 2013).

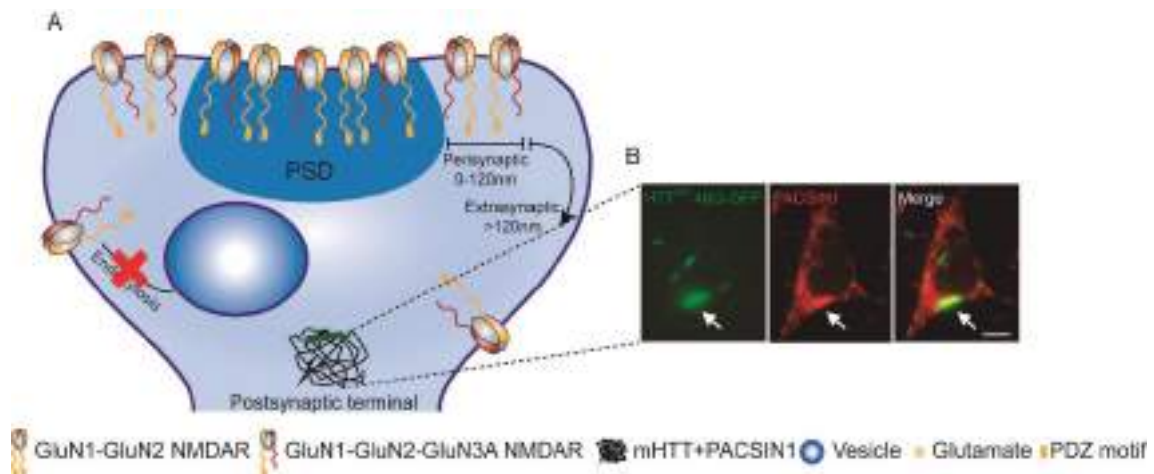


Figure 11. Glu3A-containing NMDARs location in HD dendritic spines. (A) Diagram shows enhanced membrane levels of Glu3A-containing NMDARs in HD synapses compared to WT synapses (Figure 9). (B) Representative images of MSNs neurons transfected with HTT-exon1-46Q-GFP and stained for endogenous PACSIN1 demonstrate sequestration of PACSIN1 into mHTT aggregates. Arrows point to the localization of PACSIN1 kidnapped by HTT-exon1-46Q in cytoplasmic aggregates. Scale bar: 5  $\mu$ m. Modified from Marco *et al.*, 2013.

Importantly, dendritic spine loss in MSNs was prevented by genetic deletion of Glu3A. The prevention of loss in spine numbers was associated with major improvement in striatum-dependent motor symptoms. For instance, in rotarod and vertical pole tasks, YAC128 mice showed an evident motor impairment that was rescued by genetic Glu3A deletion (Marco *et al.*, 2013). In the swimming T-maze, that test procedural learning and memory, YAC128 mice show learning defects in comparison with YAC128x*Grin3a*<sup>-/-</sup> mice, that performed as well as WT mice. All these data provide causal demonstration of aberrant Glu3A expression in synaptic and motor HD alterations (Figure 12).

### 3. Gene silencing

#### 3.1. RNA interference (RNAi)

Several processes can modify gene expression in cells. Post-transcriptional RNA silencing, mediated by small non-coding RNAs of 20–35 nucleotides that can trigger the silencing of complementary RNA sequences, is an important and

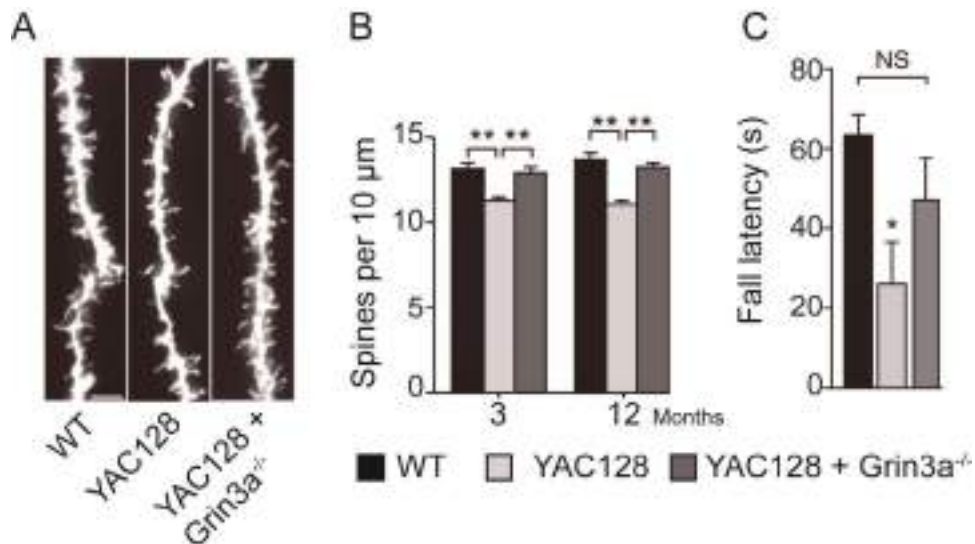


Figure 12. Genetic deletion of GluN3A in YAC128 prevents dendritic spine density loss and ameliorates motor dysfunction. (A) Dendritic segments from Golgi-impregnated MSNs of 3-month-old WT, YAC128 and YAC128 × *Grin3a*<sup>-/-</sup> mice. Scale bar: 3 μm. (B) Quantification of spine densities in MSNs from mice of the indicated ages and genotypes. (C) Fall latency from an accelerating rotarod for 10- to 12-month-old mice of the indicated genotypes. Modified from Marco *et al.*, 2013.

evolutionarily conserved form of gene regulation in eukaryotes (Ecker *et al.*, 1986; Napoli *et al.*, 1990; Fire *et al.*, 1998). Primary microRNAs (pri-miRNAs) are RNA transcripts encoded by the genome of the cell (Borchert *et al.*, 2006). They contain self-complementary as well as non-complementary segments which generate the characteristic hairpin shape with some internal mismatches along the duplex. They are later processed in the nucleus by the Drosha-DGCR8 complex into miRNAs precursors (pre-miRNA), and exported to the cytosol by exportin-5 (Lee *et al.*, 2003; Yi *et al.*, 2003; Gregory *et al.*, 2004; Han *et al.*, 2004). Mature miRNAs are generated by the catalytic action of a ribonuclease complex containing Dicer (Provost *et al.*, 2002). Then, the resulting 19-25 nucleotides-long miRNA duplexes, that shows an imperfect stem-loop secondary structure, associate with the RNA-induced silencing complex (RISC) (Khvorova *et al.*, 2003), where the antisense “guide” single strand (ssRNA) recognise the target transcript (Schwarz *et al.*, 2003), while the sense strand is degraded. Inhibition of mRNA expression can occur in two ways. If the complementarity between miRNA and mRNA is perfect or near

perfect, the process culminates with the transcript cleavage, whereas imperfect base pairing causes translational repression and mRNA destabilization (Lewis *et al.*, 2005; Guo *et al.*, 2010).

### 3.1.1 Short hairpin RNA (shRNA)

shRNA is a widely used tool that takes advantage of the cellular machinery in order to knock down the expression of genes of interest. shRNA technology was developed to mimic pre-miRNAs, and its function (Zeng *et al.*, 2002; Chung *et al.*, 2006). shRNAs are ssRNA molecules containing the antisense guide bp sequences (complementary to the target mRNA) and a sense sequence connected by a loop of unpaired nucleotides. shRNAs are encoded by exogenous plasmid or viral DNA and synthesised by the host cell under the control of polymerase III (Pol III) promoters U6 or H1 (Paul *et al.*, 2002; Sui *et al.*, 2002). shRNAs can be processed by Dicer, giving rise to small interfering RNAs (siRNA) that tap into the cellular mechanisms described above (Borel *et al.*, 2014; Bofill-De Ros *et al.*, 2016). The greater use of shRNA regarding its homolog in function, siRNA, is because physicochemical properties of siRNAs such as size, negative charges, and large molecule weight make it unstable (Wang *et al.*, 2010). Furthermore, the siRNAs can induce type I interferon responses (Kim *et al.*, 2007; Tseng *et al.*, 2009).

A main limitation of therapies using RNAi is to achieve efficient delivery to target cells. To facilitate the delivery of RNAi, different methods have been developed such as non-viral particles and viral vectors (Davidson and McCary 2011). shRNA can be linked to aptamers and cholesterol particles or introduced into nanoparticles, but this approaches would require of successive administrations, and they broad cell-type delivery, so they are not the ideal method to direct gene silencing to specific cell populations (Soutschek *et al.*, 2004; Kumar *et al.*, 2007; Dassie *et al.*, 2009). Different types of viruses have been used for the delivery of shRNA, but among them, lentivirus and adeno-associated virus (AAV) stand out among all because their low immunogenicity (Mingozzi and High 2013; Annoni *et al.*, 2018). But, lentivirus generally integrate their genomes into transcriptionally active chromatin of the host cell and this

could inactivate a tumour suppressor gene or activate an oncogene (Lombardo *et al.*, 2007). To overcome mutagenesis, AAVs are one of the most promising approaches for the delivery of shRNA.

### 3.2. AAVs

AAVs have many advantages over other systems for gene transfer in clinical applications (Lentz *et al.*, 2012). AAV belongs to the *Parvoviridae* family and require co-infection by a helper virus (adenovirus or herpesvirus) for efficient replication. Its single-stranded DNA (ssDNA) genome is 4.7 Kb-long and is encapsulated in a small (20-25nm) icosahedral capsid (Hoggan 1970; Berns 1990; Berns *et al.*, 1996). The AAV genome consists of two genes flanked by inverted terminal repeats (ITRs) (Hermonat *et al.*, 1984). Cap gene encodes the viral capsid proteins VP1, VP2 and VP3, which facilitate virion binding to cell surface receptors (Tratschin *et al.*, 1984; Ruffing *et al.*, 1992; Ni *et al.*, 1994; Young *et al.*, 2000). The other gene, Rep, encodes four regulatory proteins (Rep78, Rep68, Rep52 and Rep40) involved in replication and packaging of the genome (Chejanovsky and Carter, 1989; Weitzman *et al.*, 1994). There are 12 serotypes (AAV1-12), differentiated by capsid protein motifs that bind specific cell surface receptors for cell attachment, and more than one hundred variants of AAVs (Ikezu, 2015). AAVs recognize a variety of proteinaceous receptors and glycan attachment factors to be internalized by caveolar endocytosis, micropinocytosis, via clathrin-mediated endocytosis or by the clathrin-independent carriers (Bartlett *et al.*, 2000; Sanlioglu *et al.*, 2000; Pillay *et al.*, 2017). Endosomal vesicle pathways converge in the Golgi apparatus (Bantel-Schaal *et al.*, 2002; Nonnenmacher *et al.*, 2012; Nonnenmacher *et al.*, 2019). During the internalization process, virus can escape from the membrane complex with the intact capsid and travel to the nucleus by host factors (Bartlett *et al.*, 2000; Johnson *et al.*, 2009; Popa *et al.*, 2015). Viral ssDNA stays as a genetic unit of replication in the host cell that exist extra-chromosomally called episome (Chen *et al.*, 2001; Nakai *et al.*, 2001).



### 3.2.1. Recombinant AAVs (rAAVs)

rAAVs were generated by genetic manipulation of AAVs to allow delivery of a specific gene or genetic cassette into cells. The transgene cassette is incorporated to the ssDNA between the ITRs replacing rep and cap genes (see Materials and methods) (Surace *et al.*, 2007). Different serotypes can infect different cell types; one example is rAAV9 that can infect cells from liver, heart, muscle, brain and skeletal muscle, while rAAV5 mostly infect liver cells (Zincarelli *et al.*, 2008; Rajapaksha *et al.*, 2019). The use of rAAV *in vivo* provides several advantages:

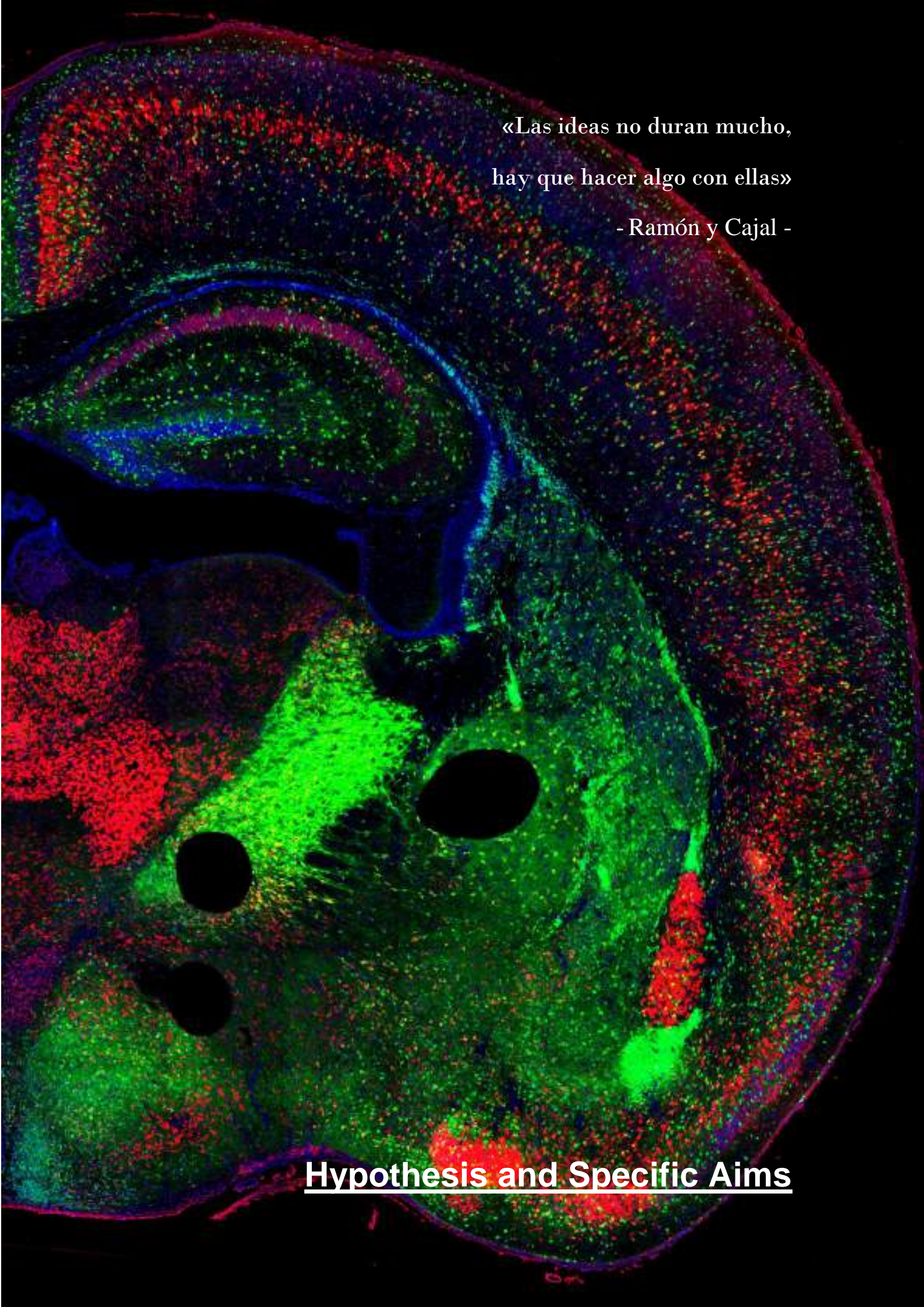
- Reduced toxicity, as AAVs induce a mild immune response (Hutson *et al.*, 2012).
- Low probability of mutagenesis, as genetic material stays as an episome (Berns 1990).
- Wide range of cell type infectivity (Zincarelli *et al.*, 2008)

In contrast, the major caveat of rAAV is its small packaging capacity, between 4.1 and 4.9 kb, which allows a maximum of 5.2 kb of genetic material, including the ITRs (Dong *et al.*, 1996; Hermonat *et al.*, 1997; Wu *et al.*, 2010). Gene silencing can be induced in a specific cell type by selecting an AAV serotype that mainly infects that cell population.

### 3.3 shRNA-AAVs as a therapeutic tool

RNAi has become a powerful tool to investigate and treat a variety of diseases (e.g., viral infections, cancer, dominant genetic disorders) (Davidson *et al.*, 2011), and specifically shRNAs have been widely used in preclinical studies of different pathologies in disease animal models (Borel *et al.*, 2014). For instance, shRNA-based approaches have been shown to efficiently knock-down ataxin-1 and *Htt* gene expression in neurodegenerative spinocerebellar ataxia type 1 and HD mouse models respectively, with aid of rAAV vector delivery into the mouse brain (Boudreau *et al.*, 2011; Keiser *et al.*, 2016), leading to a reduction of symptoms caused the specific mutation.

According to the U.S. clinical trials database, of the 66 RNAi-based finished or ongoing clinical trials, 20 of them used shRNAs (clinicaltrials.gov). rAAV delivery is the gene transfer method of choice in at least 231 ongoing clinical trials. Of all these clinical trials, 43 use rAAVs as a delivery system targeting brain areas by neurosurgery in neurodegenerative disorders such as dementia, Parkinson, Alzheimer and Huntington diseases. In the latter, different doses of rAAV5 ( $6 \times 10^{12}$ - $6 \times 10^{13}$  vg/subject) carrying a miRNA against *HTT* are administered in adults with early manifest Huntington disease by stereotaxic intrastriatal infusion. This clinical trial aims to explore safety, tolerability and efficacy of the treatment. Although the estimated date of completion of this study is the year 2026, previous studies carried out in transgenic mouse and minipig models indicated an improvement in the motor symptoms observed in those animals as a result of the reduction in the amount of the mHTT (Evers *et al.*, 2018; Spronck *et al.*, 2019). Taking this information together, the use of rAAVs as vectors to deliver shRNAs to inhibit genetic expression provides a promising tool for the development of medical treatments for a wide range of diseases, especially those caused by overexpression of a known gene.



«Las ideas no duran mucho,  
hay que hacer algo con ellas»

- Ramón y Cajal -

Hypothesis and Specific Aims





**First chapter.** “RNAi-Based GluN3A Silencing Prevents and Reverses Disease Phenotypes Induced by Mutant huntingtin”

Building upon previous work from the laboratory that demonstrated a causal relationship between aberrant expression of GluN3A subunits and HD, our goal was to validate the therapeutic benefit of suppressing/antagonizing GluN3A function. To do this we designed a rAAV-based gene therapy strategy to silence GluN3A by RNAi in vulnerable populations, and evaluated its efficacy in a mouse model of HD. The work was structured in 3 specific objectives:

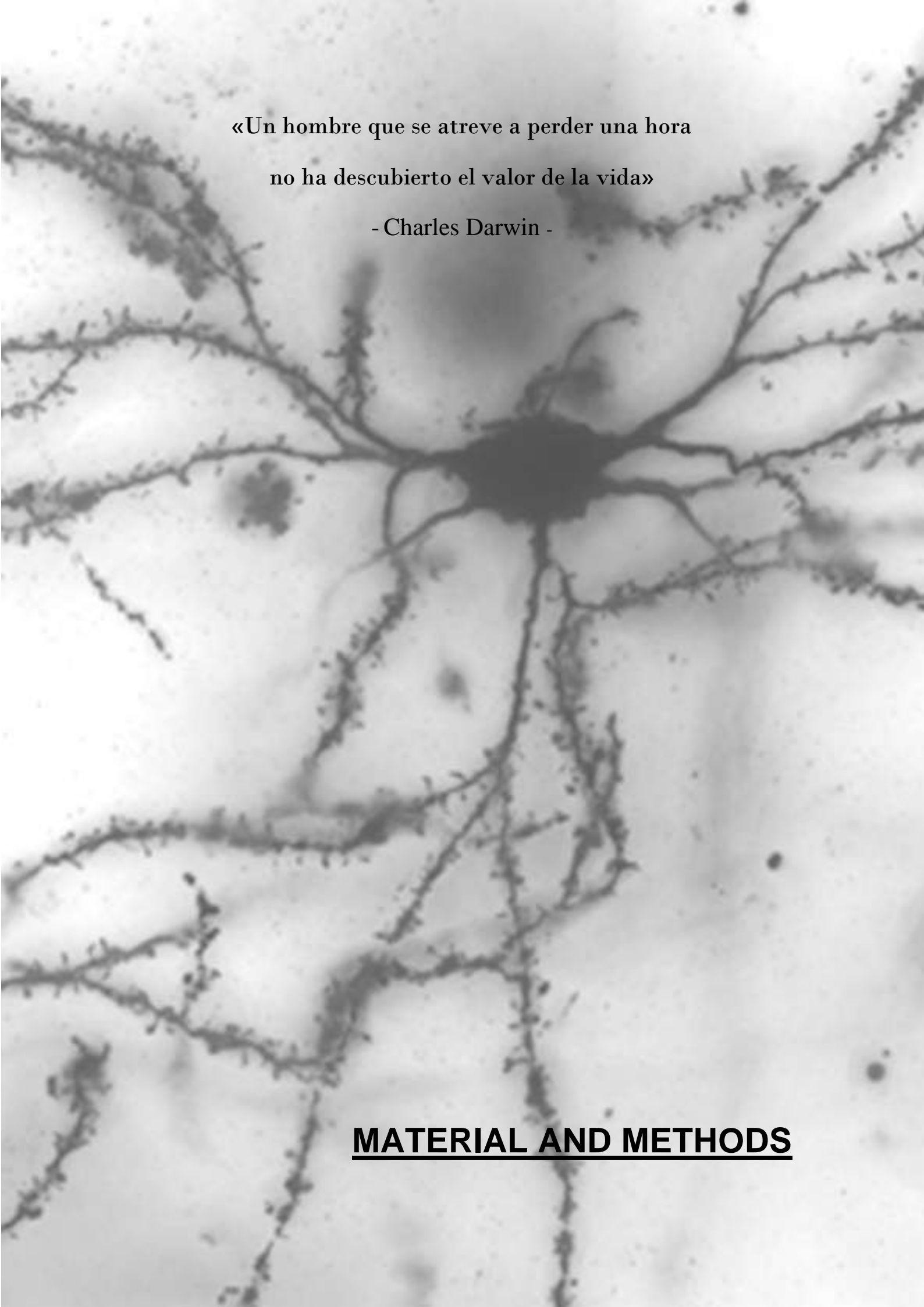
- 1) To set-up and validate a GluN3A silencing strategy based on intrastriatal rAAV injection to deliver shGluN3A to MSNs.
- 2) To define a therapeutic window of opportunity over which synapse loss can be reversed.
- 3) To evaluate the effects of GluN3A silencing on HD-like motor symptoms characteristic of YAC128 mice.

**Second chapter.** “Temporal Dynamics and Neuronal Specificity of *Grin3a* Expression in the Mouse Forebrain”

GluN3A is typically expressed during postnatal development with much lower levels observed in adult brains. This suggested that strategies based on GluN3A silencing would lack the major side-effects of previously failed therapies targeting other NMDAR subtypes. However, information on specific patterns of GluN3A expression during development and especially in adulthood was sparse. In this context, the goal of this part of the thesis was to define in detail the temporal patterns of GluN3A expression in developing and adult mouse brains and to identify the cellular types that express GluN3A. Currently available antibodies do not work well in immunohistochemistry and show non-specific signal in adult brains, and thus we used a ISH approach. Our specific aims were:

## Hypothesis and Specific Aims

- 1) To characterise the extent of *Grin3a* mRNA down-regulation into adulthood.
- 2) To generate a detailed regional map of *Grin3a* expression in young and adult brains.
- 3) To analyse temporal patterns of *Grin3a* expression and down-regulation during postnatal periods and provide a roadmap to investigate GluN3A functions in experience-dependent refinements.
- 4) To study *Grin3a* expression across different cell populations.



«Un hombre que se atreve a perder una hora  
no ha descubierto el valor de la vida»

- Charles Darwin -

**MATERIAL AND METHODS**





### 1. AAV-shGluN3A vector

To study the effect of GluN3A silencing in the striatum in HD mouse models we used a shRNA that targets rat and mouse GluN3A (shGluN3A, Table 2, target sequence in bold).

The efficiency and specificity of silencing had been previously tested in primary cortical neurons using a lentivirus construct expressing the shGluN3A (Yuan *et al.* 2013). Endogenous GluN3A protein expression was largely reduced in a dose-dependent manner without affecting postsynaptic proteins or other NMDAR subunits (Figure 13).

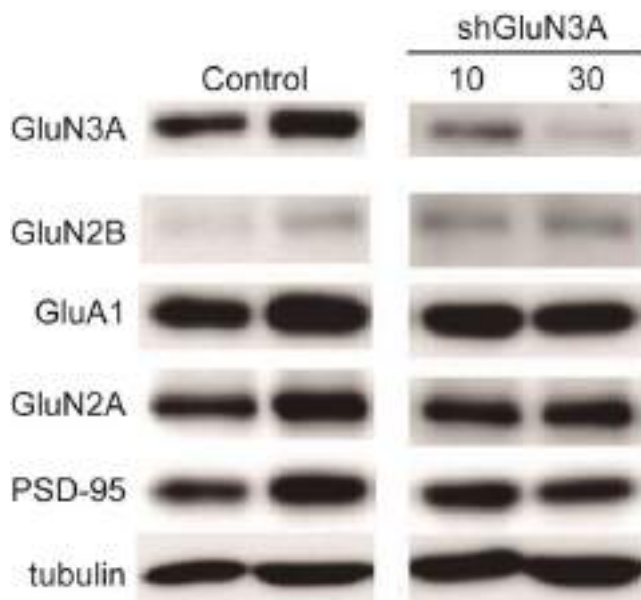


Figure 13. ShGluN3A characterization. Effect on GluN3A protein expression levels in cultures cortical neurons by the transduction of shGluN3A, showing the specific down-regulation of GluN3A expression without effects on other proteins analysed. Adapted from Yuan *et al.*, 2003.

Two shRNA promoters are generally used, U6 and H1. Although U6 promoter is more efficient (Mäkinen *et al.*, 2006) it also presents more cytotoxicity due to sequestration of endogenous silencing machinery and the appearance of off-target effects (An *et al.*, 2006; Sun *et al.*, 2013). Because of the U6 cytotoxicity, the H1 promoter was selected at the time of designing the AAV vector. shGluN3A, under the H1 promoter, was subcloned into a pAAV vector that contained EGFP (as a reporter gene) under the cytomegalovirus (CMV) promoter to enable visualization of infected cells (Figure 14). Virus

production was done by Vector Biolabs. A control shRNA was also purchased from Vector Biolabs and used as a control (Table 2).

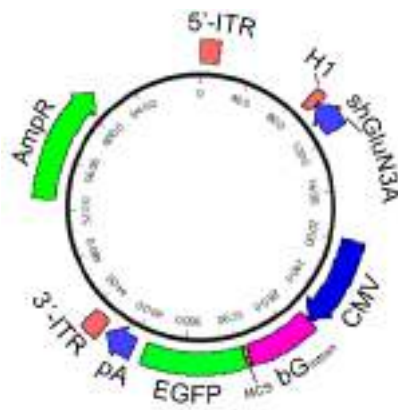


Figure 14. Schematic drawing of the generated rAAV plasmid carrying shGluN3A.

## 2. rAAV production

The production of the rAAVs used was made by transfection of three different plasmids into HEK293T cells (Figure 15):

1. H1-shGluN3A-CMV-EGFP sequence flanked by AAV2 ITRs.
2. Plasmid encoding rep and cap genes.
3. Plasmid that provides the genes isolated from helper adenovirus.

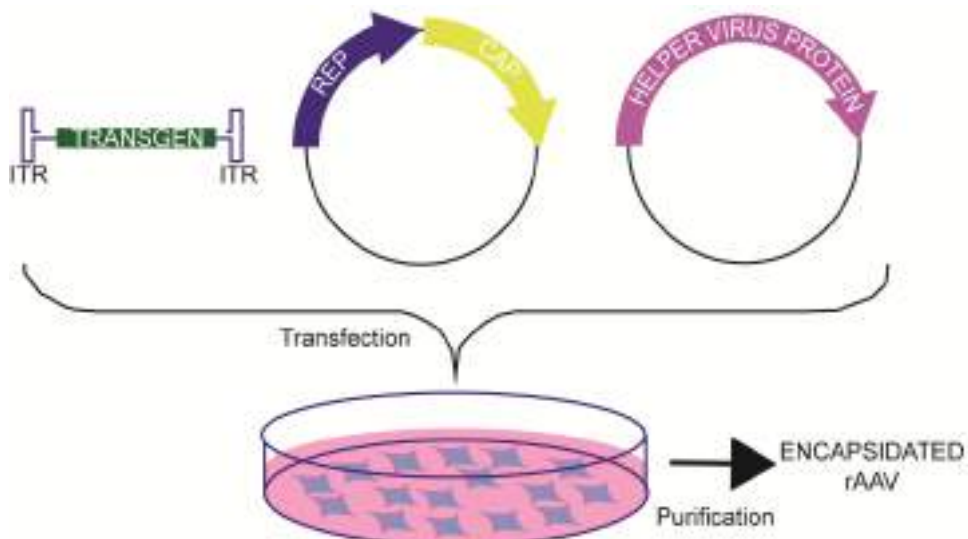


Figure 15. Schematic showing transfection of HEK293T cells with the 3 necessary plasmids to generate encapsidated rAAV. After cell lysis, rAAV are isolated by density gradient or

column purification (Penaud-Budloo *et al.*, 2018) and stored at  $-80^{\circ}\text{C}$  in phosphate buffered saline (PBS, pH 7.4) containing 5% glycerol.

The cap gene determines the serotype of the rAAV, so its variation allows us to obtain different rAAV serotypes. For our experiments 3 different rAAV serotypes (rAAV8, rAAV9 and rAAV10) were produced by the Vector Core Facility of the Universitat Autònoma de Barcelona for comparison of infection rates and neuronal selectivity. Once the best serotype (rAAV9) for our study was selected, the rAAV9-shGluN3A and shControl was produced by Vector Biolabs (Table 2), as mentioned.

Table 2. rAAV constructs used for cell infection.

Name	Capsid Serotype	Company	Insert	Physical Titer (gc/ml)
<b>rAAV8-CMV-GFP</b>	rAAV8	Vector Core Facility of The Universitat Autònoma de Barcelona (Spain)	CMV-EGFP	$2.35 \times 10^{12}$
<b>rAAV9-CMV-GFP</b>	rAAV9	Vector Core Facility of The Universitat Autònoma de Barcelona (Spain)	CMV-EGFP	$2.50 \times 10^{12}$
<b>rAAV10-CMV-GFP</b>	rAAV10	Vector Core Facility of The Universitat Autònoma de Barcelona (Spain)	CMV-EGFP	$2.50 \times 10^{12}$
<b>rAAV9-shGluN3A</b>	rAAV9	Vector Biolabs (Malvern, PA, USA)	CMV-EGFP-H1-shGluN3A (GATCCCCCTA <b>CAGCTGAGTTT</b> <b>AGAAATTCAAG</b> AGATTTCTAAA CTCAGCTGTAG TTTTAA)	$4.4 \times 10^{13}$
<b>rAAV9-shControl</b>	rAAV9	Vector Biolabs (Malvern, PA, USA)	CMV-EGFP-H1-shControl (CAACAAGATG AAAGCACCAAC TCGAGTTGGTG CTCTTCATCTT GTTGTTTTTT)	$3.2 \times 10^{13}$

### 3. Stereotaxic injections

Mice were anesthetized with an intraperitoneal injection of ketamine/xylazine (80/10 mg/kg) and placed in a World Precision Instruments stereotaxic frame. The scalp was shaved and a longitudinal incision was made to expose the skull surface. Two burr holes were drilled above the infusion sites with a hand drill (Figure 16). A 2  $\mu$ l virus suspension was stereotaxically injected with a 5 mL Hamilton syringe into one or both striata of anesthetized mice according to the Paxinos and Franklin mouse brain atlas (Paxinos *et al.*, 2001). The infusion rate was 200 nL per minute with a World Precision Instruments single-syringe infusion pump (SP100iZ), and the needle remained in place for 5 minutes after infusion for vector absorption before removal of the syringe. Finally, the site was stitched closed.

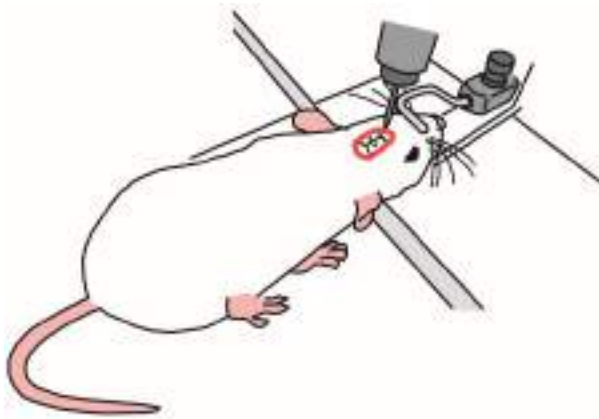


Figure 16. Schematic of mice placed into a stereotaxic frame with the skull surface exposed and two burr holes in the bone.

### 4. Spine measurement by Golgi impregnation

Mice were sacrificed, their brains extracted from the skull, and fresh brain hemispheres were incubated in Golgi-Cox solution (1% potassium dichromate; 1% mercury chloride; 0.8% potassium chromate) for three weeks in the dark. Then, tissue was washed with water several times and a final wash was made with 90% ethanol for 30 minutes to avoid “needle-like” precipitates. In a vibratome, the hemispheres were cut into 200  $\mu$ m-thick slices in 70% ethanol solution and stored no longer than 24 hours in the same solution. A reduction step with 16% ammonia solution for 1 hour was used to produce metallic mercury and the slices were fixed by incubation with 1% sodium thiosulfate solution. Slices were mounted in Superfrost slides and dehydrated through

successive immersions in increasing concentrations of alcohols. Coverslips were mounted using DPX medium.

The slides were randomly coded, and the experimenter was blind to genotype and virus injection during image acquisition and analysis. Bright-field images of Golgi-impregnated MSNs were captured with a Nikon DXM 1200F digital camera attached to a Nikon Eclipse E600 light microscope using 100x oil objective. Only fully impregnated MSNs with their soma and at least four orders of dendrites entirely within the thickness of the section were included in the analysis. Image z-stacks were taken every 0.75  $\mu\text{m}$  and analysed with Fiji software. A total of 2.536 dendritic segments (25–124  $\mu\text{m}$  long; average, 50.67  $\mu\text{m}$ ) were traced through different layers of the stack and spines counted manually. Spine density per neuron was calculated in as many tertiary dendrites of length  $>25$   $\mu\text{m}$  as could be unequivocally identified (range, 7–15 dendrites).

## 5. Western blot

### 5.1 Protein sample preparation

Mice were sacrificed and both striata were dissected. Striata were weighed (w) and homogenized into 10 volumes (w/v) of cooled homogenization buffer (0.32 M sucrose; 10 mM HEPES pH 7.4; 2 mM EDTA) supplemented with protease inhibitors (Roche). All the procedures were done at 4°C. Homogenation was carried out using 10-12 strokes of a motor-driven glass-teflon homogenizer (Heidolph RZR-1, position 3, 600-800 rpm). Samples were then centrifuged at 1000xg for 15 minutes to remove the pelleted nuclear fraction. Supernatants were sonicated (20 pulses) with a tip-sonicator (Branson Sonifier 250; duty cycle 20, output 3), and centrifuged at 16200xg for 20 minutes. Samples were stored at -80°C.

### 5.2 SDS-PAGE electrophoresis

Protein concentrations were measured using the BCA protein assay (Pierce). Twenty to fifty micrograms of total protein were resolved using sodium dodecyl

sulphate-polyacrylamide gel electrophoresis (SDS-PAGE). Gels were cast manually using Mini-Protean set (Bio-Rad). The resolving gel (Acrylamide/bisacrylamide from 5 to 10 %, 10% SDS; 1.5 M Tris-HCl pH 8.8; 10% ammonium persulfate; 0.05% TEMED) was added smoothly between two glass plates spaced 1.5 mm. A 10-well comb was placed into the stacking gel (Acrylamide/bisacrylamide from 4%; 10% SDS; 0.5 M Tris-HCl pH 6.8; 10% ammonium persulfate; 0.05% TEMED) just after being poured over resolving gel before it polymerized. After gel had polymerized glass plates containing the gel were placed into de electrophoresis module assembly and filled with electrophoresis buffer (20 mM Tris-HCl; 1% SDS; 190 mM glycine). Samples were dissolved in 4x Laemmli sample buffer (125 mM Tris-HCl; 4% SDS; 20%  $\beta$ -mercaptoethanol; 20% glycerol; 0.004% bromophenol blue), heated at 95°C for 5 minutes and loaded into the wells along with a molecular weight marker (BlueStar Prestained Protein marker plus, Nippon Genetics # MWP04). Electrophoresis was carried out at 80V until the samples entered the resolving gel and then at 100V for 1-2 hours.

### 5.3 Protein transfer to PVDF membranes

After electrophoresis, gels were equilibrated in transfer buffer (10 mM glycine; 10 mM Tris-HCl; 5% methanol). Simultaneously, polyvinylidene difluoride (PVDF) membranes were activated with methanol for 5 minutes. Transfer sandwich was prepared within a gel holder cassette with fibre pads, Whatman filter papers, the gel and the PVDF membrane. The cassette placed into the electrode module with the gel facing the cathode end and filled with transfer buffer. Transference was carried out at constant 300 mA for 2 hours at 4°C. Once the proteins were transferred to the membrane this was briefly rinsed in water and stained in Ponceau S solution.

### 5.4 Immunodetection

Membranes were blocked with 5% skimmed milk in Tris-buffer saline pH 7.6 (50 mM Tris-Cl; 150 mM NaCl; 0.05% Tween-20) (TBS-T) at room temperature

(RT) for 1 hour and then incubated overnight at 4°C in primary antibody solution (1% skimmed milk in TBS-T) with the appropriate primary antibody (Table 3). The following day, the blot was rinsed and incubated with the appropriate horseradish peroxidase-conjugated secondary antibody (1:10000, GE Healthcare) in blocking solution for 1 hour at RT. Blots were developed using enhanced chemiluminescence (ECL) plus substrate (Pierce) and exposed to a film (GE Healthcare). Films were scanned with GS-800 imaging densitometer (Bio-rad) and individual bands were quantified after background subtraction using ImageQuant studio 5.2 (Molecular dynamics) software.

Table 3. Primary antibodies used for immunodetection in WB.

Antibody	Provider	Catalog number	Host	Dilution
<b>GluN1</b>	Millipore	MAB363	Mouse	1:2000
<b>GluN3A</b>	Jim.S. Trimmer (US Davis)	K35/40	Rabbit	1:100
<b>DARPP-32</b>	BD Biosciences	611520	Mouse	1:500

## 6. *In situ* hybridization

### 6.1 *Grin3a* mRNA cloning

#### 6.1.1 Riboprobe design and synthesis

We chose to study *Grin3a* expression by *in situ* hybridization (ISH) given the lack of good, specific antibodies. First, different riboprobes against the *Grin3a* mRNA were generated and tested. One of them was selected based on its sensitivity, specificity and because the sense sequence gave no signal (Figure 17). The *Grin3a* riboprobe is complementary to nucleotides 2853 to 3392 of mouse *Grin3a* mRNA (spanning 495 bp of the C-terminal domain, Accession number NM\_001033351.2).

Templates for synthesizing the *Grin3a* riboprobe were obtained by PCR from cDNA libraries of C57BL/6 hippocampus using the following primers: (5'-3')

Forward primer: GAACACATAGTGTACAGACTGC

Reverse primer: CTAGGATTCACAAGTCCGGTT

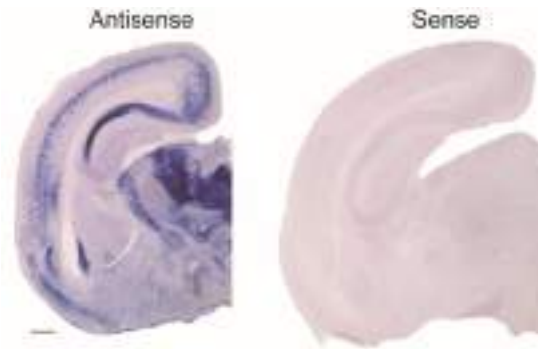


Figure 17. *Grin3a* riboprobe characterization. Representative ISH coronal sections images at P9 using antisense (left) and sense (right) riboprobe. Images show sensitivity and specificity. Scale bar: 500  $\mu$ m.

Plasmids for riboprobes against *Gad1* mRNA (bp 934-1786 of the *Gad1* cDNA, Accession number NM\_008077) were a gift from Dr. Jordi Guimer.

#### 6.1.2 Insert and vector digestion, and ligation.

To generate complementary overhanging ends, 2  $\mu$ g of insert and pBlueScript SK plasmid were digested with XhoI and EcoRI restriction enzymes in appropriate buffer conditions for 2 hours at 37°C. Linearized DNA and insert were run in a 0.8% agarose gel and the corresponding band of each were cut out. To remove agarose and obtain pure DNA, QIAquick gel extraction kit (Qiagen) was used.

For the ligation reaction, 70 ng of linearized vector DNA were mixed in a 1:3 molar ratio with the insert and 1  $\mu$ l of T4 DNA ligase in ligase buffer (New England Biolabs). The mix was incubated overnight at 16°C, and the ligase was inactivated by incubation at 70°C for 10 minutes.

#### 6.1.3 Bacterial transformation

Subcloning efficiency *Escherichia coli* (DH5 $\alpha$ ) cells (50  $\mu$ l) (Invitrogen) were transformed with 5 ng of ligation mixtures in Super Optimal broth with catabolite repression (SOC medium; 10 mM MgCl<sub>2</sub>; 20 mM Glucose) by incubation for 30 minutes in ice, followed by a 20-second heat shock (42°C) and 1-hour



incubation with SOC medium at 37°C under shaking (225 rpm). Twenty-five µl of the mix were seeded in LB-agar culture plate with 50 µg/ml of ampicillin.

#### 6.1.4 Plasmid amplification

Multiple bacterial colonies were picked and grown in LB medium with selection antibiotic and the plasmids were extracted using Qiagen Plasmid Maxi Preparation Kit (QIAGEN). The sequence of the plasmid was analysed using DNASTAR software.

#### 6.2 Riboprobe synthesis

To obtain riboprobes, we linearized each plasmid using 2 µl of restriction enzymes XhoI (for the *Grin3a* and *Gad1* mRNA antisense riboprobe, used to detect expression) or EcoRI (for the *Grin3a* and *Gad1* mRNA sense riboprobe, used as negative control) at 37°C for 2 hours in the appropriate buffer (New England Biolabs). For the synthesis of the riboprobes, 6 µg of linear plasmid was mixed with RNase-free water, transcription buffer, 2 µl of RNase inhibitors, 2 µl of T3 (for the *Grin3a* or *Gad1* mRNA antisense) or T7 (for the *Grin3a* or *Gad1* mRNA sense) polymerase and a nucleotides mix (Roche), in a total volume of 50 µl at 37°C for 2 hours. The nucleotide mix contains 10 mM ATP, 10 mM CTP, 10 mM GTP, 6.5 mM UTP and 3.5 mM UTP-Digoxigenin or UTP-Fluorescein. DNase enzyme (2 µl) was added for plasmid degradation before checking the riboprobe synthesis, by running a few µl of reaction product in a 1% agarose gel and measuring the amount of RNA in NanoDrop (One/OneC Microvolume UV-Vis Spectrophotometer; Thermo Fisher).

#### 6.3 Colorimetric ISH: Hybridization, immunodetection and amplification

After deep anesthesia with isoflurane, mice were transcardially perfused with 4% paraformaldehyde in phosphate buffered saline (PBS, pH 7.4) with a Masterflex L/S complete pump system. Brains were removed and post-fixed

overnight. Cerebra were embedded with 4% agarose in PBS solution, sectioned coronally with a vibratome in 100 µm-thick slices and stored in PBS at 4 °C. After heating the riboprobe for 10 minutes at 80°C to avoid loops, free-floating brain sections, previously permeabilized with detergent mix (1% NP40, 1% SDS, 0.5% Sodium Deoxycholate, 50 mM Tris pH 8.0, 1 mM EDTA and 150 mM NaCl) for 1 hour at RT, were incubated with antisense or sense digoxigenin-labeled riboprobes against *Grin3a* mRNA at 63°C overnight in hybridization buffer (50% formamide deionized; 2x saline-sodium citrate (SSC) pH 5.3; 50 µg/ml heparin; 50 µg/ml tRNA; 50 µg/ml Salmon Sperm DNA; 0.1% Tween-20). The following day, several washes for 2 hours with cleaning solution (50% formamide; 2x SSC pH 5.3; 1% SDS) at 63°C were necessary to remove non-specific binding mRNA-riboprobe. Later, slices were washed with 1x MABT (100 mM maleic acid; 150 mM NaCl; 190 mM NaOH; 0.1% Tween-20, pH 7.5) and subsequently incubated in blocking solution (2% Blocking Reagent and 20% sheep serum in MABT) for 1 hour to prevent non-specific antibody binding. Hybridized probes were detected using an alkaline phosphatase-conjugated anti-digoxigenin (Table 4). Slices were incubated in blocking solution with appropriate antibody overnight at 4°C. To remove non-bound antibodies, several washes in MABT buffer were made.

For visualization, sections were then incubated at RT during 6 or 22 hours in a solution containing nitroblue tetrazolium chloride (NBT) and 5-bromo-4-chloro-3'-indolyphosphate p-toluidine salt (BCIP) (purple color) substrates in NTMT buffer (100 mM NaCl; 100 mM Tris-HCl pH 9.5; 50 mM MgCl<sub>2</sub>; 1% Tween-20). Alkaline phosphatase catalyses a reaction that produces a coloured precipitate. After developing, reaction was stopped with several washes of PBS-T and post fixation step with 4% PFA in PBS was carried out. Slices were mounted in superfrost slides (Thermo Fisher) and dehydrated through successive washes with increasing concentrations of alcohols. Coverslips were mounted with DPX mounting solution.

## 6.4 FISH: Hybridization, immunodetection and amplification

Identical protocol to the described above was followed, except that sections were 80 µm-thick and they were incubated for 1 hour at RT in the dark with MABT buffer + 1% H<sub>2</sub>O<sub>2</sub> to avoid non-specific precipitates during the development step due to the activity of endogenous peroxidases. Sections were incubated with *Grin3a* mRNA digoxigenin-labeled riboprobes in hybridization buffer, followed by incubation with peroxidase-conjugated anti-digoxigenin (Table 4). A tyramide signal amplification (TSA) plus fluorescence kit was used for signal amplification and detection (Thermo Fisher, NEL744001KT). For that, slices were incubated in a mix with amplification buffer and Cy3 fluorochrome in a 1:100 dilution for 1 hour in the dark. In this step, horseradish peroxidase (POD) enzyme conjugated with antibodies catalyzes covalent deposition of fluorophores directly adjacent to the riboprobe. To remove non-specific fluorescence precipitates, the slices were rinsed in PBS for 1 hour and incubated with 4',6-diamidino-2-phenylindole (DAPI) (Invitrogen 1:50000) for 10 minutes at RT. Slices were mounted in superfrost slides (Thermo Fisher) and air-dried, and cover-slipped with fluorescence mounting medium (DAKO).

### 6.4.1 Double FISH

Double FISH was performed with dual hybridization: one probe was labeled with UTP-Digoxigenin and the other with UTP-Fluorescein (against *Grin3a* mRNA and *Gad1* mRNA respectively) followed by duplicated detection and amplification steps. For that, after *Grin3a* signal amplification and detection with Cy3 TSA plus fluorescence kit an incubation for 1 hour at RT in the dark with 1x PBS + 1% H<sub>2</sub>O<sub>2</sub> was carried out to remove endogenous peroxidase activity. The protocol continued as the first one using a different antibody (anti-fluorescein-POD, Table 4) and a different fluorochrome (Cy5).

Table 4. List of antibodies used for ISH

Antibody	Provider	Catalog number	Host	Dilution
<b>Digoxigenin-AP</b>	Roche	11093274910	Sheep	1:2000
<b>Digoxigenin-POD</b>	Roche	11207733910	Sheep	1:2000
<b>Fluorescein-POD</b>	Roche	11426346910	Sheep	1:2000

## 7. RNAscope

For RNAscope assays, the tissue was collected as indicated in the previous protocol and was immersed in 30% sucrose at 4°C and frozen in OCT. Frozen brains were sectioned at 14 µm with a cryostat and stored at -80°C. RNAscope® Multiplex Fluorescent Kit v2 (Advanced Cell Diagnostics) was used to perform *in situ* hybridizations with the following probes: *Grin3A-C1* (#551371), *GAD1-C2* (#400951-C2), *Slc17a7-C3* (*vGluT1*) (#416631-C3), *Sst-C3* (#404631-C3), and *tdTomato-C2* (#317041-C2). Briefly, slides were dried for 60 min at -20°C, washed in PBS for 5 min, then baked for 10 min at 60°C. The slides were post-fixed by immersing them in pre-chilled 4% PFA for 10 min in ice, followed by two rinses in diH<sub>2</sub>O. Slides were dehydrated for 5 min each in 50%, 70% and 100% ethanol, then dried for 5 min at RT. 5-8 drops of RNAscope hydrogen peroxide was applied to the slides for 10 min followed by diH<sub>2</sub>O washing. Then, slides were transferred to a container with RNAscope Target Retrieval Reagent and incubated at > 95°C for 5 min, followed by incubation in 100% alcohol for 3 min. After drying the slides at RT, they were treated with Protease III for 20 min at 40°C. After rinsing 2 times in diH<sub>2</sub>O, 1X target probe mixes were applied to the brain sections and incubated at 40°C for 2 hours in the HybEZ™ oven (Advanced Cell Diagnostics). Sections were then incubated with preamplifier and amplifier probes to develop HRP-C1, C2 and C3 signals with TSA Plus fluorophores (PerkinElmer) following the RNAscope® Multiplex Fluorescent Kit v2 user manual. After washing, sections were stained for 30 seconds with DAPI.

## 8. Immunohistochemistry

### 8.1 Immunohistochemistry in slices from injected mice

Animals were deeply anesthetized and transcardially perfused with 4% paraformaldehyde in 0.1 M phosphate buffer (PB) (pH 7.4). Brains were removed, post-fixed overnight, and stored in 30% sucrose in PB buffer at 4°C. Thirty-micrometer coronal sections were cut with a freezing sliding microtome and stored at -20°C in cryoprotectant solution (30% ethylene glycol; 30% glycerol; 20 mM PB) until processing. Free-floating brain sections were washed in PBS and incubated for 30 minutes in permeabilization/blocking solution (1% BSA; 0.1% Triton X-100; 4% normal goat or donkey serum (NS) in PBS). Different primary antibodies (Table 5) were incubated in 1% BSA, 0.1% Triton X-100, and 1% NS in PBS shaking overnight at 4°C. After several washes with PBS, sections were incubated with appropriate Cy3-conjugated secondary antibody (Table 6) in 1% BSA, 0.1% Triton X-100 in PBS for 1 hour at RT. After several washes in PBS and incubation for 10 minutes in DAPI, sections were mounted onto Superfrost Plus slides (Thermo Fisher Scientific), airdried, and coverslipped with Mowiol-DABCO solution.

Table 5. Primary antibodies used for immunostaining.

Antibody	Provider	Catalog number	Host	Dilution
<b>NeuN</b>	Millipore	MAB377	Mouse	1:500
<b>DARPP-32</b>	Cell Signaling	19A3#2306	Rabbit	1:500
<b>choline acetyltransferase</b>	Chemicon	AB144P	Goat	1:100
<b>GFAP</b>	Dako	20334	Rabbit	1:500
<b>Olig2</b>	Millipore	AB9610	Rabbit	1:1000
<b>Sst</b>	Millipore	MAB354	Rat	1:400
<b>GFP</b>	Synaptic systems	132002	Rabbit	1:1000
<b>Cux1 or CDP</b>	Santa Cruz biotechnology	Sc-13024	Rabbit	1:500
<b>Ctip2</b>	Abcam	Ab18465	Rat	1:500

## 8.2 Immunohistochemistry after FISH

Permeabilization and blocking step had already been conducted, so after the FISH procedure, free-floating brain sections were directly incubated with primary antibody (Table 5) overnight at 4°C as described in the section 8.1 and incubated with appropriate secondary antibody (Table 6).

Table 6. Secondary antibodies used for immunostaining.

Antibody	Provider	Catalog number	Host	Dilution
<b>Anti-Rabbit-Cy3</b>	Jackson Immunoresearch	111165003	Goat	1:500
<b>Anti-Mouse-Cy3</b>	Jackson Immunoresearch	115165003	Goat	1:500
<b>Anti-Goat-Cy3</b>	Jackson Immunoresearch	705166147	Donkey	1:500
<b>Anti-Rabbit-Cy5</b>	Jackson Immunoresearch	111175144	Goat	1:500
<b>Anti-Rat-488</b>	Invitrogen	A11006	Goat	1:500
<b>Anti-Rabbit-488</b>	Invitrogen	A11008	Goat	1:500

## 9. Image acquisition and analysis

To quantify transduction efficiency, mosaic pictures of sequential rAAV-injected brain sections (at the level of the striatum and spaced 240  $\mu\text{m}$  apart) were captured with a 2.5x objective using a Nikon Eclipse E600 epifluorescence microscope. Positive EGFP signal was defined as three times the value of fluorescent intensity in the green channel in an adjacent but non-injected region of the brain. Regions with GFP signal within the striatum were automatically detected with a set threshold of 3-fold over matched non-injected regions, and their areas were summed to calculate the total infected area.

For cell rAAV tropism, colocalization of GFP fluorescence with neuronal/glia markers was analysed with Fiji software on images acquired on a Zeiss LSM800 confocal microscope (Carl Zeiss) using 10x or 40x objectives.

Bright field images of colorimetric ISH were acquired using a Leica DM6000B microscope with 5x and 10x objectives or a MZ16FA stereomicroscope

equipped with a DC500 digital camera, and processed with Leica AF6000 software. Quantification of *Grin3a* expression across cortical layers and sensory modalities (Figure 5D, second chapter) was performed using Fiji for automatic detection of positive labelling after background subtraction. Fluorescence confocal images were captured on an Olympus FV1200 with a 20x objective or a ZEISS AxioImager M2 microscope with an Apochromat 20x objective, and processed with FV10-ASW\_Viewer and Zen Blue software respectively. The colocalization of *Grin3a*-positive cells with neuronal subtype-specific markers was quantified using Fiji software.

For anatomical analysis, identification of structures and functional interpretation, the Mouse brain in stereotaxic coordinates (Paxinos and Franklin, 2019 Edition), the Mouse nervous system (Watson, Paxinos, Puelles, 2012 Edition) and the Atlas of the developing mouse brain (Paxinos, Halliday, Watson, Koutcherov, Wang, 2007 Edition) were used.

## 10. Animals

### 10.1 Mouse models

WT and YAC128 (line 55 homozygotes; Tg(YAC128)55Hay) male mice in a FVB/N background were crossed for at least four generations into a C57Bl6J background and used in the studies described in the first part of the thesis.

In the second part, several strains of mice were used: WT, GAD67<sup>GFP</sup> (B6.Cg-Tg(Gad1-EGFP)) (Tamamaki *et al.*, 2003) and Nkx2.1-Cre::Ai9<sup>tdTomato</sup>. The latter was obtained by crossing Tg(Nkx2.1-Cre)2Sand/J (JAX 008661; Xu *et al.*, 2008) and Ai9(B6.Cg-Gt(ROSA) 26Sortm9(CAG-tdTomato)Hze/J (JAX 007909; Madisen *et al.*, 2010). Mice were housed 4-6 per cage with *ad libitum* access to food and water and maintained in a temperature-controlled environment on a 12-hr light/dark cycle at humidity between 40-60% in a standard pathogen free environment. All procedures were conducted in accordance with the European and Spanish regulations (2010/63/UE; RD53/2013) were approved by the Ethical Committee of the Government of

Navarra and by the Ethical Committee of the Government of the Generalitat Valenciana (2017/VSC/PEA/00196)

## 10.2 Real-time PCR for YAC128 mice genotyping

Mice samples were incubated in digestion buffer (100 mM Tris pH 8.8; 5 mM EDTA; 200 mM NaCl; 0.2% SDS; 100 µg/ml proteinase K) for 2 hours at 55°C with shaking. After a centrifugation step for 10 minutes at 13200xg, DNA was precipitated by addition of one volume of isopropanol to the supernatant and centrifuged at 13200xg for 10 minutes. Pellet was washed with 70% ethanol, dried and resuspended in milliQ water.

Quantitative PCR (qPCR) was carried out using the SYBR Green PCR Master Mix (Applied Biosystems) and a pair of primers specific to human *HTT*.  $\beta$ -Actin was used as housekeeping gene. (Table 7). Each qPCR reaction was run in triplicate, containing 2.5 ng of DNA sample, 10 µl of SYBR Green PCR Master Mix, 5 pmol of forward primer and 5 pmol of reverse primer in 20 µl in total mix using a 7300 Applied Biosystems apparatus. qPCR program included an enzyme activation step (95°C for 2 minutes) followed by 40 cycles of denaturation/annealing-elongation (95°C for 15 seconds and 60°C for 1 minute respectively). Relative quantification  $2^{-(CT \beta\text{-actin} - CT \textit{Htt})}$  was used to analyse results. Samples (from WT, heterozygous and homozygous YAC128 mice) with known amount of copies for human *HTT* were run in the same 96-well plate as the test samples.

Table 7. Nucleotide sequence of the different primers used for qPCR genotyping.

Primer name	Sequence (5'-3')	Host
<b>Forward huntingtin</b>	GAAAGTCAGTCCGGGTAGAACTTC	Human
<b>Reverse huntingtin</b>	CAGATACCCGCTCCATAGCAA	Human
<b>Forward <math>\beta</math>-Actin</b>	ACGGCCAGGTCATCACTATTG	Mouse/rat
<b>Reverse <math>\beta</math>-Actin</b>	CAAGAAGGAAGGCTGGAAAAGA	Mouse/rat

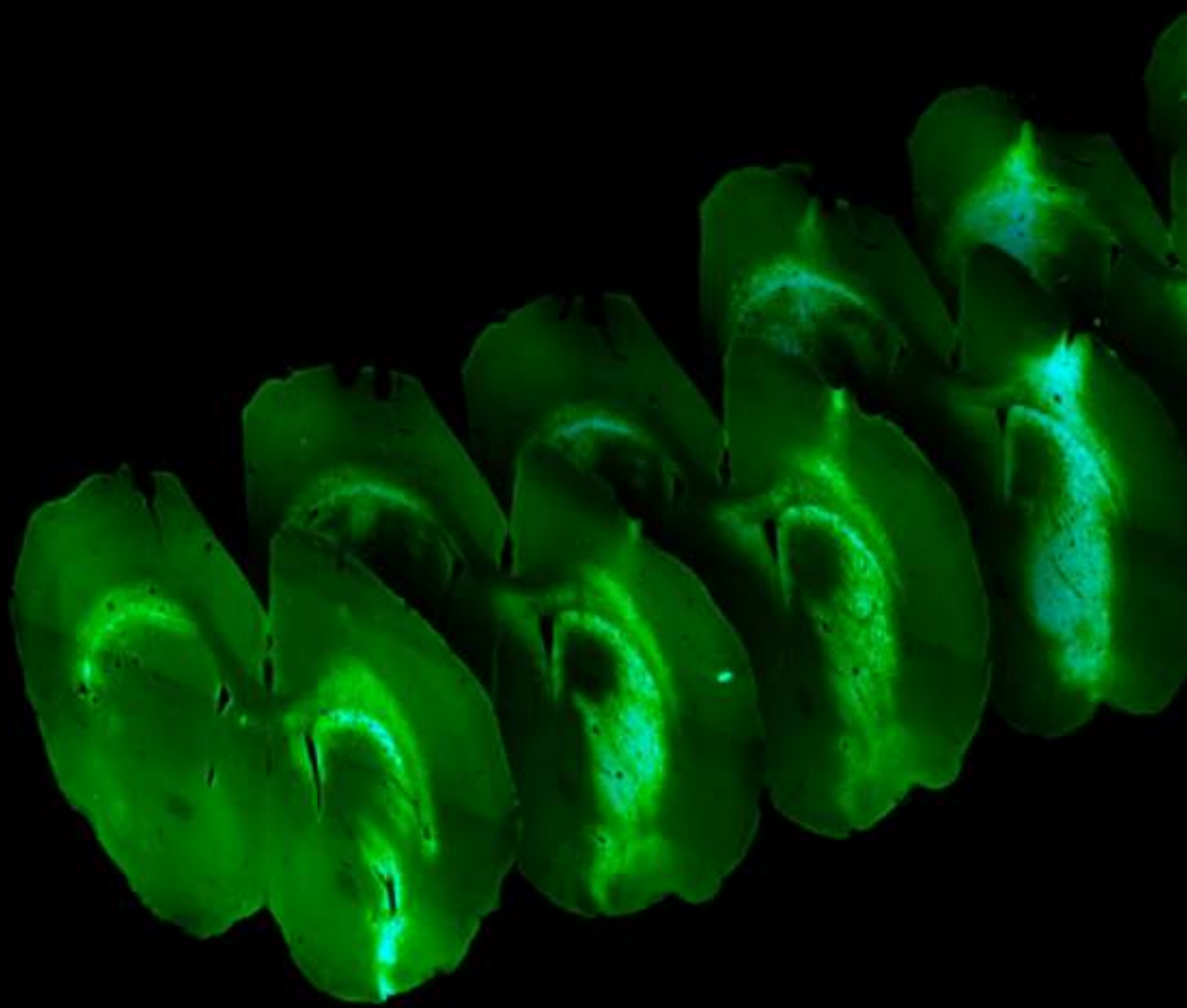


## 11. Behavioral tests

Two independent male mice cohorts of 10–12 months of age were used. For motor coordination assessment, naive mice were placed on a rotarod for 2 trials (spaced for 2 hours) with a fixed speed of 12 rpm, and the number of falls was recorded until the sum of latencies to fall reached a total of 60 seconds per trial. A balance beam test was used to evaluate fine motor coordination and balance. Mice were placed at one end of a 12-mm-wide, 90-cm-long beam, and the time to reach an escape box containing nesting material and located in the opposite end was recorded. Mice were allowed to rest for 15 seconds before next trial with a total of three consecutive trials. After 2 hours, the test was repeated using a 6-mm beam width, making the test more sensitive. To measure muscular strength, mice were placed on top of a standard wire cage lid (surrounded by tape to prevent mice walking off the edge), and after light shaking so mice gripped the wires, the lid was turned upside down. Latency to the first fall was recorded with a maximum of 60 seconds.

## 12. Statistical analysis

Statistical analysis was performed using GraphPad Prism 5-7. Sample sizes for each experiment were determined based on previous studies from our laboratory. The number of mice used for the first part “RNAi-Based GluN3A Silencing Prevents and Reverses Disease Phenotypes Induced by Mutant huntingtin” have been included in the corresponding figure legends. The following number of mice were analysed for the second part of this thesis: E17.5 (n=3), P0 (n=6), P3 (n=8), P6 (n=16, short and long exposure; n=4, FISH), P9 (n=6), P12 (n=4), adult (n=3, long exposure). One- or two-way ANOVA followed by Bonferroni *post-hoc* tests was used to assess differences between groups. In all figures, data are presented as means  $\pm$  SEM.



«El estudioso es el que lleva a los demás lo que él ha  
comprendido, la verdad»

- Santo Tomas de Aquino -



**RESULTS (First chapter)**



# RNAi-Based GluN3A Silencing Prevents and Reverses Disease Phenotypes Induced by Mutant huntingtin

Sonia Marco,<sup>1</sup> Alvaro Murillo,<sup>1,2</sup> and Isabel Pérez-Otaño<sup>1,2</sup>

<sup>1</sup>Cellular Neurobiology Laboratory, Center for Applied Medical Research (CIMA), University of Navarra Medical School, Avda Pio XII 55, 31008 Pamplona, Spain;

<sup>2</sup>Instituto de Neurociencias (CSIC-UMH), Avda Ramón y Cajal s/n, 03550 San Juan de Alicante, Spain

Huntington's disease (HD) is a dominantly inherited neurodegenerative disease caused by expansion of a polyglutamine tract in the huntingtin protein. HD symptoms include severe motor, cognitive, and psychiatric impairments that result from dysfunction and later degeneration of medium-sized spiny neurons (MSNs) in the striatum. A key early pathogenic mechanism is dysregulated synaptic transmission due to enhanced surface expression of juvenile NMDA-type glutamate receptors containing GluN3A subunits, which trigger the aberrant pruning of synapses formed by cortical afferents onto MSNs. Here, we tested the therapeutic potential of silencing GluN3A expression in YAC128 mice, a well-established HD model. Recombinant adeno-associated viruses encoding a short-hairpin RNA against GluN3A (rAAV-shGluN3A) were generated, and the ability of different serotypes to transduce MSNs was compared. A single injection of rAAV9-shGluN3A into the striatum of 1-month-old mice drove potent (>90%) and long-lasting reductions of GluN3A expression in MSNs, prevented dendritic spine loss and improved motor performance in YAC128 mice. Later delivery, when spine pathology is already apparent, was also effective. Our data provide proof-of-concept for GluN3A silencing as a beneficial strategy to prevent or reverse corticostriatal disconnectivity and motor impairment in HD and support the use of RNAi-based or small-molecule approaches for harnessing this therapeutic potential.

## INTRODUCTION

Huntington's disease (HD) is a fatal neurodegenerative disorder with motor, cognitive, and psychiatric disturbances. It is caused by abnormal expansion of a polyglutamine repeat in the huntingtin (HTT) protein that triggers its misfolding and aggregation and alters interactions of HTT with multiple binding partners. The neuropathology involves early synapse failure and loss followed by cell death, especially in the striatum where medium-sized spiny neurons (MSNs) that make 90%–95% of all neurons are selectively vulnerable.<sup>1</sup> Currently, there is no cure or treatment to slow disease progression, and therapies barely manage the symptoms.

The search for disease-modifying therapies has focused on lowering the amount of mutant HTT with antisense oligonucleotides or

RNAi.<sup>2–4</sup> Doing so while preserving wild-type (WT) protein levels has proven challenging, but ongoing clinical trials based on allele-specific or non-selective targeting of both WT and mutant HTT are beginning to yield promising results. Other therapeutic options include modulating autophagy, modifying HTT aggregation, or supplementing growth factors.<sup>5–7</sup> An alternative that has been less explored, due to insufficient knowledge of the underlying molecular mechanisms, is to arrest the pathogenic process by counteracting key initiating events. Most prominent in HD is the progressive disconnection between the cortex and the striatum, which results from dysfunction and loss of excitatory glutamatergic synapses<sup>8–10</sup> impinging on dendritic spines of MSNs. Supporting its relevance for disease pathogenesis, longitudinal imaging and clinical studies have demonstrated that degeneration of MSN spines and striatal atrophy occur in premanifest HD<sup>11–13</sup> and are robust predictors of clinical onset and progression.<sup>14,15</sup>

We recently identified aberrant expression of juvenile NMDA receptors containing GluN3A subunits (GluN3A-NMDARs)<sup>16</sup> as a major driver of the HD synaptic pathology.<sup>17</sup> Sequestration of the GluN3A-selective endocytic adaptor PACSIN1 by mutant HTT<sup>1–17</sup> causes accumulation of GluN3A-NMDARs at MSN synapses, altering MSN excitability and reactivating pruning mechanisms normally restricted to postnatal developmental stages.<sup>18,19</sup> Importantly, dysregulated GluN3A expression can be detected from very early disease stages and is a feature shared by HD brains and a variety of mouse models (expressing N-terminal or full-length HTT, and knockin mice). Suppressing GluN3A expression by crossing YAC128 mice, a well-established mouse model, with GluN3A null mice prevented all aspects of the synapse pathology, as well as cognitive and motor dysfunction and reduced MSN loss.<sup>17,18</sup> While this prevention was encouraging, genetic suppression is neither an amenable therapeutic strategy nor definitive proof of principle given known compensatory effects in knockout mice. Further validation was needed, including defining a therapeutic window and developing

Received 9 February 2018; accepted 12 May 2018.

<https://doi.org/10.1016/j.ymth.2018.05.013>

Correspondence: Isabel Pérez-Otaño, Instituto de Neurociencias (CSIC-UMH), Avda Ramón y Cajal s/n, 03550 San Juan de Alicante, Spain.  
E-mail: [otano@umh.es](mailto:otano@umh.es)



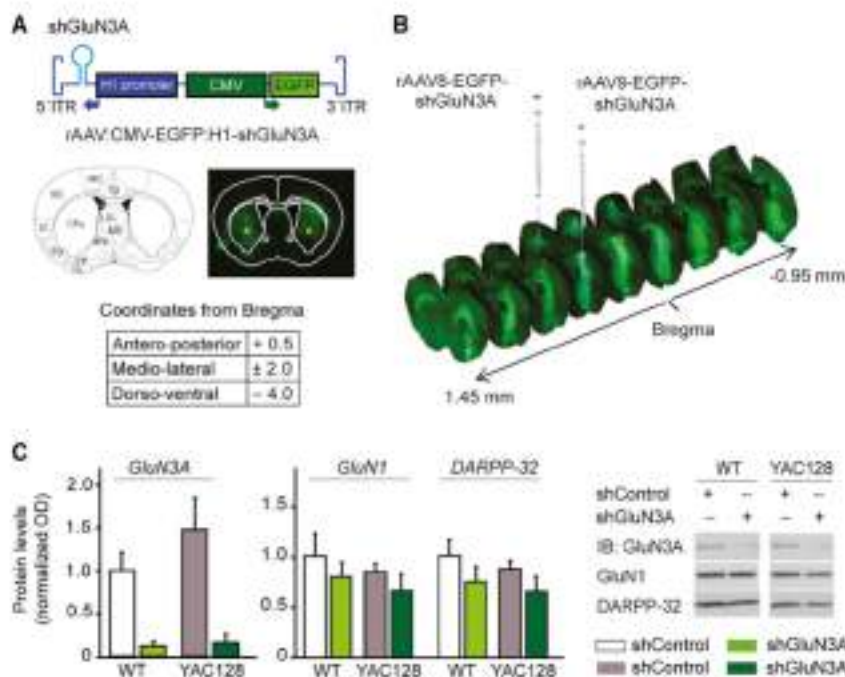


**Figure 1. Silencing GluN3A in MSNs by intrastriatal injection of rAAV9-driven shRNAs**

(A) Top, cartoon of rAAV construct encoding shRNAs against the NMDAR subunit GluN3A flanked by inverted terminal repeat (ITR) sequences. shRNA expression is driven by the H1 promoter, and expression of EGFP by the CMV promoter. Middle, schematic of the brain section where injections were placed, along with example of an injected mouse brain. Stars show the tip of the needle. CPU, caudate putamen. Bottom, stereotaxic coordinates relative to bregma (in mm). (B) Widespread viral transduction upon single rAAV9 injections into the striatum. Injection sites and antero-posterior coordinates relative to bregma (in mm) are shown. (C) Immunoblot analysis of *in vivo* silencing efficiency of rAAV9-shGluN3A. Quantification and representative immunoblots showing levels of the indicated proteins in extracts from 3-month-old WT and YAC128 mice striata receiving rAAV9-shGluN3A at 1 month of age, compared to contralateral striata injected with control rAAV9. Data are mean  $\pm$  SEM normalized to WT striatum injected with rAAV9-shControl ( $n = 5$  animals per group). Two-way ANOVA showed no interaction between genotype and shRNA treatment ( $F_{(1,16)} = 0.74$ ,  $p = 0.403$ ) but revealed a strong effect of rAAV9-shGluN3A on GluN3A protein levels relative to shControl ( $F_{(1,16)} = 19$ ,  $p = 0.0007$ ).

feasible therapeutic approaches, if possible exclusively targeted to vulnerable cell types to minimize adverse effects.

Here, we validate GluN3A as a therapeutic target by using recombinant adeno-associated vectors (rAAVs) to deliver RNAi triggers that correct the aberrant GluN3A expression. rAAVs offer many advantages for gene transfer in neurodegenerative disease, and different serotypes exhibit different tropisms allowing to target a variety of cell types.<sup>20,21</sup> Of several serotypes tested, rAAV9-driven GluN3A silencing was most efficient for stably and selectively transducing MSNs and fully prevented the synaptic pathology and motor deficits in YAC128 mice. Protection was achieved when rAAVs were delivered at the onset of pathology but also at later disease stages. Together, our results support the development of RNAi-based therapies or alternative approaches targeting GluN3A to treat HD.

## RESULTS

### Intrastriatal rAAV9-shGluN3A Drives Sustained GluN3A

#### Silencing in MSNs

We generated rAAVs expressing a previously validated short hairpin RNA (shRNA) directed to GluN3A<sup>22</sup> (shGluN3A) under the regulation of the H1 non-coding RNA promoter. A GFP reporter gene driven by a cytomegalovirus (CMV) promoter was included in the vector to aid detection of transduced cells (Figure 1A). In a first series of experiments, we compared the ability of different rAAV serotypes to spread throughout the mouse striatum and efficiently transduce MSNs, the vulnerable cell population. Serotypes 8, 9, and 10 were chosen based on previous reports.<sup>23,24</sup> Viral particles were delivered into the striatum using coordinates determined with the Paxinos

mouse brain atlas<sup>25</sup> (Figure 1A) at the doses indicated in Figure S1. GFP expression was visualized 2 weeks after surgery by fluorescence microscopy analysis of series of mosaic images spanning the entire striatum. All serotypes yielded detectable GFP expression, but a quantitative assessment demonstrated that the spread capacity of rAAV9 was higher and more consistent across individuals (Figure S1); a single injection of rAAV9 resulted in widespread transduction that extended 2.4 mm across the anteroposterior axis of the striatum (Figure 1B).

We next evaluated the *in vivo* silencing efficacy of rAAV9-shGluN3A. rAAV9s expressing shGluN3A or control shRNA were delivered into the striatum of 1-month-old WT and YAC128 mice (injection volume, 2  $\mu$ L;  $6.4$ – $8.8 \times 10^{10}$  viral genomes), and GluN3A expression was quantified 2 months after injection. Immunoblot analysis demonstrated that GluN3A protein levels were dramatically reduced in the rAAV9-shGluN3A-injected striatum relative to contralateral striata receiving rAAV9-shControl (Figure 1C;  $p = 0.0007$ ). Silencing was persistent and lasted for at least 11 months after injection, which was the latest time point analyzed; the reduction in GluN3A protein levels observed in rAAV9-shGluN3A-injected striata of old (12-month-old) WT and YAC128 mice was of similar magnitude as it was in younger animals (to 10%–15% of shControl-injected striata;  $p < 0.0001$ ). The effects of shGluN3A were target specific, as neither levels of the obligatory NMDAR subunit GluN1 nor the MSN marker DARPP-32 were altered (Figure 1C).

We finally characterized the transduction profile of rAAV9-shGluN3A by quantifying the co-localization of GFP with specific

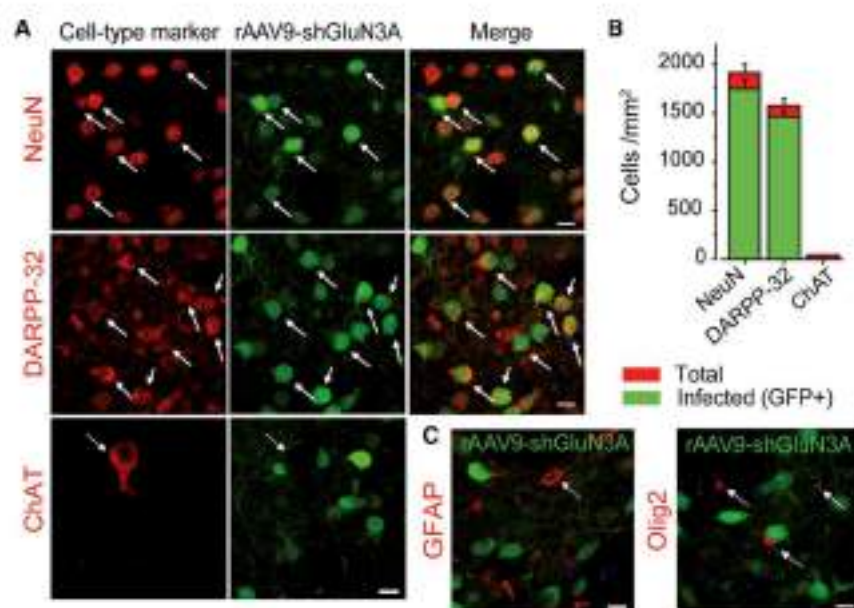


**Figure 2. In Vivo Transduction Efficiency in Immunohistochemically Identified Cell Types**

(A and C) Single confocal images of striatal sections from WT mice receiving rAAV9-shGluN3A at 1 month of age (green) and stained by immunohistochemistry for specific cell type markers upon sacrifice, 2 weeks after delivery (red) (A: NeuN, all neurons; DARPP-32, MSNs; ChAT, cholinergic neurons; C: GFAP, astrocytes; Olig2, oligodendrocytes). Solid arrows, examples of colocalization; dashed arrows, no colocalization. Scale bars, 10  $\mu$ m. (B) Quantification of striatal cells positive for a given marker transduced by rAAV9-shGluN3A. Data are mean  $\pm$  SEM ( $n = 4$  animals per group, five striatal fields at different antero-posterior levels were analyzed per mouse).

cell type markers, rAAV9-shGluN3A transduced a majority of striatal neurons and exhibited strong tropism for DARPP-32-labeled MSNs (92.6%  $\pm$  4% of MSNs were GFP positive), with virtually no cholinergic interneurons transduced (Figures 2A and 2B). Transduction of GFAP-positive astrocytes was very low and restricted to the site of injection (Figure 2C). GFP expression was also absent from striatal oligodendrocytes labeled with Olig2 (Figure 2C). Similarly, high efficiency and analogous neuronal distribution of infection by rAAV9 were observed throughout the duration of the experiment (Figure S2), in line with the sustained reductions in GluN3A protein measured by western blot. Thus, rAAV9-shGluN3A shows a specific neuronal tropism in the striatum and preferentially targets MSNs, the vulnerable population in HD, without modifying GluN3A levels in other neuronal or non-neuronal populations.

#### Intrastriatal rAAV9-shGluN3A Prevents and Reverses Spine Loss in MSNs

To evaluate the beneficial effects of suppressing GluN3A expression in MSNs, we performed single bilateral injections of rAAV9-shGluN3A or rAAV9-shControl into the striatum of WT and YAC128 mice (Figure 3A). YAC128 mice express full-length HTT with 128 glutamine repeats under the control of the human promoter and recapitulate many characteristics of HD, including early dysfunction and loss of MSN synapses prior to motor and cognitive deficits, later followed by cell death.<sup>20</sup> A first set of injections was timed to match the onset of synapse dysfunction, which can be detected by 1 month of age in YAC128 mice.<sup>17</sup> The status of synaptic connectivity was monitored over the course of disease progression (3, 6, and 12 months) by measuring spine densities on MSNs using the Golgi impregnation technique and applying quantitative criteria previously described (Figures 3A and 3B). MSNs from YAC128 mice injected with rAAV9-shControl showed significantly decreased spine densities at all ages examined,

consistent with previous work (Figures 3C and 3D, white versus gray bars). Spine loss was fully prevented by rAAV9-shGluN3A; the effect was persistent as it was observed 2, 5, and even 11 months after surgery (Figure 3D, dark green versus gray bars). By contrast, rAAV9-shGluN3A did not affect spine density in WT

MSNs at any age examined (Figure 3D, white versus bright green bars) as could be expected given the low levels of juvenile GluN3A subunits expressed by adult MSNs. This latter finding confirmed that GluN3A suppression specifically targets the pathological trait, i.e., enhanced GluN3A-mediated pruning in MSNs, without affecting physiological mechanisms used by MSNs for spine maintenance.

In order to define a potential therapeutic window, we injected rAAV9-shGluN3A or shControl into the striatum of 4- to 5-month-old mice, an age by which spine loss is well established in the YAC128 model. End-study analysis of spine density was conducted at 12 months of age. A significant reversal of spine loss was observed in YAC128 mice receiving rAAV9-shGluN3A relative to mice injected with control shRNA (Figure 3D, far right gray versus dark green bars;  $p < 0.001$ , two-way ANOVA followed by Bonferroni post-hoc test). Cumulatively, the results show that suppressing GluN3A in MSNs prevents and rescues the synaptic pathology even when treatment is started after overt spine loss has taken place.

#### Intrastriatal rAAV9-shGluN3A Improves Motor Performance

We finally investigated whether the synaptic rescue was associated to improvements in motor performance. Motor coordination and balance were assayed on 10- to 12-month-old mice bilaterally injected with rAAV9-shGluN3A or shControl. By this age, YAC128 mice displayed impairments in motor coordination in a fixed rotarod task when compared to WT (Figure 4A, white versus gray circles;  $p < 0.001$ , two-way ANOVA followed by Bonferroni post-hoc test). rAAV9-shGluN3A significantly decreased the number of falls from the fixed rotarod relative to mice receiving control shRNA (Figure 4A;  $p < 0.001$ , dark green versus gray circles;  $p < 0.001$ , two-way ANOVA followed by Bonferroni post-hoc test) and fully restored the performance of YAC128 mice upon two trials (Figure 4B).

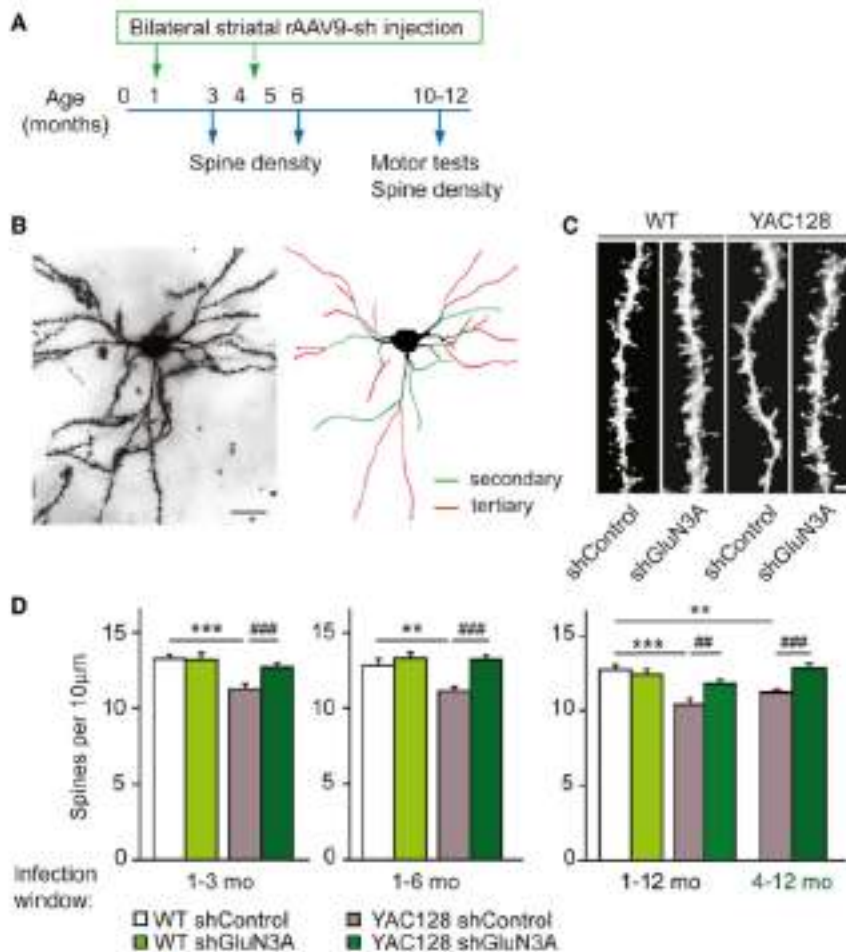


**Figure 3. GluN3A Silencing Prevents and Reverses Spine Loss**

(A) Experimental design followed in this study. Times of injection are indicated in green. (B) Photomicrograph of a Golgi-impregnated MSN from a 12-month-old YAC128 mouse reared with rAAV9-shGluN3A, along with schematic showing criteria adopted for defining secondary (green) or tertiary (red) dendrites to be used in quantification. Scale bar, 20  $\mu$ m. (C) Representative dendritic segments of tertiary dendrites from MSNs of 6-month-old WT and YAC128 mice injected with rAAV9-shControl/shGluN3A at 1 month of age. Scale bar, 2  $\mu$ m. (D) Quantification of spine densities in MSNs from mice receiving rAAV9-shControl or shGluN3A over the indicated time windows. Two-way ANOVA 1–3 months: genotype  $\times$  shRNA interaction,  $F_{(1,30)} = 9.24$ ,  $p = 0.0031$ ; shRNA,  $F_{(1,30)} = 4.76$ ,  $p = 0.0317$ ; genotype,  $F_{(1,30)} = 12.6$ ,  $p = 0.0006$ ; 1–6 months: genotype  $\times$  shRNA,  $F_{(1,70)} = 5.78$ ,  $p = 0.0188$ ; shRNA,  $F_{(1,70)} = 15$ ,  $p = 0.0002$ ; genotype,  $F_{(1,70)} = 6.80$ ,  $p = 0.016$ ; 1–12 months: genotype  $\times$  shRNA,  $F_{(1,100)} = 8.85$ ,  $p = 0.0037$ ; shRNA,  $F_{(1,100)} = 2.44$ ,  $p = 0.1214$ ; genotype,  $F_{(1,100)} = 20.4$ ,  $p < 0.0001$ ; 4–12 months: genotype  $\times$  shRNA,  $F_{(1,100)} = 11.6$ ,  $p = 0.0009$ ; shRNA,  $F_{(1,100)} = 3.88$ ,  $p = 0.0515$ ; genotype,  $F_{(1,100)} = 0.538$ ,  $p = 0.465$ . Data are mean  $\pm$  SEM ( $n = 14$ –35 neurons from 4–6 animals per group; \* $p < 0.05$ , \*\* $p < 0.001$ , ## $p < 0.01$ , ### $p < 0.001$ , post-hoc Bonferroni multiple comparison test).

pruning resulting from aberrant GluN3A expression are among the earliest events in HD pathophysiology and major drivers of the pathogenic process, and (2) genetic GluN3A suppression prevents early- to late-disease phenotypes.<sup>17,18</sup>

led us to explore viable therapeutic strategies. We show that upon a single intrastriatal injection, rAAV9s encoding shRNAs against GluN3A drove highly efficient, long-lasting GluN3A silencing that selectively targeted MSNs. Silencing expression in MSNs was sufficient for halting the synaptic pathology and restoring motor performance.

The present work corroborates and extends the earlier results and has major translational implications. First, silencing GluN3A exclusively in MSNs (that normally express low GluN3A levels in adult stages) while sparing other cell types in the striatum (such as cholinergic interneurons that retain high expression into adulthood)<sup>17</sup> permits to block specifically the pathological event, i.e., age-inappropriate reactivation of GluN3A in vulnerable populations, while sparing normal function. Such specificity could provide clinical benefit while minimizing adverse effects. The observation that injecting rAAV9-shGluN3A does not affect spine density in WT MSNs, nor motor performance, supports this rationale. Second, rAAV9-driven GluN3A silencing was effective when timed with the onset of the synaptic pathology but also when initiated later in the disease course, establishing a window of opportunity over which preexisting phenotypes can be reversed. Third, the

Similar results were observed in the balance beam test, where fine motor coordination and balance can be tested by measuring the time it takes for the mouse to traverse an elevated narrow beam to reach a safe platform. Here, two different beam widths, 12 and 6 mm, were used (Figures 5A and 5D). YAC128 mice took longer to cross a 12-mm beam than WT (albeit their performance improved across trials; Figures 5B and 5C); motor deficits were more prominent on a 6-mm beam, and practice was not sufficient to overcome the defect (Figures 5E and 5F). By contrast, YAC128 mice injected with rAAV9-shGluN3A were indistinguishable from WT animals in their ability to traverse both beams (Figures 5B, 5C, 5E, and 5F). Injection of rAAV9-shGluN3A in WT mice did not affect motor performance in either task, as noted in the rotarod task. Amelioration of the motor phenotype was not due to changes in body weight or motor strength because neither parameter was affected by rAAV9-shGluN3A in YAC128 mice (Figure 5G).

## DISCUSSION

Here, we provide validation of GluN3A as a target to treat early pathogenic mechanisms in HD and develop and test RNAi-based tools to harness this therapeutic potential. Our previous findings that (1) impaired glutamatergic synaptic transmission and excessive synapse



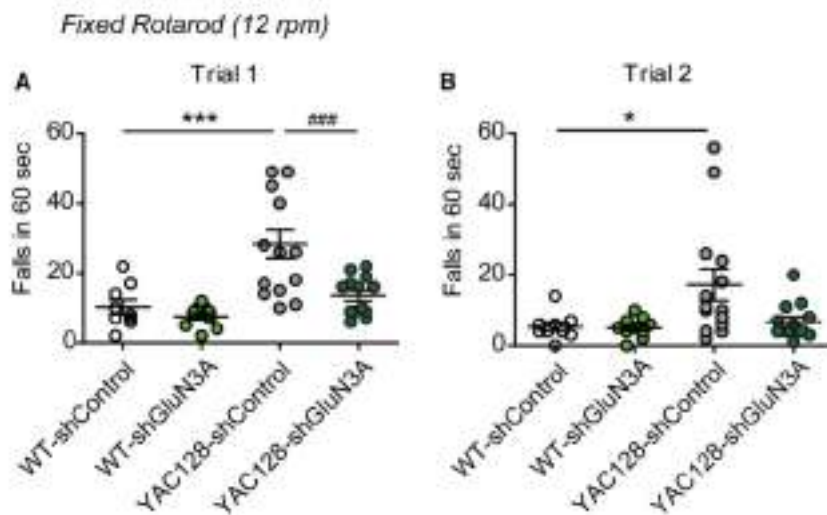


**Figure 4. rAAV9-shGluN3A Improves Motor Coordination in YAC128 Mice**

(A and B) Number of falls from a fixed rotarod set at 12 rpm for 10- to 12-month-old mice of the indicated genotypes that received bilateral intrastriatal injections of rAAV9-shControl or shGluN3A at 1 month of age. Data are represented for each of two trials conducted (trial 1, A; trial 2, B). Two-way ANOVA trial 1: genotype  $\times$  shRNA interaction,  $F_{(1,42)} = 4.53$ ,  $p = 0.0392$ ; shRNA,  $F_{(1,42)} = 9.59$ ,  $p = 0.0035$ ; genotype,  $F_{(1,91)} = 18.2$ ,  $p = 0.0001$ ; trial 2: genotype  $\times$  shRNA,  $F_{(1,42)} = 3.03$ ,  $p = 0.0893$ ; shRNA,  $F_{(1,42)} = 3.31$ ,  $p = 0.0762$ ; genotype,  $F_{(1,42)} = 5.31$ ,  $p = 0.0262$ . Data are mean  $\pm$  SEM ( $n = 9$ –14 mice per group; \* $p < 0.05$ , \*\* $p < 0.001$ , \*\*\* $p < 0.001$ , post-hoc Bonferroni multiple comparison test).

approach targets one of the earliest disease mechanisms when intervention is more likely to be efficacious and before a point of no return has been reached.<sup>27</sup> Electrophysiological and morphological evidence of early dysfunction and loss of MSN synapses is extensive in HD mouse models<sup>24,18</sup> and humans.<sup>11,12</sup> Likewise, longitudinal imaging and functional studies in humans report significant striatal atrophy years prior to diagnosable HD,<sup>28</sup> which is strongly correlated with time to disease onset, performance, and clinical progression.<sup>14,15</sup> And, GluN3A has been shown to be required for the multivariate dysfunction of synaptic transmission onto MSNs that precedes morphological signs (chosen as readout in this study), including early enhanced synaptic currents mediated by AMPA and NMDA-type glutamate receptors and NMDA "spikes" or "upstates."<sup>17,18</sup>

Within the experimental time frame of the present study, loss of MSNs is not yet detectable in YAC128 mice and we could not determine whether GluN3A knockdown would reduce the neurodegeneration that is seen at later stages. In our previous report, genetic cross of YAC128 mice with GluN3A null mice conferred partial protection from cell death,<sup>27</sup> suggesting that preventing synaptic damage preserves pro-survival signaling pathways driven by afferent synaptic activity.<sup>29</sup> However, multiple other factors such as deficient neurotrophic signaling, transcriptional dysregulation, or altered proteostasis have been linked to cell death in preclinical HD studies, and establishing whether these are related or independent of the synaptic pathology needs to be carefully addressed.

While HTT-lowering drugs seem the therapy of choice, developing allele-specific strategies has proven to be difficult and will likely require targeting single-nucleotide polymorphisms residing only in the mutant allele or alternative approaches such as genome editing.<sup>30,31</sup> Clinical trials testing the safety of allele-specific antisense oligonucleotides that silence the mutant *HTT* gene (Wave Precision-HDs) are currently active, but the polymorphisms targeted are present only in a subset of people with the HD gene and in some cases do not

discriminate between mutant and normal *HTT*.<sup>12</sup> Antisense oligonucleotides against both WT and mutant *HTT* (IONIS-HTT<sub>HD</sub>) have recently yielded promising dose-response reductions in protein levels along with appropriate safety and tolerability profiles in a completed phase I clinical trial. However, the efficacy of these approaches (as well as their tolerability over the extended periods of time likely required to treat chronic neurodegeneration) remains to be tested through larger trials. Our study provides the necessary proof-of-principle for exploring therapies targeting aberrant GluN3A expression in HD that could be used alone or in combination with HTT-lowering treatments. Efforts to be undertaken include further evaluation of the current RNA-based approach or investing in screenings for small molecules blocking GluN3A expression, function, or downstream signaling pathways. In the current RNA-based approach, delivery continues to be a challenge, as it would require direct intraparenchymal administration into the striatum. Nevertheless, our data show that rAAV9 yields remarkably long-lasting knockdown of GluN3A protein levels associated to motor improvement upon a single injection, which would limit the invasiveness of the procedure.

## MATERIALS AND METHODS

### RNAi Constructs

A 59-bp fragment encoding a 19-bp-long shRNA specific for rat and mouse GluN3A (sh-GluN3A target sequence: 5'-CTACAGCTGAGTTTAGAAA-3')<sup>22</sup> or a control shRNA were expressed under control of the H1 promoter. For serotype comparison experiments in Figure S1, rAAV expression vectors carried only EGFP driven by a CMV promoter and were produced at the Vector Core Facility of the University of Barcelona (Spain). rAAV9-shControl and rAAV9-shGluN3A were manufactured by Vector Biolabs (Malvern, PA). Titers of rAAV9-shControl or shGluN3A used ranged between 3.2 and  $4.4 \times 10^{12}$  vg/mL.

### Animals

WT and YAC128 (line 55 homozygotes) male mice in a FVB/N background crossed for at least four generations into a C57Bl6J background were used. Animals were housed four to six per cage with *ad libitum* access to food and water and maintained in a

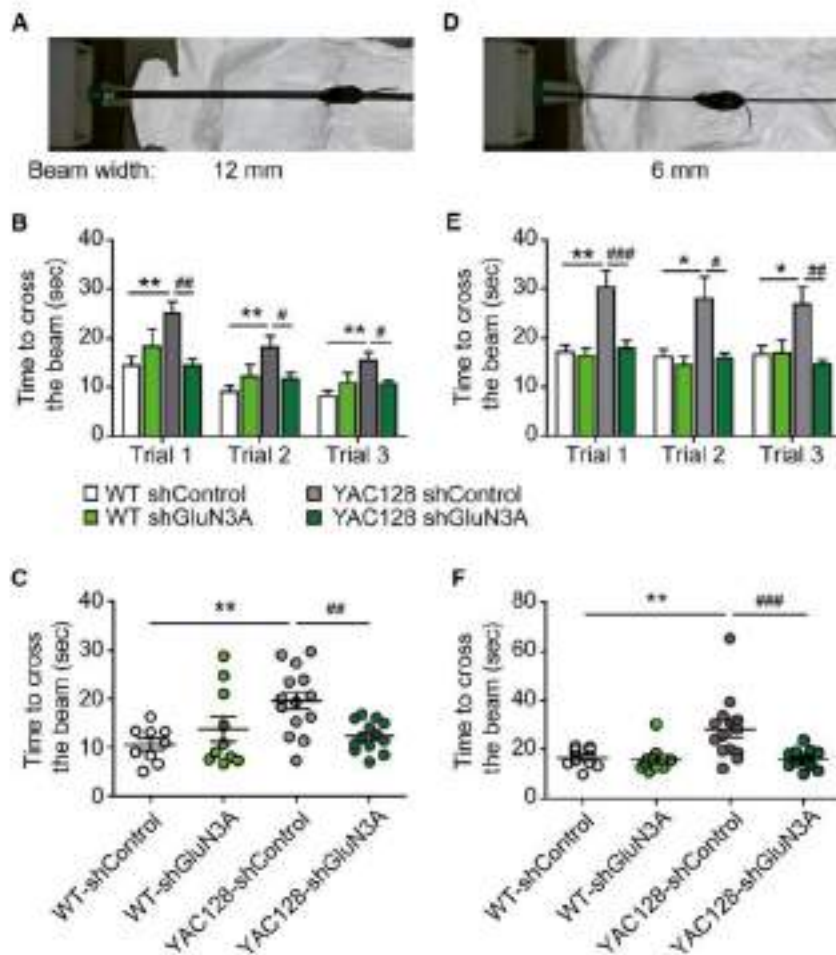


**Figure 5. Rescue of Balance Deficits by rAAV9-shGluN3A in YAC128 Mice**

(A and D) Photographs of the balance beam task showing two different beam widths (12 mm, A; 6 mm, D) and escape box to the left. (B, C, E, and F) Time to cross a 12 (B and C) or 6 (E and F)-mm-wide beam for 10- to 12-month-old mice of the indicated genotypes and treatments. Data in (B) and (E) are per trial. Two-way ANOVA genotype  $\times$  shRNA interaction: 12-mm beam trial 1,  $F_{(1,42)} = 9.82$ ,  $p = 0.0034$ ; trial 2,  $F_{(1,42)} = 5.88$ ,  $p = 0.0197$ ; trial 3,  $F_{(1,42)} = 5.851$ ,  $p = 0.020$ ; 6-mm beam trial 1,  $F_{(1,42)} = 5.45$ ,  $p = 0.0245$ ; trial 2,  $F_{(1,42)} = 3.30$ ,  $p = 0.0765$ ; trial 3,  $F_{(1,42)} = 5.633$ ,  $p = 0.0223$ . Data in (C) and (F) are individual averages across different trials. Two-way ANOVA genotype  $\times$  shRNA interaction: 12-mm beam,  $F_{(1,42)} = 9.13$ ,  $p = 0.043$ ; 6-mm beam,  $F_{(1,42)} = 5.59$ ,  $p = 0.0228$ . Data are mean  $\pm$  SEM ( $n = 9$ -14 mice per group; \* $p < 0.05$ , \*\* $p < 0.01$ , \*\*\* $p < 0.001$ , post-hoc Bonferroni multiple comparison test).

Brains were removed, post-fixed overnight, and stored in 30% sucrose in PB at 4°C. Thirty-micrometer coronal sections were cut with a freezing sliding microtome and stored at -20°C in cryoprotectant solution (30% ethylene glycol, 30% glycerol, 20 mM PB) until processing. Free-floating brain sections were washed in PBS, blocked for 30 min in 1% BSA, 0.1% Triton X-100, and 4% normal goat or donkey serum (NS) in PBS, and incubated with primary antibody in 1% BSA, 0.1% Triton X-100, and 1% NS in PBS overnight at 4°C. The following primary antibodies were used: mouse anti-NeuN (1:500, Millipore, MAB377),

temperature-controlled environment on a 12-hr dark/light cycle. All procedures were conducted in accordance with the European and Spanish regulations (86/609/EEC; RD1201/2005) and were approved by the Ethical Committee of the Government of Navarra.

#### Stereotaxic Injections

Mice were anesthetized with ketamine/xylazine (80/10 mg/kg, intraperitoneally [i.p.]) and placed in a stereotaxic frame. The scalp was shaved, a longitudinal incision was made to expose the skull surface, and two burr holes were drilled above the infusion sites. A 2- $\mu$ L virus suspension was stereotaxically injected into the striatum of anesthetized mice according to the Paxinos and Franklin mouse brain atlas.<sup>28</sup> A 5  $\mu$ L Hamilton syringe was used for the infusion (Hamilton, Reno, NV). The infusion rate was 200 nL/min, and the needle remained in place for 5 min after infusion for vector absorption before removal of the syringe. Finally, the site was stitched closed.

#### Immunohistochemistry

Animals were deeply anesthetized and transcardially perfused with 4% paraformaldehyde in 0.1 M phosphate buffer (PB) (pH 7.4).

rabbit anti-DARPP-32 (1:500, Cell Signaling, 19A3), goat anti-choline acetyltransferase (ChAT) (1:100, Chemicon AB144P), rabbit anti-GFAP (1:500, Dako, 20334), and rabbit anti-Olig2 (1:1000, Millipore AB9610). After washing with PBS, sections were incubated with appropriate Cy3-conjugated secondary antibody (1:1000, Jackson ImmunoResearch) in 1% BSA, 0.1% Triton X-100 in PBS for 1 hr at room temperature. After several washes in PBS, sections were mounted onto Superfrost Plus slides (Thermo Fisher Scientific), air-dried, and coverslipped with Mowiol-DABCO solution.

#### Image Acquisition and Analysis

To quantify transduction efficiency, mosaic pictures of sequential rAAV-injected brain sections (at the level of the striatum and spaced 240  $\mu$ m apart) were captured with a 2.5 $\times$  objective using a Nikon Eclipse E600 epifluorescence microscope. Positive EGFP signal was defined as three times the value of fluorescent intensity in the green channel in an adjacent but non-injected region of the brain. Regions with GFP signal within the striatum were automatically detected with a set threshold of 3-fold over matched non-injected regions, and their areas were summed to calculate the total infected area. For cell tropism,

colocalization of GFP fluorescence with neuronal/glia markers was analyzed with Fiji software on images acquired on a Zeiss LSM800 confocal microscope (Carl Zeiss) using 10× or 40× objectives.

#### Western Blot Analysis

Striata were dissected and homogenized into 10 volumes of cold homogenization buffer (0.32 M sucrose, 10 mM HEPES [pH 7.4], 2 mM EDTA) supplemented with protease inhibitors (Roche). Protein concentrations were determined using the BCA protein assay (Pierce). Twenty to fifty micrograms of total protein were resolved by SDS-PAGE and transferred onto PVDF membranes (GE Healthcare). Antibodies to mouse anti-GluN1 (1:2,000, Millipore MAB363), mouse anti-GluN3A (1:100, kind gift from J.S. Trimmer), and mouse anti-DARPP-32 (1:500; BD Biosciences, 611520) were used for immunoblotting, followed by incubation with horseradish peroxidase-conjugated secondary antibodies (1:10,000, GE Healthcare). Blots were developed using enhanced chemiluminescence (ECL) plus substrate (Pierce) and exposed to film (GE Healthcare), and band intensities were quantified on a densitometer (Bio-Rad).

#### Spine Measurements

Fresh brains were processed following the Golgi-Cox method.<sup>17</sup> The slides were randomly coded, and the experimenter was blind to genotype during image acquisition and analysis. Bright-field images of Golgi-impregnated MSNs were captured with a 100× oil objective. Only fully impregnated MSNs with their soma and at least four orders of dendrites entirely within the thickness of the section were included in the analysis. Image z stacks were taken every 0.75 μm and analyzed with Fiji software. A total of 2,536 dendritic segments (25–124-μm long; average, 50.67 μm) were traced through different layers of the stack and spines counted. Spine density per neuron was calculated in as many tertiary dendrites of length >25 μm as could be unequivocally identified per neuron (range, 7–15 dendrites).

#### Behavioral Tests

Two independent male mice cohorts of 10–12 months of age were used. For motor coordination assessment, naive mice were placed on a rotarod with a fixed speed of 12 rpm (two trials/day, spaced 2 hr) and the number of falls was recorded until the sum of latencies to fall reached a total of 60 s per trial. A balance beam test was used to evaluate fine motor coordination and balance.<sup>33</sup> Mice were placed at one end of a 12-mm-wide, 90-cm-long beam, and the time to reach an escape box containing nesting material and located in the opposite end was recorded. Mice were allowed to rest for 15 s before next trial with a total of three consecutive trials. After 2 hr, the test was repeated using a 6-mm beam width. Muscular strength was measured as described previously.<sup>34</sup> In brief, mice were placed on top of a standard wire cage lid (surrounded by tape to prevent mice walking off the edge), and after light shaking so mice gripped the wires, the lid was turned upside down. Latency to the first fall was recorded.

#### Statistical Analysis

Statistical analysis was performed using GraphPad Prism 5. Sample sizes for each experiment were determined based on previous studies

from our laboratory. One- or two-way ANOVA followed by Bonferroni post-hoc tests was used to assess differences between groups. In all figures, data are presented as means ± SEM.

#### SUPPLEMENTAL INFORMATION

Supplemental Information includes three figures and can be found with this article online at <https://doi.org/10.1016/j.ymtbe.2018.05.013>.

#### AUTHOR CONTRIBUTIONS

S.M. performed surgeries and behavioral experiments; S.M. and A.M. performed jointly all other experiments and data analysis. I.P.-O. and S.M. conceived the study, designed experiments, analyzed data, and wrote the paper.

#### CONFLICTS OF INTEREST

The authors have no conflict of interest.

#### ACKNOWLEDGMENTS

The authors thank Luis Garcia-Rabareda and John Wesseling for advice with the behavioral studies and manuscript writing and Miguel Pérez-Otaño for help with graphic design. Work was funded by the Spanish Ministry of Science (grants CSD2008-00005 and SAF2016-80895-R to I.P.-O., SAF2013-48983-R to I.P.-O. and J.F.W., SEV-2013-0317 to the Instituto de Neurociencias, and fellowship BES-2014-069359 to A.M.), UTE project CIMA, the Marató TV3 Foundation, Beca Josefina Garre (to I.P.-O.), and the Fundación Caja Navarra (to S.M.).

#### REFERENCES

- Wesseling J.F., and Pérez-Otaño, I. (2015). Modulation of GluN3A expression in Huntington disease: a new n-methyl-D-aspartate receptor-based therapeutic approach? *JAMA Neurol.* 72, 468–473.
- Bodreau, R.L., McBride, J.L., Martins, I., Shen, S., Xing, Y., Carter, B.J., and Dawson, B.L. (2009). Nucleus-specific silencing of mutant and wild-type huntingtin demonstrates therapeutic efficacy in Huntington's disease mice. *Mol. Ther.* 17, 1055–1063.
- Kordukiewicz, H.B., Sznack, L.M., Wozniak, E.V., Manic, C., McAlonis, M.M., Pytel, K.A., Artales, J.W., Weiss, A., Cheng, S.H., Shihabuddin, L.S., et al. (2012). Sustained therapeutic reversal of Huntington's disease by transient repression of huntingtin synthesis. *Neuron* 74, 1031–1044.
- Drouot, V., Perrin, V., Haug, B., Dufour, N., Auergan, G., Alves, S., Burmeister, G., Brouillet, E., Lüthi-Carter, K., Hamtrays, P., and Déglen, N. (2009). Sustained effects of nonallele-specific Huntington silencing. *Ann. Neurol.* 63, 276–285.
- Ravikumar, B., Vacher, C., Berger, Z., Davis, J.E., Luo, S., Oroz, L.G., Scarff, B., Easton, D.F., Duden, R., O'Kane, C.J., and Rubenstein, D.C. (2004). Inhibition of mTOR induces autophagy and reduces toxicity of polyglutamine expansions in fly and mouse models of Huntington disease. *Nat. Genet.* 36, 585–595.
- Bates, G.P., Dorsey, D., Gusella, J.F., Hayden, M.R., Kay, C., Leavitt, B.R., Nance, M., Ross, C.A., Seubert, R.L., Warde, R., et al. (2015). Huntington disease. *Nat. Rev. Dis. Primers* 1, 15005.
- Irurozqui-Sanchez, M., Lam, W., Hanna, M., Stencheva, B., Imortino, S., Fleming, A., Tarditi, A., Meneses, F., Datta, T.J., Xu, C., et al. (2013). siRNA screen identifies Q1CT as a druggable target for Huntington's disease. *Nat. Chem. Biol.* 11, 347–354.
- Ross, C.A., and Tabrizi, S.J. (2011). Huntington's disease: from molecular pathogenesis to clinical treatment. *Lancet Neurol.* 10, 83–98.

9. Millerwood, A.J., and Raymond, L.A. (2010). Early synaptic pathophysiology in neurodegeneration: insights from Huntington's disease. *Trends Neurosci.* 33, 513–523.
10. Veldman, M.D., and Yang, X.W. (2018). Molecular insights into cortico-striatal miscommunications in Huntington's disease. *Curr. Opin. Neurobiol.* 48, 79–89.
11. Crawford, G.A., Williams, R.S., and DiFiglia, M. (1985). Evidence for degenerative and regenerative changes in neostriatal spiny neurons in Huntington's disease. *Science* 227, 770–773.
12. Ferrante, R.J., Kowal, N.W., and Richardson, E.F., Jr. (1991). Proliferative and degenerative changes in striatal spiny neurons in Huntington's disease: a combined study using the section-Golgi method and calbindin D28k immunocytochemistry. *J. Neurosci.* 11, 3877–3887.
13. Tabrizi, S.J., Scahill, B.L., Durr, A., Ross, R.A., Leavitt, B.R., Jerni, R., Landwehrmeyer, G.B., Fox, N.C., Johnson, H., Hicks, S.L., et al. TRACK-HD Investigators (2011). Biological and clinical changes in premanifest and early stage Huntington's disease in the TRACK-HD study: the 12-month longitudinal analysis. *Lancet Neurol.* 10, 31–42.
14. Tabrizi, S.J., Scahill, B.L., Owen, G., Durr, A., Leavitt, B.R., Ross, R.A., Bressan, B., Landwehrmeyer, G.B., Fox, N.C., Johnson, H., et al. TRACK-HD Investigators (2013). Predictors of phenotypic progression and disease onset in premanifest and early-stage Huntington's disease in the TRACK-HD study: analysis of 36-month observational data. *Lancet Neurol.* 12, 637–649.
15. Harrington, D.L., Liu, D., Smith, M.M., Mills, J.A., Long, J.D., Ayward, E.H., and Paulsen, J.S. (2014). Neuroanatomical correlates of cognitive functioning in preclinical Huntington disease. *Brain Behav.* 4, 29–40.
16. Perez-Otano, I., Laneri, E.S., and Weisling, J.F. (2016). Emerging roles of GluN2B-containing NMDA receptors in the CNS. *Nat. Rev. Neurosci.* 17, 623–633.
17. Marco, S., Girak, A., Petrovic, M.M., Poldi, M.A., Martinez-Turillas, R., Martinez-Hernandez, I., Kohlschütter, L.S., Torres-Peña, J., Graham, R.K., Watanabe, M., et al. (2013). Suppressing aberrant GluN2A expression rescues synaptic and behavioral impairments in Huntington's disease models. *Nat. Med.* 19, 1030–1038.
18. Mahfooz, K., Marco, S., Martínez-Turillas, R., Raju, M.K., Pérez-Otano, I., and Weisling, J.F. (2016). GluN2A promotes NMDA spiking by enhancing synaptic transmission in Huntington's disease models. *Neurobiol. Dis.* 93, 47–56.
19. Kebon, L.A., Belone, C., De Ros, M., Zandieta, A., Day, P.N., Pérez-Otano, I., and Müller, D. (2014). GluN2A promotes dendritic spine pruning and destabilization during postnatal development. *J. Neurosci.* 34, 9213–9223.
20. Borel, F., Kae, M.A., and Mueller, C. (2016). Recombinant AAV as a platform for translating the therapeutic potential of RNA interference. *Mol. Ther.* 22, 692–701.
21. Davidson, B.L., and McCray, P.B., Jr. (2011). Current prospects for RNA interference-based therapies. *Nat. Rev. Genet.* 12, 329–340.
22. Yuan, T., Marsh, M., O'Connor, E.C., Day, P.N., Verpillat, C., Sala, C., Pérez-Otano, I., Madsen, C., and Belone, C. (2015). Expression of cocaine-evoked synaptic plasticity by GluN2A-containing NMDA receptors. *Neuron* 80, 1025–1034.
23. Aschauer, D.P., Krenn, S., and Buxpel, S. (2013). Analysis of transduction efficiency, tropism and axonal transport of AAV serotypes 1, 2, 5, 6, 8 and 9 in the mouse brain. *PLoS ONE* 8, e76310.
24. Cearley, G.N., Vandenberghe, J.H., Parente, M.K., Carrish, R.R., Wilson, J.M., and Walk, J.H. (2006). Expanded repertoire of AAV vector serotypes mediate unique patterns of transduction in mouse brain. *Mol. Ther.* 16, 1710–1718.
25. Paxinos, G., and Franklin, K. (2001). *The Mouse Brain in Stereotaxic Coordinates* (San Diego, CA: Elsevier Academic Press).
26. Slow, E.J., van Raamsdonk, J., Rogers, D., Coleman, S.H., Graham, R.K., Dery, Y., Oh, R., Basada, N., Hussain, S.M., Yang, Y.Z., et al. (2013). Selective striatal neuronal loss in a YAC128 mouse model of Huntington disease. *Hum. Mol. Genet.* 12, 1359–1367.
27. Rubinsteyn, D.C., and Orr, S.T. (2016). Dismantling rotors for mechanistic therapeutics with neurodegenerative disease duration? There may be a point in the course of a neurodegenerative condition where therapeutics targeting disease-causing mechanisms are futile. *BioEssays* 38, 977–984.
28. Ayward, E.H., Sparks, S.F., Field, K.M., Vallapragada, V., Shpreit, B.D., Rosenblatt, A., Brandt, J., Gintley, L.M., Liang, K., Zhou, H., et al. (2004). Onset and rate of striatal atrophy in preclinical Huntington disease. *Neurology* 63, 66–72.
29. Okamoto, S., Portadi, M.A., Talantova, M., Yao, D., Xia, P., Ibrerboeder, D.E., Zaidi, B., Clemente, A., Kuhl, M., Graham, R.K., et al. (2009). Balance between synaptic versus extrasynaptic NMDA receptor activity influences inclusion and neurotoxicity of mutant huntingtin. *Nat. Med.* 15, 1407–1413.
30. Kiser, M.S., Koriatowicz, H.B., and Michnick, J.L. (2016). Gene suppression strategies for dominantly inherited neurodegenerative diseases: lessons from Huntington's disease and spinocerebellar ataxia. *Hum. Mol. Genet.* 25 (B1), R53–R64.
31. Montoya, A.M., Hanks, V.A., Kiser, M.S., and Davidson, B.L. (2017). CRISPR/Cas9 editing of the mutant Huntington allele in vitro and in vivo. *Mol. Ther.* 23, 12–23.
32. Kay, C., Skene, N.H., Southwell, A.L., and Hayley, M.E. (2014). Personalized gene silencing therapeutics for Huntington disease. *Clin. Genet.* 86, 29–36.
33. Luong, T.N., Carlisle, H.J., Southwell, A., and Patterson, P.H. (2011). Assessment of motor balance and coordination in mice using the balance beam. *J. Vis. Exp.* <https://doi.org/10.3791/2376>.
34. Casals, J.M., Prada, J.R., Torres-Peña, J.F., Bosh, M., Martín-Baron, R., Muñoz, M.T., Mergold, C., Erdler, P., and Albrecht, J. (2004). Brain-derived neurotrophic factor regulates the onset and severity of motor dysfunction associated with encephalergic neuronal degeneration in Huntington's disease. *J. Neurosci.* 24, 7727–7738.

YMTHE, Volume 26

**Supplemental Information**

**RNAi-Based GluN3A Silencing Prevents  
and Reverses Disease Phenotypes  
Induced by Mutant huntingtin**

Sonia Marco, Alvaro Murillo, and Isabel Pérez-Otaño

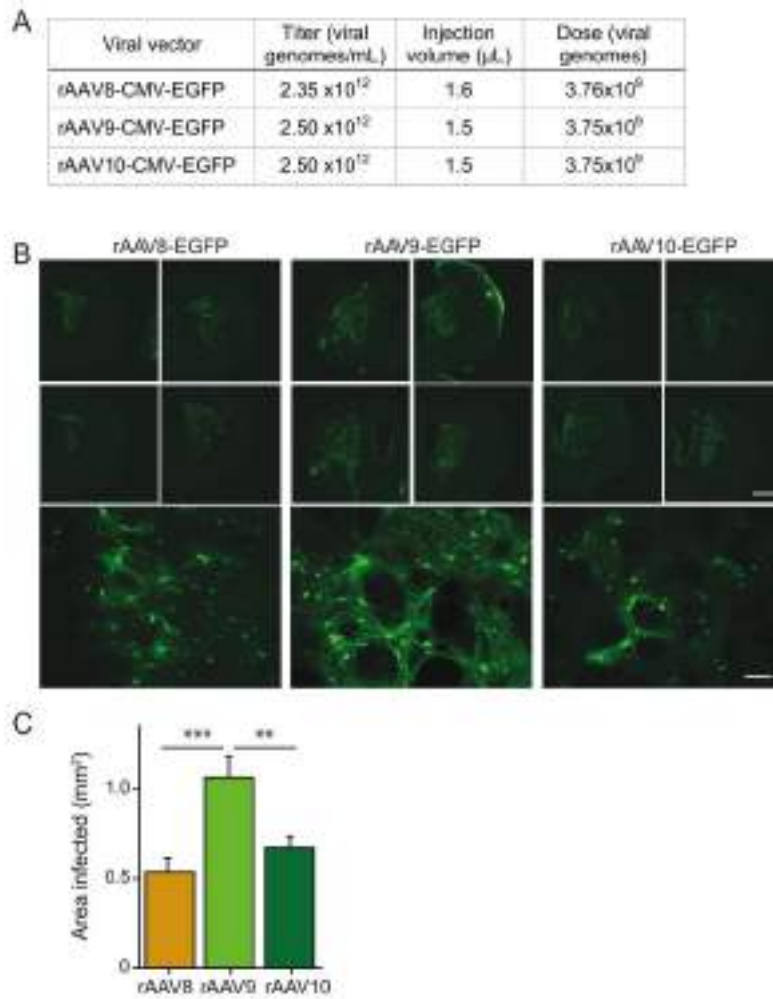


**Figure S1. Comparison of transduced striatal area between rAAV serotypes upon a single striatal injection**  
 (A) Titers and volumes of injection for rAAVs used in serotype comparison. (B) Photomicrographs of coronal sections from mice bilaterally injected into the striatum with rAAV8-, rAAV9-, or rAAV10-EGFP, and sacrificed 2 weeks later. Scale bar: 1mm and 100  $\mu$ m. (C) Quantification of striatal area displaying GFP fluorescence in series of mosaic images separated 240  $\mu$ m. Data are mean  $\pm$  S.E.M. (n=3 animals per serotype; \*\*  $P < 0.01$ , \*\*\*  $P < 0.001$ , one-way ANOVA followed by Bonferroni multiple comparison test).

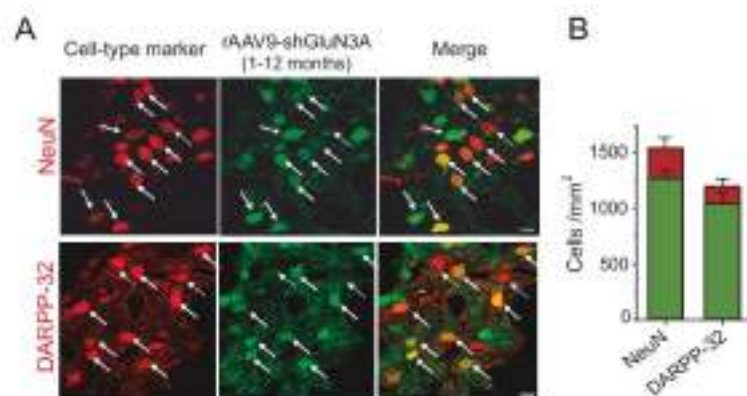


**Figure S2. Long-lasting transduction of striatal neurons by rAAV9-shGluN3A**

(A) Single confocal images of representative striatal sections from a YAC128 mouse receiving rAAV9-shGluN3A at 1 month of age (green) and stained by immunohistochemistry for NeuN or DARPP-32 at 12 months (red). Solid arrows: examples of colocalization; dashed arrows: no colocalization. Scale bar: 10  $\mu$ m.

(B) Quantification of number of striatal neurons transduced by rAAV9-shGluN3A. Data are mean  $\pm$  S.E.M. (n= 3 mice, 2-3 striatal fields analysed and averaged per mice).

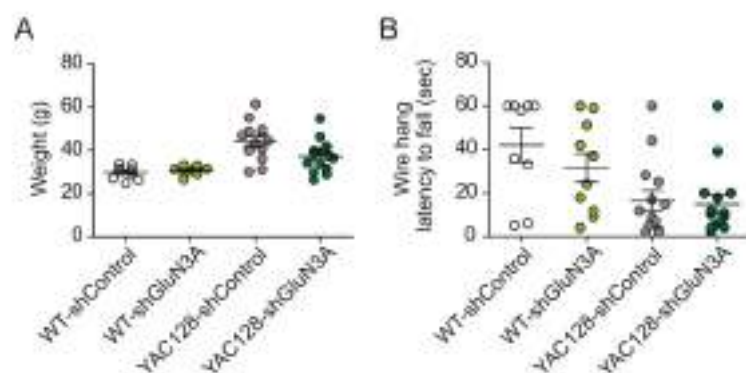


**Figure S3. Body weight and muscular strength are not affected by rAAV9-shGluN3A intrastriatal injection.**

(A) Body weight is increased in 10-12 month-old YAC128 mice compared to WT mice. Injection into the striatum of rAAV9-shGluN3A has no significant effect in body weight. Two-way ANOVA: genotype x shRNA interaction  $F(1,44) = 3.95$ ,  $P = 0.0530$ ; shRNA  $F(1,44) = 2.37$ ,  $P = 0.1305$ ; genotype  $F(1,44) = 31.3$ ,  $P < 0.0001$ .

(B) Latency to fall from the wire. Two-way ANOVA: genotype x shRNA  $F(1,44) = 0.635$ ,  $P = 0.4298$ ; shRNA  $F(1,44) = 1.14$ ,  $P = 0.2924$ ; genotype  $F(1,44) = 14.2$ ,  $P = 0.0005$ .



«Lo bueno de la ciencia es que es cierta independientemente de  
si crees o no en ella»

-Neil deGrasse Tyson-

**RESULTS (Second chapter)**

A vibrant, multi-colored nebula or galaxy core. The image features swirling patterns of blue, green, and red against a dark background, suggesting a complex, multi-colored celestial object. The colors are distributed in a way that creates a sense of depth and movement, with the blue and green appearing more prominent in the foreground and the red appearing more in the background.



## ORIGINAL ARTICLE

# Temporal Dynamics and Neuronal Specificity of Grin3a Expression in the Mouse Forebrain

Alvaro Murillo<sup>1,2</sup>, Ana I. Navarro<sup>1</sup>, Eduardo Puelles<sup>1</sup>, Yajun Zhang<sup>3</sup>, Timothy J. Petros<sup>3</sup> and Isabel Pérez-Otaño<sup>1</sup>

<sup>1</sup>Instituto de Neurociencias, Consejo Superior de Investigaciones Científicas – Universidad Miguel Hernández, 03550 Sant Joan d'Alacant, Spain, <sup>2</sup>UK Dementia Research Institute at Cardiff University, CF24 4HQ Cardiff, UK and <sup>3</sup>Eunice Kennedy Shriver National Institute of Child Health and Human Development, Bethesda, MD, USA

Address correspondence to Isabel Pérez-Otaño, Instituto de Neurociencias, CSIC-UMH, Av. Ramón y Cajal s/n, 03550 Sant Joan d'Alacant, Spain. Email: otano@umh.es

## Abstract

GluN3A subunits endow N-Methyl-D-Aspartate receptors (NMDARs) with unique biophysical, trafficking, and signaling properties. GluN3A-NMDARs are typically expressed during postnatal development, when they are thought to gate the refinement of neural circuits by inhibiting synapse maturation, and stabilization. Recent work suggests that GluN3A also operates in adult brains to control a variety of behaviors, yet a full spatiotemporal characterization of GluN3A expression is lacking. Here, we conducted a systematic analysis of *Grin3a* (gene encoding mouse GluN3A) mRNA expression in the mouse brain by combining high-sensitivity colorimetric and fluorescence *in situ* hybridization with labeling for neuronal subtypes. We find that, while *Grin3a* mRNA expression peaks postnatally, significant levels are retained into adulthood in specific brain regions such as the amygdala, medial habenula, association cortices, and high-order thalamic nuclei. The time-course of emergence and down-regulation of *Grin3a* expression varies across brain region, cortical layer of residence, and sensory modality, in a pattern that correlates with previously reported hierarchical gradients of brain maturation and functional specialization. *Grin3a* is expressed in both excitatory and inhibitory neurons, with strong mRNA levels being a distinguishing feature of somatostatin interneurons. Our study provides a comprehensive map of *Grin3a* distribution across the murine lifespan and paves the way for dissecting the diverse functions of GluN3A in health and disease.

**Key words:** circuit refinement, excitatory glycine receptors, high-order thalamus, neocortical maturation, somatostatin interneurons

## Introduction

N-Methyl-D-Aspartate receptors (NMDARs) are a family of excitatory glutamate-gated ion channels with central roles in brain plasticity, development, learning, and memory (Paoletti et al. 2013). Each receptor consists of four subunits, an obligatory GluN1 subunit and combinations of GluN2 (A-D) and GluN3 (A, B) subunits, which generates a variety of subtypes with distinct biophysical and signaling properties, distribution, and functions. Whereas GluN1 and GluN2 are expressed in the central nervous system throughout life in high concentrations, GluN3A subunits

are rarer and predominate during early postnatal stages. Heteromeric complexes composed of GluN1/GluN2/GluN3A respond to glutamate and NMDA, and are thus bona-fide NMDARs. However, they have nonconventional properties that distinguish them from classical NMDARs (GluN1/GluN2 heteromers) including lower calcium permeability, reduced voltage-dependent block by magnesium, and lesser attachment to postsynaptic densities. Because of these properties, they can work as dominant-negative regulators of NMDAR-mediated

plasticity and have been proposed to fine-tune the refinement of neural circuits during critical postnatal periods by inhibiting the stabilization of nonused synapses and promoting their pruning (Pachernegg et al. 2012; Perez-Otano et al. 2016).

Recent studies point towards broader roles of GluN3A subunits in the mammalian brain. First, GluN3A can form GluN1/GluN3 complexes that do not bind glutamate and instead generate excitatory currents activated by glycine (Perez-Otano et al. 2001; Chatterton et al. 2002). Although initially studied in recombinant systems, native GluN1/GluN3A receptors have now been identified in juvenile mouse hippocampus and adult medial habenula (Grand et al. 2018; Otsu et al. 2019). Rather than modulating plasticity, their activation potentiates basal firing rates and could have a major influence on neuronal excitability. Second, while GluN3A protein and mRNA levels are largely down-regulated after critical developmental periods, the Allen Brain Atlas documents remaining *Grin3a* mRNA expression in adult brains and a variety of phenotypes of cognition, social, and aversive behavior have been reported in adult mice lacking GluN3A, suggesting that functional relevance may continue throughout life (Mohamad et al. 2013; Lee et al. 2016; Otsu et al. 2019). Third, genetic mutations or alterations in human *GRIN3A* expression have been linked to disorders of cognition, mood, and emotion such as schizophrenia, bipolar disorder, or substance abuse, suggesting alterations in the control of affective, impulsive traits or executive functions (Mueller and Mesdor-Woodruff 2004; Yang et al. 2015; Lee et al. 2016; Huang et al. 2017). Importantly, preclinical mouse studies provided causal relationships between age-inappropriate reactivation of functional GluN3A expression and pathological spine pruning in Huntington's disease, or maladaptive forms of plasticity that predispose to drug relapse (Marco et al. 2013, 2018; Yuan et al. 2013), making GluN3A an attractive candidate for therapeutic intervention.

At present it is unclear how GluN3A subunits subserve such diverse functions and whether links to behavior or disease endophenotypes reflect adult roles of GluN3A or faults in the developmental trajectories of specific neuronal circuits. A limitation for dissecting GluN3A functions has been the lack of a comprehensive understanding of the timing and regional variations in GluN3A expression throughout development and in the adult brain, and of the cellular populations where GluN3A is expressed. To address this limitation, we have conducted a systematic analysis of *Grin3a* mRNA expression in the mouse brain from embryonic to early postnatal and adult stages using colorimetric and fluorescence in situ hybridization (ISH). We find that, while subject to a prominent down-regulation, substantial *Grin3a* expression is retained in a subset of brain regions. Specifically, adult *Grin3a* expression was highest in multimodal or associative areas such as the insular, prefrontal, and anterior cingulate cortices or the claustrum, and in areas encoding or integrating internal emotional or arousal/awareness states such as the amygdala, medial habenula, or "high-order" thalamic nuclei. Throughout postnatal development, *Grin3a* expression exhibits precise temporal dynamics that differ in neocortical areas across sensory modalities and cortical layer. At the cellular level, *Grin3a* is expressed by both excitatory and inhibitory neurons, with high expression a distinguishing feature of somatostatin (Sst) interneurons.

## Materials and Methods

### Animals and Tissue Collection

Several strains of C57BL/6 J background mice were used: WT, *GAD67<sup>Cre</sup>* (B6.Cg-Tg[Gad1-EGFP] (Tarnamaki et al. 2003) and *Nix2.1-Cre::Ai9<sup>flTm40</sup>*. The latter was obtained crossing Tg[Nkx2.1-Cre]25 and/ (JAX 008661; (Xu et al. 2008) and Ai9[B6.Cg-Gt(ROSA)26Sortm9(CAG-tdTomato)Hze/] (JAX 007909) (Madisen et al. 2010). Mice were housed 4–6 per cage with ad libitum access to food and water and maintained in a temperature-controlled environment on a 12-h light/dark cycle at humidity between 40 and 60% in a standard pathogen free environment. All procedures were conducted in accordance with the European and Spanish regulations (2010/63/UE; RD53/2013) and were approved by the Ethical Committee of the Government of the Generalitat Valenciana (2017/VSC/PEA/00196).

After deep anesthesia with isoflurane, mice were transcardially perfused with 4% paraformaldehyde in phosphate buffered saline (PBS) pH 7.4. Brains were removed and postfixed overnight at 4°C. From this step on, tissue treatment was different depending on the later technique. For colorimetric and fluorescence ISH, brains were then embedded in 4% agarose, sectioned coronally in 100 or 80  $\mu\text{m}$ -thick slices respectively with a vibrating microtome and stored in PBS at 4°C. For RNAscope assays, tissue was immersed in 30% sucrose at 4°C and frozen in OCT. Frozen brains were sectioned at 14  $\mu\text{m}$  with a cryostat and stored at  $-80^\circ\text{C}$ .

### Cloning and In Situ Hybridization

Templates for synthesizing *Grin3a* riboprobes were obtained by PCR from cDNA libraries of hippocampus of C57BL/6 using the following primers: forward GAACACATAGTGTACAGACTGC; reverse CTAGGATTCACAAGTCCGGT. The resulting amplicon was purified with QIAquick gel extraction kit- (QIAGEN) and cloned into pBlueScript SK plasmid. Plasmids for riboprobes against *Gad1* mRNA were a gift from Dr Jordi Guimer. The riboprobes were: *Grin3a*-ctd (spanning 495 bp of the C-terminal domain, accession number NM\_001033351.2) and *Gad1* (bp 934–1786 of the *Gad1* cDNA, accession number NM\_008077). Plasmids were linearized and riboprobes labeled with UTP-digoxigenin or UTP-fluorescein during *in vitro* transcription using polymerase T3 or T7 (for antisense and sense riboprobes, respectively). Riboprobes were then purified by RNeasy Mini Kit Qiagen and concentrations measured with NanoDrop.

Free-floating 100  $\mu\text{m}$ -thick brain sections were permeabilized with detergent mix (1% NP-40, 1% SDS, 0.5% sodium deoxycholate, 50 mM Tris pH 8.0, 1 mM EDTA, and 150 mM NaCl) for 1 h at room temperature, and incubated with digoxigenin-labeled riboprobes at 63°C in hybridization buffer (50% formamide; 2x saline-sodium citrate pH 5.3; 50  $\mu\text{g}/\text{mL}$  heparin; 50  $\mu\text{g}/\text{mL}$  tRNA; 50  $\mu\text{g}/\text{mL}$  salmon sperm DNA; 0.1% Tween-20) overnight. Hybridized probes were detected using an alkaline phosphatase-conjugated antidigoxigenin (Roche 11093274910, 1:2000) in blocking solution (2% Roche Blocking reagent and 20% sheep serum in MABT buffer) overnight at 4°C, followed by several washes in MABT buffer (500 mM maleic acid, 750 mM NaCl, 0.95 M NaOH, and 0.1% Tween-20, pH 7.5). For visualization, sections were then incubated at room temperature during 6 or 22 h in a solution containing

nitroblue tetrazolium chloride (NBT) and 5-bromo-4-chloro-3'-indolylphosphate p-toluidine salt (BCIP) in NTMT buffer (100 mM NaCl; 100 mM Tris-HCl pH 9.5; 50 mM MgCl<sub>2</sub>; 1% Tween-20) that produces a colored precipitate due to the reaction with alkaline phosphatase. After several washes in PBS 1x, sections were mounted onto Superfrost Plus slides (Thermo Fisher Scientific™), dehydrated, and coverslipped with DPX mounting solution.

### Fluorescence In Situ Hybridization

Identical protocol to the described above was followed, except 80 µm-thick brain sections were used. Sections were incubated with digoxigenin- and fluorescein-labeled riboprobes (against *Grin3a* and *Gad1* mRNA, respectively) in hybridization buffer, followed by incubation with peroxidase-conjugated antidigoxigenin or anti-fluorescein antibodies (Roche 11 207 733 910; Roche 11 426 346 910, 1:2000). A TSA plus fluorescence kit was used for signal amplification and detection according to the manufacturer protocol (Thermo Fisher, NEL744001KT). To avoid non-specific signal, endogenous peroxidases were inactivated by incubation with MABT-1% H<sub>2</sub>O<sub>2</sub> for 1 h in the dark. Sense probes used as control yielded no signal. Double fluorescence ISH was performed with dual hybridization and duplication of detection and amplification steps. Sections were counterstained with DAPI, mounted onto Superfrost Plus slides (Thermo Fisher), air-dried, and cover-slipped with fluorescence mounting medium (DAKO).

### Immunohistochemistry

After the fluorescence ISH procedure, free-floating brain sections were incubated with primary antibody in 1% BSA, 0.1% Triton X-100, and 1% NS in PBS overnight at 4°C. The following primary antibodies were used: rabbit anti-GFP (Synaptic systems 132 002, 1:1000), rabbit anti-Cux1 (Santa Cruz Biotechnology Sc-13024, 1:500) and rat anti-Ctip2 (Abcam Ab18465, 1:500). After washing with PBS, sections were incubated with fluorophore-conjugated secondary antibody in 1% BSA, 0.1% Triton X-100 in PBS for 1 h at room temperature. The following secondary antibodies were used: anti-rabbit-Cy3 (Jackson ImmunoResearch 111 175 144, 1:500), anti-rat-488 (Invitrogen A11006, 1:500) and anti-rabbit-488 (Invitrogen A11008, 1:500). After several washes in PBS, sections were counterstained with DAPI, mounted onto Superfrost Plus slides, air-dried, and coverslipped with fluorescence mounting medium (DAKO).

### Image Acquisition and Analysis

Bright field images were acquired using a Leica DM6000B microscope with 5X and 10X objectives or a MZ16FA stereomicroscope equipped with a DC500 digital camera, and processed with Leica AF6000 software. Quantification of *Grin3a* expression across cortical layers and sensory modalities was performed using Fiji for automatic detection of positive labeling after background subtraction. Fluorescence confocal images were captured on an Olympus FV1200 with a 20X objective or a ZEISS AxioImager M2 microscope with an Apochromat 20X objective, and processed with FV10-ASW\_Viewer and Zen Blue software, respectively. The colocalization of *Grin3a*-positive cells with neuronal subtype-specific markers was quantified using Fiji software.

For anatomical analysis, identification of structures and functional interpretation, the Mouse brain in stereotaxic

coordinates (Paxinos and Franklin, 2019 Edition), the Mouse nervous system (Watson, Paxinos, Puelles, 2012 Edition) and the Atlas of the developing mouse brain (Paxinos, Halliday, Watson, Koutcherov, Wang, 2007 Edition) were used.

### RNAscope In Situ Hybridization Assay

RNAscope® Multiplex Fluorescent Kit v2 (Advanced Cell Diagnostics) was used to perform ISH with the following probes: *Grin3a*-C1 (#551371), *Gad1*-C2 (#400951-C2), *Slc17a7*-C3 (vGlut1)(#416 631-C3), *Sst*-C3 (#404631-C3), and *tdTomato*-C2 (#317041-C2).

Briefly, slides were dried for 60 min at -20°C, washed in PBS for 5 min, then baked for 10 min at 60°C. The slides were postfixed by immersing them in prechilled 4% PFA for 10 min at ice, followed by two rinses in diH<sub>2</sub>O. Slides were dehydrated for 5 min each in 50%, 70%, and 100% ethanol, then dried for 5 min at RT. About 5–8 drops of RNAscope hydrogen peroxide was applied to the slides for 10 min followed by diH<sub>2</sub>O washing. Then, slides were transferred to a container with RNAscope target retrieval reagent and incubated at >95°C for 5 min, then incubated in 100% alcohol for 3 min. After drying the slides at RT, they were treated with Protease III for 20 min at 40°C. After rinsing two times in distilled water, 1X target probe mixes were applied to the brain sections and incubated at 40°C for 2 h in the HyBEZ™ oven (Advanced Cell Diagnostics). Sections were then incubated with preamplifier and amplifier probes and develop HRP-C1, C2, and C3 signals with TSA Plus fluorophores (PerkinElmer) by following the RNAscope® Multiplex Fluorescent Kit v2 user manual. After washing, sections were stained for 30 s with DAPI.

### Statistical Analysis

Statistical analysis was performed using GraphPad Prism 7. For qualitative and semi-quantitative analysis of colorimetric ISH data in Figures 1–4 and Supplementary Table 1, the following number of mice were analyzed: E17.5 (n = 3), P0 (n = 6), P3 (n = 6), P6 (n = 16, short and long exposure), P9 (n = 6), P12 (n = 4), adult (n = 3, long exposure). Two-way ANOVA followed by Bonferroni's multiple comparisons posthoc test was used to assess differences between groups in Figure 5D. In all figures, data are presented as means ± SEM.

## Results

### Predominant Postnatal *Grin3a* mRNA Expression and Down-Regulation into Adulthood

We began by comparing the relative levels and regional patterns of *Grin3a* mRNA expression in young (postnatal day (P) 6) and adult (3–4 months) mouse brains using colorimetric ISH. Here and for most other experiments, sections were processed using two different exposures to the developing solution. This allowed us to achieve the high sensitivity needed for detecting adult expression (22 h, high exposure, Fig. 1), while preserving a dynamic range for semi-quantitative assessment of expression levels at earlier postnatal stages (6 h, low exposure, Figs 2–4). P6 was chosen based on previous quantitative immunoblot analyses in rodent brain that reported maximal *Grin3a* expression over the P5–P9 time window (Al-Hallaq et al. 2002; Wong et al. 2002; Roberts et al. 2009).

A first inspection confirmed that highest *Grin3a* mRNA levels are found postnatally and decline dramatically in most brain regions into adulthood (Fig. 1). However, there were

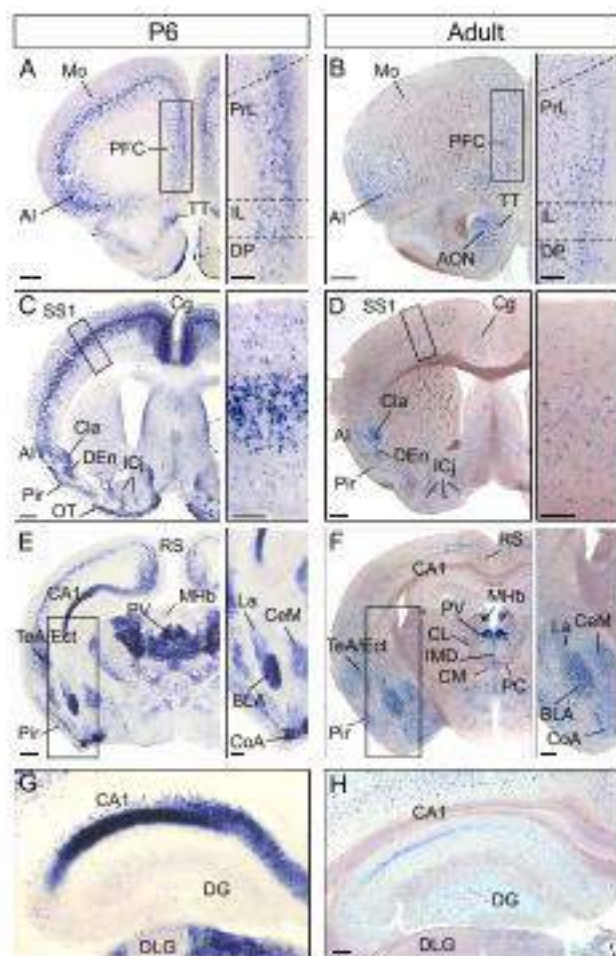


**Figure 1.** *Grin3a* expression is down-regulated into adulthood. Colorimetric ISH showing *Grin3a* mRNA expression in young (postnatal day P6; A, C, E, G) and adult mouse brain (B, D, F, H). Sections were exposed for 22 h to the developing solution to enhance sensitivity. Representative coronal sections at different rostro-caudal levels are displayed, and higher magnification images of the boxed areas are shown on the right. AI, agranular insular cortex; ACo, anterior olfactory nucleus; BLA, basolateral amygdala; CA1, Cornu Ammonis 1; CeM, central amygdala; Cg, cingulate cortex; CL, centrolateral thalamic nucleus; Cla, claustrum; CM, centromedial thalamic nucleus; CoA, cortical amygdala; DEa, dorsal endopiriform nucleus; DG, dentate gyrus; DLG, dorsal lateral geniculate nucleus; DP, dorsal peduncular cortex; Ect, ectothalamic cortex; ICj, islands of Calleja; IL, infralimbic cortex; IMD, intermediodorsal thalamic nucleus; La, lateral amygdala; MHB, medial habenula nucleus; Mo, motor cortex; OT, olfactory tubercle; PC, paracentral thalamic nucleus; PFC, prefrontal cortex; Pr, piriform cortex; PrL, prelimbic cortex; PV, paraventricular thalamic nucleus; RS, retrosplenial cortex; SS1, somatosensory cortex 1; TeA, temporal association cortex; TT, tenia tecta. Scale bars: 500  $\mu$ m (A-F), 200  $\mu$ m (G-H and insets).

notable exceptions. Substantial *Grin3a* levels were retained in specific cortical areas including the prefrontal cortex (limbic and infralimbic divisions), anterior cingulate, retrosplenial, agranular insular, temporal association, ectothalamic, and perirhinal cortices (Fig. 1B, D, F, see Supplementary Fig. 1). This adult pattern of *Grin3a* expression correlates with a cortical hierarchy of functional specialization established based on connectivity patterns or structural properties (Fulcher et al. 2019; Harris et al. 2019). High adult levels of *Grin3a* mRNA were also observed in areas of the olfactory cortex (tenia tecta, anterior olfactory nucleus, dorsoendopiriform nucleus,

islands of Calleja), in nuclei of the contiguous cortical or olfactory amygdala (anterior, ACo; and posteromedial, PMCo); and in basolateral and central amygdala (Fig. 1B, D, F, see Supplementary Fig. 1). Adult expression in the thalamus was lower and more restricted than at P6, but high levels were retained in some of the so-called “high-order” thalamic nuclei including midline (paraventricular, intermediodorsal, reuniens, rhomboid) and intralaminar nuclei (centromedial, paracentral, centrolateral) (Fig. 1F, see Supplementary Fig. 1). It is worth noting the exception of the medial habenula that displayed an opposite pattern of *Grin3a* expression, with high adult levels but low expression in young brains (Fig. 1E vs. F).

Our comparative analysis additionally revealed a clear dorso-ventral gradient of *Grin3a* expression in principal neurons of adult CA1 hippocampus (see Supplementary Fig. 2). At P6, *Grin3a* was highly expressed in CA1 pyramidal neurons throughout the entire rostrocaudal extent of the hippocampus in both dorsal and ventral divisions (Fig. 1G, see Supplementary Fig. 2A, B, D, E). In contrast, expression in dorsal CA1 was virtually absent in adults but high levels were retained in ventral CA1 pyramidal neurons (Fig. 1H, see Supplementary Fig. 2C vs. F). As previously reported (Sucher et al. 1995), no expression was detected in CA2, CA3, or dentate gyrus at either age. However, we noted a previously unappreciated strong *Grin3a* mRNA signal in a small subset of neurons in the CA1 stratum oriens which was most prominent at P6 (see Supplementary Fig. 2, insets).

As introduced above, shorter exposure to the developing solution allowed a semi-quantitative analysis of postnatal *Grin3a* expression levels across the rostro-caudal brain axis (Fig. 2 and see Supplementary Table 1). The analysis revealed a unique pattern of *Grin3a* expression with several remarkable features. First, high *Grin3a* levels were observed in most neocortical areas with predominance in deeper layers at P6 (Fig. 2A-H, see extended laminar analysis below). Expression was also high throughout the entire rostro-caudal axis of the olfactory cortex including the rostral anterior olfactory nucleus and tenia tecta, the dorsal endopiriform nucleus and piriform cortex (Fig. 2B-F); in ACo and PMCo nuclei of the cortical amygdala (Fig. 2E-H); and in the interposed cortex amygdala transition zone (Fig. 2F, G). Second, high levels were found in the basolateral, basomedial, and basoposterior divisions of the amygdala. Lower but significant levels were detected in central and lateral amygdala (Fig. 2F, G, H). Third, *Grin3a* expression was especially strong in the thalamus where it prevailed in high-order thalamic nuclei including midline thalamic nuclei (paraventricular, reuniens, rhomboid), intralaminar, mediodorsal, posterior, and lateroposterior nucleus (analogous to the primate pulvinar). By contrast, *Grin3a* was absent or expressed at very low levels in first-order, primary sensory thalamic nuclei including the dorsolateral geniculate, ventral division of the medial geniculate, or ventral posterior nuclei (Fig. 2D-F).

### Emergence and Down-regulation of *Grin3a* Expression Vary Across Brain Areas

While maximal *Grin3a* expression was previously reported in P6-P9 brains and assumed to homogeneously decline across brain regions into adulthood, earlier embryonic expression has been reported in human brains (Eriksson et al. 2002; Mueller and Meador-Woodruff 2003). Furthermore, GluN3A-NMDARs have been shown to control the propensity for precisely timed

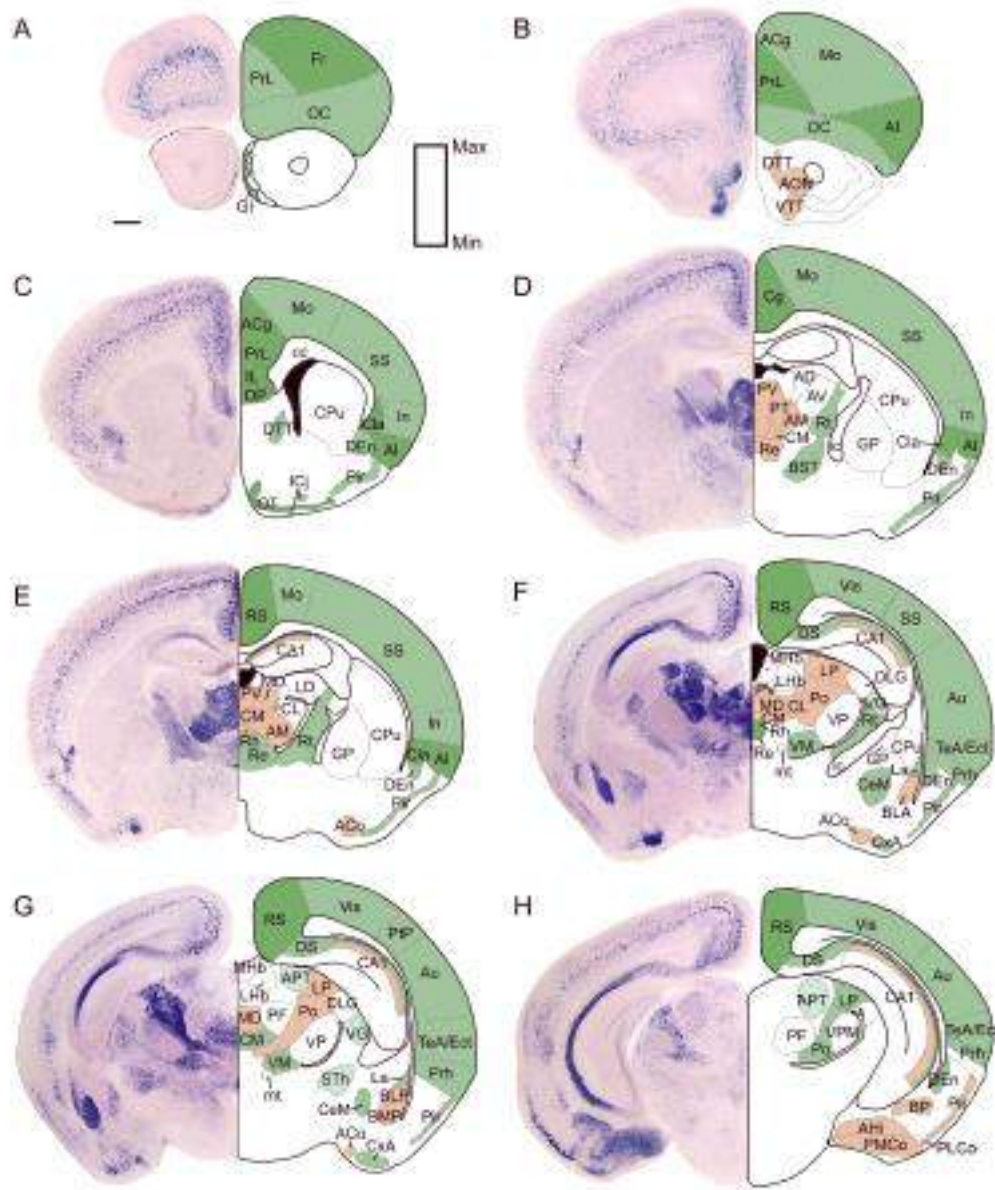


**Figure 2.** Regional distribution of *Grin3a* expression in early postnatal development. (A–H) Representative images of colorimetric ISH for *Grin3a* mRNA in coronal sections from P6 to P9 mouse brains. Here and in Figures 2–4, sections were exposed for 6 h to the developing solution. Corresponding schemes modified from the Paxinos's Atlas of the developing mouse brain are shown in the right, and mRNA expression levels are color-coded as indicated in the heatmap. The images were acquired at different rostro-caudal levels. Abbreviations are listed in Supplementary Table 1. Scale bars: 500  $\mu$ m.

forms of cortical plasticity such as the developmental onset of long-term potentiation in the hippocampus (Roberts et al. 2009) or spike-timing dependent long-term depression in visual cortex (Larsen et al. 2014) and could be predicted to display a precise timing in specific brain regions. We thus investigated the developmental time-course of *Grin3a* expression from embryonic mouse brain through multiple stages of postnatal development (P0, P3, P6, P9, P12).

We found that the age of emergence and down-regulation of *Grin3a* expression varies significantly across brain regions. By embryonic day (E) 17.5, high levels of *Grin3a* mRNA were detected in the thalamus following a similar pattern to the observed postnatally, that is, absent/low in sensory thalamus

but abundant in high-order nuclei (Fig. 3C–E). *Grin3a* was also expressed at this early time-point in the CA1 hippocampus, amygdala, cortical amygdala (Fig. 3C–E), and in the claustrum (Fig. 3B), a nucleus highly interconnected with nearly all cortical areas and involved in multimodal sensory processing (Kim et al. 2016).

*Grin3a* expression in the neocortex was low at E17.5 (Fig. 3A–E), increased postnatally, and down-regulated by P12 (Fig. 4). Yet again differences in the timing of expression were noted across neocortical areas. *Grin3a* expression appeared earliest (by P0) in cingulate, retrosplenial, and piriform cortices (Fig. 4F, K, P). By P3, expression was observed in most of the neocortex including prefrontal

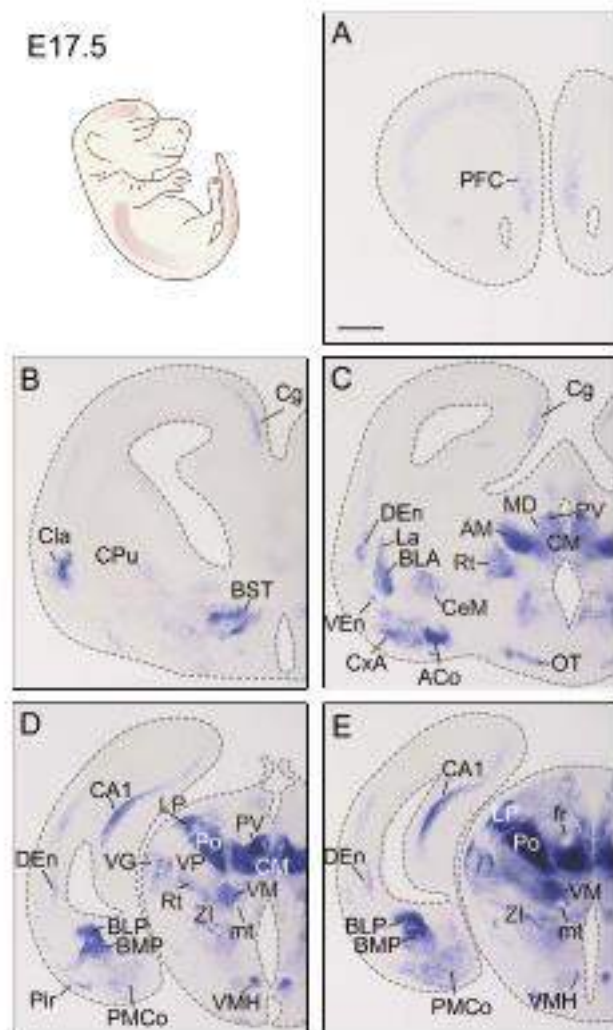


**Figure 3.** Embryonic *Grin3a* expression. (A-E) Representative images of colorimetric ISH showing *Grin3a* mRNA expression in E17.5 mouse embryos at various rostro-caudal levels. Abbreviations: ACo, anterior cortical amygdaloid nucleus; AM, anteromedial thalamic nucleus; BLA, basolateral amygdala, anterior part; BLP, basolateral amygdala, posterior part; BMP, basomedial amygdala, posterior part; BST, bed nucleus of the stria terminalis; CA1, Cornu Ammonis 1; CeM, central amygdaloid nucleus; Cg, cingulate cortex; Cla, claustrum; CM, centromedial thalamic nucleus; CPu, caudate-putamen; CxA, cortex amygdala transition zone; DEN, dorsal endopiriform nucleus; f, fasciculus retroflexus; La, lateral amygdala; LP, lateral posterior thalamic nucleus; MD, medio dorsal thalamic nucleus; mt, mammillothalamic tract; OT, olfactory tubercle; PFC, prefrontal cortex; Pir, piriform cortex; PMCo, posteromedial cortical amygdaloid nucleus; Po, posterior thalamic nucleus group; PV, paraventricular nucleus; Rt, reticular thalamic nucleus; VEn, ventral endopiriform nucleus; VG, ventrolateral geniculate nucleus; VM, ventromedial thalamic nucleus; VMH, ventromedial hypothalamic nucleus; VP, ventroposterior thalamic nucleus; ZI, zona incerta. Scale bar: 500  $\mu$ m.

and motor cortex and primary sensory cortices such as the somatosensory and auditory (Fig. 4B, G, L, Q). Expression in visual cortex was delayed and appeared around P6 (see Fig. 4P-R).

By P12, down-regulation had taken place in most regions and the characteristic adult pattern illustrated in Figure 1, with restriction to the amygdala, olfactory cortex, cortical amygdala, claustrum, and selected cortical and thalamic regions, was

reached (Fig. 4E, J, O, T). Expression in CA1 became restricted to its ventral division (Figure 4O, T, see Supplementary Fig. 2).

### Temporal Dynamics of Cortical *Grin3a* Expression Across Layers and Sensory Modalities

A major feature of developmental *Grin3a* expression in the neocortex was the initial predominance as an intense band in deeper cortical layers with later spread to other cortical laminae. To establish the laminar specificity of *Grin3a* expression, we combined fluorescence ISH with immunohistochemistry for the layer-specific markers *Ctip2* and *Cux1* that label pyramidal neurons in layer V and layers II-IV, respectively. Focused on P6 primary somatosensory cortex (SS1), we found that the highest number of *Grin3a*-positive fluorescent cells populate layer V as determined by colocalization with *Ctip2* (Fig. 5A). A subset of layer V cells could be distinguished by their strong *Grin3a* mRNA labeling (Fig. 5B, bottom panel). Only a few *Grin3a*-positive cells with much lower fluorescence signal were detected in layers II/III (Fig. 5B, upper panel).

A finer temporal analysis covering earlier to late postnatal stages revealed a highly reproducible pattern of sequential *Grin3a* expression, which extends from deep to superficial layers, but which timing varied across sensory modalities. For instance: in SS1 *Grin3a* expression begins early in layer V, with *Grin3a*-positive cells already detected in newborns (P0). A gradual increase in the number of *Grin3a*-positive cells and *Grin3a* intensity levels in layer V was observed through P3-P6. Laminar specificity became less apparent at P9 and was lost by P12 (Fig. 5C, upper panels). Quantification of signal intensities across SS1 confirmed a sharp peak of *Grin3a* expression in layer V which reached a maximum at P6, and appearance of a second peak in layers II/III by P9 (Fig. 5D, upper graph). Expression in layer V declined significantly by P9-P12 (Fig. 5D, red vs. blue and green traces; see Supplementary Table 2). A comparison with primary visual cortex (V1) demonstrated a delayed onset of *Grin3a* expression relative to SS1 (Fig. 5C, bottom panels) or motor cortex (not shown). By P6 only a few, weakly labeled, *Grin3a*-positive cells were observed in layer V of V1 and expression peaked around P9-P12 (Fig. 5D, bottom graph). The spread to upper layers had not reached statistical significance by P12 and layer V down-regulation was also delayed relative to SS1 (blue vs. green lines in Fig. 5D, see Supplementary Table 2). The analysis demonstrates a precise laminar distribution of *Grin3a* expression, which changes over postnatal development and varies across sensory modalities, as exemplified by the shift in emergence and down-regulation between SS1 and V1.

### *Grin3a* is Expressed in Excitatory and Inhibitory Neurons, with Predominance in *Sst*-Expressing Interneurons

We next aimed to achieve cellular resolution and define which neuronal subpopulations express *Grin3a*, focusing on SS1 cortex and dorsal hippocampus at P6-P9. The neocortex is composed of a majority of excitatory glutamatergic neurons (~80%) and a lower number of inhibitory GABAergic neurons (~20%). Thus, we conducted multiplex FISH assays using RNAscope probes for the vesicular glutamate transporter *vGluT1*, the GABA-synthesizing enzyme *Gad1* (glutamate decarboxylase 1), and *Grin3a* (Fig. 6A). In SS1, *Grin3a* mRNA was expressed in both excitatory and inhibitory neurons as demonstrated by colocalization of



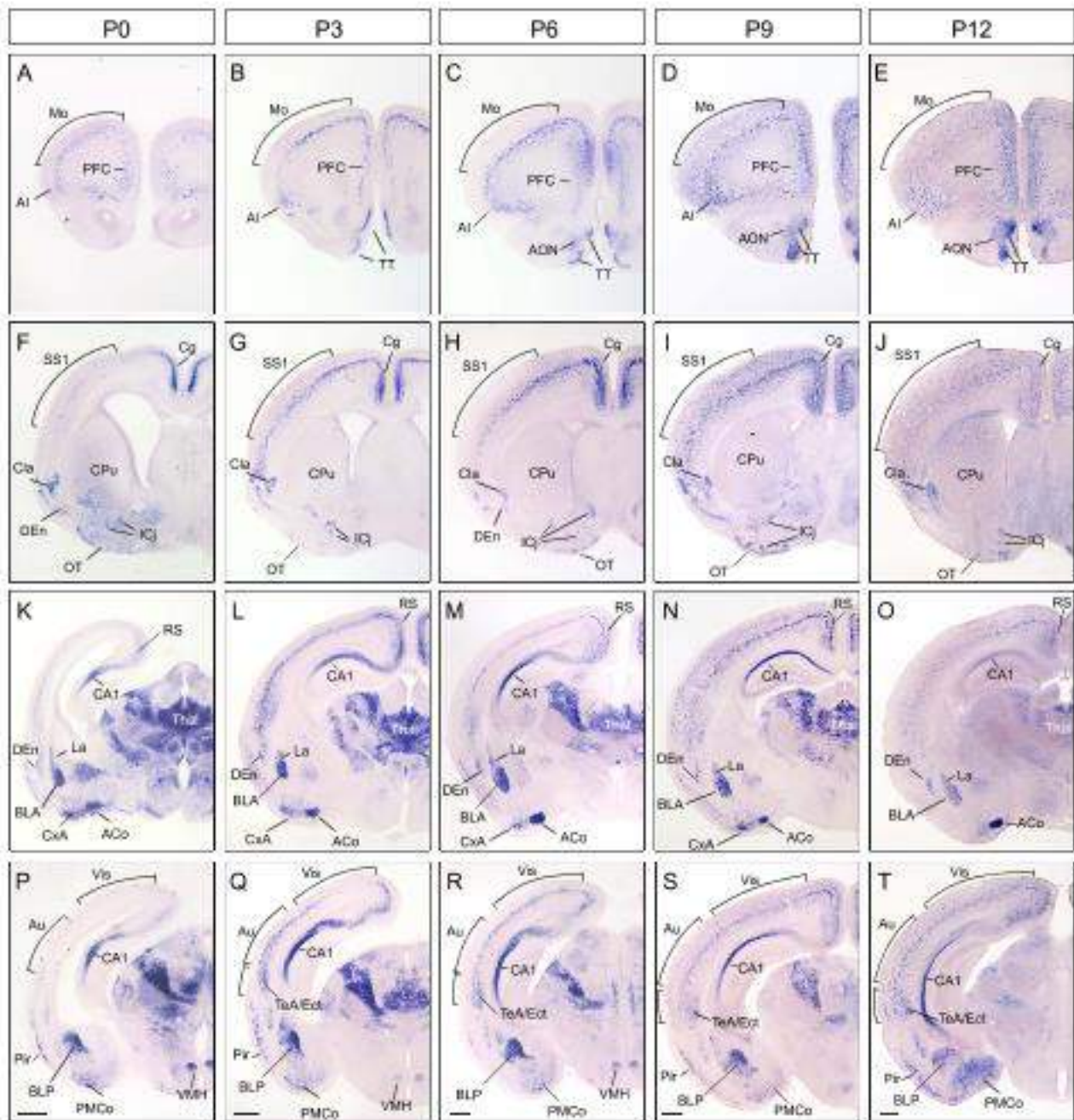


**Figure 4.** Emergence and down-regulation of *Grin3a* expression throughout postnatal developmental stages. (A-T) Colocimetric ISH for *Grin3a* mRNA in mouse brain at different postnatal (P) stages. Representative images of coronal sections at different rostro-caudal levels and indicated ages are shown. Abbreviations: ACo, anterior cortical amygdaloid nucleus; AI, agranular insular cortex; AON, anterior olfactory nucleus; Au, auditory cortex; BLA, basolateral amygdala; BLP, basolateral amygdaloid nucleus, posterior part; CA1, cornu ammonis 1; Cg, cingulate cortex; Cls, claustrum; CPu, caudate-putamen; CxA, cortex amygdala transition zone; DEn, dorsal endopiriform nucleus; Ect, ectorhinal cortex; IC, islands of Calleja; La, lateral amygdaloid nucleus; Mo, motor cortex; PFC, prefrontal cortex; OT, olfactory tubercle; Pir, piriform cortex; PMCo, posteromedial cortical amygdaloid nucleus; RS, retrosplenial cortex; SS1, somatosensory cortex 1; TeA, temporal association cortex; Thal, thalamus; TT, torus semicircularis; Vls, visual cortex; VMH, ventromedial hypothalamic nucleus. Scale bar: 100  $\mu$ m.

punctate nuclear labeling with *vGluT1* or *GAD1* mRNA (Fig. 6B). Quantitatively, about half of *Grin3a*-positive neurons were *GAD1*-positive ( $51.57\% \pm 1.63$ ) and the other half were *vGluT1*-positive ( $48.29\% \pm 1.66$ ) (Fig. 6C). Strongest expression was typically found in GABAergic interneurons (Fig. 6D). In the hippocampus, a majority of CA1 pyramidal excitatory neurons expressed *Grin3a* (Fig. 6C). We additionally identified a subpopulation

of inhibitory *GAD1*-positive neurons that displayed strong *Grin3a* labeling in the stratum oriens, whereas inhibitory interneurons intercalated in the CA1 pyramidal layer or in the stratum radiatum lacked *Grin3a* expression (Fig. 6C, E). Similar results were obtained when *Grin3a* localization in inhibitory interneurons was examined by conventional double FISH with riboprobes against *Grin3a* and *Gad1* (see Supplementary

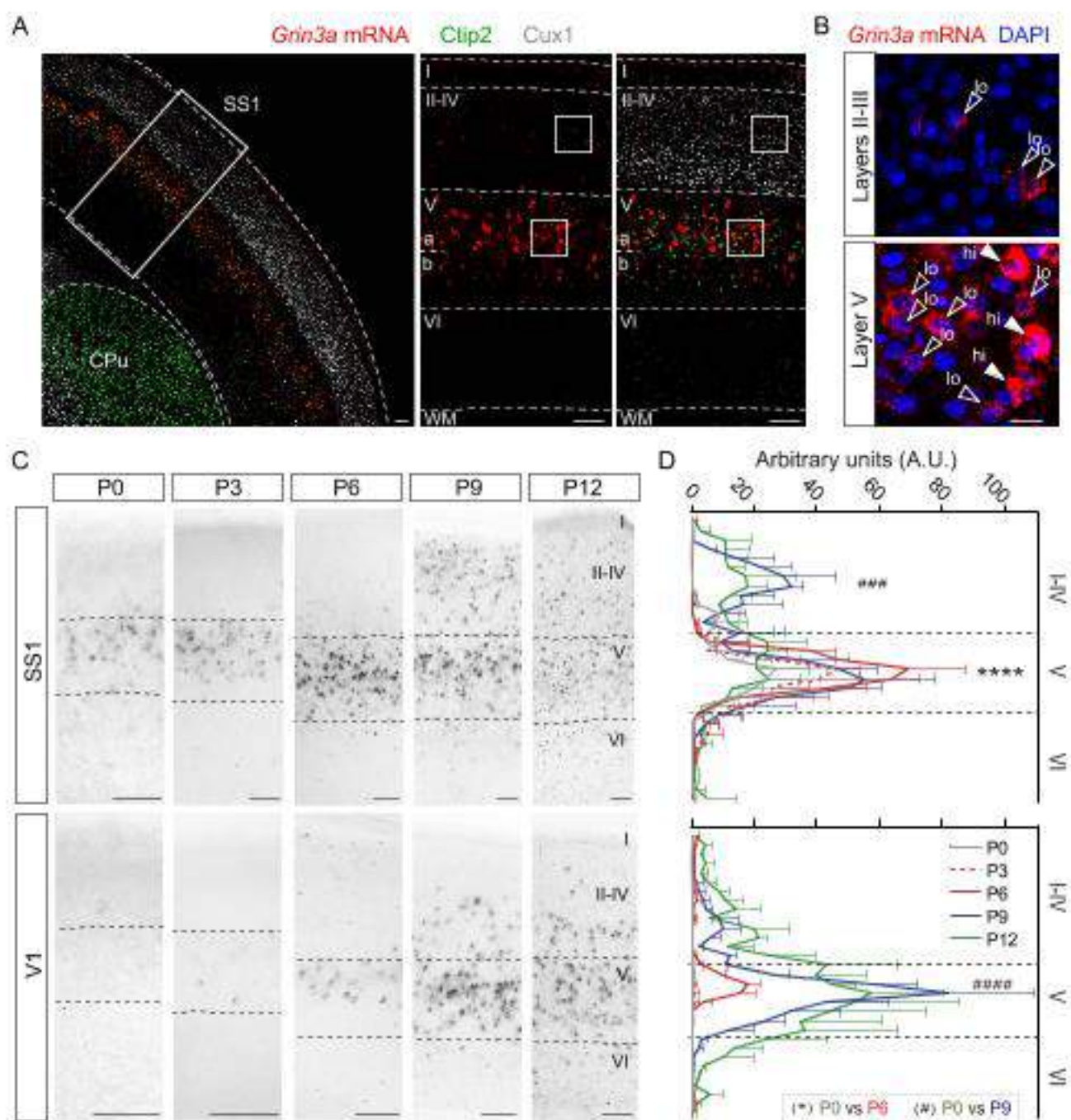


**Figure 5.** Dynamic temporal patterns of *Grin3a* expression across cortical layers and sensory modalities. (A) Left, mosaic of single confocal images of somatosensory cortex 1 (SS1) at P6 showing fluorescence ISH labeling of *Grin3a* mRNA (red) combined with immunofluorescence staining for *Cltp2* (green) and *Cux1* (gray). Middle, right: higher magnification images of the boxed area on the left. Dotted lines mark boundaries between areas (left panel) or cortical layers (middle-right panels). (B) High-magnification images of boxed areas in layers II-III and V of the middle panel in A. *Grin3a* mRNA (red) and DAPI-stained nuclei (blue) are shown. Solid arrows indicate cells with high *Grin3a* mRNA levels; empty arrows show cells with low *Grin3a* mRNA levels. (C, D) Comparative analysis of the time-courses of *Grin3a* emergence and down-regulation in SS1 and primary visual cortex (V1). (C) Representative images show colorimetric ISH for *Grin3a* mRNA in SS1 and V1 at indicated postnatal ages. Dotted lines mark layer V boundaries. (D) Graphs of *Grin3a* mRNA intensity levels across layers in SS1 (top) and V1 (bottom) at P0 (gray), P3 (dashed red), P6 (red), P9 (blue), P12 (green). Data are mean  $\pm$  S.E.M. ( $n = 3$  mice per postnatal age; 2 cortical fields taken at different levels were analyzed per mouse). Shown are statistical significances between P0 and P6 (\*\*\*\* $P < 0.0001$ ) and between P0 and P9 (\*\*\* $P < 0.001$ , \*\*\*\* $P < 0.0001$ ) calculated using two-way ANOVA followed by Bonferroni's multiple comparisons test. All others can be found in [Supplementary Table 2](#). CPU, caudate-putamen; SS1, primary somatosensory cortex 1; V1, primary visual cortex 1. Scale bars: 100  $\mu$ m (A), 20  $\mu$ m (B), 100  $\mu$ m (C).

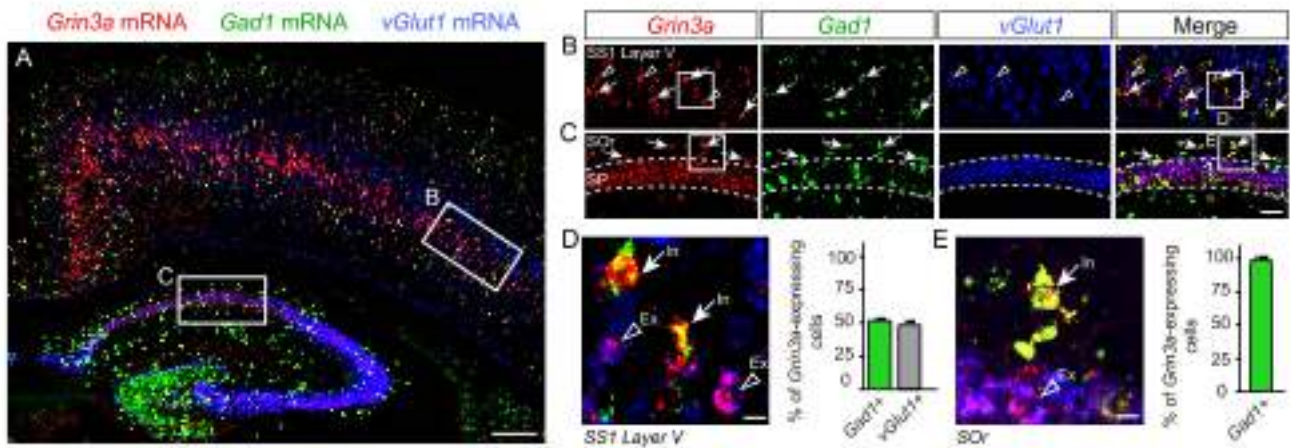


**Figure 5.** *Grin3a* expression in excitatory and inhibitory neurons. (A) Representative coronal section from a P6 wild-type mouse brain labeled by RNAscope for *Grin3a* mRNA (red) and markers of inhibitory (green: *Gad1* mRNA) and excitatory neurons (blue: *vGlut1* mRNA). (B, C) High-magnification images of the boxed areas in A corresponding to SS1 and CA1 hippocampal subfields. In (C), dotted lines mark the boundary between the different hippocampal layers. (D) Higher magnification of the boxed area in B and quantification of percentage of *Grin3a*-positive cells in SS1 layer V which express inhibitory or excitatory markers at P6–P9. (E) Higher magnification of the boxed area in C and quantification of percentage of *Grin3a* mRNA positive cells in the SOr of CA1 that colocalize with *Gad1*. Solid arrows: *Grin3a* inhibitory neurons as shown by colocalization with *Gad1* mRNA. Empty arrowheads: *Grin3a* excitatory neurons as shown by colocalization with *vGlut1* mRNA. Data are mean  $\pm$  S.E.M. ( $n=4$  animals, 6 SS1 fields, and 5 SOr of CA1 at different antero-posterior levels were analyzed). Ex, excitatory neurons; In, inhibitory neurons; SOr, stratum oriens; SS, stratum pyramidale. Scale bars: 100  $\mu$ m (A); 25  $\mu$ m (B–C); 5  $\mu$ m (D–E).

Fig. 3A) or using *GAD67<sup>Cre</sup>* mice (Tamamaki et al. 2003) (see Supplementary Fig. 3B, C).

The two most prevalent types of interneurons are fast-spiking parvalbumin-containing interneurons and low-threshold spiking Sst interneurons, which are generated in the medial ganglionic eminence (MGE) and account for  $\sim 70\%$  of all interneurons (Tricoire et al. 2011; Lim et al. 2018). To determine which interneuron populations express *Grin3a*, we used *Nbx2-1-cre:Alb<sup>tdTomato</sup>* transgenic mice where the tdTomato signal is restricted to MGE-derived interneurons (Madisen et al. 2010) (Fig. 7A–C). Quantitatively,  $52.14\% \pm 2.44$  of *Grin3a*-expressing cells colocalized with tdTomato mRNA in SS1 layer V (Fig. 7D), a figure almost identical to the 51.57% of *Grin3a*-positive cells that colocalize with *Gad1* (Fig. 6D), indicating that essentially all *Grin3a*-expressing interneurons derive from MGE progenitors. Of these, the majority expressed Sst mRNA at high levels ( $34.88\% \pm 2.45$  of the *Grin3a*-expressing population that is  $\sim 70\%$  of all *Grin3a*-positive interneurons, Fig. 7D). At present, it is unclear if the remaining tdTomato-positive/Sst-negative cells belong to a population of immature Sst-fated interneurons that have not yet upregulated Sst mRNA levels, a different MGE-derived population such as parvalbumin cells, or a subset of MGE-derived cells that do not express either parvalbumin or Sst (Petros et al. 2015). Since parvalbumin is not upregulated in cortical interneurons until the second postnatal week, we are unable to directly address this. Similar results were obtained in the stratum oriens where virtually all *Grin3a*-expressing cells expressed tdTomato and Sst (Fig. 7E). Conversely, nearly all Sst-positive interneurons expressed *Grin3a* ( $96.39\% \pm 0.98$  of the total Sst population in SS1 layer V,  $91.98\% \pm 3.10$  in stratum oriens, Fig. 7F).

## Discussion

We provide a comprehensive description of *Grin3a* expression in the mouse brain from embryonic to postnatal and adult stages. Our results recapitulate and expand with anatomical detail the

major postnatal down-regulation known a priori, and additionally reveal highly dynamic and differential *Grin3a* regulation across different brain regions. We further show that *Grin3a* is expressed in both excitatory and inhibitory neurons, and identify a previously underappreciated enrichment of *Grin3a* mRNA in Sst interneurons. The work provides a roadmap for dissecting the diverse functions attributed to GluN3A-NMDARs in brain physiology, behavior, and disease states.

During early postnatal life, neuronal circuits in the brain are massively remodeled by experience via long-lasting plasticity mechanisms that stabilize subsets of synapses but weaken or eliminate others (Katz and Shatz 1996). GluN3A-NMDARs have been proposed to control the timing and magnitude of this remodeling by limiting classical NMDAR signaling until the arrival of sensory experience, and/or fine-tuning synapse plasticity and maturation at later stages (Roberts et al. 2009; Fiuza et al. 2013; Perez-Otano et al. 2016). Our anatomical work lends support for this idea by showing early, sequential, and transient (or protracted) expression of *Grin3a* in cortical areas over postnatal development.

The variations in the timing of *Grin3a* expression and down-regulation across cortical regions correlate with differences in time-scales of cortical maturation (Guillery 2005) and degree of functional specialization (Wang 2020). For instance, transient waves of *Grin3a* expression are a characteristic of primary sensory cortices (see Figure 5), whereas expression appears early and is retained in association and multimodal areas. Primary sensory cortices provide modality-specific information, and early maturation guided by experience is needed to sculpt receptive fields and preserve the fidelity of the information. By contrast, associative and multimodal cortices play an integrative role, have long, protracted maturation periods, and maintain a potential for plastic responses that primary sensory areas lose early (Guillery 2005). Adult *Grin3a* expression was also observed in noncortical areas with strong plasticity needs into adulthood or a functional requirement for association of multiple inputs such as the olfactory system, the amygdala, or the claustrum (see Figure 1). Within primary sensory cortices,

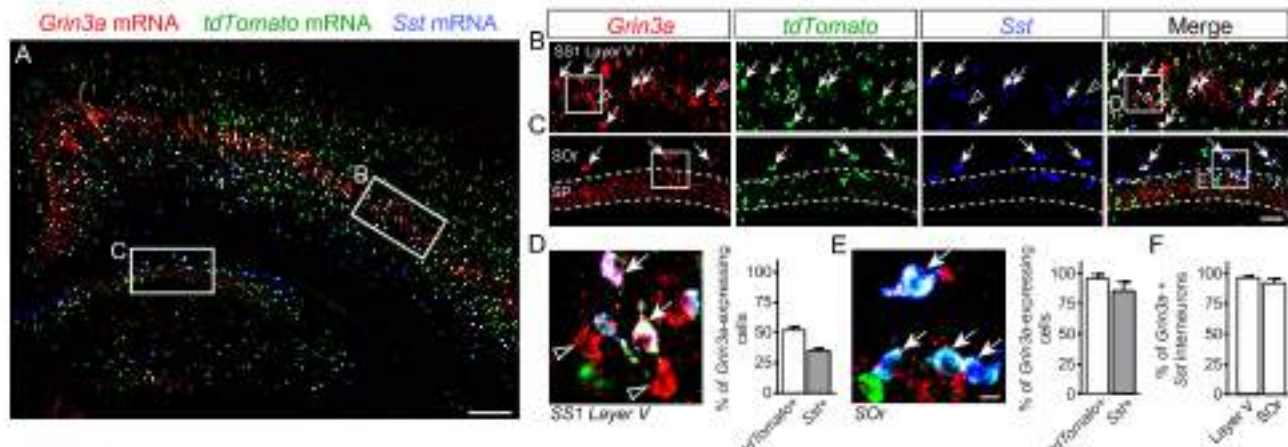


**Figure 7.** *Grin3a* expression in molecularly defined interneuron populations. RNAscope was used to assess colocalization of *Grin3a* and *Sst* mRNA in *Nbx2-1-cre:Alp<sup>tdTomato</sup>* mice that report MGE-derived interneurons. (A) Mosaic image of a P6 *Nbx2-1-cre:Alp<sup>tdTomato</sup>* mouse brain labeled for *Grin3a* mRNA (red) and specific cell-types (green: *tdTomato* mRNA; blue: *Sst* mRNA, somatostatin interneurons). Images of the corresponding boxes from SS1 (B) and CA1 area (C). Dotted lines mark the boundary between the different hippocampal layers. (D) Image of the boxed area in B (left panel) and quantification of *Grin3a*-positive cells that colocalize with *tdTomato* or *Sst* mRNA in SS1 layer V of P6–P9 mice (right panel). (E) Image of the boxed area in C (left panel) and quantification of *Grin3a*-positive cells that colocalize with *tdTomato* or *Sst* mRNA in the CA1 stratum oriens of P6–P9 mice (right panel). (F) Quantification of *Sst* mRNA positive cells that express *Grin3a* mRNA in SS1 layer V and stratum oriens. Solid arrows: *Grin3a* MGE-derived *Sst* interneurons as shown by colocalization with *tdTomato* and *Sst* mRNA. Empty arrowheads do not show colocalization and are likely *Grin3a*-positive excitatory neurons. Data are mean  $\pm$  S.E.M ( $n = 4$  animals, 5–6 fields at different rostro-caudal levels were analyzed). SOx, stratum oriens; SR, stratum pyramidale. Scale bars: 100  $\mu$ m (A); 25  $\mu$ m (B–C); 5  $\mu$ m (D–E).

*Grin3a* expression follows a stereotyped sequential pattern with initial restriction to layer V followed by expression in outer layers and overall down-regulation (see Figure 5), which resembles the inside-out patterning model of cortical maturation. While this stereotyped pattern is conserved across motor and sensory cortices, its timing varies and is coupled to the arrival of sensory experience as exemplified by the delayed *Grin3a* expression in visual cortex, an area of the neocortex that matures later coinciding with eyelid opening (Yoshii et al. 2003).

Our findings confirm and expand a recent report that found *Grin3a* expression in adult mouse brain to be one of the strongest correlates with a hierarchical gradient of functional integration—from primary sensory to transmodal association cortices, established using the T1w/T2w magnetic resonance imaging ratio (Fulcher et al. 2019). In primate and mouse cortex, the T1w/T2w ratio inversely correlates with structural markers of increased differentiation and stability across cortices (García-Cabezas et al. 2017; Wang 2020). Low T1w/T2w ratios and high *Grin3a* expression were found to be typical of functionally integrative areas in mouse and human brains (Fulcher et al. 2019), as also observed here. This is the case of the agranular cortex that receives not only sensory inputs but integrates multimodal information, or of the temporal association and rhinal cortices and the prefrontal cortex (Gogolja 2017). It is worth noting that genetic variations in human *GRIN3A* have been reported to modulate prefrontal cerebral activity during selective attention tasks (Gallinat et al. 2007), supporting a role in higher cognitive processing.

A number of parameters that vary over postnatal development and along the cortical hierarchy to fulfill specific functional requirements could be related to the *Grin3a* expression described here. For instance, *GluN3A* enhances spine turnover (Kehoe et al. 2014), and high rates of disassembly and formation of synapses and spines during postnatal critical periods are thought to be permissive for refinement while low spine turnover leads to circuit stabilization. *GluN3A* subunits have

also been shown to control the developmental onset of long-term forms of plasticity such as hippocampal long-term potentiation (Roberts et al. 2009), spike-timing dependent long-term depression in V1 (Larsen et al. 2014), or the synaptic incorporation of *GluN2A* subunits and AMPA receptors (Henson et al. 2012). Other properties such as the maintenance of persistent or recurrent activity in the prefrontal cortex could reflect roles of *GluN3A*-NMDARs or excitatory *GluN1/GluN3A* receptors on NMDA spiking activity or neuronal excitability (Mahfooz et al. 2016; Otsu et al. 2019). Finally, association and frontal areas contain a greater proportion of *Sst* interneurons that innervate dendrites and have an “input-modulating function,” while sensory areas contain more parvalbumin interneurons that innervate the soma and axon initial segment and have an “output-modulating” function.

*Grin3a* expression is very high in the thalamus where it prevails in higher order thalamic nucleus, while primary sensory thalamic areas lack *Grin3a* or express it at low levels. Information from the sensory periphery is first transmitted to the cerebral cortex via the primary sensory, or first-order, thalamic nuclei including the lateral geniculate in visual thalamus, ventral division of the medial geniculate in auditory thalamus, and ventral posterior nuclei in somatosensory thalamus. By contrast, higher order thalamic nuclei do not receive substantial input from the sensory periphery and instead form extensive cortico-thalamic-cortical circuits or connect functionally related cortical and subcortical regions. They provide a route for cortico-cortical communication which integrates cortical and subcortical inputs, linking cognition and motivated behavior to internal states and levels of consciousness (Sherman 2007). Of relevance here, highest adult *Grin3a* expression was observed in midline and intralaminar nuclei such as the centromedial and paraventricular, involved in arousal and wakefulness, and in the medial habenula, an epithalamic structure that controls negatively valued emotional associations (Van der Werf et al. 2002; Ren et al. 2018; Redinbaugh et al. 2020). Consistent with

these findings, unbiased mammalian reverse genetics detected alterations in wakefulness-sleep transitions in *Grin3a* knockout mice (Sunagawa et al. 2016), and GluN1/GluN3A glycine receptors in the medial habenula have been implicated in mediating conditioned place-aversion (Otsu et al. 2019).

Finally, our data revealed particularly high *Grin3a* mRNA levels in *Sst* interneurons of SS1 and hippocampus from early postnatal stages. This is in-line with single-cell RNAseq analyses of gene expression in adult mouse somatosensory and visual cortex interneurons (Pfeffer et al. 2013; Paul et al. 2017) (T Petros, et al, unpublished data). Publicly available transcriptome datasets indicate that *Grin3a* expression might be a conserved feature of *Sst* interneurons across species (<http://interneuron.mccarrolllab.org>). Moreover, a recent genome-wide epigenomic analysis identified the *Grin3a* locus as a site of open chromatin and low DNA methylation (mCG) in *Sst* interneurons (Yao et al. 2020). Both epigenetic marks are typical of actively expressed genes and are thought to promote and maintain cell-type specific expression and cell identity.

Together these data provide strong validation of *Grin3a* expression as a secondary marker for *Sst* interneurons. They further suggest that GluN3A subunits might play more general roles than currently envisioned in modulating the development of neural circuits. Along with the well-studied refinements of connections between excitatory principal neurons, circuit formation requires the network integration of local interneurons that also involves a refinement of excitatory synaptic inputs onto these inhibitory cells (De Marco Garcia et al. 2015; Tunçdemir et al. 2016). For example, *Sst* interneurons in infragranular layers of SS1 receive dense but transient thalamocortical innervation during the first postnatal week. This innervation is required for the later functional maturation and synaptic integration of parvalbumin interneurons, but is reduced by 4-fold by P14 (Tunçdemir et al. 2016). Our data show that *Grin3a* is highly expressed between P3 and P9 in layer V *Sst* interneurons, providing a candidate mechanism for mediating the refinement of thalamocortical inputs. Excitatory synapses onto MGE-derived interneurons undergo a defined program of synapse maturation, with predominance of GluN2B-NMDARs in neonates which are later replaced by GluN2A-NMDARs (Matta et al. 2013; Porszyk et al. 2016). This developmental switch in subunit composition resembles the experienced by excitatory neurons, in which GluN3A down-regulation has been implicated (Perez-Otano and Ehlers 2004; Henson et al. 2012).

In sum, our study offers new insight onto the spatiotemporal patterns of *Grin3a* distribution in the brain and opens up important cell biological and functional questions. At the cell biological level, further investigations on regulation will be needed to define the transcriptional and epigenetic mechanisms that determine the area-to-area and temporal variations in *Grin3a* expression. Is experience a critical determinant factor, as suggested by the observation that rearing rats in the dark prevents GluN3A down-regulation in visual cortex (Larsen et al. 2014); or is regulation by the calcium-regulated transcription factor CaRF (Lyons et al. 2016)? In terms of function, the transient expression of *Grin3a* in cortical areas and temporal correlation with hierarchical cortical maturation emphasizes the concept of GluN3A as a key controller of the timing of brain maturation and its coupling to experience. Further advances will require selective deletion of the *Grin3a* gene at specific times and in specific neuronal populations, combined with tools to distinguish roles of GluN3A-NMDARs from those of the yet more enigmatic excitatory GluN1/GluN3 receptors.

## Supplementary Material

Supplementary material can be found at *Cerebral Cortex* online.

## Notes

We are grateful to Francisca Almagro-García for expert technical help, to Drs Francisco Clascá, Eloísa Herrera, Salvador Martínez, Elisa Mengual, John Wesseling, and Óscar Elía-Zudaire for advice on manuscript preparation, and Miguel Pérez-Otano for help with graphic design.

We acknowledge support of the publication fee by the CSIC Open Access Publication Support Initiative through its Unit of Information Resources for Research (URICI). *Conflict of Interest:* None declared.

## Funding

Spanish Ministry of Education and Science (BES-2014-069359 fellowship to A.M., SAF2016-80895-R grant to I.P.O., Severo-Ochoa Excellence Awards SEV-2013-0317 and SEV-2017-0723); the Generalitat Valenciana (PROMETEO 2019/020 grant to I.P.O.); a NARSAD Independent Investigator Award (to I.P.O.); and NICHD Intramural Funding (to Y.Z. and T.J.P.).

## References

- Al-Hallaq RA, Jarabek BR, Fu Z, Vicini S, Wolfe BB, Yasuda RP. 2002. Association of NR3A with the N-methyl-D-aspartate receptor NR1 and NR2 subunits. *Mol Pharmacol*. 62:1119–1127.
- Chatterton JE, Awobuluyi M, Premkumar LS, Takahashi H, Talantova M, Shin Y, Cui J, Tu S, Sevarino KA, Nakanishi N et al. 2002. Excitatory glycine receptors containing the NR3 family of NMDA receptor subunits. *Nature*. 415:793–798.
- De Marco Garcia NV, Priya R, Tunçdemir SN, Fishell G, Karayannis T. 2015. Sensory inputs control the integration of neurogliaform interneurons into cortical circuits. *Nat Neurosci*. 18:393–401.
- Eriksson M, Nilsson A, Froelich-Fabre S, Akesson E, Dunker J, Selger A, Folkesson R, Benedikz E, Sundstrom E. 2002. Cloning and expression of the human N-methyl-D-aspartate receptor subunit NR3A. *Neurosci Lett*. 321:177–181.
- Fluzza M, Gonzalez-Gonzalez I, Perez-Otano I. 2013. GluN3A expression restricts spine maturation via inhibition of GIT1/Rac1 signaling. *Proc Natl Acad Sci USA*. 110:20807–20812.
- Fulcher BD, Murray JD, Zerbi V, Wang XJ. 2019. Multimodal gradients across mouse cortex. *Proc Natl Acad Sci USA*. 116:4689–4695.
- Gallinat J, Gotz T, Kalus P, Bajbouj M, Sander T, Winterer G. 2007. Genetic variations of the NR3A subunit of the NMDA receptor modulate prefrontal cerebral activity in humans. *J Cogn Neurosci*. 19:59–68.
- García-Cabezas MA, Joyce MKP, John YJ, Zikopoulos B, Barbas H. 2017. Mirror trends of plasticity and stability indicators in primate prefrontal cortex. *Eur J Neurosci*. 46:2392–2405.
- Gogolla N. 2017. The insular cortex. *Curr Biol*. 27:R580–R586.
- Grand T, Abi Gerges S, David M, Diana MA, Paoletti P. 2018. Unmasking GluN1/GluN3A excitatory glycine NMDA receptors. *Nat Commun*. 9:4769.
- Guillery RW. 2005. Is postnatal neocortical maturation hierarchical? *Trends Neurosci*. 28:512–517.
- Harris JA, Mihalas S, Hirokawa KE, Whitesell JD, Choi H, Bernard A, Bohn P, Caldejon S, Casal L, Cho A et al. 2019. Hierarchical

- organization of cortical and thalamic connectivity. *Nature*. 575:195–202.
- Henson MA, Larsen RS, Lawson SN, Perez-Otano I, Nakanishi N, Lipton SA, Philpot BD. 2012. Genetic deletion of NR3A accelerates glutamatergic synapse maturation. *PLoS One*. 7:e42327.
- Huang X, Chen YY, Shen Y, Cao X, Li A, Liu Q, Li Z, Zhang LB, Dai W, Tan T et al. 2017. Methamphetamine abuse impairs motor cortical plasticity and function. *Mol Psychiatry*. 22:1274–1281.
- Katz LC, Shatz CJ. 1996. Synaptic activity and the construction of cortical circuits. *Science*. 274:1133–1138.
- Kehoe LA, Bellone C, De Roo M, Zandua A, Dey PN, Perez-Otano I, Muller D. 2014. GluN3A promotes dendritic spine pruning and destabilization during postnatal development. *J Neurosci*. 34:9213–9221.
- Kim J, Matney CJ, Roth RH, Brown SP. 2016. Synaptic organization of the neuronal circuits of the claustrum. *J Neurosci*. 36:773–784.
- Larsen RS, Smith IT, Miriyala J, Han JE, Corlew RJ, Smith SL, Philpot BD. 2014. Synapse-specific control of experience-dependent plasticity by presynaptic NMDA receptors. *Neuron*. 83:879–893.
- Lee JH, Wei L, Deveau TC, Gu X, Yu SP. 2016. Expression of the NMDA receptor subunit GluN3A (NR3A) in the olfactory system and its regulatory role on olfaction in the adult mouse. *Brain Struct Funct*. 221:3259–3273.
- Lim L, Mi D, Llorca A, Marin O. 2018. Development and functional diversification of cortical interneurons. *Neuron*. 100:294–313.
- Lyons MR, Chen LF, Deng JV, Finn C, Pfenning AR, Sabblok A, Wilson KM, West AE. 2016. The transcription factor calcium-response factor limits NMDA receptor-dependent transcription in the developing brain. *J Neurochem*. 137:164–176.
- Madisen L, Zwingman TA, Sunkin SM, Oh SW, Zariwala HA, Gu H, Ng LL, Palmiter RD, Hawrylycz MJ, Jones AR et al. 2010. A robust and high-throughput Cre reporting and characterization system for the whole mouse brain. *Nat Neurosci*. 13:133–140.
- Mahfooz K, Marco S, Martinez-Turrillas R, Raja MK, Perez-Otano I, Wesseling JF. 2016. GluN3A promotes NMDA spiking by enhancing synaptic transmission in Huntington's disease models. *Neurobiol Dis*. 93:47–56.
- Marco S, Giralt A, Petrovic MM, Pouladi MA, Martinez-Turrillas R, Martinez-Hernandez J, Kaltenbach LS, Torres-Peraza J, Graham RK, Watanabe M et al. 2013. Suppressing aberrant GluN3A expression rescues synaptic and behavioral impairments in Huntington's disease models. *Nat Med*. 19:1030–1038.
- Marco S, Murillo A, Perez-Otano I. 2018. RNAi-based GluN3A silencing prevents and reverses disease phenotypes induced by mutant Huntington. *Mol Ther*. 26:1965–1972.
- Matta JA, Pelkey KA, Craig MT, Chittajallu R, Jeffries BW, McBain CJ. 2013. Developmental origin dictates interneuron AMPA and NMDA receptor subunit composition and plasticity. *Nat Neurosci*. 16:1032–1041.
- Mohamad O, Song M, Wei L, Yu SP. 2013. Regulatory roles of the NMDA receptor GluN3A subunit in locomotion, pain perception and cognitive functions in adult mice. *J Physiol*. 591:149–168.
- Mueller HT, Meador-Woodruff JH. 2003. Expression of the NR3A subunit of the NMDA receptor in human fetal brain. *Ann N Y Acad Sci*. 1003:448–451.
- Mueller HT, Meador-Woodruff JH. 2004. NR3A NMDA receptor subunit mRNA expression in schizophrenia, depression and bipolar disorder. *Schizophr Res*. 71:361–370.
- Otsu Y, Darq E, Pietrajtis K, Matyas F, Schwartz E, Bessaib T, Abi Gerges S, Rousseau CV, Grand T, Dieudonne S et al. 2019. Control of aversion by glycine-gated GluN1/GluN3A NMDA receptors in the adult medial habenula. *Science*. 366:250–254.
- Pachernegg S, Strutz-Seebohm N, Hollmann M. 2012. GluN3 subunit-containing NMDA receptors: not just one-trick ponies. *Trends Neurosci*. 35:240–249.
- Paoletti P, Bellone C, Zhou Q. 2013. NMDA receptor subunit diversity: impact on receptor properties, synaptic plasticity and disease. *Nat Rev Neurosci*. 14:383–400.
- Paul A, Crow M, Raudales R, He M, Gillis J, Huang ZJ. 2017. Transcriptional architecture of synaptic communication delineates GABAergic neuron identity. *Cell*. 171:522, e520–539.
- Paxinos G, Franklin K. 2019. *Mouse brain in stereotaxic coordinates*. 5th ed. Amsterdam (Netherlands): Academic Press.
- Paxinos G, Halliday G, Watson C, Koutcherov Y, Wang H. 2007. *Atlas of the developing mouse brain*. 1st ed. Amsterdam (Netherlands): Academic Press.
- Perez-Otano I, Ehlers MD. 2004. Learning from NMDA receptor trafficking: clues to the development and maturation of glutamatergic synapses. *Neurosignals*. 13:175–189.
- Perez-Otano I, Larsen RS, Wesseling JF. 2016. Emerging roles of GluN3-containing NMDA receptors in the CNS. *Nat Rev Neurosci*. 17:623–635.
- Perez-Otano I, Schulteis CT, Contractor A, Lipton SA, Trimmer JS, Sucher NJ, Heinemann SF. 2001. Assembly with the NR1 subunit is required for surface expression of NR3A-containing NMDA receptors. *J Neurosci*. 21:1228–1237.
- Perszyk RE, DiRaddo JO, Strong KI, Low CM, Ogden KK, Khatri A, Vargish GA, Pelkey KA, Tricolre L, Liotta DC et al. 2016. GluN2D-containing N-methyl-D-aspartate receptors mediate synaptic transmission in hippocampal interneurons and regulate interneuron activity. *Mol Pharmacol*. 90:689–702.
- Petroc TJ, Bultje RS, Ross ME, Fishell G, Anderson SA. 2015. Apical versus basal neurogenesis directs cortical interneuron subclass fate. *Cell Rep*. 13:1090–1095.
- Pfeffer CK, Xue M, He M, Huang ZJ, Scanziani M. 2013. Inhibition of inhibition in visual cortex: the logic of connections between molecularly distinct interneurons. *Nat Neurosci*. 16:1058–1076.
- Redinbaugh MJ, Phillips JM, Kambi NA, Mohanta S, Andryk S, Dooley GL, Afrasiabi M, Raz A, Saalman YB. 2020. Thalamus modulates consciousness via layer-specific control of cortex. *Neuron*. 106:66, e12–75.
- Ren S, Wang Y, Yue F, Cheng X, Dang R, Qiao Q, Sun X, Li X, Jiang Q, Yao J et al. 2018. The paraventricular thalamus is a critical thalamic area for wakefulness. *Science*. 362:429–434.
- Roberts AC, Díez-García J, Rodríguez RM, Lopez IP, Lujan R, Martínez-Turrillas R, Pico E, Henson MA, Bernardo DR, Jarrett TM et al. 2009. Downregulation of NR3A-containing NMDARs is required for synapse maturation and memory consolidation. *Neuron*. 63:342–356.
- Sherman SM. 2007. The thalamus is more than just a relay. *Curr Opin Neurobiol*. 17:417–422.
- Sucher NJ, Akbarian S, Chi CL, Leclerc CL, Awobuluyi M, Deitcher DL, Wu MK, Yuan JP, Jones EG, Lipton SA. 1995. Developmental and regional expression pattern of a novel NMDA receptor-like subunit (NMDAR-L) in the rodent brain. *J Neurosci*. 15:6509–6520.
- Sunagawa GA, Sumiyama K, Ukai-Tadenuma M, Ferrin D, Fujishima H, Ukai H, Nishimura O, Shi S, Ohno RI, Narumi

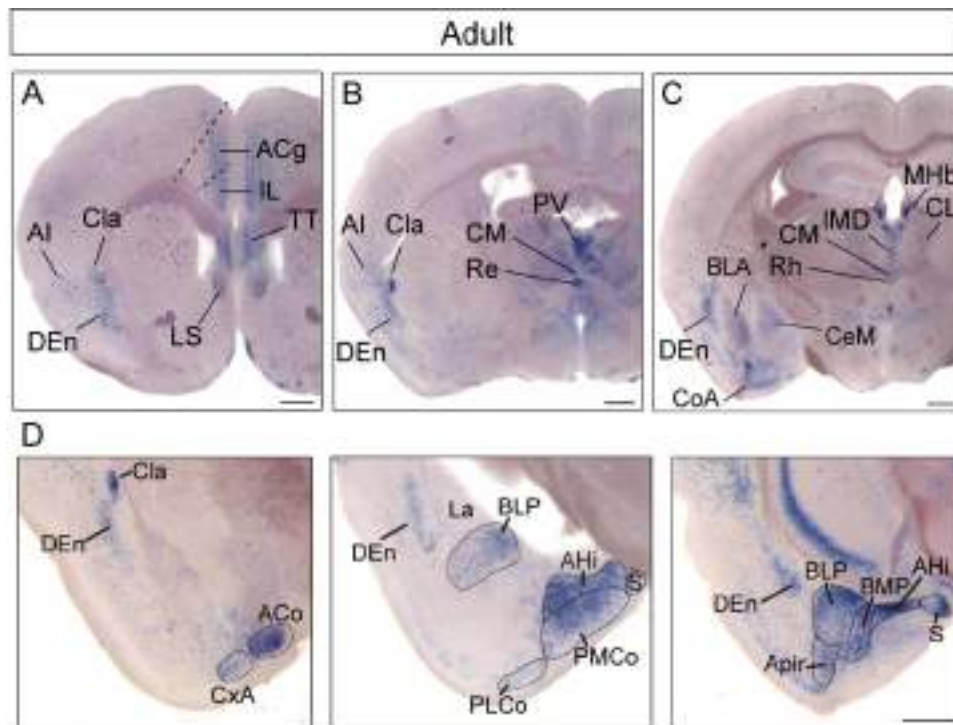
- R et al. 2016. Mammalian reverse genetics without crossing reveals Nr3a as a short-sleeper gene. *Cell reports*. 14:662–677.
- Tamamaki N, Yanagawa Y, Tomioka R, Miyazaki J, Obata K, Kaneko T. 2003. Green fluorescent protein expression and colocalization with calretinin, parvalbumin, and somatostatin in the GAD67-GFP knock-in mouse. *J Comp Neurol*. 467:60–79.
- Tricoire L, Pelkey KA, Erkkila BE, Jeffries BW, Yuan X, McBain CJ. 2011. A blueprint for the spatiotemporal origins of mouse hippocampal interneuron diversity. *J Neurosci*. 31:10948–10970.
- Tuncdemir SN, Wamsley B, Stam FJ, Osakada F, Goulding M, Callaway EM, Rudy B, Fishell G. 2016. Early Somatostatin interneuron connectivity mediates the maturation of deep layer cortical circuits. *Neuron*. 89:521–535.
- Van der Werf YD, Witter MP, Groenewegen HJ. 2002. The intralaminar and midline nuclei of the thalamus. Anatomical and functional evidence for participation in processes of arousal and awareness. *Brain Res Brain Res Rev*. 39:107–140.
- Wang XJ. 2020. Macroscopic gradients of synaptic excitation and inhibition in the neocortex. *Nat Rev Neurosci*. 21:169–178.
- Watson C, Paxinos G, Puelles L. 2012. *Mouse nervous system*. 1st ed. Amsterdam (Netherlands): Academic Press.
- Wong HK, Liu XB, Matos MF, Chan SF, Perez-Otano I, Boysen M, Cui J, Nakanishi N, Trimmer JS, Jones EG et al. 2002. Temporal and regional expression of NMDA receptor subunit NR3A in the mammalian brain. *J Comp Neurol*. 450:303–317.
- Xu Q, Tam M, Anderson SA. 2008. Fate mapping Nlxx2.1-lineage cells in the mouse telencephalon. *J Comp Neurol*. 506:16–29.
- Yang J, Wang S, Yang Z, Hodgkinson CA, Izrikova P, Ma JZ, Payne TJ, Goldman D, Li MD. 2015. The contribution of rare and common variants in 30 genes to risk nicotine dependence. *Mol Psychiatry*. 20:1467–1478.
- Yao Z, Liu H, Xie F, Fischer S, Boeshaghi AS, Adkins RS, Aldridge AI, Ament SA, Pinto-Duarte A, Bartlett A et al. 2020. An integrated transcriptomic and epigenomic atlas of mouse primary motor cortex cell types. *bioRxiv*. doi: <https://doi.org/10.1101/2020.02.29.970558>.
- Yoshii A, Sheng MH, Constantine-Paton M. 2003. Eye opening induces a rapid dendritic localization of PSD-95 in central visual neurons. *Proc Natl Acad Sci USA*. 100:1334–1339.
- Yuan T, Mameli M, EC OC, Dey PN, Verpelli C, Sala C, Perez-Otano I, Luscher C, Bellone C. 2013. Expression of cocaine-evoked synaptic plasticity by GluN3A-containing NMDA receptors. *Neuron*. 80:1025–1038.

## **SUPPLEMENTARY INFORMATION**

### ***Temporal Dynamics and Neuronal Specificity of Grin3a Expression in the Mouse Forebrain***

Alvaro Murillo, Ana Isabel Navarro, Eduardo Puelles, Yajun Zhang, Timothy J. Petros and  
Isabel Pérez Otaño

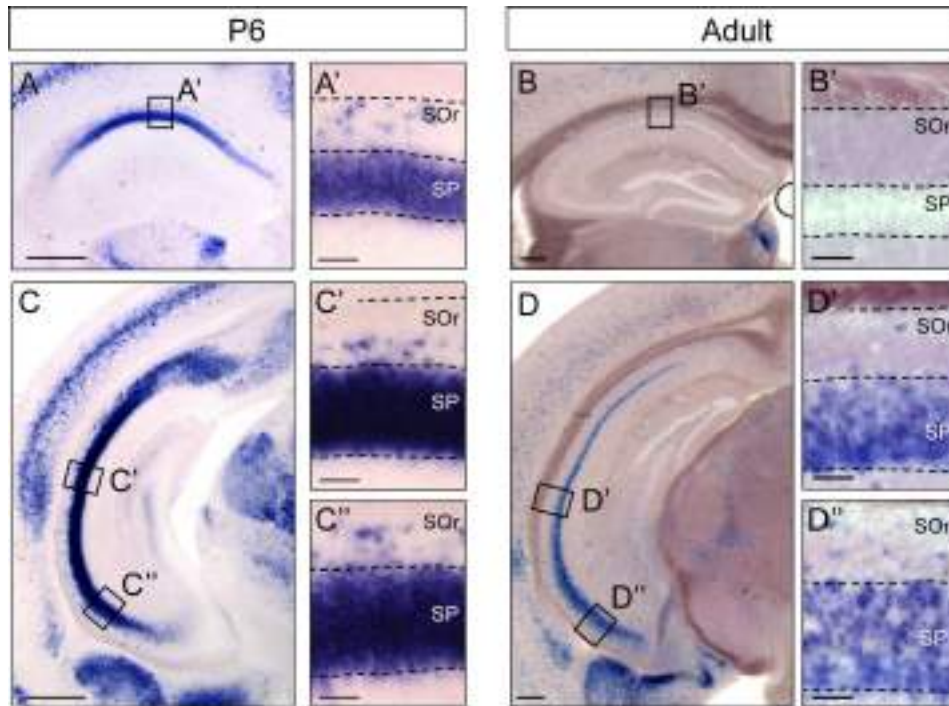




**Supplementary Figure 1 (related to Figure 1). Adult *Grin3a* expression in the thalamus and cortical amygdala**

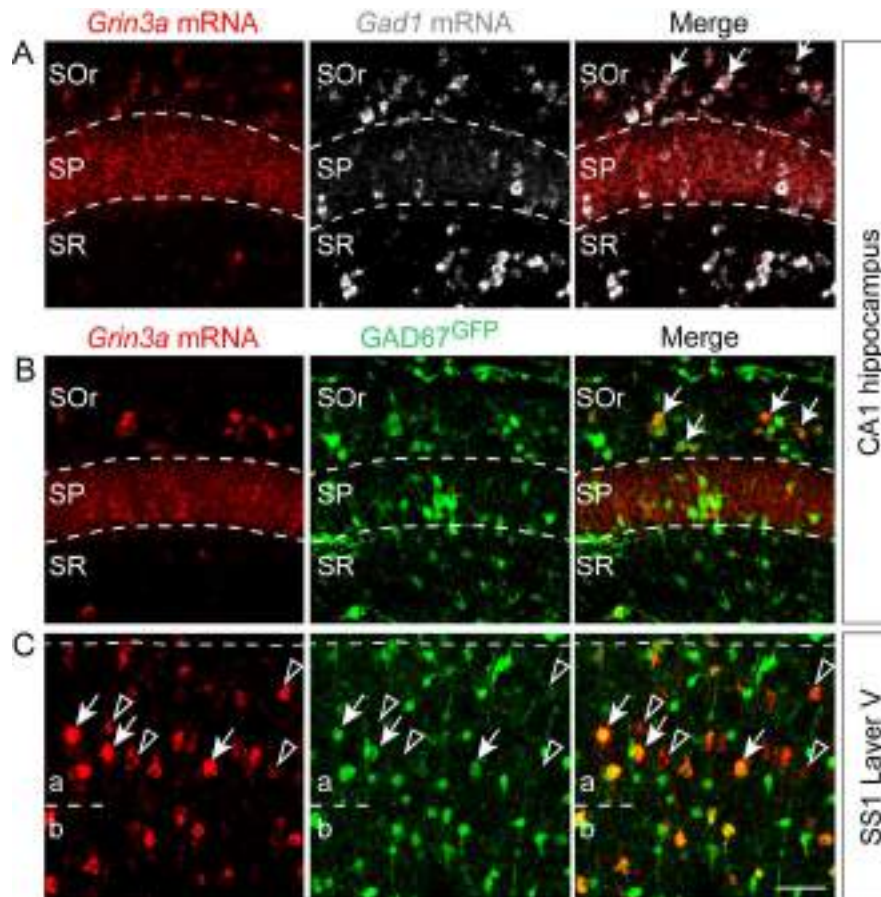
(A-C) Coronal sections of adult mouse brain showing further detail of *Grin3a* expression in subcortical structures. (D) Higher magnification images of *Grin3a* expression in ventral cortical amygdala nuclei.

ACg, anterior cingulate cortex; ACo, anterior cortical amygdaloid nucleus; AHi, amygdalohippocampal area; AI, agranular insular cortex; APir, amygdalo-piriform transition area; BLA, basolateral amygdala, anterior part; BLP, basolateral amygdala, posterior part; BMP, basomedial amygdala, posterior part; CeM, central amygdala; CL, centrolateral thalamic nucleus; Cla, claustrum; CM, centromedial thalamic nucleus; CoA, cortical amygdala; CxA, cortex amygdala transition zone; DEn, dorsal endopiriform nucleus; IL, infralimbic cortex; IMD, intermediodorsal thalamic nucleus; La, lateral amygdala; LS, lateral septum; MHb, medial habenula nucleus; PLCo, posterolateral cortical amygdaloid nucleus; PMCo, posteromedial cortical amygdaloid nucleus; PV, paraventricular thalamic nucleus; Re, reuniens thalamic nucleus; Rh, rhomboid thalamic nucleus; S, subiculum; TT, tenia tecta. Scale bars: 500  $\mu$ m.



**Supplementary Figure 2 (related to Figure 1). Dorso-ventral gradient of *Grin3a* expression in adult CA1 hippocampus**

ISH photomicrographs show representative images of *Grin3a* mRNA expression in dorsal (A, B) and ventral CA1 (C, D) in postnatal (P6) and adult young brains. High magnification images for the corresponding boxes (A', B', C', C'', D', D'') are shown. Dotted lines mark the boundary between the different hippocampal layers. SO<sub>r</sub>, stratum oriens; SP, stratum pyramidale. Scale bars: 500  $\mu$ m (A-D); 50  $\mu$ m (A'-D'; C'', D'').



**Supplementary Figure 3 (related to Figure 6). High *Grin3a* mRNA expression in a subpopulation of GABAergic neurons**

(A) Maximal projection images from double FISH show *Grin3a* mRNA (red) colocalization with *Gad1* mRNA (white) in the CA1 stratum oriens of P6 mice. (B, C) Single confocal images of *Grin3a* mRNA FISH (red) and GFP signal (green) in *GAD67<sup>GFP</sup>* mice identify a subpopulation of GABA interneurons expressing high levels of *Grin3a* mRNA in CA1 (B) and layer V of somatosensory cortex 1. (C) Solid arrows: colocalization of *Grin3a* mRNA with GABAergic markers *Gad1* mRNA or *GAD67<sup>GFP</sup>*. Empty arrows: non-GABAergic *Grin3a*-positive cells. Dashed lines mark the boundary between cortical or hippocampal layers. CA1, cornu ammonis 1; SOr, stratum oriens; SP, stratum pyramidale; SR, stratum radiatum; SS1, somatosensory cortex 1. Scale bar: 20  $\mu\text{m}$ .

**Supplementary Table 1 (related to Figure 2).** Semi-quantitative analysis of *Grin3a* mRNA levels at postnatal times of maximal expression (P6-P9).

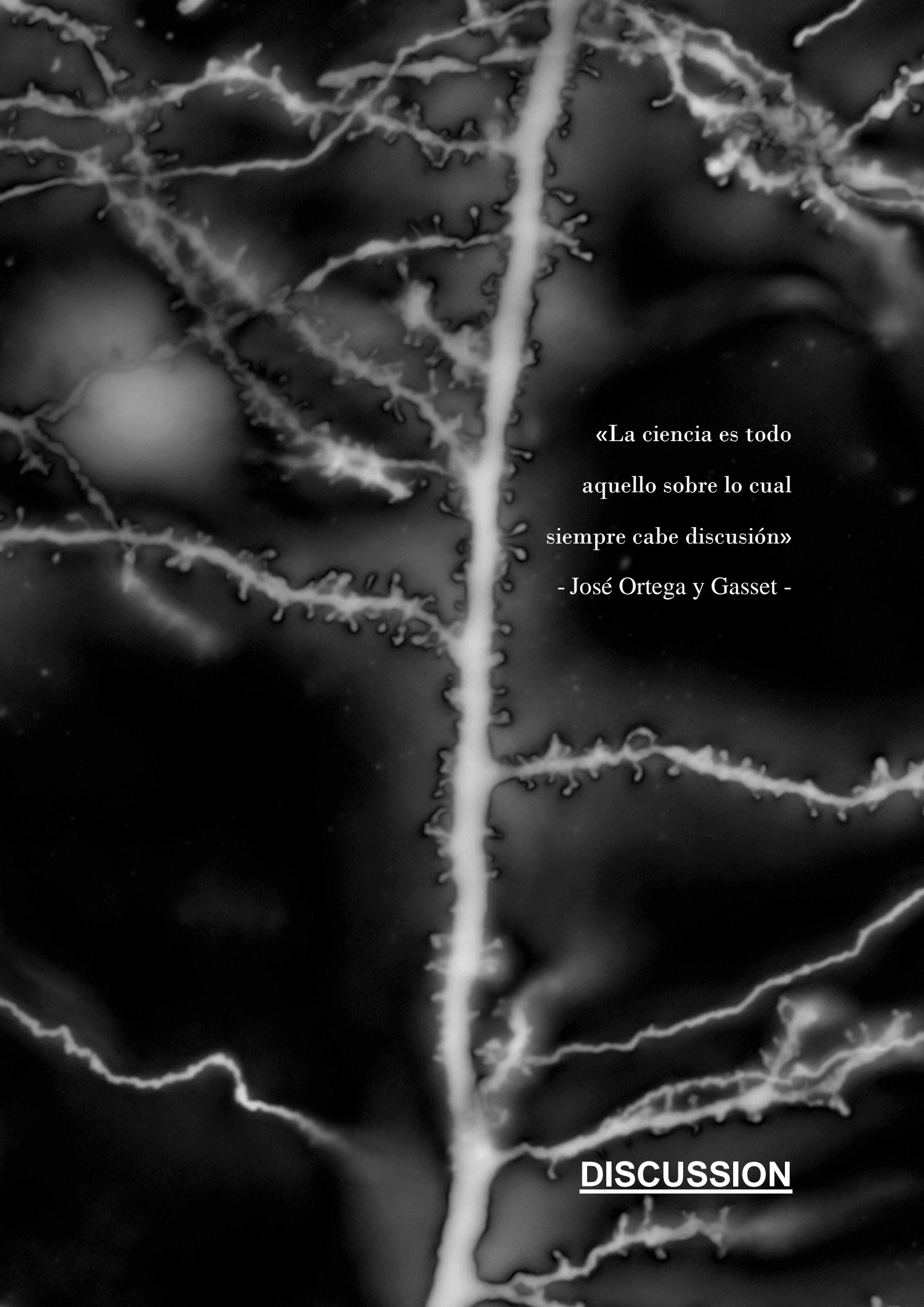
Degree of *Grin3a* expression estimated from P6-P9 brains (n= 6 mice per age; absent (-), low (+), moderate (++) , medium (+++) and strong expression (++++).

<b><i>Grin3a</i> mRNA expression</b>	<b>Abbreviation</b>	<b>Qualitative intensity</b>
Agranular insular cortex	AI	+++
Anterior cingulate cortex	ACg	++
Anterior olfactory nucleus	AON	++++
Anterior pretectal nucleus	APT	+
Auditory cortex	Au	++
Baso amygdaloid nucleus, posterior part	BP	++++
Basolateral amygdaloid nucleus, posterior part	BLP	++++
Basomedial amygdaloid nucleus, posterior part	BMP	++++
Basolateral amygdaloid nucleus, anterior part	BLA	++++
Bed nucleus of the stria terminalis	BST	++
Caudate-putamen	CPu	(-/+)
Central amygdaloid nucleus, medial division	CeM	++
Cingulate cortex	Cg	+++
Clastrum	Cla	+++
Corpus callosum	cc	n.a.
Cortex amygdala transition zone	CxA	++
Cortical amygdala	CoA	
Amygdalohippocampal area	AHi	++++
Anterior cortical amygdaloid nucleus	ACo	++++
Posterolateral cortical amygdaloid nucleus	PLCo	++++
Posteromedial cortical amygdaloid nucleus	PMCo	++++
Dorsal endopiriform nucleus	DEn	++
Dorsal subiculum	DS	++
Frontal association cortex	Fr	+++
Globus pallidus	GP	(-)
Glomerular layer of the olfactory bulb	Gl	++
Hippocampus	Hipp	
Cornu Ammonis 1	CA1	
Stratum oriens	SOr	++
Stratum pyramidale	SP	++++
Stratum radiatum	SR	(-)
Cornu Ammonis 2	CA2	(-)
Cornu Ammonis 3	CA3	(-)
Dentate gyrus	DG	(-)
Indusium griseum	IG	++
Insular cortex	In	++
Internal capsule	ic	n.a.
Islands of Calleja	ICj	++
Lateral amygdaloid nucleus	La	++
Lateral habenula	LHb	(-)

Mammillary tract	mt	n.a.
Medial habenula	MHb	+
Mitral cell layer of the olfactory bulb	Mia	++++
Motor cortex	Mo	++
Olfactory tubercle	OT	+++
Orbitofrontal cortex	OC	++
Parafascicular thalamic nucleus	PF	(-)
Parietal cortex, posterior part	PtP	++
Piriform cortex	Pir	++
Prefrontal cortex	PFC	
Dorsal peduncular cortex	DP	+++
Infralimbic cortex	IL	+++
Prelimbic cortex	PrL	+++
Retrosplenial cortex	RS	+++
Rhinal cortices	Rhi	
Ectorhinal cortex	Ect	++
Perirhinal cortex	PRh	++
Somatosensory cortex	SS	++
Subthalamic nucleus	STh	+
Temporal association cortex	TeA	++
Tenia tecta	TT	
Dorsal tenia tecta	DTT	++++
Ventral tenia tecta	VTT	++++
Thalamus	Thal	
Anterodorsal thalamic nucleus	AD	(-)
Anteromedial thalamic nucleus	AM	++++
Anteroventral thalamic nucleus	AV	(-)
Centrolateral thalamic nucleus	CL	++++
Centromedial thalamic nucleus	CM	++++
Dorsal lateral geniculate nucleus	DLG	(-)
Lateral posterior thalamic nucleus	LP	++++
Laterodorsal thalamic nucleus	LD	(-)
Mediodorsal thalamic nucleus	MD	++++
Paracentral thalamic nucleus	PC	++++
Paratenial thalamic nucleus	PT	++++
Paraventricular thalamic nucleus	PV	++++
Posterior thalamic nuclear group	Po	++++
Reticular thalamic nucleus	Rt	++
Reuniens thalamic nucleus	Re	+++
Rhomboid thalamic nucleus	Rh	++++
Ventral lateral geniculate nucleus	VG	+
Ventral posterior thalamic nucleus	VP	(-)
Ventral posterolateral thalamic nucleus	VPL	(-)
Ventral posteromedial thalamic nucleus	VPM	(-)
Ventromedial thalamic nucleus	VM	++
Ventromedial hypothalamic nucleus	VMH	+++
Visual cortex	Vis	++

**Supplementary Table 2 (related to Figure 5D).** Statistical analyses of the time-courses of *Grin3a* emergence and downregulation in primary somatosensory (SS1) and visual cortex (V1) (n = 3 mice per postnatal age; 2 cortical fields taken at different levels were analysed per mouse).

2-way ANOVA plus Bonferroni post-hoc test					
SS1	Upper layers	Layer V	V1	Upper layers	Layer V
P0 vs P3	n.s.	0.072 (↑)	P0 vs P3	n.s.	n.s.
P0 vs P6	n.s.	**** (↑)	P0 vs P6	n.s.	n.s.
P0 vs P9	### (↑)	0.078	P0 vs P9	n.s.	#### (↑)
P0 vs P12	n.s.	n.s.	P0 vs P12	n.s.	**** (↑)
P3 vs P6	n.s.	* (↑)	P3 vs P6	n.s.	n.s.
P6 vs P9	***	* (↓)	P6 vs P9	n.s.	**** (↑)
P9 vs P12	n.s.	** (↓)	P9 vs P12	n.s.	n.s.



«La ciencia es todo  
aquello sobre lo cual  
siempre cabe discusión»  
- José Ortega y Gasset -

DISCUSSION







The first chapter of my Thesis provides proof-of-principle validation of GluN3A as a target to treat early pathogenic mechanisms in HD, and develop and test RNAi-based tools to harness this therapeutic potential. The strategy was based on previous findings from our laboratory that impaired glutamatergic synaptic transmission and excessive synapse pruning resulting from aberrant GluN3A expression are among the earliest events in HD pathophysiology and major drivers of the pathogenic process. Genetic GluN3A suppression prevented early-to-late disease phenotypes including altered AMPA and NMDA receptor currents and spine loss (Marco *et al.*, 2013; Mahfooz *et al.*, 2016), leading us to explore viable therapeutic strategies. We were able to demonstrate that upon a single intrastriatal injection, rAAV9s encoding shRNAs against GluN3A drive highly efficient, long-lasting GluN3A silencing that targets selectively MSNs. Silencing expression in MSNs was sufficient for halting the synaptic pathology and restoring motor performance.

The work corroborates and extends the earlier results and has major translational implications. First, silencing GluN3A exclusively in MSNs (that normally express low GluN3A levels in adult stages) whilst sparing other cell types in the striatum (such as cholinergic interneurons that retain high expression into adulthood (Marco *et al.*, 2013)) enables to block specifically the pathological event, i.e. age-inappropriate reactivation of GluN3A in vulnerable populations. Such specificity could provide clinical benefit while minimizing adverse effects. The observation that injecting rAAV9-shGluN3A does not affect spine density in WT MSNs, nor motor performance, supports this rationale. Second, rAAV9-driven GluN3A silencing turned out to be effective when timed with the onset of the synaptic pathology but also when initiated later in the disease course, establishing a window of opportunity over which pre-existing phenotypes can be reversed. Third, our approach targets one of the earliest disease mechanism, when intervention is more likely to be efficacious and before a point of no-return has been reached (Rubinsztein *et al.*, 2016). In this regard, electrophysiological and morphological evidence of early dysfunction and loss of MSN synapses is extensive in HD mouse models (Milnerwood *et al.*, 2010; Mahfooz *et al.*, 2016) and humans (Graveland *et al.*, 21985; Ferrante *et*

*et al.*, 1991). Likewise, longitudinal imaging and functional studies in humans report significant striatal atrophy years prior to diagnosable HD (Aylward *et al.*, 2004), which is strongly correlated with time to disease onset, performance and clinical progression (Tabrizi *et al.*, 2013; Harrington *et al.*, 2014). And, GluN3A has been shown to be required not only for spine loss (chosen as a read-out in this study) but also for the multivariate dysfunction of synaptic transmission onto MSNs that precedes morphological signs, including early enhanced synaptic currents mediated by AMPA and NMDA-type glutamate receptors and NMDA “spikes” or “upstates” (Marco *et al.*, 2013; Mahfooz *et al.*, 2016). Within the experimental time-frame of the present study, death of MSNs is not yet detectable in YAC128 mice and we could not determine whether GluN3A knockdown would reduce the neurodegeneration that is seen at later stages. In our previous report, genetic cross of YAC128 mice with GluN3A knock-outs conferred partial protection from cell death (Marco *et al.*, 2013), indicating that preventing synaptic damage preserves pro-survival signaling pathways driven by afferent synaptic activity (Keiser *et al.*, 2016). However, multiple other factors such as deficient neurotrophic signalling, transcriptional dysregulation or altered proteostasis have been linked to cell death in preclinical and human HD studies, and establishing whether these are related or independent of the synaptic pathology still needs to be addressed.

While HTT-lowering drugs seem the therapy of choice, developing allele-specific strategies has proven to be difficult and will likely require to target single-nucleotide polymorphisms residing only in the mutant allele or alternative approaches such as genome editing (Keiser *et al.*, 2016; Monteys *et al.*, 2017). Clinical trials testing the safety of allele-specific antisense oligonucleotides that silence the mutant *HTT* gene (Wave Precision-HDs) are currently active, but the polymorphisms targeted are present only in a subset of people with the HD gene and in some cases do not discriminate between mutant and normal HTT. Furthermore, the polymorphism variability is large across geographic populations, where the prevalence of polymorphisms are much lower in the general population in China, Japan, and Nigeria compared to HD patients of European origin (Warby *et al.*, 2009). Using RNAi for the strategy of selecting polymorphisms in the mutant allele requires that the variations in *mHTT* allele

must be present in mature RNA, thus limiting available target sequences (Kay *et al.*, 2014). Alternative strategies are based on specific silencing by RNAi of the expanded polyQ stretch. But when the mutated and WT allele do not differ much in the number of CAG repeats (e.g. 44/15, respectively), the treatment does not discriminate and silences the two alleles (Yu *et al.*, 2012). Therefore, this therapy does not work in patients with a short HD repeat. Another caveat is the possibility of off-target effects, since there are 66 protein-coding transcripts that carry CAG repeats (Butland *et al.*, 2007), and this treatment could silence their expression. All this emphasizes the need for a personalized treatment strategies based on patient genotypes. Nevertheless, antisense oligonucleotides against both WT and mutant *HTT* (IONIS-HTT<sub>Rx</sub>), by bolus intrathecal administration, have recently yielded promising dose-response reductions in HTT protein levels in cerebrospinal fluid and showed appropriate safety and tolerability profiles in a completed phase 1 clinical trial (Tabrizi *et al.*, 2019). However, the efficacy of these approaches in the reduction of mHTT expression in CNS (as well as their tolerability over the extended periods of time likely required to treat chronic neurodegeneration) remains to be tested through larger trials. More generally, the use of RNAi to treat diseases such as cancer, viral infection, diabetes or cardiovascular disease, has become increasingly applied (Chen *et al.*, 2018). In our RNA-based approach for neurodegenerative disease, delivery continues to be a challenge as it would require direct intraparenchymal administration into the striatum. However, non-viral particles could provide alternatives to carry shRNAs to the brain and target cells. Liposomes, solid lipid nanoparticles, nanostructured lipid carriers, polymer-based delivery and aptamers are the more widely used. These RNAi delivery systems show excellent physical stability, low toxicity, ease of preparation and stability for storage (Naseri *et al.*, 2015). However, since high therapeutic doses are required when using non-viral technologies, and the resulting gene expression is generally transient, most gene therapies now rely on viral vectors which allow long-term expression of the transgene.

Specifically, the use of rAAVs for transgene delivery continues to be seen as one of the safest methods to treat different diseases including neurodegenerative disorders such as dementia, Parkinson and Alzheimer

diseases (Martier *et al.*, 2020). The neural feature of non-division allows long-term expression of transgenes with a single administration of rAAVs, whereas other delivery systems require successive administrations, which is a great disadvantage in the CNS. In addition, rAAVs have been tested in more than 200 clinical trials, and shown to be safe (Hudry *et al.*, 2019). rAAVs have also been used as a shRNA delivery in clinical trials. In chronic hepatitis C virus, shRNAs against well-conserved hepatitis C virus genome sequences delivered by rAAV have shown long-term and dose-dependent shRNA expression. This clinical trial indicated that the treatment is tolerable and safe for patients (Patel *et al.*, 2016). Studies have suggested that combination of rAAVs treatment together with new non-invasive techniques, such as the use of ultrasound to direct the virus to the striatum (Stavarache *et al.*, 2019), could expand its use in humans. However, our data show that rAAV9 yields remarkably long-lasting knock-down of GluN3A protein levels associated to motor improvement upon a single injection, which would limit the invasiveness of the procedure.

In summary, our study grants the necessary proof-of-principle for exploring therapies targeting aberrant GluN3A expression in HD, that could be used alone or in combination with HTT-lowering treatments. Efforts to be undertaken in the future include further evaluation of the current RNAi-based approach or investing on screenings for small molecules blocking GluN3A expression, function or downstream signalling pathways. Rationale for the treatment stemmed out from a unique feature of GluN3A subunits, which are predominantly expressed on early postnatal stages and pathologically reactivated in animal models and HD patients (Marco *et al.*, 2013). Such combination of features suggested that side-effects would be minimum if therapies started in late life. Yet a detailed knowledge of GluN3A expression patterns in adult or even postnatal life has been conspicuously absent, so they cannot be not ruled out.

To fill that gap we embarked on a comprehensive analysis of GluN3A expression in the mouse brain from embryonic to postnatal and adult stages. This part constitutes the Second Chapter of my Thesis.

One of the main contributions is a fine anatomical detailed map of the postnatal down-regulation known *a priori*, which reveals a highly dynamic and differential *Grin3a* regulation across different brain regions. During early postnatal life, neuronal circuits in the brain are massively remodelled by experience: large subsets of synapses are strengthened and mature but may others weaken and are eliminated (Katz and Shatz 1996). GluN3A-NMDARs have been proposed to control the timing and magnitude of this remodelling by limiting classical NMDAR signalling until the arrival of sensory experience, and/or fine-tuning synapse plasticity and maturation at later stages (Roberts *et al.*, 2009; Fiuza *et al.*, 2013; Perez-Otano *et al.*, 2016). Our anatomical work lends support for this idea by showing early, sequential, and transient expression of *Grin3a* in many cortical areas over postnatal development.

The variations in the timing of *Grin3a* expression and down-regulation across cortical regions correlate remarkably with differences in time-scales of cortical maturation (Guillery 2005) and degree of functional specialization (Wang 2020). For instance, transient waves of *Grin3a* expression are a characteristic of primary sensory and motor cortices, whereas expression appears early and is retained in association and multimodal areas. Primary sensory cortices provide modality-specific information, and early maturation guided by experience is needed to sculpt receptive fields and preserve the fidelity of the information. By contrast, associative and multimodal cortices play an integrative role, have long, protracted maturation periods and maintain a potential for plastic responses that lower areas lose early (Guillery 2005). Of relevance here, adult *Grin3a* expression was also observed in non-cortical areas with strong plasticity needs into adulthood, or high functional requirements such as association of multiple inputs such are the olfactory system, the amygdala, the claustrum, or ventral hippocampus.

Within primary sensory cortices, *Grin3a* expression follows a stereotyped sequential pattern with initial restriction to layer V followed by expression in outer layers and overall down-regulation, which resembles the inside-out patterning model of cortical maturation. While this stereotyped pattern is conserved across motor and sensory cortices, its timing varies and is coupled to the arrival of sensory experience as exemplified by the delayed *Grin3a*

expression in visual cortex, an area of the neocortex that matures later coinciding with eyelid opening (Yoshii *et al.*, 2003).

Our findings confirm and expand a recent report that found *Grin3a* expression in adult mouse brain to be one of the strongest correlates with a hierarchical gradient of functional integration, from primary sensory to transmodal association cortices, established using the T1w/T2w magnetic resonance imaging ratio (Fulcher *et al.*, 2019). In primate and mouse cortex, the T1w/T2w ratio inversely correlates with structural properties such as levels of intracortical myelination, laminar elaboration, abundance of parvalbumin interneurons or perineuronal nets, all considered markers of increased differentiation and stability across cortices (Garcia-Cabezas *et al.*, 2017; Wang 2020). Low T1w/T2w ratios and high *Grin3a* expression are typical of functionally integrative areas, such as insular cortices, temporal association areas, cingulate cortex, ectorhinal cortex, etc (Figure 18A). Correlation between T1w:T2w ratios and *Grin3a* levels are consistent between mice and humans (Figure 18B) (Fulcher *et al.*, 2019). It is worth noting that genetic variations in human GRIN3A have been reported to modulate prefrontal cerebral activity during selective attention tasks (Gallinat *et al.* 2007), supporting a role in higher cognitive processing.

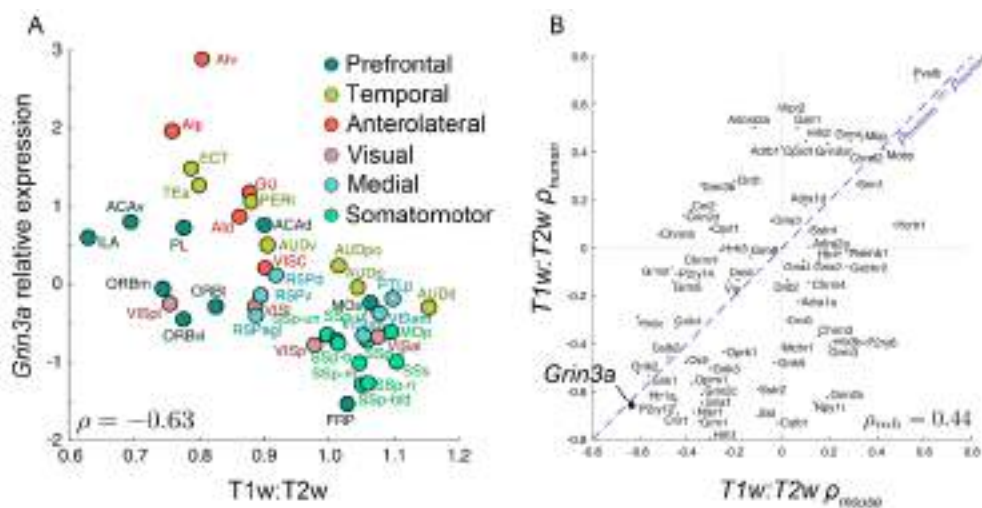


Figure 18. Correlation between T1w:T2w ratios and *Grin3a* relative expression (A) Scatter plot of T1w:T2w vs z-score normalized levels of *Grin3a* transcription in different adult mouse brain areas. (B) The plot shows the correlation between T1w:T2w and transcription levels for 70 brain-related genes in mice (horizontal axis) and humans (vertical axis), where

*Grin3a* levels are consistent between humans and mice. Modified from Fulcher *et al.*, 2019. Abbreviations for cortical areas and genes are defined in Fulcher *et al.*, 2019.

A number of parameters that vary over postnatal development and along the cortical hierarchy to fulfil specific functional requirements could be related to the GluN3A expression described here. For instance, *Grin3a* enhances spine turnover (Kehoe *et al.*, 2014), and high rates of disassembly and formation of synapses and spines during postnatal critical periods are thought to be permissive for refinement while low spine turnover leads to circuit stabilization. GluN3A subunits have also been shown to control the developmental onset of long-term forms of plasticity such as hippocampal long-term potentiation (Roberts *et al.*, 2009), spike-timing dependent long-term depression in V1 (Larsen *et al.*, 2014), or the synaptic incorporation of GluN2A subunits and AMPA receptors (Henson *et al.*, 2012). Other properties such as the maintenance of persistent or recurrent activity in the prefrontal cortex could reflect roles of GluN3A-NMDARs or excitatory GluN1/GluN3A receptors on NMDA spiking activity or neuronal excitability (Mahfooz *et al.*, 2016; Otsu *et al.*, 2019). Finally, association and frontal areas contain a greater proportion of Sst interneurons that innervate dendrites and have an “input-modulating function”, while sensory areas contain more parvalbumin interneurons that innervate the soma and axon initial segment and have an “output-modulating” function.

*Grin3a* expression is very high in the thalamus where it prevails in higher order thalamic nucleus, while primary sensory thalamic areas lack *Grin3a* or express it at low levels. Information from the sensory periphery is first transmitted to the cerebral cortex via the primary sensory, or first-order, thalamic nuclei including the lateral geniculate in visual thalamus, ventral division of the medial geniculate in auditory thalamus, and ventral posterior nuclei in somatosensory thalamus. By contrast, higher order thalamic nuclei do not receive substantial input from the sensory periphery and instead form extensive cortico-thalamic-cortical circuits or connect functionally related cortical and subcortical regions. They provide a route for cortico-cortical communication which integrates cortical and subcortical inputs, linking cognition and motivated behavior to internal states and levels of consciousness (Sherman 2007). Of

relevance here, highest adult *Grin3a* expression was observed in midline and intralaminar nuclei such as the centromedial and paraventricular, involved in arousal and wakefulness (Van der Werf *et al.*, 2002; Ren *et al.*, 2018; Redinbaugh *et al.*, 2020). Consistent with these findings, unbiased mammalian reverse genetics detected alterations in wakefulness-sleep transitions in *Grin3a* knockout mice (Sunagawa *et al.*, 2016), and GluN1/GluN3A glycine receptors in the medial habenula have been implicated in mediating conditioned place-aversion (Otsu *et al.*, 2019). Particularly intriguing is the gradient of *Grin3a* expression throughout the hippocampus with a greater presence in the ventral hippocampus in adult stages. The dorsal hippocampus is mostly related to memory and spatial navigation, while the ventral hippocampus mediates anxiety-related behaviours (Bannerman *et al.*, 2004). In addition, the areas of the hippocampus where *Grin3a* mRNA is present are anatomically linked to areas of social behavior, such as amygdala nuclei and prefrontal cortex that also show high levels of expression in adult mice (Kishi *et al.*, 2006; Sun *et al.*, 2020). A previous report defines GluN3A expression as a key regulatory protein in the development and execution of normal social behavioral mice interaction. In a variety of social behavioral tests, GluN3A KO adult mice show social deficits, which is due to the effect of lack of GluN3A on oxytocin receptor levels in prefrontal cortex (Lee *et al.*, 2018), which directly relates GluN3A expression to social development in mice. Another area with high expression of *Grin3a* is the DEN the function of which is unknown. Different results indicate that DEN belongs to the limbic processing network, which interacts with the ipsilateral amygdala complexes and prefrontal cortex (Behan *et al.*, 1999; Watson *et al.*, 2016). We could conclude that the function of GluN3A in stages of development would be what is well known so far, which is the function of refinement of neuronal circuits by immature synapse pruning, but in adult animals, GluN3A function is related to motivated, arousal and wakefulness, wakefulness-sleep transitions, social, emotional and anxiety behavior elements.

Finally, our data revealed particularly high *Grin3a* mRNA levels in Sst interneurons of SS1 and hippocampus from early postnatal stages (Figure 19A). This is in-line with single-cell RNAseq analyses of gene expression in adult mouse somatosensory, motor and visual cortex interneurons (Pfeffer *et al.*,



2013; Paul *et al.*, 2017). In adult (16 week-old mice) somatosensory and motor cortices, Sst interneurons were distinguished from other GABA interneurons by a high expression of *Grin3a* (Figure 19B) (Paul *et al.*, 2017). *Grin3a* expression was highest in Sst Martinotti cells that appear in the stratum oriens of hippocampus (Leão *et al.*, 2012) and within the neocortex, in layers V and somewhat less in 2-3 (Harris *et al.*, 2014). Single-cell RNAseq of adult visual cortex also detected high expression of *Grin3a* in Sst compared to other types of interneurons (Figure 19C) (Pfeffer *et al.*, 2013). Publicly available transcriptome datasets indicate that *Grin3a* expression might be a conserved feature of Sst interneurons across species (<http://interneuron.mccarrolllab.org/>). Moreover, a recent genome-wide epigenomic analysis identified the *Grin3a* locus as a site of open chromatin and low DNA methylation (mCG) in Sst interneurons (Yao *et al.*, 2020). Both epigenetic marks are typical of actively expressed genes and are thought to promote and maintain cell-type specific expression and cell identity.

Together, these data provide strong validation of *Grin3a* expression as a secondary marker for Sst interneurons, which may explain some of their particular features in terms of synaptic communication. They further suggest that GluN3A subunits might play more general roles than currently envisioned in modulating the development of neural circuits. Along with the well-studied refinements of connections between excitatory principal neurons, circuit formation requires the network integration of local interneurons that also involves a refinement of excitatory synaptic inputs onto these inhibitory cells (De Marco Garcia *et al.*, 2015; Tuncdemir *et al.*, 2016). For example, Sst interneurons in infragranular layers of SS1 receive dense but transient thalamocortical innervation during the first postnatal week. This innervation is required for the later functional maturation and synaptic integration of parvalbumin interneurons, but is reduced by 4-fold by P14 (Tuncdemir *et al.*, 2016). Our data show that *Grin3a* is highly expressed between P3-P9 in layer V Sst interneurons, providing a candidate mechanism for mediating the refinement of thalamocortical inputs. Excitatory synapses onto MGE-derived interneurons undergo a defined program of synapse maturation, with predominance of GluN2B-NMDARs in neonates which are later replaced by GluN2A-NMDARs (Matta *et al.*, 2013; Perszyk *et al.*, 2016). This developmental

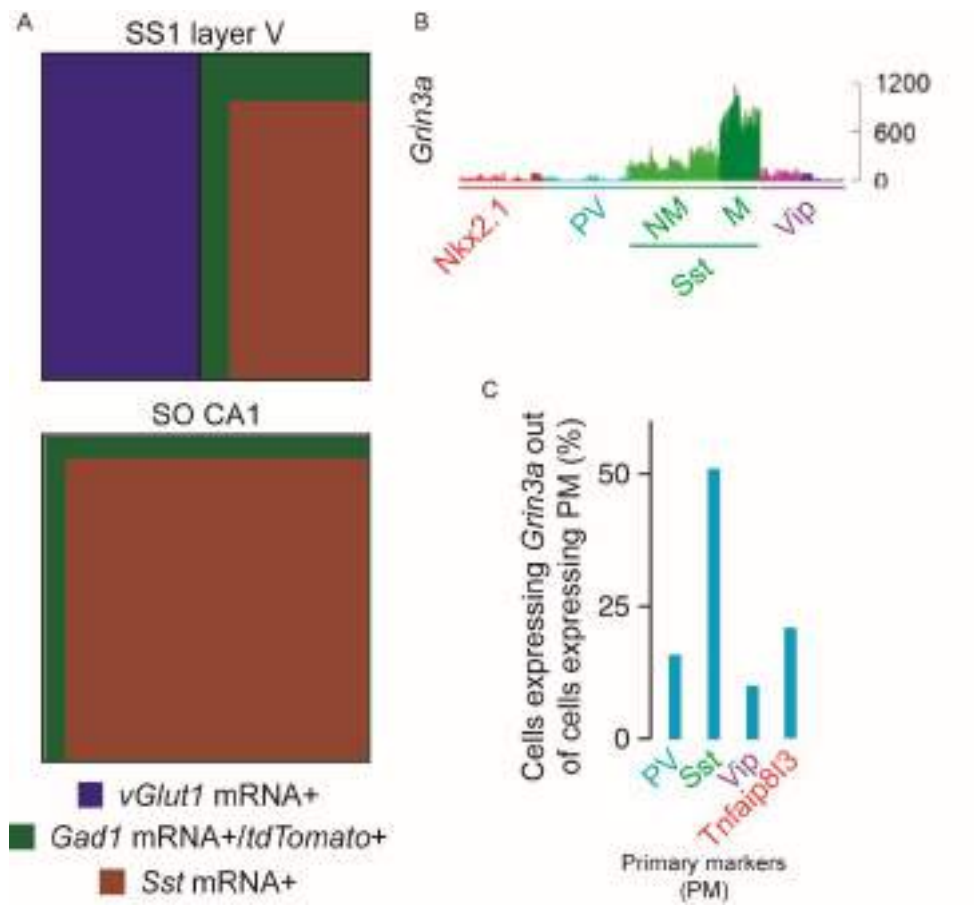
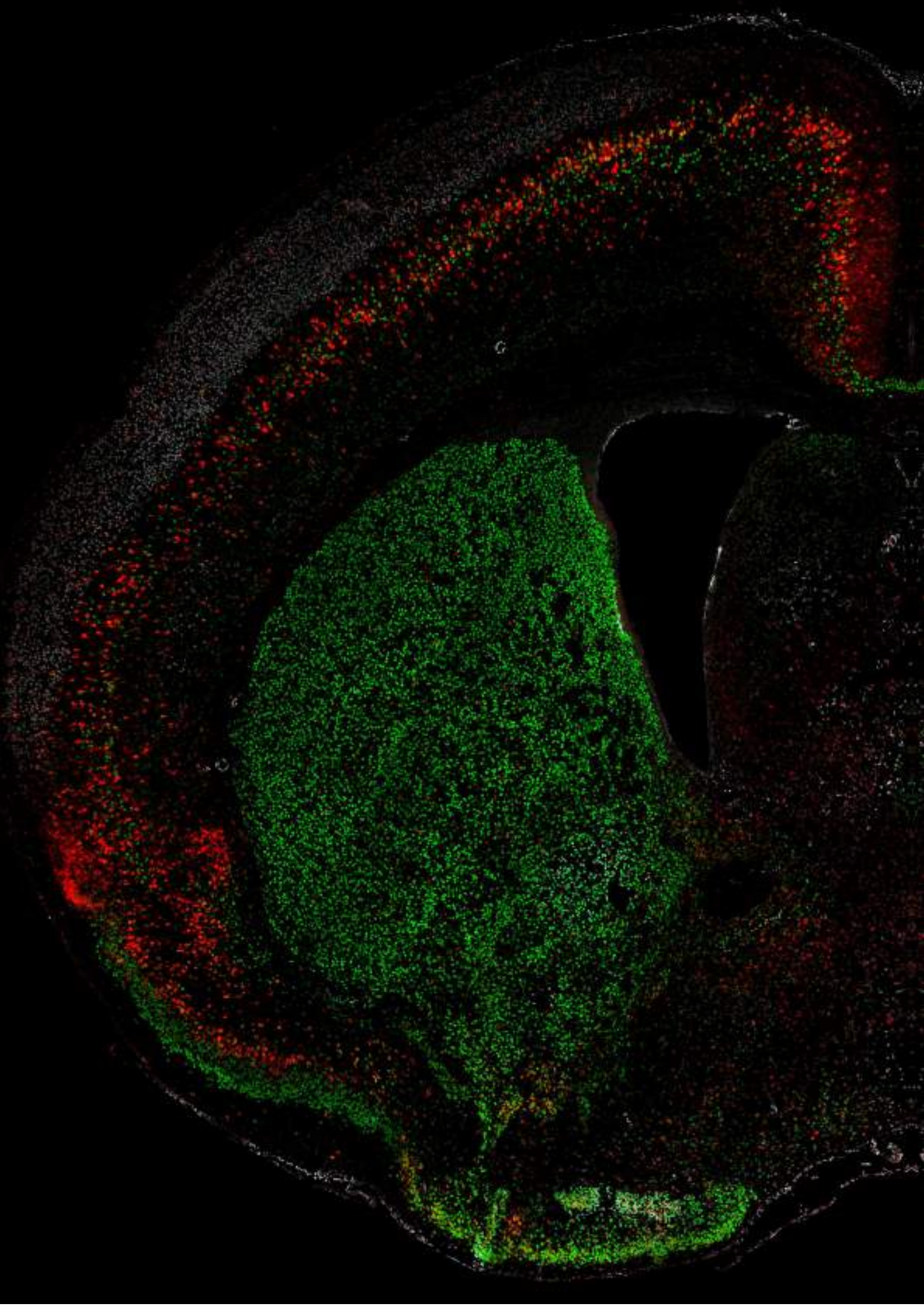
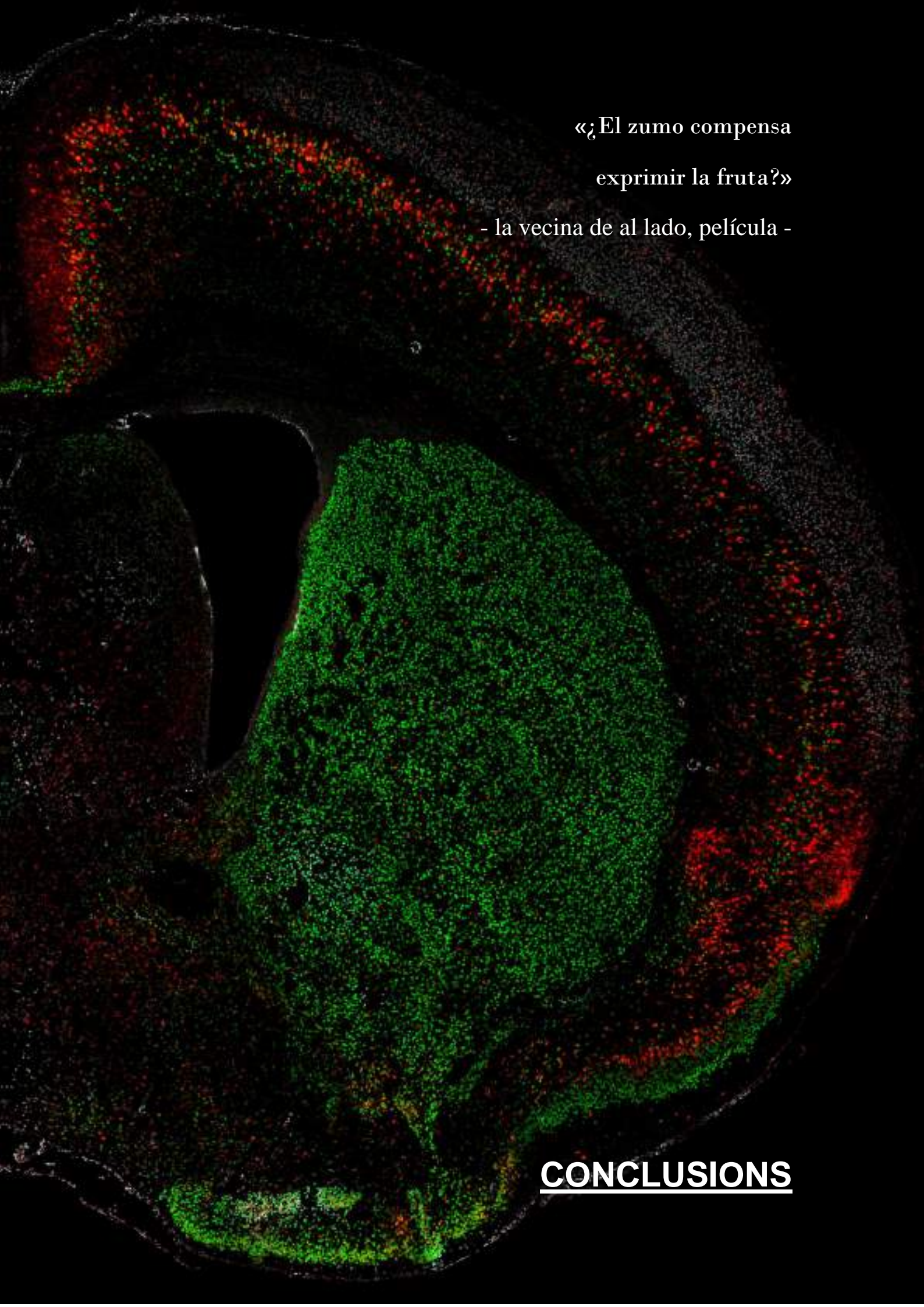


Figure 19. High *Grin3a* mRNA levels in Sst interneurons. (A) Percentage of *Grin3a*-positive cells in different neuronal populations. The area size illustrates the percentage of *Grin3a* mRNA+ neurons (total square) colocalizing with each neuronal marker in layer V of SS1 (top) and SO of CA1 (bottom). (B) *Grin3a* mRNA expression measured by RNA-seq in SS cortex single cells. Modified from Paul *et al.*, 2017. (C) Coexpression of primary interneuron markers (PM) and *Grin3a* based on the analysis of 474 single cells by scRT-PCR. Modified from Pfeffer *et al.*, 2013. Abbreviations: *Gad1* mRNA label GABAergic neurons; M, Martinotti cells; SO, stratum oriens; SS1, somatosensory cortex 1; *Sst* mRNA label somatostatin interneurons; *Nkx2.1-tdTomato* and *Nkx2.1* label interneurons from MGE; NM, Non-Martinotti cells; PV, parvalbumin interneurons; *tnfaip8l3*, TNF Alpha Induced Protein 8 Like 3; *vGlut1* mRNA label glutamatergic neurons; Vip, vasoactive intestinal peptide interneurons.

switch in subunit composition resembles the experienced by excitatory neurons, in which GluN3A down-regulation has been implicated (Perez-Otano and Ehlers 2004; Henson *et al.*, 2012).

In sum, our study offers entirely new insight onto the spatiotemporal patterns of *Grin3a* distribution in the brain, provides a roadmap for dissecting the diverse functions attributed to GluN3A-NMDARs in brain physiology, behaviour and disease states, and opens up important cell biological and functional questions. At the cell biological level, further investigations on regulation will be needed to define the transcriptional and epigenetic mechanisms that determine the area-to-area and temporal variations in *Grin3a* expression. Is experience a critical determinant factor, as suggested by the observation that rearing rats in the dark prevents GluN3A down-regulation in visual cortex (Larsen *et al.*, 2014) or is regulation by the calcium-regulated transcription factor CaRF (Lyons *et al.*, 2016)? In terms of function, the transient expression of *Grin3a* in cortical areas and temporal correlation with hierarchical cortical maturation emphasizes the concept of GluN3A as a key controller of the timing of brain maturation and its coupling to experience. Further advances will require selective deletion of the *Grin3a* gene at specific times and in specific neuronal populations, combined with tools to distinguish roles of GluN3A-NMDARs from those of the yet more enigmatic excitatory GluN1/GluN3 receptors.





«¿El zumo compensa  
exprimir la fruta?»

- la vecina de al lado, película -

**CONCLUSIONS**





All the results presented in the First Chapter of my Thesis: “RNAi-Based GluN3A Silencing Prevents and Reverses Disease Phenotypes Induced by Mutant huntingtin” are summarized in the following points:

- 1) The spread capacity of rAAV9 in striatum was higher and more consistent across individuals than that of rAAV8 or rAAV10, as was thus chosen for our gene therapy approach.
- 2) A single injection of the rAAV9-shGluN3A silenced persistently and specifically the expression of GluN3A subunits without affecting other proteins analysed.
- 3) rAAV9-shGluN3A showed neuronal tropism in the striatum and preferentially targets medium spiny neurons, the vulnerable population in Huntington’s disease, without modifying GluN3A levels in other neuronal or non-neuronal populations.
- 4) rAAV9-driven GluN3A silencing was effective when timed with the onset of the synaptic pathology but also when initiated later in the disease course, establishing a broad window of opportunity over which pre-existing phenotypes can be reversed.
- 5) Silencing expression in medium spiny neurons was sufficient for restoring motor performance in a Huntington’s disease mice model.

All the results presented in the Second Chapter of my Thesis: “Temporal Dynamics and Neuronal Specificity of *Grin3a* Expression in the Mouse Forebrain” are summarized in the following points:

- 1) Despite a major down-regulation, *Grin3a* mRNA expression is retained into adulthood in a subset of brain areas such as the prefrontal cortex, anterior cingulate, retrosplenial, agranular insular, temporal association, ectorhinal, and perirhinal cortices, amygdala and ventral hippocampus.

- 2) A stereotyped, layer-specific profile of *Grin3a* expression is observed in sensory and motor cortices at early postnatal stages, with early restriction to layer V and later appearance in upper layer neurons. The timing however varies across sensory modalities and correlates with the timing of arrival of sensory experience and associated neural circuit refinements.
- 3) *Grin3a* is expressed in both excitatory and inhibitory neurons, with GABAergic interneurons showing particularly high *Grin3a* mRNA levels in somatosensory cortex and stratum oriens of the hippocampus. Virtually all *Grin3a*-positive interneurons are Nkx2.1-positive which shows a common origin in the medial ganglionic eminence.
- 4) Virtually all somatostatin interneurons in cortex and hippocampus express high levels of *Grin3a* mRNA, indicating that *Grin3a* expression can be used as a secondary marker for somatostatin interneurons.




## CONCLUSIONES

Los resultados presentados en el primer capítulo de mi tesis "El silenciamiento de GluN3A basado en ARNi previene y revierte los fenotipos de enfermedad inducidos por huntingtina mutante" están resumidos en los siguientes puntos:

- 1) La capacidad de difusión del rAAV9 en el estriado fue mayor y más consistente entre diferentes ratones inyectados que los rAAV8 o rAAV10, por lo que se escogió como vector para nuestra estrategia de terapia génica.
- 2) Una única inyección de rAAV9-shGluN3A silenció de forma persistente y específica la expresión de las subunidades GluN3A sin afectar a otras proteínas analizadas.
- 3) rAAV9-shGluN3A presenta un tropismo neuronal en el estriado con preferencia significativa por neuronas espinosas medianas, la población vulnerable en la enfermedad de Huntington, sin modificar los niveles de GluN3A en otras poblaciones neuronales (interneuronas colinérgicas) o no neuronales (oligodendrocitos).
- 4) El silenciamiento de GluN3A dirigido por rAAV9 fue eficaz cuando se sincronizó con el inicio de la patología sináptica, pero también cuando se inició más tarde en el curso de la enfermedad. Esta observación establece una amplia ventana de oportunidad sobre la cual se pueden revertir los fenotipos preexistentes.
- 5) El silenciamiento de la expresión en neuronas espinosas medianas fue suficiente para restaurar el rendimiento motor en un modelo de ratones con enfermedad de Huntington.

Los resultados presentados en el segundo capítulo de mi tesis "Dinámica temporal y especificidad neuronal de la expresión de *Grin3a* en el prosencéfalo del ratón" están resumidos en los siguientes puntos:

- 1) A pesar de una importante reducción a partir del pico de expresión postnatal, se observan niveles significativos del ARNm de *Grin3a* hasta la edad adulta en un subconjunto de áreas cerebrales que incluyen la corteza prefrontal, cíngulo anterior, retrosplenial, corteza insular agranulada, temporal asociativa, cortezas ectorrinal y perirrinal, amígdala e hipocampo ventral.
- 2) La expresión de *Grin3a* sigue un perfil estereotipado y específico de capa en las cortezas sensoriales primarias y motoras en las primeras etapas posnatales, con una restricción temprana a capa V y aparición posterior en las neuronas de las capas superiores. Sin embargo, el curso temporal varía según la modalidad sensorial y se correlaciona con la llegada de la experiencia sensorial y refinamientos asociados del circuito neuronal.
- 3) *Grin3a* se expresa tanto en neuronas excitadoras como inhibitoras, con niveles de ARNm particularmente elevados en interneuronas GABAérgicas de corteza somatosensorial y stratum oriens del hipocampo. Virtualmente todas las interneuronas que expresan *Grin3a* son positivas para el marcador Nkx2.1 lo que muestra un origen común en la eminencia ganglionar media.
- 4) Virtualmente todas las interneuronas somatostatinérgicas en corteza e hipocampo expresan altos niveles de *Grin3a* ARNm, indicando que la expresión de *Grin3a* puede usarse como marcador secundario de interneuronas somatostatinérgicas.



«La vida no se mide por las  
veces que respiramos, sino por los  
momentos que nos dejan sin aliento»

- Will Smith -

**APPENDIX**





## General abbreviations

### A

AAV, adeno-associated virus

Ab, antibody

AMPA,  $\alpha$ -amino-3-hydroxy-5-methyl-4-isoxazolepropionic acid

ANOVA, analysis of variance

AP2, clathrin adaptor protein 2

AP-5, D-2-amino-5-phosphonovaleric acid

### B

BAC, bacterial artificial chromosome

BCIP, 5-bromo-4-chloro-3'-indolyphosphate p-toluidine salt

### C

C-terminal, carboxy-terminal

Ca<sup>2+</sup>, calcium ions

CAA, cytosine-adenine-adenine nucleotides

CAG, cytosine-adenine-guanine nucleotides

CaMKII, calcium-calmodulin-dependent protein kinase II

Cap genes, capsid genes

CC, motif required for redox modulation with two cysteine residues

Chat, cholinergic interneurons

CMV, cytomegalovirus promoter

CNS, central nervous system

Ctip2, chicken ovalbumin upstream promoter transcription factor-interacting protein 2

Cux1, cut Like Homeobox 1 protein

Cy, cyanine

**D**

D1, dopamine receptor 1 positive neurons

D2, dopamine receptor 2 positive neurons

DAPI, 4',6-diamidino-2-phenylindole

DARPP-32, Dopamine and cAMP regulated phosphoprotein 32

DNA, deoxyribonucleic acid

dNTPs, deoxyribonucleotide triphosphates

**E**

E, embryonic day

ECL, enhanced chemiluminescence

EDTA, ethylenedinitrilotetraacetic acid

EGFP, enhance GFP

EH, enfermedad de Huntington

EM, electron microscopy

ER, endoplasmic reticulum

**F**

fEPSP, field excitatory postsynaptic potential

FISH, fluorescent ISH

**G**

GABA, gamma-aminibutyric

Gad1, Glutamate decarboxylase 1

GAD67, glutamic acid decarboxylase 67

GFP, green fluorescent protein

GIT1, G-protein coupled receptor kinase interacting protein

GluD,  $\delta$ -Receptors

GluN3A, glutamate NMDA receptor subunit 3A

GluN3A-S, C-terminal short length GluN3A

GluN3A-L, C-terminal long length GluN3A

GRIN, glutamate receptor ionotropic N-methyl-D-aspartate

*Grin3a*, glutamate receptor ionotropic N-methyl-D-aspartate 3a

## H

HEAT, Huntingtin, Elongator factor3, PR65/A regulatory subunit of PP2A and Tor1

HEPES, 4-(2-hydroxyethyl)-1-piperazineethanesulfonic acid

HFS, high-frequency stimulation

HTT, huntingtin protein

*HTT*, human huntingtin gene

*Htt*, mouse huntingtin gene

HD, Huntington's disease

## I

IT15, interesting transcript 15 gene

ITRs, inverted terminal repeats

ISH, *in situ* hybridization

## K

K<sup>+</sup>, potassium ions

Kb, kilo bases

kD, kilo Daltons

KO, knock out

## L

LTP, long-term potentiation

## M

M1-4, transmembrane helices 1-4

MAPs, microtubule-associated proteins

Mg<sup>2+</sup>, magnesium ions

mHtt, mutant Huntingtin

miRNAs, micro RNAs

mRNA, messenger RNA

Ms, milliseconds

MSNs, medium spiny neurons

mTOR, mammalian target of rapamycin

mTORC1, mammalian target of rapamycin complex

## **N**

Na<sup>+</sup>, sodium ions

NBT, nitroblue tetrazolium chloride

NMDAR, N-methyl-D-aspartate receptors

N-terminal, amino-terminal

NSE, specific enolase promoter

## **O**

Oligos, oligonucleotides

## **P**

P(number), postnatal day

PACSLN1, protein kinase C and casein kinase substrate in neurons 1

PAK1, p21-activated kinase 1

PB, phosphate buffer

PBS, phosphate buffered saline

PCR, polymerase chain reaction

PFA, paraformaldehyde

PKA, protein kinase A

PKC, protein kinase C

PP2A, protein phosphatase 2A

POD, horseradish peroxidase



PolyQ, poly glutamine repeats

PRD, proline-rich domain

Pre-miRNAs, pre-mature miRNAs

Pri-miRNAs, primary microRNAs

Prnp, mouse prion promoter

pS, picosiemens

PSD, postsynaptic density

PSD-95, postsynaptic density protein-95

PTK, protein phosphatase 2A

PVDF, polyvinylidene difluoride

## **Q**

Q/R/N, Glutamine/arginine/asparagine

## **R**

rAAV, recombinant adeno-associated virus

Rep gene, replication gene

Rheb, Ras-GTPase activating proteins

RISC, RNA-induced silencing complex

RNA, Ribonucleic acid

Rpm, Revolutions per minute

RT, room temperature

RT-PCR, reverse transcriptase polymerase chain reaction

RXR, arginine/any/arginine

## **S**

SDS-PAGE, sodium dodecyl sulphate polyacrylamide gel electrophoresis

SEM, standard error of the mean

shRNA, short-hairpin-RNA

siRNAs, small interfering RNAs

ssDNA, single-stranded DNA

ssRNA, single strand

Sst, somatostatin

Syndapin, synaptic dynamin-associated protein

## **T**

TBS, Tris buffer saline

TEMED, N,N,N',N'-Tetramethylethylenediamine

TSA, tyramide signal amplification

## **V**

vGlut1, vesicular glutamate transporter 1

## **W**

WT, wild-type

## **X**

xg, relative centrifugal force

## **Y**

YAC, yeast artificial chromosome

YWL, Tyrosine-tryptophan-leucine

## **Anatomical abbreviations**

### **A**

ACg, anterior cingulate cortex

ACo, anterior cortical amygdaloid nucleus

AD, anterior/dorsal thalamic nucleus

AHi, amygdalohippocampal area

AI, agranular insular cortex

AM, anterior/medial thalamic nucleus

AON, anterior olfactory nucleus

APT, anterior pretectal nucleus

Au, auditory cortex

AV, anteriorventral thalamic nucleus

## **B**

BMP, basomedial amygdaloid nucleus, posterior part

BLA, basolateral amygdala

BLP, basolateral amygdaloid nucleus

BP, baso amygdaloid nucleus, posterior part

BST, bed nucleus of the stria terminalis

## **C**

CA1, cornu ammonis 1

cc, corpus callosum

CeM, central amygdaloid nucleus, medial division

Cg, cingulate cortex

CL, centrolateral thalamic nucleus

Cla, claustrum

CM, centromedial thalamic nucleus

CoA, cortical amygdala

CPu, caudate-putamen

CxA, cortex amygdala transition zone

## **D**

DEn, dorsal endopiriform nucleus

DLG, dorsolateral geniculate nucleus

DP, dorsal peduncular cortex

DG, dentate gyrus

DS, dorsal subiculum

DTT, dorsal tenia tecta

**F**

Fr, frontal cortex

Fr, fasciculus retroflexus

**E**

Ect, ectorhinal cortex

**G**

GP, globus pallidus

GPe, external segment of the globus pallidus

GPi, internal segment of the globus pallidus

**H**

Hb, habenula

**I**

Ic, internal capsule

ICj, islands of Calleja

ICjM, major island of Calleja

IG, Indusium griseum

In, insular cortex

IL, infralimbic cortex

IM, intercalated amygdaloid nucleus, main part

IMD, intermediodorsal thalamic nucleus

In, insular cortex

**L**

La, lateral amygdala

LD, laterodorsal thalamic nucleus

LHb, lateral habenula

LP, lateral posterior thalamic nucleus

LS, lateral septal nucleus

LTD, long-term depression

LTP, long-term potentiation

## **M**

MD, medial dorsal thalamic nucleus

MGE, medial ganglionic eminence

MHb, medial habenular nucleus

Mia, Mitral cell layer of the olfactory bulb

Mo, motor cortex

mt, mammillothalamic tract

## **O**

OC, orbital cortex

OFC, orbitofrontal cortex

ON, olfactory nerve

OT, Olfactory tubercle

## **P**

PC, Paracentral thalamic nucleus

PF, Parafascicular thalamic nucleus

PFC, prefrontal cortex

Pir, piriform cortex

PLCo, posteriorlateral cortical amygdala nucleus

PMCo, posteriomedial cortical amygdala nucleus

Po, posterior thalamic nuclear group

PRh, perirhinal cortex

PrL, prelimbic cortex

PT, paratenial thalamic nucleus

PtP, parietal cortex, posterior part

PV, paraventricular thalamic nucleus

Pyr, pyramidal layer

## **R**

Re, reuniens thalamic nucleus

Rh, rhomboid thalamic nucleus

Rhi, rhinal cortices

RNA, ribonucleic acid

RS, retrosplenial cortex

Rt, reticular thalamic nucleus

## **S**

S, subiculum

SN, substantia nigra

SNC, substantia nigra *pars compacta*

SNr, substantia nigra *pars reticulata*

SOr, stratum oriens

SP, stratum pyramidale

SR, stratum radiatum

SS, somatosensory cortex

ST, bed nucleus of the stria terminalis

STh, subthalamic nucleus

STN, subthalamic nucleus

## **T**

Thal, thalamus

TeA, temporal association cortex

TT, tenia tecta

Tu, olfactory tubercle

## **V**

VA, ventral-anterior thalamic nucleus

VEn, ventral endopiriform nucleus

VG, Ventral lateral geniculate nucleus

Vis, visual cortex

VL, ventral-lateral thalamic nucleus

VM, ventromedial thalamic nucleus

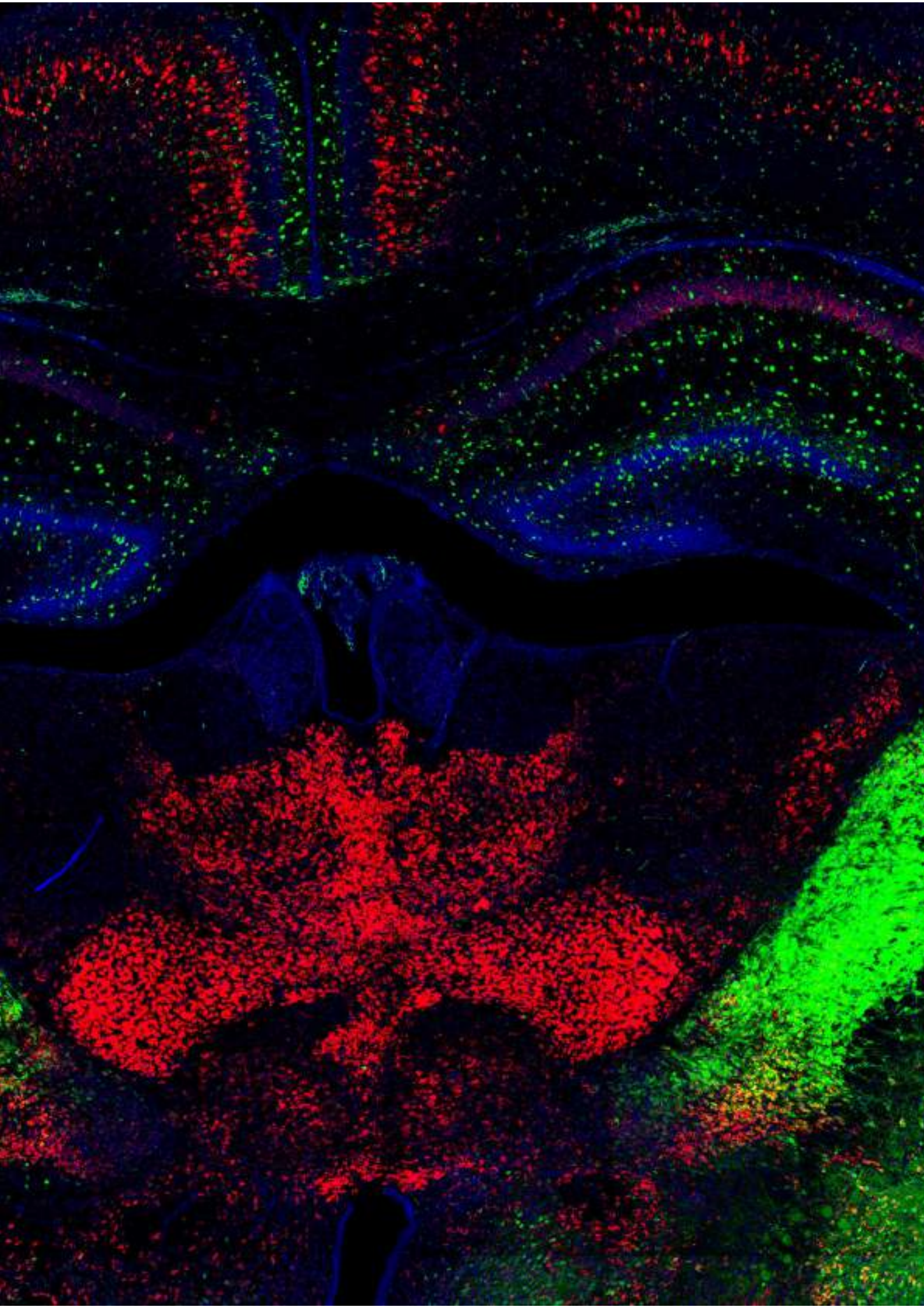
VMH, ventromedial hypothalamic nucleus

VP, ventral posterior thalamic nucleus

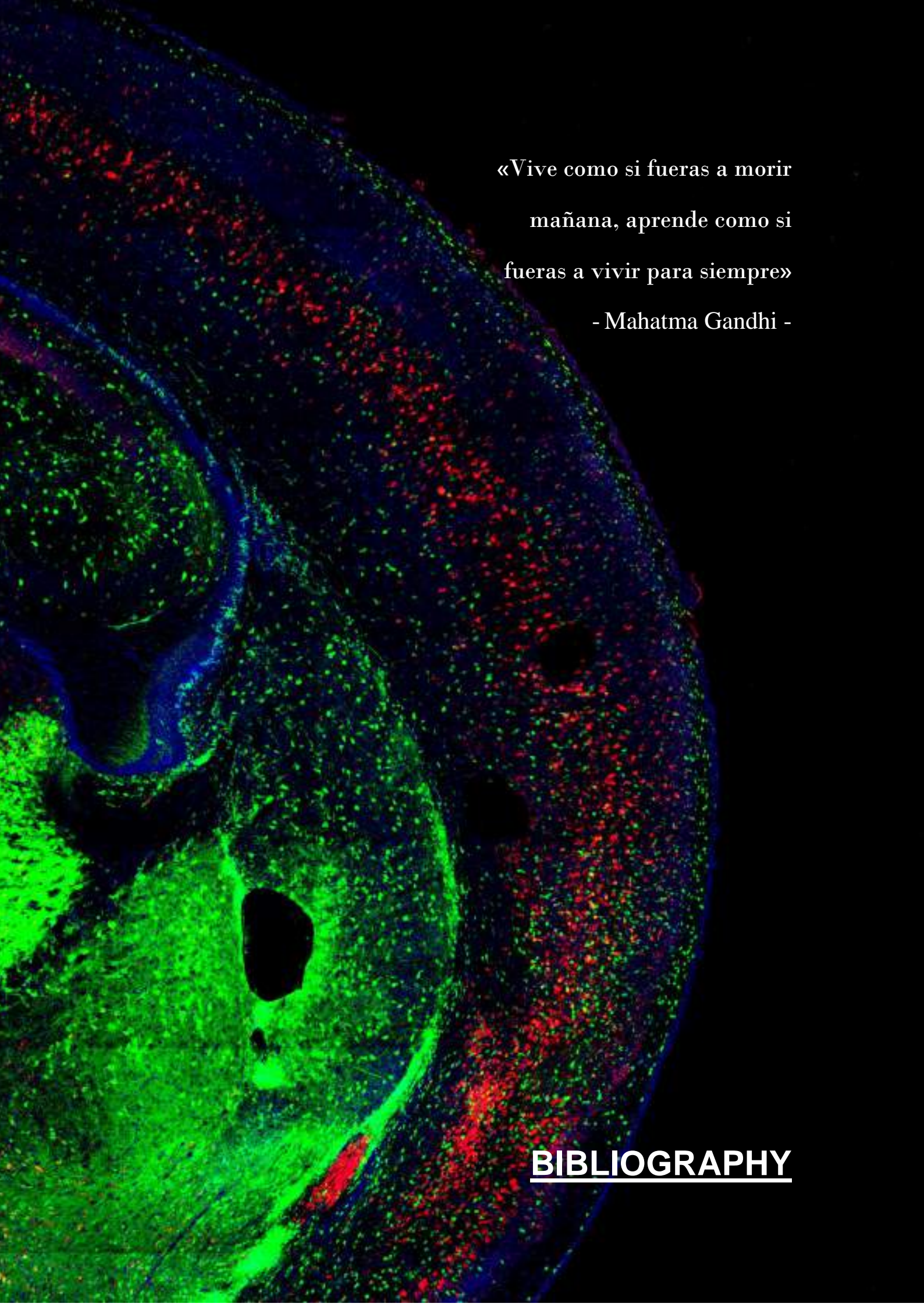
VTT, ventral tenia tecta

## **Z**

ZI, zona incerta







«Vive como si fueras a morir  
mañana, aprende como si  
fueras a vivir para siempre»  
- Mahatma Gandhi -

**BIBLIOGRAPHY**





- Albin, R. L., A. B. Young and J. B. Penney. 1989. "The functional anatomy of basal ganglia disorders ". *Trends in Neuroscience*, 12(10).
- Albin, R. L., A. Reiner, K. D. Anderson, J. B. Penney and A. B. Young. 1990. "Striatal and Nigral Neuron Subpopulations in Rigid Huntington's Disease: Implications for the Functional Anatomy of Chorea and Rigidity-akinesia." *Annals of Neurology* 27(4):357–65.
- Al-Hallaq, R. A., B. R. Jarabek, Z. Fu, S. Vicini, B. B. Wolfe and R. P. Yasuda. 2002. "Association of NR3A with the N-Methyl-D-Aspartate Receptor NR1 and NR2 Subunits." *Molecular Pharmacology* 62(5):1119–27.
- An, D. S., F. X. Qin, V. C. Auyeung, S. H. Mao, K. P. Sam, D. Baltimore and I. S. Y. Chen. 2006. "Optimization and Functional Effects of Stable Short Hairpin RNA Expression in Primary Human Lymphocytes via Lentiviral Vectors." *Molecular Therapy* 14(4):494–504.
- Andersson, O., A. Stenqvist, A. Attersand and G. V. Euler. 2001. "Nucleotide Sequence, Genomic Organization, and Chromosomal Localization of Genes Encoding the Human NMDA Receptor Subunits NR3A and NR3B." *Genomics* 78(3):178–84.
- André, V. M., C. Cepeda, Y. E. Fisher, M. Huynh, N. Bardakjian, S. Singh, X. W. Yang, and M. S. Levine. 2011. "Differential Electrophysiological Changes in Striatal Output Neurons in Huntington's Disease." *Journal of Neuroscience* 31(4):1170–82.
- Andrich, J., L. Arning, S. Wieczorek, P. H. Kraus, R. Gold and C. Saft. 2008. "Huntington's Disease as Caused by 34 CAG Repeats." *Movement Disorders* 23(6):879–81.
- Annoni, A., S. Gregori, L. Naldini, and A. Cantore. 2018. "Modulation of Immune Responses in Lentiviral Vector-Mediated Gene Transfer." *Cellular Immunology*. 342:103802.
- Arrasate, M., S. Mitra, E. S. Schweitzer, M. R. Segal, and S. Finkbeiner. 2004. "Inclusion Body Formation Reduces Levels of Mutant Huntingtin and the Risk of Neuronal Death." *Nature* 431(7010):805–10.
- Arrasate, M., and S. Finkbeiner. 2012. "Protein Aggregates in Huntington's Disease." *Experimental Neurology* 238(1):1–11.

Arsham, A. M. and T. P. Neufeld. 2006. "Thinking Globally and Acting Locally with TOR." *Current Opinion in Cell Biology* 18(6):589–97.

Aschauer, D. F., S. Kreuz and S. Rumpel. 2013. "Analysis of Transduction Efficiency, Tropism and Axonal Transport of AAV Serotypes 1, 2, 5, 6, 8 and 9 in the Mouse Brain." *PLoS ONE* 8(9):1–16.

Atwal, R. S., J. Xia, D. Pinchev, J. Taylor, R. M. Epand and R. Truant. 2007. "Huntingtin Has a Membrane Association Signal That Can Modulate Huntingtin Aggregation, Nuclear Entry and Toxicity." *Human Molecular Genetics* 16(21):2600–2615.

Awobuluyi, M., J. Yang, Y. Ye, J. E. Chatterton, A. Godzik, S. A. Lipton and D. Zhang. 2007. "Subunit-Specific Roles of Glycine-Binding Domains in Activation of NR1/NR3 N-Methyl-D-Aspartate Receptors." *Molecular Pharmacology* 71(1):112–22.

Aylward, E. H., B. F. Sparks, K. M. Field, V. Yallapragada, B. D. Shpritz, A. Rosenblatt, J. Brandt, L. M. Gourley, K. Liang, H. Zhou, R. L. Margolis, and C. A. Ross. 2004. "Onset and Rate of Striatal Atrophy in Preclinical Huntington Disease." *Neurology* 63(1):66–72.

Banke, T. G., S. M. Dravid, and S. F. Traynelis. 2005. "Protons Trap NR1/NR2B NMDA Receptors in a Nonconducting State." *Journal of Neuroscience* 25(1):42–51.

Bannerman, D. M., J. N. P. Rawlins, S. B. McHugh, R. M. J. Deacon, B. K. Yee, T. Bast, W. N. Zhang, H. H. J. Pothuizen and J. Feldon. 2004. "Regional Dissociations within the Hippocampus - Memory and Anxiety." *Neuroscience and Biobehavioral Reviews* 28(3):273–83.

Bantel-Schaal, U., B. Hub and J. Kartenbeck. 2002. "Endocytosis of Adeno-Associated Virus Type 5 Leads to Accumulation of Virus Particles in the Golgi Compartment." *Journal of Virology* 76(5):2340–49.

Bartlett, J. S., R. Wilcher and R. J. Samulski. 2000. "Infectious Entry Pathway of Adeno-Associated Virus and Adeno-Associated Virus Vectors." *Journal of Virology* 74(6):2777–85.

Barria, A. and R. Malinow. 2002. "Subunit-Specific NMDA Receptor Trafficking to Synapses." *Neuron*, Vol. 35, 345–353.

Bates, G. P., R. Dorsey, J. F. Gusella, M. R. Hayden, C. Kay, B. R. Leavitt, M. Nance, C. A. Ross, R. I. Scahill, R. Wetzel, E. J. Wild, and S. J. Tabrizi. 2015. "Huntington Disease." *Nature Reviews Disease Primers* 1(April):1–21.

Beal M. F., Kowall N. W. , Ellison D. W. , Mazurek M. F. , Swartz K. J. , and Martin J. B. 1986. "Replication of the Neurochemical Characteristics of Huntington's Disease by Quinolinic Acid. ." *Nature* 321(May):168–71.

Beal, M. F., E. Brouillet, B. G. Jenkins, R. J. Ferrante, N. W. Kowall, E. Storey, R. Srivastava, B. F. Rosen, and B. T. Hyman. 1993. "Neurochemical and Histologic Characterization of Striatal Excitotoxic Lesions Produced by the Mitochondrial Toxin 3-Nitropropionic Acid." *The Journal of Neuroscience*, 13(10): 4181-4192

Beckstead, R. M. and C. J. Cruz. 1986. "Striatal Axons to the Globus Pallidus, Entopeduncular Nucleus and Substantia Nigra Come Mainly from Separate Cell Populations in Cat." *Neuroscience* 19(1):147–58.

Beckstead, R. M. 1988. "Association of Dopamine d<sub>1</sub> and D<sub>2</sub> Receptors with Specific Cellular Elements in the Basal Ganglia of the Cat: The Uneven Topography of Dopamine Receptors in the Striatum Is Determined by Intrinsic Striatal Cells, Not Nigrostriatal Axons." *Neuroscience* 27(3):851–63.

Behan, M. and L. B. Haberly. 1999. "Intrinsic and Efferent Connections of the Endopiriform Nucleus in Rat." *Journal of Comparative Neurology* 408(4):532–48.

Benn, C. L., C. Landles, H. Li, A. D. Strand, B. Woodman, K. Sathasivam, S. H. Li, S. Ghazi-Noori, E. Hockly, S. M. N. N. Faruque, J. H. J. Cha, P. T. Sharpe, J. M. Olson, X. J. Li and G. P. Bates. 2005. "Contribution of Nuclear and Extranuclear PolyQ to Neurological Phenotypes in Mouse Models of Huntington's Disease." *Human Molecular Genetics* 14(20):3065–78.

Berns, K. I. 1990. "Parvovirus Replication." *Microbiological Reviews* 54(3):316–29.

Berns, K. I. and C. Giraud. 1996. "Biology of Adeno-Associated Virus." *Adeno-Associated Virus (AAV) Vectors in Gene Therapy. Current Topics in Microbiology and Immunology*, vol 2181–23.

Bofill-De Ros, X., and S. Gu. 2016. "Guidelines for the Optimal Design of MiRNA-Based ShRNAs." *Methods* 103:157–66.

Bolam, J. P., B. H. Wainer, and A. D. Smith. 1984. "Characterization of Cholinergic Neurons in the Rat Neostriatum. A Combination of Choline Acetyltransferase Immunocytochemistry, Golgi-Impregnation and Electron Microscopy." *Neuroscience* 12(3):711–18.

Borchert, G. M., W. Lanier, and B. L. Davidson. 2006. "RNA Polymerase III Transcribes Human MicroRNAs." *Nature Structural and Molecular Biology* 13(12):1097–1101.

Borel, F., M. A. Kay, and C. Mueller. 2014. "Recombinant AAV as a Platform for Translating the Therapeutic Potential of RNA Interference." *Molecular Therapy* 22(4):692–701.

Boudreau, R. L., I. Martins, and B. L. Davidson. 2009. "Artificial MicroRNAs as SiRNA Shuttles: Improved Safety as Compared to ShRNAs in Vitro and In Vivo." *Molecular Therapy* 17(1):169–75.

Boudreau, R. L., R. M. Spengler, and B. L. Davidson. 2011. "Rational Design of Therapeutic SiRNAs: Minimizing off-Targeting Potential to Improve the Safety of RNAi Therapy for Huntington's Disease." *Molecular Therapy* 19(12):2169–77.

Brody, S. A., N. Nakanishi, S. Tu, S. A. Lipton and M. A. Geyer. 2005. "A Developmental Influence of the N-Methyl-D-Aspartate Receptor NR3A Subunit on Prepulse Inhibition of Startle." *Biological Psychiatry* 57(10):1147–52.

Burzomato, V., G. Frugier, I. Pérez-Otaño, J. T. Kittler and D. Attwell. 2010. "The Receptor Subunits Generating NMDA Receptor Mediated Currents in Oligodendrocytes." *Journal of Physiology* 588(18):3403–14.

Butland, S. L., R. S. Devon, Y. Huang, C. L. Mead, A. M. Meynert, S. J. Neal, S. S. Lee, A. Wilkinson, G. S. Yang, M. M. S. Yuen, M. R. Hayden, R. A. Holt, Blair R. Leavitt, and B. F. Franci. Ouellete. 2007. "CAG-Encoded Polyglutamine Length Polymorphism in the Human Genome." *BMC Genomics* 8:1–18.

Canals, J. M., J. R. Pineda, J. F. Torres-Peraza, M. Bosch, R. Martín-Ibañez, M. T. Muñoz, G. Mengod, P. Ernfors, and J. Alberch. 2004. "Brain-Derived Neurotrophic Factor Regulates the Onset and Severity of Motor Dysfunction Associated with Enkephalinergic Neuronal Degeneration in Huntington's Disease." *Journal of Neuroscience* 24(35):7727–39.

Cannella, M., C. Gellera, V. Maglione, P. Giallonardo, G. Cislighi, M. Muglia, A. Quattrone, F. Pierelli, S. Di Donato and F. Squitieri. 2004. "The Gender Effect in Juvenile Huntington Disease Patients of Italian Origin." *American Journal of Medical Genetics* 125B(1):92–98.

Carter, R. J., L. A. Lione, T. Humby, L. Mangiarini, A. Mahal, G. P. Bates, S. B. Dunnett, and A. J. Morton. 1999. "Characterization of Progressive Motor Deficits in Mice Transgenic for the Human Huntington's Disease Mutation." *Journal of Neuroscience* 19(8):3248–57.

- Cavara, N. A. and M. Hollmann. 2008. "Shuffling the Deck Anew: How NR3 Tweaks NMDA Receptor Function." *Molecular Neurobiology* 38(1):16–26.
- Caviness, V. S. and D. O. Frost. 1980. "Tangential Organization of Thalamic Projections to the Neocortex in the Mouse." *Journal of Comparative Neurology* 194(2):335–67.
- Cearley, C. N., L. H. Vandenberghe, M. K. Parente, E. R. Carnish, J. M. Wilson and John H. Wolfe. 2008. "Expanded Repertoire of AAV Vector Serotypes Mediate Unique Patterns of Transduction in Mouse Brain." *Molecular Therapy* 16(10):1710–18.
- Cepeda, C., R. S. Hurst, C. R. Calvert, E. Hernández-Echeagaray, O. K. Nguyen, E. Jocoy, L. J. Christian, M. A. Ariano, and M. S. Levine. 2003. "Transient and Progressive Electrophysiological Alterations in the Corticostriatal Pathway in a Mouse Model of Huntington's Disease." *Journal of Neuroscience* 23(3):961–69.
- Chan, S. F. and N. J. Sucher. 2001. "An NMDA Receptor Signaling Complex with Protein Phosphatase 2A." *Journal of Neuroscience* 21(20):7985–92.
- Chatterton, J. E., M. Awobuluyi, L. S. Premkumar, H. Takahashi, M. Talantova, Y. Shin, J. Cul, S. Tu, K. A. Sevarino, N. Nakanishi, G. Tong, S. A. Lipton and D. Zhang. 2002. "Excitatory Glycine Receptors Containing the NR3 Family of NMDA Receptor Subunits." *Nature* 415(6873):793–98.
- Chejanovsky, N. and B. J. Carter. 1989. "Mutagenesis of an AUG Codon in the Adeno-Associated Virus Rep Gene: Effects on Viral DNA Replication." *Virology* 173(1):120–28.
- Chen, B. S. and K. W. Roche. 2007. "Regulation of NMDA Receptors by Phosphorylation." *Neuropharmacology* 53(3):362–68.
- Chen, J., Y. Ma, R. Fan, Z. Yang and M. D. Li. 2018. "Implication of Genes for the N-Methyl-d-Aspartate (NMDA) Receptor in Substance Addictions." *Molecular Neurobiology* 55(9):7567–78.
- Chen, J., Q. Liu, R. Fan, H. Han, Z. Yang, W. Cui, G. Song, and M. D. Li. 2020. "Demonstration of Critical Role of GRIN3A in Nicotine Dependence through Both Genetic Association and Molecular Functional Studies." *Addiction Biology* 25(1):1–11.
- Chen, Z. Y., S. R. Yant, C. Y. He, L. Meuse, S. Shen and M. A. Kay. 2001. "Linear DNAs Concatemere *in Vivo* and Result in Sustained Transgene Expression in Mouse Liver." *Molecular Therapy* 3(3):403–10.

Chowdhury, D., S. Marco, I. M. Brooks, A. Zanduetta, Y. Rao, V. Haucke, J. F. Wesseling, S. J. Tavalin and I. Pérez-Otaño. 2013. "Tyrosine Phosphorylation Regulates the Endocytosis and Surface Expression of GluN3A-Containing NMDA Receptors." *Journal of Neuroscience* 33(9):4151–64.

Chung, K. H., C. C. Hart, S. Al-Bassam, A. Avery, J. Taylor, P. D. Patel, A. B. Vojtek and D. L. Turner. 2006. "Polycistronic RNA Polymerase II Expression Vectors for RNA Interference Based on BIC/MiR-155." *Nucleic Acids Research* 34(7).

Ciabarra, A. M., J. M. Sullivan, L. G. Gahn, G. Pecht, S. Heinemann and K. A. Sevarino. 1995. "Cloning and Characterization of  $\alpha$ -1: A Developmentally Regulated Member of a Novel Class of the Ionotropic Glutamate Receptor Family." *Journal of Neuroscience* 15(10):6498–6508.

Ciabarra, A. M. and K. A. Sevarino. 1997. "An Anti- $\alpha$ -1 Antibody Recognizes a Heavily Glycosylated Protein in Rat Brain." *Molecular Brain Research* 46(1–2):85–90.

Colin, E., D. Zala, G. Liot, H. Rangone, M. Borrell-Pagès, X. J. Li, F. Saudou and S. Humbert. 2008. "Huntingtin Phosphorylation Acts as a Molecular Switch for Anterograde/Retrograde Transport in Neurons." *EMBO Journal* 27(15):2124–34.

Colonnese, M. T. and M. Constantine-Paton. 2006. "Developmental Period for N-Methyl-D-Aspartate (NMDA) Receptor-Dependent Synapse Elimination Correlated with Visuotopic Map Refinement." *Journal of Comparative Neurology* 494(5):738–51.

Coyle, J. T. and R. Schwarcz. 1976. "Lesion of striatal neurones with kainic acid provides a model for Huntington's chorea." *Nature* Vol. 263.

Culver, B. P., J. N. Savas, S. K. Park, J. H. Choi, S. Zheng, S. O. Zeitlin, J. R. Yates and N. Tanese. 2012. "Proteomic Analysis of Wild-Type and Mutant Huntingtin-Associated Proteins in Mouse Brains Identifies Unique Interactions and Involvement in Protein Synthesis." *Journal of Biological Chemistry* 287(26):21599–614.

Das, S., Y. F. Sasaki, T. Rothe, L. S. Premkumar, M. Takasu, J. E. Crandalli, P. Dikkes, D. A. Conner, P. V. Rayudu, W. Cheung, C. Vincent, S. A. Lipton and N. Nakanish. 1998. "Increased NMDA Current and Spine Density in Mice Lacking the NMDA Receptor Subunit NR3A." *Nature* 393(6683):377–81.

Dassie, J. P., X. Liu, G. S. Thomas, R. M. Whitaker, K. W. Thiel, K. R. Stockdale, D. K. Meyerholz, A. P. Mccaffrey, J. O. Mcnamara li, and P. H.



- Giangrande. 2009. "Articles Systemic Administration of Optimized Aptamer-SiRNA Chimeras Promotes Regression of PSMA-Expressing Tumors." *Nature biotechnology*. 27(9).
- Davidson, B. L., and P. B. McCray. 2011. "Current Prospects for RNA Interference-Based Therapies." *Nature Reviews Genetics* 12(5):329–40.
- De Marco García, N. V., R. Priya, S. N. Tuncdemir, G. Fishell, and T. Karayannis. 2015. "Sensory Inputs Control the Integration of Neurogliaform Interneurons into Cortical Circuits." *Nature Neuroscience* 18(3):393–403.
- Del Toro, D., J. Alberch, F. Lázaro-Diéguez, R. Martín-Ibáñez, X. Xifró, G. Egea and J. M. Canals. 2009. "Mutant Huntingtin Impairs Post-Golgi Trafficking to Lysosomes by Delocalizing Optineurin/Rab8 Complex from the Golgi Apparatus." *Molecular Biology of the Cell* 20:2673–83.
- DeLong, M. R. 1990. "Primate Models of Movement Disorders of Basal Ganglia Origin." *Trends in Neurosciences* 13(7):281–85.
- Deng, Y. P., R. L. Albin, J. B. Penney, A. B. Young, K. D. Anderson and A. Reiner. 2004. "Differential Loss of Striatal Projection Systems in Huntington's Disease: A Quantitative Immunohistochemical Study." *Journal of Chemical Neuroanatomy* 27(3):143–64.
- Di Maio, L., F. Squitieri, G. Napolitano, G. Campanella, J. A. Trofatter and P. M. Conneally. 1993. "Onset Symptoms in 510 Patients with Huntington's Disease." *Journal of Medical Genetics* 30(4):289–92.
- Dingledine, R., K. Borges, D. Bowie, and S. F. Traynelis. 1999. "The Glutamate Receptor Ion Channels." *Pharmacological Reviews* 51(1):7–61.
- Diprospero, N. A., E. Y. Chen, V. Charles, M. Plomann, J. H. Kordower, and D. A. Tagle. 2004. "Early Changes in Huntington's Disease Patient Brains Involve Alterations in Cytoskeletal and Synaptic Elements." *Journal of Neurocytology* 33(5):517–33.
- Djousse, L., B. Knowlton, L. A. Cupples, K. Marder, I. Shoulson and R. H. Myers. 2002. "Weight Loss in Early Stage of Huntington's Disease." *Neurology* 59(9):1325–30.
- Dong, J., P. Fan and R. A. Frizzell. 1996. "Quantitative Analysis of the Packaging Capacity Recombinant Adeno-Associated Virus of." 2112:2101–12.

Donoghue, J. P. and M. Herkenham. 1986. "Neostriatal Projections from Individual Cortical Fields Conform to Histochemically Distinct Striatal Compartments in the Rat." *Brain Research* 365(2):397–403.

Dragatsis, I., M. S. Levine and S. Zeitlin. 2000. "Inactivation of Hdh in the Brain and Testis Results in Progressive Neurodegeneration and Sterility in Mice." *Nature Genetics* 26(3):300–306.

Drouet, V., V. Perrin, R. Hassig, N. Dufour, G. Auregan, S. Alves, G. Bonvento, E. Brouillet, R. Luthi-Carter, P. Hantraye, and N. Déglon. 2009. "Sustained Effects of Nonallele-Specific Huntingtin Silencing." *Annals of Neurology* 65(3):276–85.

Dubé, L., A. D. Smith and J. P. Bolam. 1988. "Identification of Synaptic Terminals of Thalamic or Cortical Origin in Contact with Distinct Medium-size Spiny Neurons in the Rat Neostriatum." *Journal of Comparative Neurology* 267(4):455–71.

Dubinsky, R. M. 2005. "No Going Home for Hospitalized Huntington's Disease Patients." *Movement Disorders* 20(10):1316–22.

Duff, K., J. S. Paulsen, Leigh J. Beglinger, D. R. Langbehn, C. Wang, J. C. Stout, C. A. Ross, E. Aylward, N. E. Carlozzi, S. Queller, and P. 2010. "Before the Diagnosis of Huntington's Disease and Their Relationship to Markers of Disease Progression : Evidence of Early Lack of Awareness." *J Neuropsychiatry Clin Neurosci.* 196–207.

Dumas, T. C. 2005. "Developmental Regulation of Cognitive Abilities: Modified Composition of a Molecular Switch Turns on Associative Learning." *Progress in Neurobiology* 76(3):189–211.

Ecker, J. R. and R. W. Davis. 1986. "Inhibition of Gene Expression in Plant Cells by Expression of Antisense RNA." *Proceedings of the National Academy of Sciences of the United States of America* 83(15):5372–76.

Elias, S., M. S. Thion, H. Yu, C. M. Sousa, C. Lasgi, X. Morin, and S. Humbert. 2014. "Huntingtin Regulates Mammary Stem Cell Division and Differentiation." *Stem Cell Reports* 2(4):491–506.

Engelender, S, A. H. Sharp, V. Colomer, M. K. Tokito, A. Lanahan, P. Worley, E. L. F. Holzbaur and C. A. Ross. 1997. "Huntingtin-Associated Protein 1 (HAP1) Interacts with the P150 Glued Subunit of Dynactin". *Oxford University Press* 6(13):2205–12.

Engqvist-Goldstein, Å. E. Y., R. A. Warren, M. M. Kessels, J. H. Keen, J. Heuser and D. G. Drubin. 2001. "The Actin-Binding Protein Hip1R Associates with Clathrin during Early Stages of Endocytosis and Promotes Clathrin Assembly in Vitro." *Journal of Cell Biology* 154(6):1209–23.

Eriksson, M., A. Nilsson, S. Froelich-Fabre, E. Åkesson, J. Dunker, Å. Seiger, R. Folkesson, E. Benedikz and E. Sundström. 2002. "Cloning and Expression of the Human N-Methyl-D-Aspartate Receptor Subunit NR3A." *Neuroscience Letters* 321(3):177–81.

Eriksson, M., A. Nilsson, H. Samuelsson, E. Samuelsson, L. Mo, E. Åkesson, E. Benedikz and E. Sundström. 2007. "On the Role of NR3A in Human NMDA Receptors." *Physiology and Behavior* 92(1–2):54–59.

Eriksson, M., H. Samuelsson, S. Björklund, E. Tortosa, J. Avila, E. B. Samuelsson, E. Benedikz, and E. Sundström. 2010. "MAP1B Binds to the NMDA Receptor Subunit NR3A and Affects NR3A Protein Concentrations." *Neuroscience Letters* 475(1):33–37.

Evers, M. M., J. Miniarikova, S. Juhas, A. Vallès, B. Bohuslavova, J. Juhasova, H. K. Skalnikova, P. Vodicka, I. Valekova, C. Brouwers, B. Blits, J. Lubelski, H. Kovarova, Z. Ellederova, S. J. Van Deventer, H. Petry, and J. Motlik. 2018. "AAV5-MiHTT Gene Therapy Demonstrates Broad Distribution and Strong Human Mutant Huntingtin Lowering in a Huntington's Disease Minipig Model." *Molecular Therapy* 26(9):2163–77.

Faber, P. W., J. R. Alter, M. E. Macdonald and A. C. Hart. 1999. "Polyglutamine-Mediated Dysfunction and Apoptotic Death of a Caenorhabditis Elegans Sensory Neuron." *Proceedings of the National Academy of Sciences of the United States of America* 96(1):179–84.

Feldman, D. E., R. A. Nicoll, R. C. Malenka and J. T. R. Isaac. 1998. "Long-Term Depression at Thalamocortical Synapses in Developing Rat Somatosensory Cortex." *Neuron* 21(2):347–57.

Ferrante, R. J., N. W. Kowall and E. P. Richardson. 1991. "Proliferative and Degenerative Changes in Striatal Spiny Neurons in Huntington's Disease: A Combined Study Using the Section-Golgi Method and Calbindin D28k Immunocytochemistry." *Journal of Neuroscience* 11(12):3877–87.

Fienberg, A. A. and P. Greengard. 2000. "The DARPP-32 Knockout Mouse." *Brain Research Reviews* 31(2–3):313–19.

Fire, A., S. Xu, M. K. Montgomery, S. A. Kostas, S. E. Driver and C. C. Mello. 1998. "Potent and specific genetic interference by double-stranded RNA in *Caenorhabditis elegans*". *Nature* 49(1234):431–34.

Fiuza, M., I. González-González and I. Pérez-Otaño. 2013. "GluN3A Expression Restricts Spine Maturation via Inhibition of GIT1/Rac1 Signaling." *Proceedings of the National Academy of Sciences of the United States of America* 110(51):20807–12.

Folstein, S.E., M. H. Abbott, G. A. Chase, B. A. Jensen and M. F. Folstein. 1983. "The Association of Affective Disorder with Huntington's Disease in a Case Series and in Families." *Psychological Medicine* 13(3):537–42.

Fulcher, B. D., J. D. Murray, V. Zerbi, and X. J. Wang. 2019. "Multimodal Gradients across Mouse Cortex." *Proceedings of the National Academy of Sciences of the United States of America* 116(10):4689–95.

Furukawa, H. and E. Gouaux. 2003. "Mechanisms of Activation, Inhibition and Specificity: Crystal Structures of the NMDA Receptor NR1 Ligand-Binding Core." *EMBO Journal* 22(12):2873–85.

Furukawa, H., S. K. Singh, R. Mancusso and E. Gouaux. 2005. "Subunit Arrangement and Function in NMDA Receptors." *Nature* 438(7065):185–92.

Gagnon, D., S. Petryszyn, M. G. Sanchez, C. Bories, J. M. Beaulieu, Y. De Koninck, A. Parent and M. Parent. 2017. "Striatal Neurons Expressing D1 and D2 Receptors Are Morphologically Distinct and Differently Affected by Dopamine Denervation in Mice." *Scientific Reports* 7(December 2016):9–17.

Gallinat, J., T. Götz, P. Kalus, M. Bajbouj, T. Sander, and G. Winterer. 2007. "Genetic Variations of the NR3A Subunit of the NMDA Receptor Modulate Prefrontal Cerebral Activity in Humans." *Journal of Cognitive Neuroscience* 19(1):59–68.

Gambrill, A. C. and A. Barria. 2011. "NMDA Receptor Subunit Composition Controls Synaptogenesis and Synapse Stabilization." *Proceedings of the National Academy of Sciences of the United States of America* 108(14):5855–60.

Garcia-Cabezas M. A., M. K. P. Joyce, Y. J. John, B. Zikopoulos, H. Barbas. 2017. "Mirror trends of plasticity and stability indicators in primate prefrontal cortex." *Eur J Neurosci*. 46:2392-2405.

Gerfen, C. R. 1984. "The neostriata I mosaic: compartmentalization of corticostriatal input and striatonigral output systems" *Nature* Vol. 311

Gerfen, C. R. 1988. "Synaptic Organization of the Striatum." *Journal of Electron Microscopy Technique* 10(3):265–81.

Gerfen, C. R., T. M. Engber, L. C. Mahan, Z. Susel, T. N. Chase, and F. J. Jr. Monsma. 1990. "D1 and D2 Dopamine Receptor-Regulated Gene Expression of Striatonigral and Striatopallidal Neurons." *Science* 250(1986):1429–32.

Gladding, C. M., and L. A. Raymond. 2011. "Mechanisms Underlying NMDA Receptor Synaptic/Extrasynaptic Distribution and Function." *Molecular and Cellular Neuroscience* 48(4):308–20.

Glantz, L. A. and David A. Lewis. 2000. "Decreased Dendritic Spine Density on Prefrontal Cortical Pyramidal Neurons in Schizophrenia." *Archives of General Psychiatry* 57(1):65–73.

Glass, M., M. Dragunow and R. L. M. Faull. 2000. "The Pattern of Neurodegeneration in Huntington's Disease: A Comparative Study of Cannabinoid, Dopamine, Adenosine and GABA(A) Receptor Alterations in the Human Basal Ganglia in Huntington's Disease." *Neuroscience* 97(3):505–19.

Goehler, H., M. Lalowski, U. Stelzl, S. Waelter, M. Stroedicke, U. Worm, A. Droege, K. S. Lindenberg, M. Knoblich, C. Haenig, M. Herbst, J. Suopanki, E. Scherzinger, C. Abraham, B. Bauer, R. Hasenbank, A. Fritzsche, A. H. Ludewig, K. Buessow, S. H. Coleman, C. A. Gutekunst, B. G. Landwehrmeyer, H. Lehrach, and E. E. Wanker. 2004. "A Protein Interaction Network Links GIT1, an Enhancer of Huntingtin Aggregation, to Huntington's Disease." *Molecular Cell* 15(6):853–65.

Gogolla, N. 2017. "The Insular Cortex." *Current Biology* 27(12):R580–86.

Goldberg Y. P., D.W. Nicholson, D.M. Rasper, M.A. Kalchman, H.B. Koide, R.K. Graham, M. Bromm, P. Kazemi-Esfarjani, N.A. Thornberry, J.P. Vaillancourt, and M.R. Hayden. 1996. "Cleavage of Huntingtin by Apopain, A Proapoptotic Cysteine Protease, Is Modulated by The Polyglutamine Tract." *Nature Medicine* 2(4):534–39.

Graham, R. K., M. A. Pouladi, P. Joshi, G. Lu, Y. Deng, N. P. Wu, B. E. Figueroa, M. Metzler, V. M. André, E. J. Slow, L. Raymond, R. Friedlander, M. S. Levine, B. R. Leavitt and M. R. Hayden. 2009. "Differential Susceptibility to Excitotoxic Stress in YAC128 Mouse Models of Huntington Disease between Initiation and Progression of Disease." *Journal of Neuroscience* 29(7):2193–2204.

Grand T, Abi Gerges S, David M, Diana MA, and Paoletti P. 2018. "Unmasking GluN1/GluN3A excitatory glycine NMDA receptors". *Nature Communication*. 9:4769.

Graveland, G. A. and M. Difiglia. 1985. "The Frequency and Distribution of Medium-Sized Neurons with Indented Nuclei in the Primate and Rodent Neostriatum." *Brain Research* 327(1–2):307–11.

Graveland, G. A., R. S. Williams and M. Difiglia. 1985. "Evidence for Degenerative and Regenerative Changes in Neostriatal Spiny Neurons in Huntington's Disease." *Science* 227(4688):770–73.

Gray, M., D. I. Shirasaki, C. Cepeda, V. M. André, B. Wilburn, X. H. Lu, J. Tao, I. Yamazaki, S. H. Li, Y. E. Sun, X. J. Li, M. S. Levine and X. W. Yang. 2008. "Full-Length Human Mutant Huntingtin with a Stable Polyglutamine Repeat Can Elicit Progressive and Selective Neuropathogenesis in BACHD Mice." *Journal of Neuroscience* 28(24):6182–95.

Gregory, R. I., K. P. Yan, G. Amuthan, T. Chendrimada, B. Doratotaj, N. Cooch and Ramin Shiekhattar. 2004. "The Microprocessor Complex Mediates the Genesis of MicroRNAs." *Nature* 432(7014):235–40.

Guillery, R. W. 2005. "Is Postnatal Neocortical Maturation Hierarchical?" *Trends in Neurosciences* 28(10):512–17.

Guo, H., N. T. Ingolia, J. S. Weissman and D. P. Bartel. 2010. "Mammalian MicroRNAs Predominantly Act to Decrease Target mRNA Levels." *Nature* 466(7308):835–40.

Gutekunst, C. A., A. I. Levey, C. J. Heilman, W. L. Whaley, H. Yi, N. R. Nash, H. D. Rees, J. J. Madden and S. M. Hersch. 1995. "Identification and Localization of Huntingtin in Brain and Human Lymphoblastoid Cell Lines with Anti-Fusion Protein Antibodies." *Proceedings of the National Academy of Sciences of the United States of America* 92(19):8710–14.

Haber, S. N., J. L. Fudge and N. R. McFarland. 2000. "Striatonigrostriatal Pathways in Primates Form an Ascending Spiral from the Shell to the Dorsolateral Striatum." *Journal of Neuroscience* 20(6):2369–82.

Han, J., Y. Lee, K. Yeom, Y. Kim, H. Jin and V. N. Kim. 2004. "The Drosha–DGCR8 complex in primary microRNA processing." *Genes & Development* 18:3016–302.

Hansson, O., Å. Petersén, M. Leist, P. Nicotera, R. F. Castilho, and P. Brundin. 1999. "Transgenic Mice Expressing a Huntington's Disease Mutation Are

Resistant to Quinolinic Acid-Induced Striatal Excitotoxicity." *Proceedings of the National Academy of Sciences of the United States of America* 96(15):8727–32.

Hansson, O., E. Guatteo, N. B. Mercuri, G. Bernardi, X. J. Li, R. F. Castilho, and P. Brundin. 2001. "Resistance to NMDA Toxicity Correlates with Appearance of Nuclear Inclusions, Behavioural Deficits and Changes in Calcium Homeostasis in Mice Transgenic for Exon 1 of the Huntington Gene." *European Journal of Neuroscience* 14(9):1492–1504.

Harjes, P. and E. E. Wanker. 2003. "The Hunt for Huntingtin Function: Interaction Partners Tell Many Different Stories." *Trends in Biochemical Sciences* 28(8):425–33.

Harrington, D. L., D. Liu, M. M. Smith, J. A. Mills, J. D. Long, E. H. Aylward, and J. S. Paulsen. 2014. "Neuroanatomical Correlates of Cognitive Functioning in Prodromal Huntington Disease." *Brain and Behavior* 4(1):29–40.

Harris, A. Z., and D. L. Pettit. 2007. "Extrasynaptic and Synaptic NMDA Receptors Form Stable and Uniform Pools in Rat Hippocampal Slices." *Journal of Physiology* 584(2):509–19.

Harris, J. A., K. E. Hirokawa, S. A. Sorensen, H. Gu, M. Mills, L. L. Ng, P. Bohn, M. Mortrud, B. Ouellette, J. Kidney, K. A. Smith, C. Dang, S. Sunkin, A. Bernard, S. W. Oh, L. Madisen and H. Zeng. 2014. "Anatomical Characterization of Cre Driver Mice for Neural Circuit Mapping and Manipulation." *Frontiers in Neural Circuits* 8:1–16.

Harris, J. A., S. Mihalas, K. E. Hirokawa, J. D. Whitesell, H. Choi, A. Bernard, P. Bohn, S. Caldejon, L. Casal, A. Cho, A. Feiner, D. Feng, N. Gaudreault, C. R. Gerfen, N. Graddis, P. A. Groblewski, A. M. Henry, A. Ho, R. Howard, J. E. Knox, L. Kuan, X. Kuang, J. Lecoq, P. Lesnar, Y. Li, J. Luviano, S. McConoughey, M. T. Mortrud, M. Naeemi, L. Ng, S. W. Oh, B. Ouellette, E. Shen, S. A. Sorensen, W. Wakeman, Q. Wang, Y. Wang, A. Williford, J. W. Phillips, A. R. Jones, C. Koch, and H. Zeng. 2019. "Hierarchical Organization of Cortical and Thalamic Connectivity." *Nature* 575(7781):195–202.

Harry, H. W. C. N. Still and R. K. Abramson. 1981. "Huntington's Disease in Black Kindreds in South Carolina." *Neurol*, Vol 38.

Heng, M. Y., S. J. Tallaksen-Greene, P. J. Detloff and R. L. Albin. 2007. "Longitudinal Evaluation of the Hdh<sup>(CAG)<sup>150</sup></sup> Knock-in Murine Model of Huntington's Disease." *Journal of Neuroscience* 27(34):8989–98.

Henson, M. A., A. C. Roberts, K. Salimi, S. Vadlamudi, R. M. Hamer, J. H. Gilmore, L. F. Jarskog and B. D. Philpot. 2008. "Developmental Regulation of

the NMDA Receptor Subunits, NR3A and NR1, in Human Prefrontal Cortex." *Cerebral Cortex* 18(11):2560–73.

Henson, M. A., A. C. Roberts, I. Pérez-Otaño and B. D. Philpot. 2010. "Influence of the NR3A Subunit on NMDA Receptor Functions." *Progress in Neurobiology* 91(1):23–37.

Henson, M. A., R. S. Larsen, S. N. Lawson, I. Pérez-Otaño, N. Nakanishi, S. A. Lipton and B. D. Philpot. 2012. "Genetic Deletion of NR3A Accelerates Glutamatergic Synapse Maturation." *PLoS ONE* 7(8).

Hering, H., M. Sheng, and H. H. Medical. 2001. "Dendritic Spines: Structure, Dynamics and Regulation." *Nature reviews*. 880–88.

Hermonat, P. L., M. A. Labow, R. Wright, K. I. Berns and N. Muzyczka. 1984. "Genetics of Adeno-Associated Virus: Isolation and Preliminary Characterization of Adeno-Associated Virus Type 2 Mutants." *Journal of Virology* 51(2):329–39.

Hermonat, P. L., R. T. Plott, A. D. Santin, G. P. Parham and J. T. Flick. 1997. "Adeno-Associated Virus Rep78 Inhibits Oncogenic Transformation of Primary Human Keratinocytes by a Human Papillomavirus Type 16-Ras Chimeric." *Gynecologic Oncology* 66(3):487–94.

Hickey, M. A., A. Kosmalska, J. Enayati, R. Cohen, S. Zeitlin, M. S. Levine and M. F. Chesselet. 2008. "Extensive Early Motor and Non-Motor Behavioral Deficits Are Followed by Striatal Neuronal Loss in Knock-in Huntington's Disease Mice." *Neuroscience* 157(1):280–95.

Hodgson, J. G., N. Agopyan, C. A. Gutekunst, B. R. Leavitt, F. Lepiane, R. Singaraja, D. J. Smith, N. Bissada, K. McCutcheon, J. Nasir, L. Jamot, L. Xiao-Jiang, M. E. Stevens, E. Rosemond, J. C. Roder, A. G. Phillips, E. M. Rubin, S. M. Hersch and M. R. Hayden. 1999. "A YAC Mouse Model for Huntington's Disease with Full-Length Mutant Huntingtin, Cytoplasmic Toxicity, and Selective Striatal Neurodegeneration." *Neuron* 23(1):181–92.

Hoggan, M.D. 1970. "Adenovirus associated viruses." *Prog. Med. Virol.* 12, 211–239.

Hollmann, M. and S. Heinemann. 1994. "Cloned Glutamate Receptors." *Annual Review of Neuroscience* 17:31–108.

Holtmaat, A. J. G. D., J. T. Trachtenberg, L. Wilbrecht, G. M. Shepherd, X. Zhang, G. W. Knott and Karel Svoboda. 2005. "Transient and Persistent Dendritic Spines in the Neocortex *in Vivo*." *Neuron* 45(2):279–91.



Hoogeveen, A. T., R. Willemsen, N. Meyer, K. E. de Rooij, R. A. C. Roos, G. J. B. va. Ommen and H. Galjaard. 1993. "Characterization and Localization of the Huntington Disease Gene Product." *Human Molecular Genetics* 2(12):2069–73.

Huang, X., Chen, YY., Shen, Y., Cao, X., Li, A., Liu Q, Li Z, Zhang LB, Dai W, Tan T, Arias-Carrion O, Xue Y-X, Su H and Yuan T-F. 2017. "Methamphetamine abuse impairs motor cortical plasticity and function". *Molecular psychiatry*. 22:1274-1281.

Hudry, E., and L. H. Vandenberghe. 2019. "Therapeutic AAV Gene Transfer to the Nervous System: A Clinical Reality." *Neuron* 101(5):839–62.

Hughes, A. C., M. Mort, L. Elliston, R. M. Thomas, S. P. Brooks, S. B. Dunnett and Lesley Jones. 2014. "Identification of Novel Alternative Splicing Events in the Huntingtin Gene and Assessment of the Functional Consequences Using Structural Protein Homology Modelling." *Journal of Molecular Biology* 426(7):1428–38.

Hutson, T. H., E. Foster, J. M. Dawes, R. Hindges, R. J. Yáñez-Muñoz and L. D. F. Moon. 2012. "Lentiviral Vectors Encoding Short Hairpin RNAs Efficiently Transduce and Knockdown LINGO-1 but Induce an Interferon Response and Cytotoxicity in Central Nervous System Neurons." *Journal of Gene Medicine* 14(5):299–315.

Ikezu, T. 2015. "The Use of Viral Vectors to Enhance Cognition". Elsevier Inc.

Ilinsky, I. A. and K. Kultas-Ilinsky. 1987. "Sagittal Cytoarchitectonic Maps of the Macaca Mulatta Thalamus with a Revised Nomenclature of the Motor-related Nuclei Validated by Observations on Their Connectivity." *Journal of Comparative Neurology* 262(3):331–64.

Ishihama, K. and J. E. Turman. 2006. "NR3 Protein Expression in Trigeminal Neurons during Postnatal Development." *Brain Research* 1095(1):12–16.

Jahanshahi, A., R. Vlamings, A. H. Kaya, L. W. Lim, M. L. F. Janssen, S. Tan, V. Visser-Vandewalle, H. W. M. Steinbusch and Y. Temel. 2010. "Hyperdopaminergic Status in Experimental Huntington Disease." *Journal of Neuropathology and Experimental Neurology* 69(9):910–17.

Jantzie, L. L., D. M. Talos, M. C. Jackson, H. K. Park, D. A. Graham, M. Lechpammer, R. D. Folkerth, J. J. Volpe and F. E. Jensen. 2015. "Developmental Expression of N-Methyl-d-Aspartate (NMDA) Receptor Subunits in Human White and Gray Matter: Potential Mechanism of Increased Vulnerability in the Immature Brain." *Cerebral Cortex* 25(2):482–95.

Jimenez-Sanchez, M., W. Lam, M. Hannus, B. Sönnichsen, S. Imarisio, A. Fleming, A. Tarditi, F. Menzies, T. Ed Dami, C. Xu, E. Gonzalez-Couto, G. Lazzeroni, F. Heitz, D. Diamanti, L. Massai, V. P. Satagopam, G. Marconi, C. Caramelli, A. Nencini, M. Andreini, G. L. Sardone, N. P. Caradonna, V. Porcari, C. Scali, R. Schneider, G. Pollio, C. J. O'Kane, A. Caricasole, and D. C. Rubinsztein. 2015. "SiRNA Screen Identifies QPCT as a Druggable Target for Huntington's Disease." *Nature Chemical Biology* 11(5):347–54.

Jin, Z., A. K. Bhandage, I. Bazov, O. Kononenko, G. Bakalkin, E. R. Korpi and B. Birnir. 2014. "Selective Increases of AMPA, NMDA, and Kainate Receptor Subunit MRNAs in the Hippocampus and Orbitofrontal Cortex but Not in Prefrontal Cortex of Human Alcoholics." *Frontiers in Cellular Neuroscience* 8(JAN):1–10.

Johnson, J. S. and R. J. Samulski. 2009. "Enhancement of Adeno-Associated Virus Infection by Mobilizing Capsids into and Out of the Nucleolus." *Journal of Virology* 83(6):2632–44.

Johnson, J. W. and P. Ascher. 1987. "Glycine Potentiates the NMDA Response in Cultured Mouse Brain Neurons." *Nature* 325(6104):529–31.

Joubert, J. and M. C. Botha. 1987. "Huntington Disease in South African Blacks. A Report of 8 Cases." *South African Medical Journal* 73(8):489–94.

Kagel, M. C. and N. A. Leopold. 1992. "Dysphagia in Huntington's Disease: A 16-Year Retrospective." *Dysphagia* 7(2):106–14.

Kaltenbach, L. S., E. Romero, R. R. Becklin, R. Chettier, R. Bell, A. Phansalkar, A. Strand, C. Torcassi, J. Savage, A. Hurlburt, G. H. Cha, L. Ukani, C. L. Chepanoske, Y. Zhen, S. Sahasrabudhe, J. Olson, C. Kurschner, L. M. Ellerby, J. M. Peltier, J. Botas and Robert E. Hughes. 2007. "Huntingtin Interacting Proteins Are Genetic Modifiers of Neurodegeneration." *PLoS Genetics* 3(5):689–708.

Katz L. C., C. J. Shatz. 1996. "Synaptic activity and the construction of cortical circuits." *Science*. 274:1133-1138.

Kawaguchi, Y., C. J. Wilson and P. C. Emson. 1990. "Projection Subtypes of Rat Neostriatal Matrix Cells Revealed by Intracellular Injection of Biocytin." *Journal of Neuroscience* 10(10):3421–38.

Kay, C., N. H. Skotte, A. L. Southwell and M. R. Hayden. 2014. "Personalized Gene Silencing Therapeutics for Huntington Disease." *Clinical Genetics* 86(1):29–36.

- Kehoe, L. A., Y. Bernardinelli and D. Muller. 2013. "GluN3A: An NMDA Receptor Subunit with Exquisite Properties and Functions." *Neural Plasticity* 2013.
- Kehoe, L. A., C. Bellone, M. De Roo, A. Zanduetta, P. N. Dey, I. Pérez-Otaño and D. Muller. 2014. "GluN3A Promotes Dendritic Spine Pruning and Destabilization during Postnatal Development." *Journal of Neuroscience* 34(28):9213–21.
- Keiser, M. S., H. B. Kordasiewicz and J. L. McBride. 2016. "Gene Suppression Strategies for Dominantly Inherited Neurodegenerative Diseases: Lessons from Huntington's Disease and Spinocerebellar Ataxia." *Human Molecular Genetics* 25(R1):R53–64.
- Kennedy, L., E. Evans, C. M. Chen, L. Craven, P. J. Detloff, M. Ennis and P. F. Shelbourne. 2003. "Dramatic Tissue-Specific Mutation Length Increases Are an Early Molecular Event in Huntington Disease Pathogenesis." *Human Molecular Genetics* 12(24):3359–67.
- Kenney, C., S. Powell and Joseph Jankovic. 2007. "Autopsy-Proven Huntington's Disease with 29 Trinucleotide Repeats." *Movement Disorders* 22(1):127–30.
- Keryer, G., J. R. Pineda, G. Liot, J. Kim, P. Dietrich, C. Benstaali, K. Smith, F. P. Cordelières, N. Spassky, R. J. Ferrante, I. Dragatsis and F. Saudou. 2011. "Ciliogenesis Is Regulated by a Huntingtin-HAP1-PCM1 Pathway and Is Altered in Huntington Disease." *Journal of Clinical Investigation* 121(11):4372–82.
- Kessler, S. and M. Bloch. 1989. "Social System Responses to Huntington Disease." *Family Process* 28(1):59–68.
- Kessels, M. M. and B. Qualmann. 2002. "Syndapins Integrate N-WASP in Receptor-Mediated Endocytosis." *EMBO Journal* 21(22):6083–94
- Kessels, M. M. and B. Qualmann. 2004. "The Syndapin Protein Family: Linking Membrane Trafficking with the Cytoskeleton." *Journal of Cell Science* 117(15):3077–86.
- Khvorova, A., A. Reynolds and S. D. Jayasena. 2003. "Functional siRNAs and miRNAs Exhibit Strand Bias." *Cell* 115(2):209–16.
- Kim, D. H., and J. J. Rossi. 2007. "Strategies for Silencing Human Disease Using RNA Interference." *Nature Reviews Genetics* 8(3):173–84.

Kim, J., C. J. Matney, R. H. Roth, and S. P. Brown. 2016. "Synaptic Organization of the Neuronal Circuits of the Claustrum." *Journal of Neuroscience* 36(3):773–84.

Kishi, T., T. Tsumori, S. Yokota and Y. Yasui. 2006. "Topographical Projection from the Hippocampal Formation to the Amygdala: A Combined Anterograde and Retrograde Tracing Study in the Rat." *Journal of Comparative Neurology* 496(3):349–68.

Klapstein, G. J., R. S. Fisher, H. Zanjani, C. Cepeda, E. S. Jokel, M. F. Chesselet, and M. S. Levine. 2001. "Electrophysiological and Morphological Changes in Striatal Spiny Neurons in R6/2 Huntington's Disease Transgenic Mice." *Journal of Neurophysiology* 86(6):2667–77.

Komure, O., A. Sano, N. Nishino, N. Yamauchi, S. Ueno, K. Kondoh, N. Sano, M. Takahashi, N. Murayama, I. Kondo, S. Nagafuchi, M. Yamada and I. Kanazawa. 1995. "DNA Analysis in Hereditary Dentatorubral-Pallidoluysian Atrophy: Correlation between Cag Repeat Length and Phenotypic Variation and the Molecular Basis of Anticipation." *Neurology* 45(1):143–49.

Kordasiewicz, H. B., L. M. Stanek, E. V. Wancewicz, C. Mazur, M. M. McAlonis, K. A. Pytel, J. W. Artates, A. Weiss, S. H. Cheng, L. S. Shihabuddin, G. Hung, C. F. Bennett, and D. W. Cleveland. 2012. "Sustained Therapeutic Reversal of Huntington's Disease by Transient Repression of Huntingtin Synthesis." *Neuron* 74(6):1031–44.

Kosinski, C. M., J. H. Cha, A. B. Young, L. Mangiarini, G. Bates, J. Schiefer, and M. Schwarz. 1999. "Intranuclear Inclusions in Subtypes of Striatal Neurons in Huntington's Disease Transgenic Mice." *NeuroReport* 10(18):3891–96.

Kremer, Berry., Goldberg, Paul., Andrew, Susan E., Theilman, Jane., Telenius, Hakan., Zeisler, Jutta., Squitieri, Ferninando., Lin, Biaoyang., Bassett, Ann., Almqvist, Elizabeth., Bird, Thomas D., and Hayden, Michael R. 1994. "A Worldwide Study of the Huntington's Disease Mutation." *The New England Journal of Medicine* 331(8):481.

Kumar, P., H. Wu, J. L. McBride, K. Jung, M. H. Kim, B. L. Davidson, S. Kyung, P. Shankar, and N. Manjunath. 2007. "Transvascular Delivery of Small Interfering RNA to the Central Nervous System." *Nature*. 448(July):3–9.

Laforet, G. A., E. Sapp, K. Chase, C. McIntyre, F. M. Boyce, M. Campbell, B. A. Cadigan, L. Warzecki, D. A. Tagle, P. H. Reddy, C. Cepeda, C. R. Calvert, E. S. Jokel, G. J. Klapstein, M. A. Ariano, M. S. Levine, M. DiFiglia and N. Aronin. 2001. "Changes in Cortical and Striatal Neurons Predict Behavioral and

Electrophysiological Abnormalities in a Transgenic Murine Model of Huntington's Disease." *Journal of Neuroscience* 21(23):9112–23.

Lanciego, J. L., N. Luquin and J. A. Obeso. 2012. "Functional Anatomy of the Basal Ganglia." *Handbook of Dystonia* 45–56.

Landwehrmeyer, G. B., S. M. McNeil, L. S. Dure, P. Ge, H. Aizawa, Q. Huang, C. M. Ambrose, M. P. Duyao, E. D. Bird, E. Bonilla, M. de Young, A. J. Avila-Gonzales, N. S. Wexler, M. DiFiglia, J. F. Gusella, M. E. MacDonald, J. B. Penney, A. B. Young and J. Vonsattel. 1995. "Huntington's Disease Gene: Regional and Cellular Expression in Brain of Normal and Affected Individuals." *Annals of Neurology* 37(2):218–30.

Lapper, S. R. and J. P. Bolam. 1992. "Input from the Frontal Cortex and the Parafascicular Nucleus to Cholinergic Interneurons in the Dorsal Striatum of the Rat." *Neuroscience* 51(3):533–45.

Larsen, R. S., R. J. Corlew, M. A. Henson, A. C. Roberts, M. Mishina, M. Watanabe, S. A. Lipton, N. Nakanishi, I. Pérez-Otaño, R. J. Weinberg and B. D. Philpot. 2011. "NR3A-Containing NMDARs Promote Neurotransmitter Release and Spike Timing-Dependent Plasticity." *Nature Neuroscience* 14(3):338–44.

Larsen, R. S., I. T. Smith, J. Miriyala, J. E. Han, R. J. Corlew, S. L. Smith and B. D. Philpot. 2014. "Synapse-Specific Control of Experience-Dependent Plasticity by Presynaptic NMDA Receptors." *Neuron* 83(4):879–93.

Lau, C. G. and R. S. Zukin. 2007. "NMDA Receptor Trafficking in Synaptic Plasticity and Neuropsychiatric Disorders." *Nature Reviews Neuroscience* 8(6):413–26.

Leão, R. N., S. Mikulovic, K. E. Leão, H. Munguba, H. Gezelius, A. Enjin, K. Patra, A. Eriksson, L. M. Loew, A. B. L. Tort and K. Kullander. 2012. "OLM Interneurons Differentially Modulate CA3 and Entorhinal Inputs to Hippocampal CA1 Neurons." *Nature Neuroscience* 15(11):1524–30.

Leavitt, B. R., J. M. Van Raamsdonk, J. Shehadeh, H. Fernandes, Z. Murphy, R. K. Graham, C. L. Wellington, L. A. Raymond and Michael R. Hayden. 2006. "Wild-Type Huntingtin Protects Neurons from Excitotoxicity." *Journal of Neurochemistry* 96(4):1121–29.

Lee, J. H., L. Wei, T. C. Deveau, X. Gu and S. P. Yu. 2015. "Expression of the NMDA Receptor Subunit GluN3A (NR3A) in the Olfactory System and Its Regulatory Role on Olfaction in the Adult Mouse." *Brain Structure and Function* 221(6):3259–73.

Lee, J. H., J. Y. Zhang, Z. Z. Wei, and S. P. Yu. 2018. "Impaired Social Behaviors and Minimized Oxytocin Signaling of the Adult Mice Deficient in the N-Methyl-D-Aspartate Receptor GluN3A Subunit." *Experimental Neurology* 305(March):1–12.

Lee, M., K. K. Ting, S. Adams, B. J. Brew, R. Chung and G. J. Guillemin. 2010. "Characterisation of the Expression of NMDA Receptors in Human Astrocytes." *PLoS ONE* 5(11):1–11.

Lee, Y., C. Ahn, J. Han, H. Choi, J. Kim, J. Yim, J. Lee, P. Provost, O. Rådmark, S. Kim and V. N. Kim. 2003. "The Nuclear RNase III Drosha Initiates MicroRNA Processing." *Nature* 425(6956):415–19.

Lentz, T. B., S. J. Gray, and R. J. Samulski. 2012. "Viral Vectors for Gene Delivery to the Central Nervous System." *Neurobiology of Disease* 48(2):179–88.

Lerma, J., R. S. Zukin and M. V. L. Bennett. 1990. "Glycine Decreases Desensitization of N-Methyl-D-Aspartate (NMDA) Receptors Expressed in *Xenopus* Oocytes and Is Required for NMDA Responses." *Proceedings of the National Academy of Sciences of the United States of America* 87(6):2354–58.

Levine, M. S., G. J. Klapstein, A. Koppel, E. Gruen, C. Cepeda, M. E. Vargas, E. S. Jokel, E. M. Carpenter, H. Zanjani, R. S. Hurst, A. Efstratiadis, S. Zeitlin and M. F. Chesselet. 1999. "Enhanced Sensitivity to N-Methyl-D-Aspartate Receptor Activation in Transgenic and Knockin Mouse Models of Huntington's Disease." *Journal of Neuroscience Research* 58(4):515–32.

Lewis, B. P., C. B. Burge and D. P. Bartel. 2005. "Conserved Seed Pairing, Often Flanked by Adenosines, Indicates That Thousands of Human Genes Are MicroRNA Targets." *Cell* 120(1):15–20.

Li, S. H., G. Schilling, W. S. Young, X. Li, R. L. Margolis, O. C. Stine, M. V. Wagster, M. H. Abbott, M. L. Franz, N. G. Ranen, S. E. Folstein, J. C. Hedreen and C. A. Ross. 1993. "Huntington's Disease Gene (IT15) Is Widely Expressed in Human and Rat Tissues." *Neuron* 11(5):985–93.

Li, S., C. A. Gutekunst, S. M. Hersch and X. J. Li. 1998. "Interaction of Huntingtin-Associated Protein with Dynactin P150<sup>Glued</sup>." *Journal of Neuroscience* 18(4):1261–69.

Lim L, Mi D, Llorca A, and Marin O. 2018. "Development and Functional Diversification of Cortical Interneurons". *Neuron*. 100:294-313.

- Lin, C. H., S. Tallaksen-Greene, W. Chien, J. A. Cearley, W. S. Jackson, A. B. Crouse, S. Ren, X. Li, R. L. Albin and P. J. Detloff. 2001. "Neurological Abnormalities in a Knock-in Mouse Model of Huntington's Disease." *Human Molecular Genetics* 10(2):137–44.
- Logan, S. M., J. G. Partridge, J. A. Matta, A. Buonanno, and S. Vicini. 2007. "Long-Lasting NMDA Receptor-Mediated EPSCs in Mouse Striatal Medium Spiny Neurons." *Journal of Neurophysiology* 98(5):2693–2704.
- Lombardo, A., P. Genovese, C. M. Beausejour, S. Colleoni, Y. Lee, K. A. Kim, D. Ando, F. D. Urnov, C. Galli, P. D. Gregory, M. C. Holmes, and L. Naldini. 2007. "Gene Editing in Human Stem Cells Using Zinc Finger Nucleases and Integrase-Defective Lentiviral Vector Delivery." *Nature biotechnology*. 25(11):1298–1306.
- Low, C. and K. S. L. Wee. 2010. "New Insights into the Not-so-New NR3 Subunits of N-Methyl-D-Aspartate Receptor: Localization, Structure, and Function." *Molecular Pharmacology* 78(1):1–11.
- Luong, T.N., Carlisle, H.J., Southwell, A., and Patterson, P.H. 2011. "Assessment of motor balance and coordination in mice using the balance beam." *J. Vis. Exp.*
- Lynd-Balta, E. and S. N. Haber. 1994. "The Organization of Midbrain Projections to the Striatum in the Primate: Sensorimotor-Related Striatum versus Ventral Striatum." *Neuroscience* 59(3):625–40.
- Lyons, M. R., L. F. Chen, J. V. Deng, C. Finn, A. R. Pfenning, A. Sabhlok, K. M. Wilson, and A. E. West. 2016. "The Transcription Factor Calcium-Response Factor Limits NMDA Receptor-Dependent Transcription in the Developing Brain." *Journal of Neurochemistry* 137(2):164–76.
- Ma, L., Q. Qiao, J. W. Tsai, G. Yang, W. L., and W. B. Gan. 2016. "Experience-Dependent Plasticity of Dendritic Spines of Layer 2/3 Pyramidal Neurons in the Mouse Cortex." *Developmental Neurobiology* 76(3):277–86.
- Ma, Q., J. Yang, T. A. Milner, J. P. G. Vonsattel, M. E. Palko, L. Tessarollo, and B. L. Hempstead. 2017. "SorCS2-Mediated NR2A Trafficking Regulates Motor Deficits in Huntington's Disease." *JCI Insight* 2(9).
- McClymont, D. W., J. Harris, and I. R. Mellor. 2012. "Open-Channel Blockade Is Less Effective on GluN3B than GluN3A Subunit-Containing NMDA Receptors." *European Journal of Pharmacology* 686(1–3):22–31.

Macdonald, V., G. M. Halliday, R. J. Trent and E. A. McCusker. 1997. "Significant Loss of Pyramidal Neurons in the Angular Gyrus of Patients with Huntington's Disease." *Neuropathology and Applied Neurobiology* 23(6):492–95.

Macdonald, V. and G. Halliday. 2002. "Pyramidal Cell Loss in Motor Cortices in Huntington's Disease." *Neurobiology of Disease* 10(3):378–86.

Madisen, L., T. A. Zwingman, S. M. Sunkin, S. W. Oh, H. A. Zariwala, H. Gu, L. L. Ng, R. D. Palmiter, M. J. Hawrylycz, A. R. Jones, E. S. Lein and H. Zeng. 2010. "A Robust and High-Throughput Cre Reporting and Characterization System for the Whole Mouse Brain." *Nature Neuroscience* 13(1):133–40.

Mahant, N., E. A. Mccusker, K. Byth, S. Graham and The Huntington Study Group. 2003. "Huntington ' s Disease." *Neurology* 1607–15.

Mahfooz, K., S. Marco, R. Martínez-Turrillas, M. K. Raja, I. Pérez-Otaño, and J. F. Wesseling. 2016. "GluN3A Promotes NMDA Spiking by Enhancing Synaptic Transmission in Huntington's Disease Models." *Neurobiology of Disease* 93:47–56.

Majewska, A. and M. Sur. 2003. "Motility of Dendritic Spines in Visual Cortex *in Vivo*: Changes during the Critical Period and Effects of Visual Deprivation." *Proceedings of the National Academy of Sciences of the United States of America* 100(26):16024–29.

Mäkinen, P. I., J. K. Koponen, A. M. Kärkkäinen, T. M. Malm, K. H. Pulkkinen, J. Koistinaho, M. P. Turunen and S. Ylä-Herttua. 2006. "Stable RNA Interference: Comparison of U6 and H1 Promoters in Endothelial Cells and in Mouse Brain." *Journal of Gene Medicine* 8(4):433–41.

Mangiarini, L., K. Sathasivam, M. Seller, B. Cozens, A. Harper, C. Hetherington, M. Lawton, Y. Trottier, H. Lehrach, S. W. Davies and G. P. Bates. 1996. "Exon 1 of the HD Gene with an Expanded CAG Repeat Is Sufficient to Cause a Progressive Neurological Phenotype in Transgenic Mice." 87:493–506.

Marco, S., A. Giralt, M. M. Petrovic, M. A. Pouladi, R. Martínez-Turrillas, J. Martínez-Hernández, L. S. Kaltenbach, J. Torres-Peraza, R. K. Graham, M. Watanabe, R. Luján, N. Nakanishi, S. A. Lipton, D. C. Lo, M. R. Hayden, J. Alberch, J. F. Wesseling and I. Pérez-Otaño. 2013. "Suppressing Aberrant GluN3A Expression Rescues Synaptic and Behavioral Impairments in Huntington's Disease Models." *Nature Medicine* 19(8):1030–38.



Marco, S., A. Murillo, and I. Pérez-Otaño. 2018. "RNAi-Based GluN3A Silencing Prevents and Reverses Disease Phenotypes Induced by Mutant Huntingtin." *Molecular Therapy* 26(8).

Mariotti, C., B. Castellotti, D. Pareyson, D. Testa, M. Eoli, C. Antozzi, V. Silani, R. Marconi, F. Tezzon, G. Siciliano, C. Marchini, C. Gellera and S. Di Donato. 2000. "Phenotypic Manifestations Associated with CAG-Repeat Expansion in the Androgen Receptor Gene in Male Patients and Heterozygous Females: A Clinical and Molecular Study of 30 Families." *Neuromuscular Disorders* 10(6):391–97.

Marsh, J. L., J. Pallos and L. M. Thompson. 2003. "Fly Models of Huntington's Disease." *Human Molecular Genetics* 12(suppl 2):R187–93.

Martier, R., and P. Konstantinova. 2020. "Gene Therapy for Neurodegenerative Diseases: Slowing Down the Ticking Clock." *Frontiers in Neuroscience* 14.

Martin, B., E. Golden, O. D. Carlson, P. Pistell, J. Zhou, W. Kim, B. P. Frank, S. Thomas, W. A. Chadwick, N. H. Greig, G. P. Bates, K. Sathasivam, M. Bernier, S. Maudsley, M. P. Mattson and J. M. Egan. 2009. "Exendin-4 Improves Glycemic Control, Ameliorates Brain and Pancreatic Pathologies, and Extends Survival in a Mouse Model of Huntington's Disease." *Diabetes* 58(2):318–28.

Martínez-Turrillas, R., E. Puerta, D. Chowdhury, S. Marco, M. Watanabe, N. Aguirre and I. Pérez-Otaño. 2012. "The NMDA Receptor Subunit GluN3A Protects against 3-Nitropropionic-Acid-Induced Striatal Lesions via Inhibition of Calpain Activation." *Neurobiology of Disease* 48(3):290–98.

Matsuda, K., M. Fletcher, Y. Kamiya and M. Yuzaki. 2003. "Specific Assembly with the NMDA Receptor 3B Subunit Controls Surface Expression and Calcium Permeability of NMDA Receptors." *Journal of Neuroscience* 23(31):10064–73.

Matsuda, K., Y. Kamiya, S. Matsuda and M. Yuzaki. 2002. "Cloning and Characterization of a Novel NMDA Receptor Subunit NR3B: A Dominant Subunit That Reduces Calcium Permeability." *Molecular Brain Research* 100(1–2):43–52.

Matta, J. A., K. A. Pelkey, M. T. Craig, R. Chittajallu, B. W. Jeffries, and C. J. McBain. 2013. "Developmental Origin Dictates Interneuron AMPA and NMDA Receptor Subunit Composition and Plasticity." *Nature Neuroscience* 16(8):1032–41.

McBride, J. L., S. Ramaswamy, M. Gasmi, R. T. Bartus, C. D. Herzog, E. P. Brandon, L. Zhou, M. R. Pitzer, E. M. Berry-Kravis and J. H. Kordower. 2006. "Viral Delivery of Glial Cell Line-Derived Neurotrophic Factor Improves Behavior

and Protects Striatal Neurons in a Mouse Model of Huntington's Disease." *Proceedings of the National Academy of Sciences of the United States of America* 103(24):9345–50.

Meade, C. A., Y. P. Deng, F. R. Fusco, N. Del Mar, S. Hersch, D. Goldowitz, and A. Reiner. 2002. "Cellular Localization and Development of Neuronal Intranuclear Inclusions in Striatal and Cortical Neurons in R6/2 Transgenic Mice." *Journal of Comparative Neurology* 449(3):241–69.

Meddows, E., B. Le Bourdellès, S. Grimwood, K. Wafford, S. Sandhu, P. Whiting and R. A. Jeffre. McIlhinney. 2001. "Identification of Molecular Determinants That Are Important in the Assembly of N-Methyl-D-Aspartate Receptors." *Journal of Biological Chemistry* 276(22):18795–803.

Menalled, L. B., J. D. Sison, Y. Wu, M. Olivieri, X. J. Li, H. Li, S. Zeitlin and M. Chesselet. 2002. "Early Motor Dysfunction and Striosomal Distribution of Huntingtin Microaggregates in Huntington's Disease Knock-in Mice." *Journal of Neuroscience* 22(18):8266–76.

Menalled, L. B., J. D. Sison, I. Dragatsis, S. Zeitlin and M. Françoise Chesselet. 2003. "Time Course of Early Motor and Neuropathological Anomalies in a Knock-in Mouse Model of Huntington's Disease with 140 CAG Repeats." *Journal of Comparative Neurology* 465(1):11–26.

Meredith, G. E. and F. G. Wouterlood. 1990. "Hippocampal and Midline Thalamic Fibers and Terminals in Relation to the Choline Acetyltransferase-immunoreactive Neurons in Nucleus Accumbens of the Rat: A Light and Electron Microscopic Study." *Journal of Comparative Neurology* 296(2):204–21.

Milnerwood, A. J., C. M. Gladding, M. A. Pouladi, A. M. Kaufman, R. M. Hines, J. D. Boyd, R. W. Y. Ko, O. C. Vasuta, R. K. Graham, M. R. Hayden, T. H. Murphy and L. A. Raymond. 2010. "Early Increase in Extrasynaptic NMDA Receptor Signaling and Expression Contributes to Phenotype Onset in Huntington's Disease Mice." *Neuron* 65(2):178–90.

Milnerwood, A. J., and L. A. Raymond. 2010. "Early Synaptic Pathophysiology in Neurodegeneration: Insights from Huntington's Disease." *Trends in Neurosciences* 33(11):513–23.

Mingozi, F., and K. A. High. 2016. "Immune Responses to AAV Vectors: Overcoming Barriers to Successful Gene Therapy." *The American Society of Hematology*. 122(1):23–37.

Modregger, J., N. A. DiProspero, V. Charles, D. A. Tagle, and M. Plomann. 2002. "PACSIN 1 Interacts with Huntingtin and Is Absent from Synaptic

Varicosities in Presymptomatic Huntington's Disease Brains." *Human Molecular Genetics* 11(21):2547–58.

Mohamad, O., M. Song, L. Wei and S. P. Yu. 2013. "Regulatory Roles of the NMDA Receptor GluN3A Subunit in Locomotion, Pain Perception and Cognitive Functions in Adult Mice." *Journal of Physiology* 591(1):149–68.

Monteys, A. M., S. A. Ebanks, M. S. Keiser and B. L. Davidson. 2017. "CRISPR/Cas9 Editing of the Mutant Huntingtin Allele *In Vitro* and *In Vivo*." *Molecular Therapy* 25(1):12–23.

Monyer, H., N. Burnashev, D. J. Laurie, B. Sakmann and P. H. Seeburg. 1994. "Developmental and Regional Expression in the Rat Brain and Functional Properties of Four NMDA Receptors." *Neuron* 12(3):529–40.

Monyer, H., R. Sprengel, R. Schoepfer, A. Herb, M. Higuchi, H. Lomeli, N. Burnashev, B. Sakmann and P. H. Seeburg. 1992. "Heteromeric NMDA Receptors: Molecular and Functional Distinction of Subtypes." *Science* 256(5060):1217–21.

Mueller, H. T. and J. H. Meador-Woodruff. 2003. "Expression of the NR3A Subunit of the NMDA Receptor in Human Fetal Brain." *Annals of the New York Academy of Sciences* 1003:448–51.

Mueller, H. T. and J. H. Meador-Woodruff. 2004. "NR3A NMDA Receptor Subunit MRNA Expression in Schizophrenia, Depression and Bipolar Disorder." *Schizophrenia Research* 71(2–3):361–70.

Murmu, R. Prity, W. Li, A. Holtmaat, and J. Li. 2013. "Dendritic Spine Instability Leads to Progressive Neocortical Spine Loss in a Mouse Model of Huntington's Disease." *Neurobiology of Disease*. 33(32):12997–9.

Naarding, P., H. P. H. Kremer and F. G. Zitman. 2001. "Huntington's Disease: A Review of the Literature on Prevalence and Treatment of Neuropsychiatric Phenomena." *European Psychiatry* 16(8):439–45.

Nakai, H., S. R. Yant, T. A. Storm, S. Fuess, L. Meuse, and M. A. Kay. 2001. "Extrachromosomal Recombinant Adeno-Associated Virus Vector Genomes Are Primarily Responsible for Stable Liver Transduction *In Vivo*." *Journal of Virology* 75(15):6969–76.

Nakanishi, N., S. Tu, Y. Shin, J. Cui, T. Kurokawa, D. Zhang, H. S. V. Chen, G. Tong and S. A. Lipton. 2009. "Neuroprotection by the NR3A Subunit of the NMDA Receptor." *Journal of Neuroscience* 29(16):5260–65.

Napoli, C., C. Lemieux and R. Jorgensen. 1990. "Introduction of a Chimeric Chalcone Synthase Gene into Petunia Results in Reversible Co-Suppression of Homologous Genes in Trans." *Plant Cell* 2(4):279–89.

Naseri, N., H. Valizadeh, and P. Zakeri-Milani. 2015. "Solid Lipid Nanoparticles and Nanostructured Lipid Carriers: Structure Preparation and Application." *Advanced Pharmaceutical Bulletin* 5(3):305–13.

Nasir, J., S. B. Floresco, J. R. O'Kusky, V. M. Diewert, J. M. Richman, J. Zeisler, A. Borowski, J. D. Marth, A. G. Phillips, and M. R. Hayden. 1995. "Targeted Disruption of the Huntington's Disease Gene Results in Embryonic Lethality and Behavioral and Morphological Changes in Heterozygotes." *Cell* 81(5):811–23.

Neueder, A., C. Landles, R. Ghosh, D. Howland, R. H. Myers, R. L. M. Faull, S. J. Tabrizi, and G. P. Bates. 2017. "The Pathogenic Exon 1 HTT Protein Is Produced by Incomplete Splicing in Huntington's Disease Patients." *Scientific Reports* 7(1):1–10.

Ni, T., X. Zhou, D. M. McCarty, I. Zolotukhin and Nicholas Muzyczka. 1994. "In Vitro Replication of Adeno-Associated Virus DNA." *Proceedings of the National Academy of Sciences of the United States of America* 89(10):4673–77.

Nilsson, A., M. Eriksson, E. C. Muly, E. Åkesson, E. B. Samuelsson, N. Bogdanovic, E. Benedikz and E. Sundström. 2007. "Analysis of NR3A Receptor Subunits in Human Native NMDA Receptors." *Brain Research* 1186(1):102–12.

Nishi, M., H. Hinds, H. P. Lu, M. Kawata and Y. Hayashi. 2001. "Motoneuron-Specific Expression of NR3B, a Novel NMDA-Type Glutamate Receptor Subunit That Works in a Dominant-Negative Manner." *The Journal of Neuroscience: The Official Journal of the Society for Neuroscience* 21(23):1–6.

Nonnenmacher, M. and T. Weber. 2012. "Intracellular Transport of Recombinant Adeno-Associated Virus Vectors." *Gene Therapy* 19(6):649–58.

Nonnenmacher, M. E., J. Cintrat, D. Gillet and T. Weber. 2015. "Syntaxin 5-Dependent Retrograde Transport to the trans-Golgi Network Is Required for Adeno-Associated Virus Transduction." *Journal of Virology* 89(3):1673–87.

O'Hearn, E., S. E. Holmes, P. C. Calvert, C. A. Ross and R. L. Margolis. 2001. "SCA-12: Tremor with Cerebellar and Cortical Atrophy Is Associated with a CAG Repeat Expansion." *Neurology* 56(3):299–303.

O'Kusky, J. R., J. Nasir, F. Cicchetti, A. Parent and M. R. Hayden. 1999. "Neuronal Degeneration in the Basal Ganglia and Loss of Pallido-Subthalamic

Synapses in Mice with Targeted Disruption of the Huntington's Disease Gene." *Brain Research* 818(2):468–79.

Okamoto, S. I., M. A. Pouladi, M. Talantova, D. Yao, P. Xia, D. E. Ehrnhoefer, R. Zaidi, A. Clemente, M. Kaul, R. K. Graham, D. Zhang, H. S. Vincent Chen, G. Tong, M. R. Hayden, and S. A. Lipton. 2009. "Balance between Synaptic versus Extrasynaptic NMDA Receptor Activity Influences Inclusions and Neurotoxicity of Mutant Huntingtin." *Nature Medicine* 15(12):1407–13.

On, K. M. and N. J. Sucher. 2004. "Molecular Interaction of NMDA Receptor Subunit NR3A with Protein Phosphatase 2A." *NeuroReport* 15(9):1447–50.

Otsu, Y., E. Darcq, K. Pietrajtis, F. Mátyás, E. Schwartz, T. Bessaih, S. Abi Gerges, C. V. Rousseau T. Grand, S. Dieudonné, P. Paoletti, L. Acsády, C. Agulhon, B. L. Kieffer, and M. A. Diana. 2019. "Control of Aversion by Glycine-Gated GluN1/GluN3A NMDA Receptors in the Adult Medial Habenula." *Science* 366(6462):250–54.

Ouimet, C. C., K. C. Langley-Gullion, and P. Greengard. 1998. "Quantitative Immunocytochemistry of DARPP-32-Expressing Neurons in the Rat Caudatoputamen." *Brain Research* 808(1):8–12.

Paas, Y. 1998. "The Macro- and Microarchitectures of the Ligand-Binding Domain of Glutamate Receptors." *Trends in Neurosciences* 21(3):117–25.

Pachernegg, S., N. Strutz-Seebohm and M. Hollmann. 2012. "GluN3 Subunit-Containing NMDA Receptors: Not Just One-Trick Ponies." *Trends in Neurosciences* 35(4):240–49.

Pal, A., F. Severin, B. Lommer, A. Shevchenko and M. Zerial. 2006. "Huntingtin-HAP40 Complex Is a Novel Rab5 Effector That Regulates Early Endosome Motility and Is up-Regulated in Huntington's Disease." *Journal of Cell Biology* 172(4):605–18.

Palidwor, G. A., S. Shcherbinin, M. R. Huska, T. Rasko, U. Stelzl, A. Arumughan, R. Foulle, P. Porras, L. Sanchez-Pulido, E. E. Wanker and M. A. Andrade-Navarro. 2009. "Detection of Alpha-Rod Protein Repeats Using a Neural Network and Application to Huntingtin." *PLoS Computational Biology* 5(3).

Paoletti, P., P. Ascher and J. Neyton. 1997. "High-Affinity Zinc Inhibition of NMDA NR1-NR2A Receptors." *Journal of Neuroscience* 17(15):5711–25.

Paoletti, P. and J. Neyton. 2007. "NMDA Receptor Subunits: Function and Pharmacology." *Current Opinion in Pharmacology* 7(1):39–47.

Paoletti, P. 2011. "Molecular Basis of NMDA Receptor Functional Diversity." *European Journal of Neuroscience* 33(8):1351–65.

Paoletti, P., C. Bellone, and Q. Zhou. 2013. "NMDA Receptor Subunit Diversity: Impact on Receptor Properties, Synaptic Plasticity and Disease." *Nature Reviews Neuroscience* 14(6):383–400.

Parent, A., F. Sato, Y. Wu, J. Gauthier, M. Lévesque and M. Parent. 2000. "Organization of the Basal Ganglia: The Importance of Axonal Collateralization." *Trends in Neurosciences* 23(10 SUPPL.):20–27.

Patel, K., G. Kilfoil, D. L. Wyles, S. Naggie, E. Lawitz, S. Bradley, P. Lindell, and D. Suhy. 2016. "258. Phase I/IIa Study of TT-034, a DNA-Directed RNA Interference (DdRNAi) Agent Delivered as a Single Administration for the Treatment of Subjects with Chronic Hepatitis C Virus (HCV)." *Molecular Therapy* 24(May):S102.

Paul, A., M. Crow, R. Raudales, M. He, J. Gillis, and Z. J. Huang. 2017. "Transcriptional Architecture of Synaptic Communication Delineates GABAergic Neuron Identity." *Cell* 171(3):522-539.e20.

Paul, C. P., P. D. Good, I. Winer and D. R. Engelke. 2002. "Effective Expression of Small Interfering RNA in Human Cells." *Nature Biotechnology* 20(5):505–8.

Paulsen, J. S., K. F. Hoth, C. Nehl and L. Stierman. 2005. "Critical Periods of Suicide Risk in Huntington's Disease." *American Journal of Psychiatry* 162(4):725–31.

Paxinos, G., and Franklin, K.B.J. 2001. "The Mouse Brain in Stereotaxic Coordinates". Academic Press.

Paxinos G., Halliday G., Watson C., Koutcherov Y., and Wang H. 2007. "Atlas of the developing mouse brain". 1st Edition. Academic Press

Paxinos G., and Franklin K. 2019. "Mouse Brain in Stereotaxic Coordinates". 5th Edition. Academic Press.

Penaud-Budloo, M., A. François, N. Clément and E. Ayuso. 2018. "Pharmacology of Recombinant Adeno-Associated Virus Production." *Molecular Therapy - Methods and Clinical Development* 8(March):166–80.

Percheron G, François C, Talbi B, Yelnik J, Fénelon G.1996 "The primate motor thalamus." *Brain Res Brain Res Rev.*22(2):93-181.

Pérez-Otaño, I., C. T. Schulteis, A. Contractor, S. A. Lipton, J. S. Trimmer, N. J. Sucher and S. F. Heinemann. 2001. "Assembly with the NR1 Subunit Is

Required for Surface Expression of NR3A-Containing NMDA Receptors.” *Journal of Neuroscience* 21(4):1228–37.

Pérez-Otaño, I. and M. D. Ehlers. 2004. “Learning from NMDA Receptor Trafficking: Clues to the Development and Maturation of Glutamatergic Synapses.” *NeuroSignals* 13(4):175–89.

Pérez-Otaño, I., R. Luján, S. J. Tavalin, M. Plomann, J. Modregger, X. B. Liu, E. G. Jones, S. F. Heinemann, D. C. Lo and M. D. Ehlers. 2006. “Endocytosis and Synaptic Removal of NR3A-Containing NMDA Receptors by PACSIN1/Syndapin1.” *Nature Neuroscience* 9(5):611–21.

Pérez-Otaño, I., R. S. Larsen and J. F. Wesseling. 2016. “Emerging Roles of GluN3-Containing NMDA Receptors in the CNS.” *Nature Reviews Neuroscience* 17(10):623–35.

Perszyk, R. E., J. O. DiRaddo, K. L. Strong, C. M. Low, K. K. Ogden, A. Khatri, G. A. Vargish, K. A. Pelkey, L. Tricoire, D. C. Liotta, Y. Smith, C. J. McBain, and S. F. Traynelis. 2016. “GluN2D-Containing N-Methyl-D-Aspartate Receptors Mediate Synaptic Transmission in Hippocampal Interneurons and Regulate Interneuron Activity.” *Molecular Pharmacology* 90(6):689–702.

Petros TJ, Bultje RS, Ross ME, Fishell G, and Anderson SA. 2015. “Apical versus Basal Neurogenesis Directs Cortical Interneuron Subclass Fate”. *Cell Rep.* 13:1090-1095.

Pfeffer, C. K., M. Xue, M. He, Z. J. Huang and M. Scanziani. 2013. “Inhibition of Inhibition in Visual Cortex: The Logic of Connections between Molecularly Distinct Interneurons.” *Nature Neuroscience* 16(8):1068–76.

Piccioni, F., S. Simeoni, I. Andriola, E. Armatura, S. Bassanini, P. Pozzi and A. Poletti. 2001. “Polyglutamine Tract Expansion of the Androgen Receptor in a Motoneuronal Model of Spinal and Bulbar Muscular Atrophy.” *Brain Research Bulletin* 56(3–4):215–20.

Pickel, V. M., and A. Heras. 1996. “Ultrastructural Localization of Calbindin-D28 K and Gaba In The Matrix Compartment Of The Rat Caudate-Putamen Nuclei.” *Neuroscience* 167-178

Pillay, S. and J. E. Carette. 2017. “Host Determinants of Adeno-Associated Viral Vector Entry.” *Current Opinion in Virology* 24:124–31.

Piña-Crespo, J. C., M. Talantova, I. Micu, B. States, H. S. V. Chen, S. Tu, N. Nakanishi, G. Tong, D. Zhang, S. F. Heinemann, G. W. Zamponi, P. K. Stys and S A. Lipton. 2010. “Excitatory Glycine Responses of CNS Myelin Mediated

by NR1/NR3 'NMDA' Receptor Subunits." *Journal of Neuroscience* 30(34):11501–5.

Popa, A., W. Zhang, M. S. Harrison, K. Goodner, T. Kazakov, E. C. Goodwin, A. Lipovsky, C. G. Burd and D. DiMaio. 2015. "Direct Binding of Retromer to Human Papillomavirus Type 16 Minor Capsid Protein L2 Mediates Endosome Exit during Viral Infection." *PLoS Pathogens* 11(2):1–21.

Pouladi, M. A., A. J. Morton, and M. R. Hayden. 2013. "Choosing an Animal Model for the Study of Huntington's Disease." *Nature Reviews Neuroscience* 14(10):708–21.

Powell, T. P. S. and W. M. Cowan. 1956. "A Study of Thalamo-Striate Relations in the Monkey." *Brain* 79:364–90.

Pridmore, S. A. 1990. "The large Huntington's disease family of Tasmania". *The medical journal of Australia* Vol 153, Issue 10.

Provost, P., D. Dishart, J. Doucet, D. Friendewey, B. Samuelsson and O. Radmark. 2002. "Ribonuclease activity and RNA binding of recombinant human Dicer." *The EMBO journal* 21(21).

Prybylowski, K., K. Chang, N. Sans, L. Kan, S. Vicini, and R. J. Wenthold. 2005. "The Synaptic Localization of NR2B-Containing NMDA Receptors Is Controlled by Interactions with PDZ Proteins and AP-2." *Neuron* 47(6):845–57.

Qualmann, B., J. Roos, P. J. DiGregorio and R. B. Kelly. 1999. "Syndapin I, a Synaptic Dynamin-Binding Protein That Associates with the Neural Wiskott-Aldrich Syndrome Protein." *Molecular Biology of the Cell* 10(2):501–13.

Racca, C., F. A. Stephenson, P. Streit, J. D. B. Roberts and P. Somogyi. 2000. "NMDA Receptor Content of Synapses in Stratum Radiatum of the Hippocampal CA1 Area." *Journal of Neuroscience* 20(7):2512–22.

Rajapaksha, I., P. Angus and C. Herath. 2019. "Adeno-Associated Virus (AAV)-Mediated Gene Therapy for Disorders of Inherited and Non-Inherited Origin." *In Vivo and Ex Vivo Gene Therapy for Inherited and Non-Inherited Disorders*.

Rakic, P., J. P. Bourgeois, M. F. Eckenhoff, N. Zecevic and P. S. Goldman-Rakic. 1986. "Concurrent Overproduction of Synapses in Diverse Regions of the Primate Cerebral Cortex." *Science* 232(4747):232–35.

Ramaswamy, S., J. L. McBride, I. Han, E. M. Berry-Kravis, L. Zhou, C. D. Herzog, M. Gasmi, R. T. Bartus and J. H. Kordower. 2009. "Intrastriatal CERE-120 (AAV-Neurturin) Protects Striatal and Cortical Neurons and Delays Motor



Deficits in a Transgenic Mouse Model of Huntington's Disease." *Neurobiology of Disease* 34(1):40–50.

Ratovitski, T., E. Chighladze, N. Arbez, T. Boronina, S. Herbrich, R. N. Cole and C. A. Ross. 2012. "Huntingtin Protein Interactions Altered by Polyglutamine Expansion as Determined by Quantitative Proteomic Analysis." *Cell Cycle* 11(10):2006–21.

Ravikumar, B., C. Vacher, Z. Berger, J. E. Davies, S. Luo, L. G. Oroz, F. Scaravilli, D. F. Easton, R. Duden, C. J. O'Kane, and D. C. Rubinsztein. 2004. "Inhibition of MTOR Induces Autophagy and Reduces Toxicity of Polyglutamine Expansions in Fly and Mouse Models of Huntington Disease." *Nature Genetics* 36(6):585–95.

Raymond, L. A., V. M. André, C. Cepeda, C. M. Gladding, A. J. Milnerwood, and M. S. Levine. 2011. "Pathophysiology of Huntington's Disease: Time-Dependent Alterations in Synaptic and Receptor Function." *Neuroscience* 198:252–73.

Redinbaugh, M. J., J. M. Phillips, N. A. Kambi, S. Mohanta, S. Andryk, G. L. Dooley, M. Afrasiabi, A. Raz, and Y. B. Saalman. 2020. "Thalamus Modulates Consciousness via Layer-Specific Control of Cortex." *Neuron* 106(1):66-75.e12.

Reed, T. E. and J. H. CHandler. 1958. "Huntington's Chorea in Michigan. I. Demography and Genetics." *American Journal of Human Genetics* 10(2):201–25.

Reiner, A., R. L. Albin, K. D. Anderson, C. J. D'Amato, J. B. Penney and A. B. Young. 1988. "Differential Loss of Striatal Projection Neurons in Huntington Disease." *Proceedings of the National Academy of Sciences of the United States of America* 85(15):5733–37.

Reiner, A, I. Dragatsis and P. Dietrich. 2011. "Genetics and Neuropathology of Huntington's Disease." *International Review of Neurobiology*, vol. 98

Ren, K., B. Guo, C. Dai, H. Yao, T. Sun, X. Liu, Z. Bai, W. Wang and S. Wu. 2017. "Striatal Distribution and Cytoarchitecture of Dopamine Receptor Subtype 1 and 2: Evidence from Double-Labeling Transgenic Mice." *Frontiers in Neural Circuits* 11(August):57.

Ren, S., Y. Wang, F. Yue, X. Cheng, R. Dang, Q. Qiao, X. Sun, X. Li, Q. Jiang, J. Yao, H. Qin, G. Wang, X. Liao, D. Gao, J. Xia, J. Zhang, B. Hu, J. Yan, Y. Wang, M. Xu, Y. Han, X. Tang, X. Chen, C. He, and Z. Hu. 2018. "The Paraventricular Thalamus Is a Critical Thalamic Area for Wakefulness." *Science* 362(6413):429–34.

Richards, P., C. Didszun, S. Campesan, A. Simpson, B. Horley, K. W. Young, P. Glynn, K. Cain, C. P. Kyriacou, F. Giorgini, and P. Nicotera. 2011. "Dendritic Spine Loss and Neurodegeneration Is Rescued by Rab11 in Models of Huntington's Disease." *Cell Death and Differentiation* 18(2):191–200.

Roberts, A. C., J. Díez-García, R. M. Rodríguez, I. P. López, R. Luján, R. Martínez-Turrillas, E. Picó, M. A. Henson, D. R. Bernardo, T. M. Jarrett, D. J. Clendeninn, L. López-Mascaraque, G. Feng, D. C. Lo, J. F. Wesseling, W. C. Wetsel, B. D. Philpot and I. Pérez-Otaño. 2009. "Downregulation of NR3A-Containing NMDARs Is Required for Synapse Maturation and Memory Consolidation." *Neuron* 63(3):342–56.

Rosas, H. D., S. Y. Lee, A. C. Bender, A. K. Zaleta, M. Vangel, P. Yu, B. Fischl, V. Pappu, C. Onorato, J. Cha, D. H. Salat, and S. M. Hersch. 2010. "NeuroImage Altered White Matter Microstructure in the Corpus Callosum in Huntington's Disease: Implications for Cortical 'Disconnection'." *Neuro Image* 49(4):2995–3004.

Rosenblatt, A. and I. Leroi. 2000. "Neuropsychiatry of Huntington's Disease and Other Basal Ganglia Disorders." *Psychosomatics* 41(1):24–30.

Ross, C. A., and S. J. Tabrizi. 2011. "Huntington's Disease: From Molecular Pathogenesis to Clinical Treatment." *The Lancet Neurology* 10(1):83–98.

Ross, C. A., E. H. Aylward, E. J. Wild, D. R. Langbehn, J. D. Long, J. H. Warner, R. I. Scahill, B. R. Leavitt, J. C. Stout, J. S. Paulsen, R. Reilmann, P. G. Unschuld, A. Wexler, R. L. Margolis, and S. J. Tabrizi. 2014. "Huntington Disease: Natural History, Biomarkers and Prospects for Therapeutics." *Nature Reviews Neurology* 10(4):204–16.

Rubinsztein, D. C., and H. T. Orr. 2016. "Diminishing Return for Mechanistic Therapeutics with Neurodegenerative Disease Duration?: There May Be a Point in the Course of a Neurodegenerative Condition Where Therapeutics Targeting Disease-Causing Mechanisms Are Futile." *BioEssays* 38(10):977–80.

Ruffing, M., H. Zentgraf and J. A. Kleinschmidt. 1992. "Assembly of Viruslike Particles by Recombinant Structural Proteins of Adeno-Associated Virus Type 2 in Insect Cells." *Journal of Virology* 66(12):6922–30.

Ruzo, A., I. Ismailoglu, M. Popowski, T. Haremake, G. F. Croft, A. Deglincerti and A. H. Brivanlou. 2015. "Discovery of Novel Isoforms of Huntingtin Reveals a New Hominid-Specific Exon." *PLoS ONE* 10(5):1–13.

- Salter, M. G. and R. Fern. 2005. "NMDA Receptors Are Expressed in Developing Oligodendrocyte Processes and Mediate Injury." *Nature* 438(7071):1167–71.
- Sanlioglu, S., P. K. Benson, J. Yang, E. M. Atkinson, T. Reynolds and J. F. Engelhardt. 2000. "Endocytosis and Nuclear Trafficking of Adeno-Associated Virus Type 2 Are Controlled by Rac1 and Phosphatidylinositol-3 Kinase Activation." *Journal of Virology* 74(19):9184–96.
- Sans, N., R. S. Petralia, Y. Wang, J. Blahos li, J. W. Hell, and R. J. Wenthold. 1996. "For Review, See Sheng." *The Journal of Neuroscience* 20(3):1260–71.
- Sasaki, Y. F., T. Rothe, L. S. Premkumar, S. Das, J. Cui, M. V. Talantova, H. Wong, X. Gong, S. F. Chan, D. Zhang, N. Nakanishi, N. J. Sucher and S. A. Lipton. 2002. "Characterization and Comparison of the NR3A Subunit of the NMDA Receptor in Recombinant Systems and Primary Cortical Neurons." *Journal of Neurophysiology* 87(4):2052–63.
- Sathasivam, K., C. Hobbs, L. Mangiarini, A. Mahal, M Turmaine, P. Doherty, S. W. Davies, and G P. Bates. 1999. "Transgenic Models of Huntington's Disease." *The Royal Society*, 354, 963-969
- Saudou, F. and S. Humbert. 2016. "The Biology of Huntingtin." *Neuron* 89(5):910–26.
- Savtchouk, I., M. A. Di Castro, R. Ali, H. Stubbe, R. Luján and A. Volterra. 2019. "Circuit-Specific Control of the Medial Entorhinal Inputs to the Dentate Gyrus by Atypical Presynaptic NMDARs Activated by Astrocytes." *Proceedings of the National Academy of Sciences of the United States of America* 116(27):13602–10.
- Schaefer, M. H., J. F. Fontaine, A. Vinayagam, P. Porras, E. E. Wanker and M. A. Andrade-Navarro. 2012. "Hippie: Integrating Protein Interaction Networks with Experiment Based Quality Scores." *PLoS ONE* 7(2):1–8.
- Schilling, G., M. W. Becher, A. H. Sharp, H. A. Jinnah, K. Duan, J. A. Kotzuk, H. H. Slunt, T. Ratovitski, J. K. Cooper, N. A. Jenkins, N. G. Copeland, D. L. Price, C. A. Ross and D. R. Brochelt. 1999. "Intranuclear Inclusions and Neuritic Aggregates in Transgenic Mice Expressing a Mutant N-Terminal Fragment of Huntingtin." *Human Molecular Genetics* 8(3):397–407.
- Schorge, S. and D. Colquhoun. 2003. "Studies of NMDA Receptor Function and Stoichiometry with Truncated and Tandem Subunits." *Journal of Neuroscience* 23(4):1151–58.

Schröder, K.F., Hopf, A., Lange, H., and Thorner, G. 1975. "Morphometrisch-Statistische Strukturanalysen Des Striatum, Pallidum und Nucleus Subthalamicus Beim Menschen." *Journal Für Hirnforschung*.

Schwarz, D. S., G. Hutvágner, T. Du, Z. Xu, N. Aronin and P. D. Zamore. 2003. "Asymmetry in the Assembly of the RNAi Enzyme Complex." *Cell* 115(2):199–208.

Seeburg, P. H. 1993. "The TIPS/TINS Lecture: The Molecular Biology of Mammalian Glutamate Receptor Channels." *Trends in Pharmacological Sciences* 14(8):297–303.

Selemon, L. D. and P. S. Goldman-Rakic. 1985. "Longitudinal Topography and Interdigitated Projections in the Rhesus Monkey." *The Journal of Neuroscience* 5(3):776–94.

Seo, H., W. Kim and O. Isacson. 2008. "Compensatory Changes in the Ubiquitin-Proteasome System, Brain-Derived Neurotrophic Factor and Mitochondrial Complex II/III in YAC72 and R6/2 Transgenic Mice Partially Model Huntington's Disease Patients." *Human Molecular Genetics* 17(20):3144–53.

Seong, I. S., J. M. Woda, J. J. Song, A. Lloret, P. D. Abeyrathne, C. J. Woo, G. Gregory, J. M. Lee, V. C. Wheeler, T. Walz, R. E. Kingston, J. F. Gusella, R. A. Conlon and M. E. MacDonald. 2010. "Huntingtin Facilitates Polycomb Repressive Complex 2." *Human Molecular Genetics* 19(4):573–83.

Shelbourne, P. F., N. Killeen, R. F. Hevner, H. M. Johnston, L. Tecott, M. Lewandoski, M. Ennis, L. Ramirez, Z. Li, C. Iannicola, D. R. Littman and R. M. Myers. 1999. "A Huntington's Disease CAG Expansion at the Murine Hdh Locus Is Unstable and Associated with Behavioural Abnormalities in Mice." *Human Molecular Genetics* 8(5):763–74.

Sherman, S. Murray. 2007. "The Thalamus Is More than Just a Relay." *Current Opinion in Neurobiology* 17(4):417–22.

Shink, E., M. D. Bevan, J. P. Bolam and Y. Smith. 1996. "The Subthalamic Nucleus and The External Pallidum: Two Tightly Interconnected Structures that Control the Output of the Basal Ganglia in the Monkey." *Neuroscience* 73(2):335–57.

Shirasaki, D. I., E. R. Greiner, I. Al-Ramahi, M. Gray, P. Boontheung, D. H. Geschwind, J. Botas, G. Coppola, S. Horvath, J. A. Loo, and X. W. Yang. 2012. "Network Organization of the Huntingtin Proteomic Interactome in Mammalian Brain." *Neuron* 75(1):41–57.

Shiwach, R. 1994. "Psychopathology in Huntington's Disease Patients." *Acta Psychiatrica Scandinavica* 90(4):241–46.

Simmons, D. A., N. P. Belichenko, T. Yang, C. Condon, M. Monbureau, M. Shamloo, D. Jing, S. M. Massa, and F. M. Longo. 2013. "A Small Molecule TrkB Ligand Reduces Motor Impairment and Neuropathology in R6/2 and BACHD Mouse Models of Huntington's Disease." *Journal of Neuroscience* 33(48):18712–27.

Skrenkova, K., S. Lee, K. Lichnerova, M. Kaniakova, H. Hansikova, M. Zapotocky, Y. H. Suh and M. Horak. 2018. "N-Glycosylation Regulates the Trafficking and Surface Mobility of GluN3A-Containing NMDA Receptors." *Frontiers in Molecular Neuroscience* 11(June):1–16.

Slow, E. J., J. van Raamsdonk, D. Rogers, S. H. Coleman, R. K. Graham, Y. Deng, R. Oh, N. Bissada, S. M. Hossain, Y. Z. Yang, X. J. Li, E. M. Simpson, C. A. Gutekunst, B. R. Leavitt and M. R. Hayden. 2003. "Selective Striatal Neuronal Loss in a YAC128 Mouse Model of Huntington Disease." *Human Molecular Genetics* 12(13):1555–67.

Smothers, C. T. and J. J. Woodward. 2007. "Pharmacological Characterization of Glycine-Activated Currents in HEK 293 Cells Expressing N-Methyl-D-Aspartate NR1 and NR3 Subunits." *Journal of Pharmacology and Experimental Therapeutics* 322(2):739–48.

Sobolevsky, A. I., M. P. Rosconi and E. Gouaux. 2009. "X-Ray Structure, Symmetry and Mechanism of an AMPA-Subtype Glutamate Receptor." *Nature* 462(7274):745–56.

Solberg, O. K., P. Filkuková, J. C. Frich and K. J. Billau. Feragen. 2018. "Age at Death and Causes of Death in Patients with Huntington Disease in Norway in 1986-2015." *Journal of Huntington's Disease* 7(1):77–86.

Soutschek, J, A. Akinc, B. Bramlage, K. Charisse, R. Constien, M. Donoghue, S. Elbashir, A. Geick, P. Hadwiger, J. Harborth, M. John, V. Kesavan, G. Lavine, R. K. Pandey, T. Racie, K. G. Rajeev, I. Rohl, I. Toudjarska, G. Wang, S. Wuschko, D. Bumcrot, V. Kotliansky, S. Limmer, M. Manoharan, and H. Vornlocher. 2004. "Therapeutic Silencing of an Endogenous Gene by Systemic Administration of Modified SiRNAs." *Nature*. 173–78.

Spargo, E., I. P. Everall and P. L. Lantos. 1993. "Neuronal Loss in the Hippocampus in Huntington's Disease: A Comparison with HIV Infection." *Journal of Neurology, Neurosurgery and Psychiatry* 56(5):487–91.

Spronck, E. A., C. C. Brouwers, A. Vallès, M. De Haan, H. Petry, S. J. Van Deventer, P. Konstantinova, and M. M. Evers. 2019. "AAV5-MiHTT Gene Therapy Demonstrates Sustained Huntingtin Lowering and Functional Improvement in Huntington Disease Mouse Models." *Molecular Therapy: Methods & Clinical Development* 13(June):334–43.

Squitieri, F., M. Cannella and M. Simonelli. 2002. "CAG Mutation Effect on Rate of Progression in Huntington's Disease." *Neurological Sciences* 23(SUPPL. 2):107–8.

Srivastava T, Lal V, Prabhakar S. 1999. "Juvenile Huntington's disease." *Neurology India* 47 (4): 340-1.

Stavarache, M. A., N. Petersen, E. M. Jurgens, E. R. Milstein, Z. B. Rosenfeld, D. J. Ballon and M. G. Kaplitt. 2019. "Safe and Stable Noninvasive Focal Gene Delivery to the Mammalian Brain Following Focused Ultrasound." *Journal of Neurosurgery* 130(3):989–98.

Steffan, J. S., A. Kazantsev, O. Spasic-Boskovic, M. Greenwald, Y. Z. Zhu, H. Gohler, E. E. Wanker, G. P. Bates, D. E. Housman and L. M. Thompson. 2000. "The Huntington's Disease Protein Interacts with P53 and CREB-Binding Protein and Represses Transcription." *Proceedings of the National Academy of Sciences of the United States of America* 97(12):6763–68.

Strack, S., J. A. Zaucha, F. F. Ebner, R. J. Colbran and B. E. Wadzinski. 1998. "Brain Protein Phosphatase 2A: Developmental Regulation and Distinct Cellular and Subcellular Localization by B Subunits." *Journal of Comparative Neurology* 392(4):515–27.

Strong, T. V., D. A. Table, J. M. Valdes, L. W. Elmer, K. Boehm, M. Swaroop, K. W. Kaatz, F. S. Collins and R. L. Albin. 1993. "Widespread Expression of the Human and Rat Huntington's Disease Gene in Brain and Nonneural Tissues." *Nature Genetics* 4:221–26.

Sucher, N. J., S. Akbarian, C. L. Chi, C. L. Leclerc, M. Awobuluyi, D. L. Deitcher, M. K. Wu, J. P. Yuan, E. G. Jones and S. A. Lipton. 1995. "Developmental and Regional Expression Pattern of a Novel NMDA Receptor-like Subunit (NMDAR-L) in the Rodent Brain." *Journal of Neuroscience* 15(10):6509–20.

Sucher, N. J., K. Kohler, L. Tenneti, H. K. Wong, T. Gründer, S. Fauser, T. Wheeler-Schilling, N. Nakanishi, S. A. Lipton and E. Guenther. 2003. "N-Methyl-D-Aspartate Receptor Subunit NR3A in the Retina: Developmental Expression, Cellular Localization, and Functional Aspects." *Investigative Ophthalmology and Visual Science* 44(10):4451–56.

Sucher, N. J., E. Yu, S. F. Chan, M. Miri, B. J. Lee, B. Xiao, P. F. Worley and F. E. Jensen. 2011. "Association of the Small GTPase Rheb with the NMDA Receptor Subunit NR3A." *NeuroSignals* 18(4):203–9.

Sui, G., C. Soohoo, E. B. Affar, F. Gay, Y. Shi, W. C. Forrester and Y. Shi. 2002. "A DNA Vector-Based RNAi Technology to Suppress Gene Expression in Mammalian Cells." *Proceedings of the National Academy of Sciences of the United States of America* 99(8):5515–20.

Sun, C., T. Wu, C. Chen, P. Wu, Y. Shih, K. Tsuneyama and M. Tao. 2013. "Studies of Efficacy and Liver Toxicity Related to Adeno-Associated Virus-Mediated RNA Interference." *Human Gene Therapy* 24(8):739–50.

Sun, L., F. L. Margolis, M. T. Shipley and M. S. Lidow. 1998. "Identification of a Long Variant of MRNA Encoding the NR3 Subunit of the NMDA Receptor: Its Regional Distribution and Developmental Expression in the Rat Brain." *FEBS Letters* 441(3):392–96.

Sunagawa, G. A., K. Sumiyama, M. Ukai-Tadenuma, D. Perrin, H. Fujishima, H. Ukai, O. Nishimura, S. Shi, R. i. Ohno, R. Narumi, Y. Shimizu, D. Tone, K. L. Ode, S. Kuraku, and H. R. Ueda. 2016. "Mammalian Reverse Genetics without Crossing Reveals Nr3a as a Short-Sleeper Gene." *Cell Reports* 14(3):662–77.

Surace, E. M. and A. Auricchio. 2008. "Versatility of AAV Vectors for Retinal Gene Transfer." *Vision Research* 48(3):353–59.

Tabrizi, S. J., R. I. Scahill, A. Durr, R. A. C. Roos, B. R. Leavitt, R. Jones, G. B. Landwehrmeyer, N. C. Fox, H. Johnson, S. L. Hicks, C. Kennard, D. Craufurd, C. Frost, D. R. Langbehn, R. Reilmann, and J. C. Stout. 2011. "Biological and Clinical Changes in Premanifest and Early Stage Huntington's Disease in the TRACK-HD Study: The 12-Month Longitudinal Analysis." *The Lancet Neurology* 10(1):31–42.

Tabrizi, S. J., R. I. Scahill, G. Owen, A. Durr, B. R. L., R. A. Roos, B. Borowsky, B. Landwehrmeyer, C. Frost, H. Johnson, D. Craufurd, R. Reilmann, J. C. Stout, and D. R. Langbehn. 2013. "Predictors of Phenotypic Progression and Disease Onset in Premanifest and Early-Stage Huntington's Disease in the TRACK-HD Study: Analysis of 36-Month Observational Data." *The Lancet Neurology* 12(7):637–49.

Tabrizi, S. J., B. R. Leavitt, G. B. Landwehrmeyer, E. J. Wild, C. Saft, R. A. Barker, N. F. Blair, D. Craufurd, J. Priller, H. Rickards, A. Rosser, H. B. Kordasiewicz, C. Czech, E. E. Swayze, D. A. Norris, T. Baumann, I. Gerlach, S. A. Schobel, E. Paz, A. V. Smith, C. F. Bennett, and R. M. Lane. 2019.

“Targeting Huntingtin Expression in Patients with Huntington’s Disease.” *New England Journal of Medicine* 380(24):2307–16.

Takano, H., G. Cancel, T. Ikeuchi, D. Lorenzetti, R. Mawad, G. Stevanin, O. Didierjean, A. Dürr, M. Oyake, T. Shimohata, R. Sasaki, R. Koide, S. Igarashi, S. Hayashi, Y. Takiyama, M. Nishizawa, H. Tanaka, H. Zoghbi, A. Brice and S. Tsuji. 1998. “Close Associations between Prevalences of Dominantly Inherited Spinocerebellar Ataxias with CAG-Repeat Expansions and Frequencies of Large Normal CAG Alleles in Japanese and Caucasian Populations.” *American Journal of Human Genetics* 63(4):1060–66.

Tamamaki, N., Y. Yanagawa, R. Tomioka, J. I. Miyazaki, K. Obata and T. Kaneko. 2003. “Green Fluorescent Protein Expression and Colocalization with Calretinin, Parvalbumin, and Somatostatin in the GAD67-GFP Knock-In Mouse.” *Journal of Comparative Neurology* 467(1):60–79.

Tartari, M., C. Gissi, V. Lo Sardo, C. Zuccato, E. Picardi, G. Pesole and E. Cattaneo. 2008. “Phylogenetic Comparison of Huntingtin Homologues Reveals the Appearance of a Primitive PolyQ in Sea Urchin.” *Molecular Biology and Evolution* 25(2):330–38.

Tong, G., H. Takahashi, S. Tu, Y. Shin, M. Talantova, W. Zago, P. Xia, Z. Nie, T. Goetz, D. Zhang, S. A. Lipton and N. Nakanishi. 2008. “Modulation of NMDA Receptor Properties and Synaptic Transmission by the NR3A Subunit in Mouse Hippocampal and Cerebrocortical Neurons.” *Journal of Neurophysiology* 99(1):122–32.

Tratschin, J. D., I. L. Miller and B. J. Carter. 1984. “Genetic Analysis of Adeno-Associated Virus: Properties of Deletion Mutants Constructed *in Vitro* and Evidence for an Adeno-Associated Virus Replication Function.” *Journal of Virology* 51(3):611–19.

Traynelis, S. F., L. P. Wollmuth, C. J. McBain, F. S. Menniti, K. M. Vance, K. K. Ogden, K. B. Hansen, H. Yuan, S. J. Myers and R. Dingledine. 2010. “Glutamate Receptor Ion Channels: Structure, Regulation, and Function.” *Pharmacological Reviews* 14(1):37–40.

Tricoire L, Pelkey KA, Erkkila BE, Jeffries BW, Yuan X, and McBain CJ. 2011. “A blueprint for the spatiotemporal origins of mouse hippocampal interneuron diversity”. *Journal Neuroscience*. 31:10948- 10970.

Tseng, Y., S. Mozumdar, and L. Huang. 2009. “Lipid-Based Systemic Delivery of siRNA.” *Advanced Drug Delivery Reviews* 61(9):721–31.



Tuncdemir, S. N., B. Wamsley, F. J. Stam, F. Osakada, M. Goulding, E. M. Callaway, B. Rudy, and G. Fishell. 2016. "Early Somatostatin Interneuron Connectivity Mediates the Maturation of Deep Layer Cortical Circuits." *Neuron* 89(3):521–35.

Turmaine, M., A. Raza, A. Mahal, L. Mangiarini, G. P. Bates, and S. W. Davies. 2000. "Nonapoptotic Neurodegeneration in a Transgenic Mouse Model of Huntington's Disease." *Proceedings of the National Academy of Sciences of the United States of America* 97(14):8093–97.

Van Der Werf, Y. D., M. P. Witter, and H. J. Groenewegen. 2002. "The Intralaminar and Midline Nuclei of the Thalamus" *Anatomical and Functional Evidence for Participation in Processes of Arousal and Awareness*. Vol. 39.

Van Raamsdonk, J. M., Z. Murphy, E. J. Slow, B. R. Leavitt and M. R. Hayden. 2005a. "Selective Degeneration and Nuclear Localization of Mutant Huntingtin in the YAC128 Mouse Model of Huntington Disease." *Human Molecular Genetics* 14(24):3823–35.

Van Raamsdonk, J. M., J. Pearson, D. A. Rogers, N. Bissada, A. W. Vogl, M. R. Hayden and B. R. Leavitt. 2005b. "Loss of Wild-Type Huntingtin Influences Motor Dysfunction and Survival in the YAC128 Mouse Model of Huntington Disease." *Human Molecular Genetics* 14(10):1379–92.

Van Vugt, J. P. P., S. Siesling, K. K. E. Piet, A. H. Zwinderman, H. A. M. Middelkoop, J. J. van Hilten and R. A. C. Roos. 2001. "Quantitative Assessment of Daytime Motor Activity Provides a Responsive Measure of Functional Decline in Patients with Huntington's Disease." *Movement Disorders* 16(3):481–88.

Veldman, M. B., and X. W. Yang. 2018. "Molecular Insights into Cortico-Striatal Miscommunications in Huntington's Disease." *Current Opinion in Neurobiology* 48:79–89.

Vincent, S. R., and W. Staines. 1983. "Histochemical Demonstration of Separate Populations of Somatostatin and cholinergic Neurons in the Rat Striatum." 35:111–14.

Vogt C, Vogt O. 1941. "Thalamusstudien I-III. Sur Einfu"rung. II. Homogenita"t und Grenzgestaltung der Grisea des Thalamus. III. Das Griseum centrale (centrum medianum Luys)". *I. Psychol Neurol (Leipzig)* 50: 31–154.

Vonsattel, J. P., R. H. Myers, T. J. Stevens, R. J. Ferrante, E. D. Bird and E. P. Richardson. 1985. "Neuropathological Classification of Huntington's Disease." *Journal of Neuropathology and Experimental Neurology* 44(6):559–77.

Walker, F. 2007. "Huntington's Disease."

Wang, J., Z. Lu, M. G. Wientjes, and J. L. Au. 2010. "Delivery of SiRNA Therapeutics: Barriers and Carriers." *The AAPS Journal*. 12(4):492–503.

Wang, X., C. Zhang, G. Szábo, and Q. Quan Sun. 2013. "Distribution of CaMKII $\alpha$  Expression in the Brain in Vivo, Studied by CaMKII $\alpha$ -GFP Mice." *Brain Research* 1518:9–25.

Wang, X. J. 2020. "Macroscopic Gradients of Synaptic Excitation and Inhibition in the Neocortex." *Nature Reviews Neuroscience* 21(3):169–78.

Wanker, E. E., A. Ast, F. Schindler, P. Trepte, and S. Schnoegl. 2019. "The pathobiology of perturbed mutant huntingtin protein-protein interactions in Huntington's Disease." *Journal of Neurochemistry*. 151,507-519.

Warby, S. C., A. Montpetit, A. R. Hayden, J. B. Carroll, S. L. Butland, H. Visscher, J. A. Collins, A. Semaka, T. J. Hudson, and M. R. Hayden. 2009. "CAG Expansion in the Huntington Disease Gene Is Associated with a Specific and Targetable Predisposing Haplogroup." *American Journal of Human Genetics* 84(3):351–66.

Watanabe, M., Y. Inoue, K. Sakimura, and M. Mishina. 1992. "Developmental Changes in Distribution of Nmda Receptor Channel Subunit m Rim As." *Neuron Report* 3(12):1138–40.

Watson C., Paxinos G., and Puelles L. 2012. "Mouse nervous system". 1st Edition. Academic Press.

Watson, G. D. R., J. B. Smith and K. D. Alloway. 2017. "Interhemispheric Connections between the Infralimbic and Entorhinal Cortices: The Endopiriform Nucleus Has Limbic Connections That Parallel the Sensory and Motor Connections of the Claustrum." *Journal of Comparative Neurology* 525(6):1363–80.

Weitzman, M. D., S. R. M. Kyosti, R. M. Kotin, and R. A. Owens. 1994. "Adeno-associated virus (AAV) Rep proteins mediate complex formation between AAV DNA and its integration site in human DNA." *Proc Natl Acad Sci USA* 91(June):5808–12.

Wesseling, J. F., and I. Pérez-Otaño. 2015. "Modulation of GluN3A Expression in Huntington Disease a New N-Methyl-D-Aspartate Receptor-Based Therapeutic Approach?" *JAMA Neurology* 72(4):468–73.

- Wexler, N. S. 1991. "Molecular Approaches to Hereditary Diseases of the Nervous System: Huntington's Disease as A Paradigm." *Annual Review of Neuroscience* 14(1):503–29.
- Wheeler, V. C., W. Auerbach, J. K. White, J. Srinidhi, A. Auerbach, A. Ryan, M. P. Duyao, V. Vrbanac, M. Weaver, J. F. Gusella, A. L. Joyner and M. E. MacDonald. 1999. "Length-Dependent Gametic CAG Repeat Instability in the Huntington's Disease Knock-in Mouse." *Human Molecular Genetics* 8(1):115–22.
- Wheeler, V. C., C. Gutekunst, V. Vrbanac, L. Lebel, G. Schilling, S. Hersch, R. M. Friedlander, J. F. Gusella, J. Vonsattel, D. R. Borchelt and M. E. MacDonald. 2002. "Early Phenotypes That Presage Late-Onset Neurodegenerative Disease Allow Testing of Modifiers in Hdh CAG Knock-in Mice." *Human Molecular Genetics* 11(6):633–40.
- Whitworth, A. L., N. H. Mann, and A. W. D. Larkum. 2006. "This Article Is Protected by Copyright. All Rights 1 Reserved." *Ultrasound Obstet Gynecol.* 50(6):776–80.
- Williams K 1993. "Ifenprodil discriminates subtypes of the N-methyl-D-aspartate receptor: selectivity and mechanisms at recombinant heteromeric receptors." *Molecular pharmacology* 44(4):851-9
- Wilson, Charles J., and P. M. Groves. 2004. "Fine Structure and Synaptic Connections of the Common Spiny Neuron of the Rat Neostriatum: A Study Employing Intracellular Injection of Horseradish." *The Journal of Comparative Neurology*. 194:599-615 615(April 1979):1–17.
- Wong, H., X. Liu, M. F. Matos, S. F. Chan, I. Pérez-Otaño, M. Boysen, J. Cui, N. Nakanishi, J. S. Trimmer, E. G. Jones, S. A. Lipton and N. J. Sucher. 2002. "Temporal and Regional Expression of NMDA Receptor Subunit NR3A in the Mammalian Brain." *Journal of Comparative Neurology* 450(4):303–17.
- Wu, J., D. A. Ryskamp, X. Liang, P. Egorova, O. Zakharova, G. Hung, and I. Bezprozvanny. 2016. "Enhanced Store-Operated Calcium Entry Leads to Striatal Synaptic Loss in a Huntington's Disease Mouse Model." *Journal of Neuroscience* 36(1):125–41.
- Wu, Y., S. Richard and A. Parent. 2000. "The Organization of the Striatal Output System: A Single-Cell Juxtacellular Labeling Study in the Rat." *Neuroscience Research* 38(1):49–62.
- Wu, Z., H. Yang and P. Colosi. 2010. "Effect of Genome Size on AAV Vector Packaging." *Molecular Therapy* 18(1):80–86.

Xu, Qing., Tam, Melissa., And Anderson Stewart A. 2008. "Fate Mapping Nkx2.1-Lineage Cells in the Mouse Telencephalon" *The Journal of Comparative Neurology* 506:16–29

Yamamoto, A., J. J. Lucas and R. Hen. 2000. "Reversal of Neuropathology and Motor Dysfunction in a Conditional Model of Huntington's Disease." *Cell* 101:57–66.

Yang J, S. Wang, Z. Yang, CA. Hodgkinson, P. Iarikova, JZ. Ma, TJ. Payne, D. Goldman, and MD. Li. 2015. "The contribution of rare and common variants in 30 genes to risk nicotine dependence." *Molecular Psychiatry*. 20:1467-1478.

Yao, Y. and M. L. Mayer. 2006. "Characterization of a Soluble Ligand Binding Domain of the NMDA Receptor Regulatory Subunit NR3A." *Journal of Neuroscience* 26(17):4559–66

Yao, Y., C. B. Harrison, P. L. Freddolino, K. Schulten and M. L. Mayer. 2008. "Molecular Mechanism of Ligand Recognition by NR3 Subtype Glutamate Receptors." *EMBO Journal* 27(15):2158–70.

Yao, Z., H. Liu, F. Xie, S. Fischer, A. S. Boeshaghi, R. S. Adkins, A. I. Aldridge, S. A. Ament, A. Pinto-Duarte, A. Bartlett, et al. 2020. "An integrated transcriptomic and epigenomic atlas of mouse primary motor cortex cell types." *bioRxiv*.2020.2002.2029.970558.

Yi, R., Y. Qin, I. G. Macara, and B. R. Cullen. 2003. "Exportin-5 Mediates the Nuclear Export of Pre-MicroRNAs and Short Hairpin RNAs." *Genes and Development* 17(24):3011–16.

Yoshii, A., M. H. Sheng, and M. Constantine-Paton. 2003. "Eye Opening Induces a Rapid Dendritic Localization of PSD-95 in Central Visual Neurons." *Proceedings of the National Academy of Sciences of the United States of America* 100(3):1334–39.

Young, A. B., I. Shoulson, J. B. Penney, S. Starosta-Rubinstein, F. Gomez, H. Travers, M. A. Ramos-Arroyo, S. R. Snodgrass, E. Bonilla, H. Moreno and N. S. Wexler. 1986. "Huntington's Disease in Venezuela: Neurologic Features and Functional Decline." *Neurology* 36(2):244–49.

Young, S. M., D. M. McCarty, N. Degtyareva, and R. J. Samulski. 2000. "Roles of Adeno-Associated Virus Rep Protein and Human Chromosome 19 in Site-Specific Recombination." *Journal of Virology* 74(9):3953–66.

Yu, D., H. Pendergraff, J. Liu, H. B. Kordasiewicz, D. W. Cleveland, E. E. Swayze, W. F. Lima, S. T. Croke, T. P. Prakash, and D. R. Corey. 2012.

“Single-Stranded RNAs Use RNAi to Potently and Allele-Selectively Inhibit Mutant Huntingtin Expression.” *Cell* 150(5):895–908.

Yu, Z., S. Li, J. Evans, A. Pillarisetti, H. Li and X. Jiang Li. 2003. “Mutant Huntingtin Causes Context-Dependent Neurodegeneration in Mice with Huntington’s Disease.” *Journal of Neuroscience* 23(6):2193–2202.

Yuan, T., M. Mameli, E. C. O’Connor, P. N. Dey, C. Verpelli, C. Sala, I. Perez-Otano, C. Lüscher and C. Bellone. 2013. “Expression of Cocaine-Evoked Synaptic Plasticity by GluN3A-Containing NMDA Receptors.” *Neuron* 80(4):1025–38.

Zeng, Y., E. J. Wagner and B. R. Cullen. 2002. “Both Natural and Designed Micro RNAs Can Inhibit the Expression of Cognate MRNAs When Expressed in Human Cells.” *Molecular Cell* 9(6):1327–33.

Zhang, H., D. J. Webb, H. Asmussen and A. F. Horwitz. 2003. “Synapse Formation Is Regulated by the Signaling Adaptor GIT1.” *Journal of Cell Biology* 161(1):131–42.

Zhang, X., A. Liu, D. Ruan and J. Liu. 2002. “Effect of Developmental Lead Exposure on the Expression of Specific NMDA Receptor Subunit mRNAs in the Hippocampus of Neonatal Rats by Digoxigenin-Labeled in Situ Hybridization Histochemistry.” *Neurotoxicology and Teratology* 24(2):149–60.

Zincarelli, C., S. Soltys, G. Rengo and J. E. Rabinowitz. 2008. “Analysis of AAV Serotypes 1-9 Mediated Gene Expression and Tropism in Mice after Systemic Injection.” *Molecular Therapy* 16(6):1073–80.

Zuccato, C., M. Tartari, A. Crotti, D. Goffredo, M. Valenza, L. Conti, T. Cataudella, B. R. Leavitt, M. R. Hayden, T. Timmusk, D. Rigamonti, and E. Cattaneo. 2003. “Huntingtin Interacts with REST/NRSF to Modulate the Transcription of NRSE-Controlled Neuronal Genes.” *Nature Genetics* 35(1):76–83.

Zuo, Y., A. Lin, P. Chang and W. Gan. 2005. “Development of Long-Term Dendritic Spine Stability in Diverse Regions of Cerebral Cortex.” *Neuron* 46(2):181–89

